**TECHNISCHE UNIVERSITÄT MÜNCHEN**

Wissenschaftszentrum Weihenstephan für Ernährung, Landnutzung und Umwelt
Lehrstuhl für Molekulare Ernährungsmedizin

# Diet-induced obesity in inbred mouse strains – identification of proximate causes, reversibility of metabolic alterations and heredity of resistance

Caroline Kleß

Vollständiger Abdruck der von der Fakultät Wissenschaftszentrum Weihenstephan für Ernährung, Landnutzung und Umwelt der Technischen Universität München zur Erlangung des Grades eines

Doktors der Naturwissenschaften

genehmigte Dissertation.

| | |
|---|---|
| Vorsitzender: | Prof. Dr. Dirk Haller |
| Prüfer der Dissertation: | 1. Prof. Dr. Martin Klingenspor |
| | 2. Prof. Dr. Hannelore Daniel |

Die Dissertation wurde am 04.04.2017 bei der Technischen Universität München eingereicht und durch die Fakultät Wissenschaftszentrum Weihenstephan für Ernährung, Landnutzung und Umwelt am 06.08.2017 angenommen.

# TABLE OF CONTENTS

# SUMMARY

The worldwide prevalence of obesity has been rising for decades and presents a serious risk factor for chronic metabolic disorders like diabetes mellitus. Obesity results from a continuing energy surplus caused by an imbalance of energy intake and energy expenditure. Considering the complexity of human obesity development which is mostly polygenetic and implicates environmental influences, mouse models offer a fundamental contribution to the understanding of obesity progression. By conducting several feeding experiments in inbred mouse strains, the present study aimed to identify proximate causes of diet-induced obesity (DIO), to clarify reversibility of DIO-caused metabolic alterations and to characterize heredity of DIO.

Firstly, high-fat diet (HFD) feeding experiments revealed the impact of feeding duration, quantity and quality of fat in C57BL/6J mice on glucose tolerance and fat mass accumulation, as main read-outs for HFD-induced metabolic changes. After evaluating the response of HFD in various inbred mouse strains, mice of the AKR/J and SWR/J strain were chosen due to differences in DIO. Precise analysis of both sides of energy balance with appropriate adjustment of data was performed during the first days of HFD feeding in DIO-prone AKR/J and DIO-resistant SWR/J mice. This is the first study to unravel metabolic predispositions and the contribution of metabolizable and expanded energy to the proximate causes of DIO. Additionally the difference in positive energy balance between strains was related to accumulated fat mass.

Due to examination of mice with different DIO susceptibility, development of HFD-induced impairments of glucose homeostasis could be divided into two parts: the initial diet-dependent phase due to acute over-eating of HFD and secondly the obesity-dependent phase in which development of obesity through continuing HFD feeding is responsible for chronically reduced glucose and insulin tolerance. However, DIO-induced impaired metabolic parameters were reversible through reduction of energy intake, independent of the diet's macronutrient composition. Epididymal white adipose tissue of still obese AKR/J mice with normal glucose tolerance due to catabolic metabolism was analyzed using RNA sequencing. Furthermore, continuing weight loss in formerly obese AKR/J mice reduced energy expenditure proportionally, hampering a yo-yo-effect in body mass. Finally the F1-generation of an intercross of AKR/J and SWR/J mice was characterized. The progeny displayed complexity of polygenetic heredity of DIO and glucose tolerance, of which could neither be associated with one parental strain nor was the phenotype intermediate.

Conclusively, this comprehensive study contributes to a better understanding of DIO by identifiying proximate causes of DIO on both sides of the energy balance, differentiation of obesity- and diet-induced metabolic alterations, as well as itemization of reversibility of DIO-caused changes and characterization of the complex and polygenetic heredity of DIO.

# ZUSAMMENFASSUNG

Weltweit steigt die Adipositasprävalenz seit Jahrzehnten an. Adipositas stellt einen bedeutenden Risikofaktor für chronische metabolische Erkrankungen wie Diabetes mellitus dar. Übergewicht/Adipositas ist durch einen länger anhaltenden Energieüberschuss bedingt, dessen Ursache das Ungleichgewicht von Energieaufnahme und Energieverbrauch ist. In Anbetracht der komplexen Entstehung von Übergewicht beim Menschen, die meist polygenetisch und von der Umwelt beeinflusst ist, bieten Mausmodelle einen wesentlichen Beitrag zum Verständnis der Übergewichtsprogression. Das Ziel dieser Arbeit ist es, durch verschiedene Fütterungsexperimente in Maus-Inzuchtlinien unmittelbare Ursachen für diätinduzierte Adipositas zu identifizieren, die Reversibilität von metabolischen Veränderungen zu prüfen, die durch diätinduzierte Adipositas verursacht wurden und die Erblichkeit von diätinduzierter Adipositas zu beschreiben.

Die ersten Fütterungsexperimente mit Hochfett-Futter in C57BL/6J Mäusen zeigten den Einfluss von Fütterungsdauer, Qualität und Quantität von Fett auf die Glukosetoleranz. Letztere sowie die Fettmassezunahme wurden als Hauptindikatoren für metabolische Veränderungen durch Hochfett-Fütterung herangezogen. Nachdem die Reaktion von verschiedenen Mausstämmen auf Hochfett-Futter beurteilt worden war, wurden für weitere Experimente Mäuse der Stämme AKR/J und SWR/J gewählt, da beide sich deutlich in ihrer Empfänglichkeit für diätinduzierte Adipositas unterscheiden. Sowohl bei AKR/J Mäusen, die empfänglich für diätinduzierte Adipositas sind als auch bei SWR/J Mäusen, die Resistenz gegenüber diätinduzierter Adipositas zeigen, wurden während der ersten Tage mit Hochfett-Fütterung beide Seiten des Energiehaushalts genau analysiert und angemessen adjustiert. Diese Studie ist die Erste, die stammbedingte Stoffwechselveranlagungen und die Beteiligung von metabolisierbarer Energie und Energieverbrauch an der unmittelbaren Entstehung von diätinduzierter Adipositas aufdeckt. Zusätzlich wurde die Differenz an Energieüberschuss zwischen den Mausstämmen in Relation zur akkumulierten Fettmasse gesetzt.

Indem Mäuse mit unterschiedlicher Empfänglichkeit für diätinduzierte Adipositas untersucht wurden, konnte die Entstehung von Veränderungen in der Glukosehomöostase, die durch Hochfett-Fütterung hervorgerufen wurden, in zwei Abschnitte unterteilt werden: die erste diätabhängige Phase, die durch akutes Überfressen von Hochfettdiät gekennzeichnet ist und zweitens die übergewichtsabhängige Phase, in der das durch anhaltende Hochfett-Fütterung verursachte Übergewicht für die chronisch reduzierte Glukose- und Insulintoleranz verantwortlich ist. Dennoch waren alle Stoffwechselveränderungen, die durch diätinduzierte Adipositas verursacht wurden, durch reduzierte Energieaufnahme umkehrbar. Dabei war die Zusammensetzung der Makronährstoffe in der Diät nicht von Bedeutung. Epididymales weißes

Fettgewebe von AKR/J Mäusen, die zwar noch übergewichtig waren, aber normale Glukosetoleranz zeigten, da sie sich in einem katabolen Stoffwechselzustand befanden, wurde mittels RNA Sequenzierung analysiert. Des Weiteren reduziert sich der Energieverbrauch durch anhaltenden Gewichtsverlust in ehemals übergewichtigen AKR/J Mäusen proportional zum Körpergewicht, was einen Jo-Jo-Effekt des Körpergewichts verhinderte. Abschließend wurde die F1-Generation einer Kreuzung von AKR/J und SWR/J Mäusen charakterisiert. Die Nachkommen spiegelten die Komplexität der polygenetischen Vererbung der diätinduzierten Adipositas und Glukosetoleranz wieder, da sie weder einem elterlichen Stamm zugeordnet werden konnten noch einen intermediären Phänotyp zeigten.

Zusammenfassend trägt diese umfangreiche Arbeit dazu bei, diätinduzierte Adipositas besser zu verstehen. Unmittelbare Ursachen für diätinduzierte Adipositas wurden auf beiden Seiten der Energiebilanz identifiziert. Es konnte differenziert werden, ob Stoffwechselveränderungen durch Übergewicht oder das fettreiche Futter selbst herbeigeführt wurden. Die Umkehrbarkeit von durch diätinduzierte Adipositas hervorgerufenen Stoffwechselveränderungen wurde aufgeschlüsselt und die komplexe Vererbbarkeit von diätinduzierter Adipositas gezeigt.

# 1. INTRODUCTION

## 1.1. Causes and consequences of obesity

Alarming facts about overweight and obesity were recently updated by the World Health Organization (WHO): worldwide obesity has more than doubled since 1980 (WHO 2016). According to the WHO more than 1.9 billion adults were overweight in 2014. Of these, more than 600 million were obese. Meanwhile, worldwide rates of excess weight and obesity are linked to more deaths than those from being underweight (WHO 2016). An adult with a body mass index (BMI = weight [kg] divided by the square of height [m]) of more than 25 is defined as being overweight while obesity starts with a BMI over 30. By definition both overweight and obesity are characterized by excessive or abnormal fat accumulation which may impair health (UNAIDS 2000; Grundy 2004). Adverse physiological and metabolic consequences for health may be elevated blood glucose levels (Nakatsuji et al. 2010), insulin resistance (Xu et al. 2003; Ye 2013), increased inflammation (Greenberg and Obin 2006; Sam and Mazzone 2014), elevated free fatty acids, dyslipidemia and hypertension (Khaodhiar et al. 1999; Klop et al. 2013). So permanently, both, overweight and, more especially obesity are major risk factors in cardiovascular diseases, the leading cause of death in 2012, as well as chronic diseases like diabetes mellitus and some types of cancers (Bray 1996; Khaodhiar et al. 1999; WHO 2016).
Reversibility of obesity means that weight loss is achieved by reduction of caloric intake or by increasing energy expenditure, for example by exercising. In addition to subjectively better quality of life most of the obesity related metabolic alterations and comorbidities can also be improved (Hariri and Thibault 2010; Viardot et al. 2010; Franz et al. 2015; Kroes et al. 2016).

In general, overweight and obesity result from a chronic energy surplus caused by an imbalance of energy intake and energy expenditure. The “thrifty genes” hypothesis provides an explanation for susceptibility to obesity. During evolution individuals with genes favoring efficient storage of excess energy in the form of fat, might have had a selective advantage for survival in periods of limited food resources (Neel 1962; Prentice 2001; Chakravarthy and Booth 2004). Over the years this hypothesis has been further developed and debated (Prentice et al. 2008; Ayub et al. 2014; Wang and Speakman 2016). Essentially, today’s environment is marked by unlimited excess to high caloric, energy dense foods accompanied by a modern lifestyle with reduced physical activity. In addition to environmental influences and behavior, genetic make-up can be an individual risk or protection factor for obesity (Young et al. 2007). In rare cases, genetic susceptibility to obesity is caused by single gene mutation (Mutch and Clement 2006). An inherited propensity for monogenetic forms of obesity obeys Mandelian patterns of inheritance

(Farooqi and O'Rahilly 2005). However, body weight regulation and development of obesity are mostly influenced by a large number of gene variants (Aberle et al. 2008; Rojas et al. 2013). It is acknowledged that the interplay of all three factors - environment, behavior and genetics - leads to the development of obesity (Comuzzie and Allison 1998; Hill and Peters 1998; Speakman et al. 2011). How much influence can be apportioned to the three variables is quite individual (Speakman 2004). The estimated genetic contribution to polygenetic obesity has been estimated in numerous family, twin and adaption studies (Maes et al. 1997) and ranges in total from about 40 % to 70 % (Barsh et al. 2000). Epigenetic mechanisms can explain varying phenotype levels between genetically identical monogenetic twins (Bell and Spector 2011; Castillo-Fernandez et al. 2014). This means that environmental stimuli impact gene expression, for example through DNA methylation.

## 1.2. Energy balance

### 1.2.1. Components of energy balance

Energy balance describes the relationship of energy inflow ($E_{in}$) and energy outflow ($E_{out}$). Energy intake is ensured by the consumption of food (figure 1). In the intestine, macronutrients are broken down chemically and enzymatically to low molecular components like amino acids, glucose and fatty acids. Part of the ingested energy is not available for assimilation and is released via feces or by microbial heat dissipation (Tremaroli and Backhed 2012). Furthermore, a fraction of the assimilated energy that cannot be oxidized completely is voided as urine (Street et al. 1964). Remaining metabolizable energy is available for energy expenditure processes. Most of the energy is expended on the basal metabolic rate, including maintenance of the body's biochemical system (Lam and Ravussin 2016). Moreover energy is used for spontaneous and voluntary physical activity, growth, specific dynamic reactions to food and thermoregulation of a stable body core temperature. Both sides of the energy balance equation are complex and highly dynamic. Related to the development of obesity, maintaining a balance depends on behavior, environment and genetic equipment, for example the regional/seasonal availability of food, ambient temperature, gastrointestinal function or sufficient physical activity. If energy consuming processes are not in balance with metabolizable energy, the metabolism gains ($E_{in} > E_{out}$) or loses energy ($E_{out} > E_{in}$). Continuously positive energy balance drives the accumulation of excess energy in endogenous energy stores. Energy is mainly chemically bound as fat, and in small amounts as carbohydrates. Energy stores can be mobilized to compensate temporary energy depletion (Rozman et al. 2014). But in the longer term, persistent energy surplus leads to excess weight and obesity.

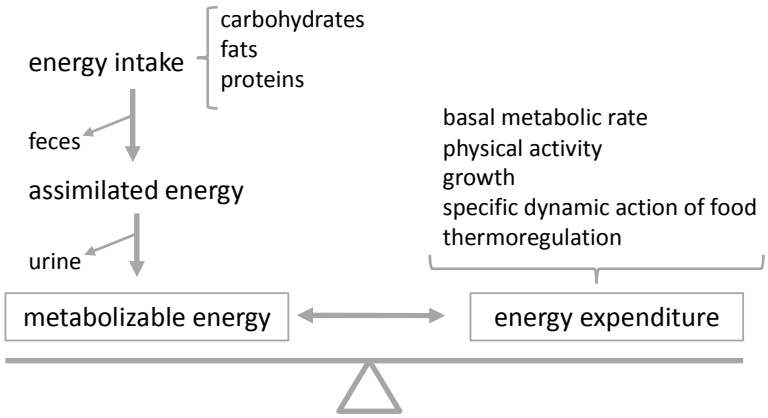


**Figure 1: Components of energy balance.** Energy balance is the relation of metabolizable energy and energy expenditure. Metabolizable energy results from food energy reduced by energy loss via feces and urine. 5 parameters contribute to energy expenditure with the basal metabolic rate as the main energy-consuming process.

### 1.2.2. Assessment of energy balance

For a convincing assessment of energy balance, it is preferable that any component be measured. Reviews of literature summarize and evaluate practicable methods and give recommendations for data analysis (Levine 2005; Even and Nadkarni 2012; Tschop et al. 2012; Lam and Ravussin 2016).

Basically, methods of energy balance determination are similar for rodents and humans. This includes the calculation of energy influx, the documentation and quantification of food intake, and voiding as urine and feces. In rodent studies, however, food intake can be measured easily by weighing food baskets with the offered food at the beginning and the end of the intervention. In humans, food dairies, recalls or questionnaires are used to report food consumption. The energy content of food and feces is assessed by direct/bomb calorimetry basing on Hess's law of constant heat summation. The caloric value of food or feces can be extrapolated by measuring the released heat detected in a bomb calorimeter when burning a sample completely under high pressure and excess oxygen. Endogenous energy stores are measured using body composition analysis for discrimination of fat and fat-free/lean mass. In addition to weighing and destructive methods inapplicable to humans, non-invasive analyses form the preferred approach, for example bioelectrical impedance analysis, dual-energy X-ray absorptiometry, (quantitative) magnetic resonance spectroscopy and imaging (Wells and Fewtrell 2006; Lee and Gallagher 2008; Tschop et al. 2012).

In the 18$^{th}$ century, first experiments in the field of energy efflux analysis assessed animal energy expenditure by direct measurement of heat production. Lavoisier and Laplace quantified the amount of melted ice in an insulated chamber that contained both ice and a living test subject

(Kaiyala and Ramsay 2011). In this context, and supported by the findings of Crawford, these researchers postulated a correlation between heat loss and carbon dioxide production, that oxygen consumption is proportional to heat production, and that animals produce energy via a form of combustion (Underwood 1944; Blaxter 1978). The next milestone in calorimetry was reached by Atwater and Rosa, when measurements in a human direct calorimeter were combined with respiratory gas exchange analysis. Results of studies using this dual calorimetric device (Atwater and Rosa 1899; Atwater and Benedict 1903) enabled empirical justification of standard tables and formulas for the calculation of caloric equivalents for gas exchange of oxygen and carbon dioxide (Kaiyala and Ramsay 2011). Thus, at the present time, and due to developments in methodology and technical innovations, indirect calorimetry is the standard method for assessing energy expenditure through calculation of the amount of energy released by oxidation of energy substrates. Direct calorimetry is seldom used, as it is technically challenging, limited in its detection of acute energy expenditure changes, and since it requires measurements of all heat transfers including radiation, convection, conduction and heat loss due to evaporation (Webb 1980; Lam and Ravussin 2016). Lots of recommended approaches for the analysis and interpretation of collected energy balance data are addressed in the literature (Arch et al. 2006; Kaiyala et al. 2010; Even and Nadkarni 2012; Rozman et al. 2014). When the results from individuals with different body mass and composition are compared, data relating to metabolizable and expended energy needs to be adjusted thoughtfully (Tschop et al. 2012; Speakman et al. 2013). Furthermore, monitoring of activity and body temperature is particularly helpful when establishing precise energy expenditure.

In general, energy balance is assessed in order to reveal disorders leading to obesity. In humans, quantifying the parameters of an energy balance equation presents a huge challenge. Measurements of daily energy expenditure are elaborate and cannot be performed in the habitual environment (Rosenbaum et al. 1996; Levine 2005). Conscious report of food intake, as well as the collection of feces and urine, can change daily routine and be highly biased by compliance on the part of individual subjects (Tucker 2007). Consequently, in human study cohorts uncontrollable environmental variables and inter-individual differences in body weight gain make it extremely difficult to reveal the causes of obesity development. Remarkably, comprehensive measurements of energy balance are also poorly reported for rodent models in obesity research, although most research laboratories are equipped with highly sophisticated technology for the assessment of key parameters. Finally, in the last few years a consensus relating to the analysis and normalization of assessed data was reached. Previously simple ratio calculations are now adopted from regressions-based approaches, such as the analysis of covariance and general linear modeling (Kaiyala and Schwartz 2011; Tschop et al. 2012;

Speakman et al. 2013). At any rate, recommendations are not applied consequently to both sides of the energy balance in human and rodent experiments.

## 1.3. Glucose and insulin sensitivity

### 1.3.1. Physiological regulation

Glucose is a ubiquitous source of energy and the 'classical' circulating blood sugar. The pancreatic hormones insulin and glucagon are the key players for regulation of glucose concentrations in the blood. Under conditions of hypoglycemia glucagon is released by α-cells of the pancreas stimulating hepatic cells to produce glucose by glycogenolysis. Insulin is responsible for the uptake of glucose by the targeting cells of different tissues and thereby for a lowering of blood glucose levels. Postprandial nutrients are taken up into circulation via the hepatic portal vein. Glucose is transported via Glut2 into hepatocytes and pancreatic cells. In the pancreas, β-cells are stimulated to secrete insulin (figure 2). In the liver insulin and the sensing of increased glucose concentrations inhibit hepatic glucose production and fortify lipogenesis and glycogenesis. Binding of circulating insulin to insulin receptors on the surface of target cells such as adipocytes, hepatocytes, erythrocytes and myocytes induces an intracellular cascade resulting in fusion of vesicles containing Glut4 with the plasma membrane leading to the uptake of glucose (whole paragraph, (Saltiel and Kahn 2001; Leto and Saltiel 2012; Kowalski and Bruce 2014)).

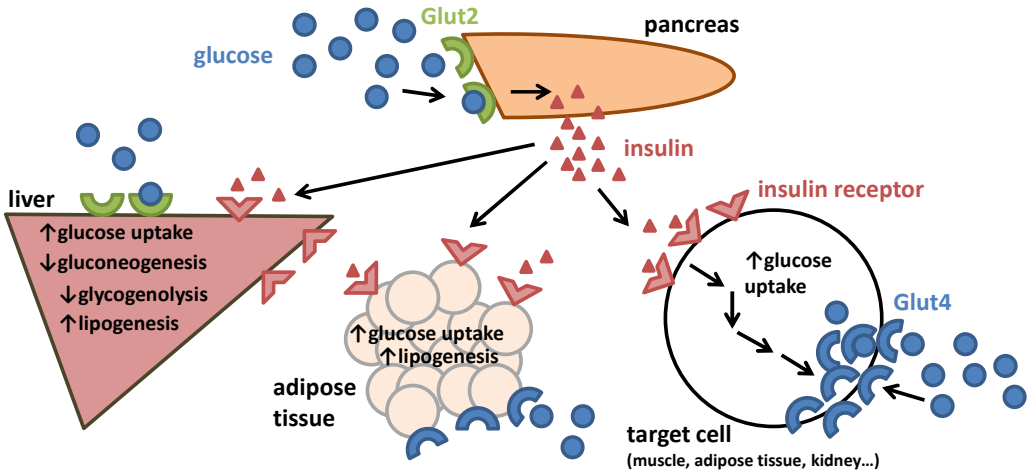


**Figure 2: Function of insulin.** In healthy, insulin sensitive subjects elevated glucose concentrations in the circulation lead to glucose uptake in the liver and the pancreas via Glut2. Pancreatic β-cells secrete insulin. In the target cells, binding of insulin to the receptor mediates glucose uptake by Glut4. Additionally lipogenesis is upregulated in adipocytes and hepatocytes whereas hepatic glucose production is reduced.

Nearly every cell needs glucose. Erythrocytes generate energy exclusively from glucose breakdown. Likewise, the brain covers its tremendous need for energy primarily with glucose. In brief, intracellular glycolysis degrades glucose to pyruvate producing high-energy ATP. Furthermore, pyruvate is decarboxylated generating acetyl-CoA which is also a breakdown product of fatty acid and amino acids. Acetyl-CoA undergoes citric acid cycle. During several chemical processes more chemical energy is bound in the form of ATP and precursors of various metabolites are also provided, as well as the reducing agent NADH. Different types of cells use generated metabolites from glucose breakdown as starting products for the production of lactate and amino acids or for fatty acid synthesis. Finally, in preferred oxidative phosphorylation more ATP is synthesized by electron transport chain forming a proton gradient across the inner mitochondrial membrane. Since glucose is essential, availability needs to be assured in times of shortage. In liver and muscle tissue, excess glucose is stored as glycogen. Whereas glucose generated from muscle glycogen can only be used as an energy substrate in muscle itself, liver glycogen can be degraded to buffer blood glucose level. The second possibility for maintaining euglycemia during fasting periods is gluconeogenesis. A lot of metabolites from peripheral tissue like lactate, glycerol and amino acids are substrates for hepatic glucose production (figure 3).

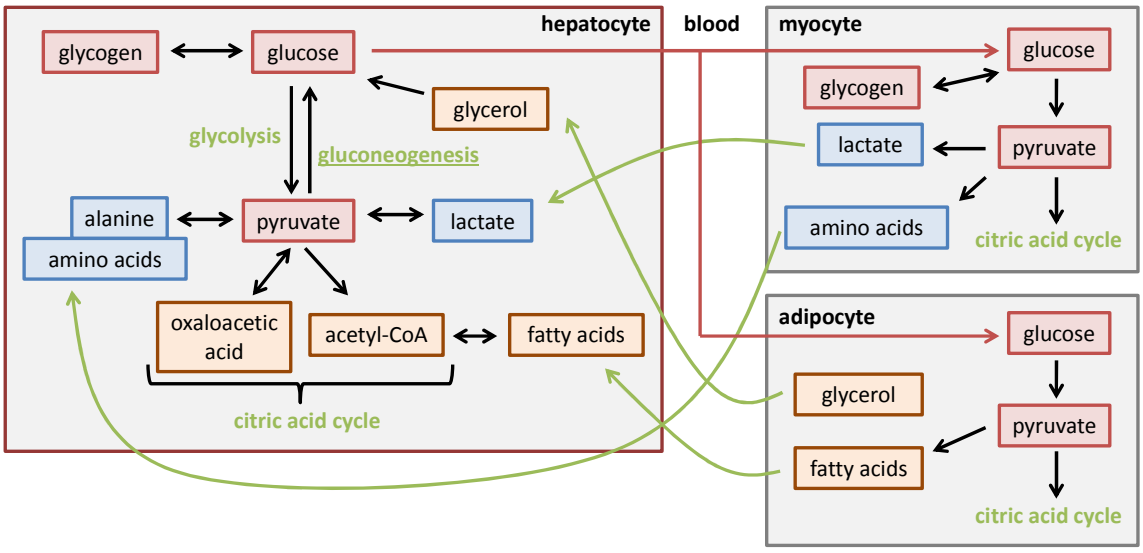


**Figure 3: Glucose as essential substrate for cells.** Glucose serves as a fuel substrate for energy production and as precursor for a lot of metabolites. In times of threatening hypoglycemia hepatocytes can generate glucose by gluconeogenesis.

### 1.3.2. Changes due to high-fat diet and obesity

Diabetes mellitus describes a group of metabolic diseases manifested by high blood sugar level over a prolongued period. Other than type 1 diabetes, or the pancreatic failure to produce sufficient insulin, type 2 diabetes starts with insulin resistance provoked by an unhealthy

lifestyle (Tuomilehto et al. 2001; Kahn et al. 2006; Keller 2006). In advance of insulin resistance and the manifestation of diabetes the action of insulin or rather the sensitivity to insulin is diminished. Inadequate insulin signalling in certain tissues leads to decreased glucose uptake and increased hepatic glucose production (Curtis et al. 2005) (figure 4).

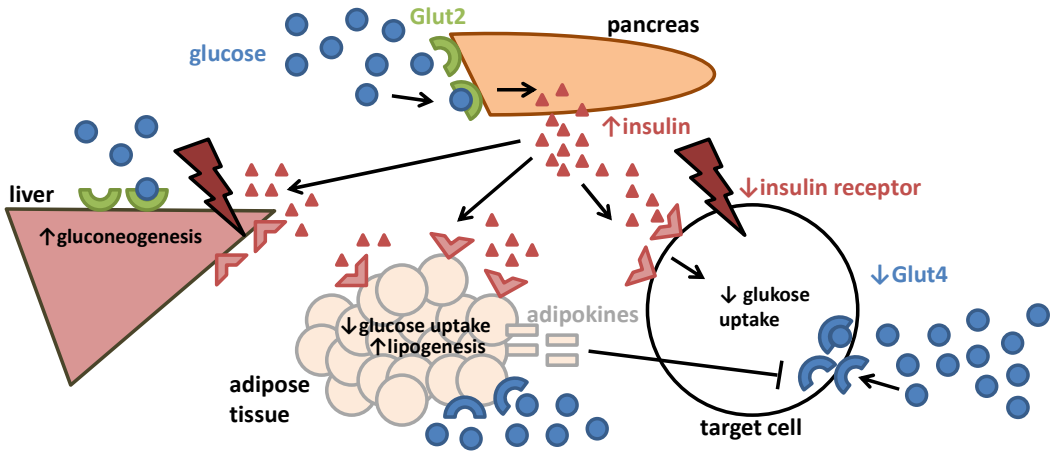


**Figure 4: Impact of decreased insulin sensitivity.** Increased intake of high-fat diet and/or obesity leads to reduced blood glucose lowering the action of insulin, possibly by diminished insulin receptor signaling, inhibition of glucose uptake by adipokines and misdirected compensatory processes in the pancreas and liver.

How the modern western lifestyle, especially excessive high-fat diet and/or obesity influence insulin sensitivity has been extensively reviewed in the literature (Greenfield and Campbell 2006; Kahn et al. 2006; Keller 2006; Johnson and Olefsky 2013). Identification of cause and effect and considering the influence of all organs and metabolites involved is challenging. Simply put, constant intake of high-caloric food increases insulin secretion to above normal levels in order to dispose of elevated blood glucose levels (Curtis et al. 2005). High insulin levels and the availability of excess nutrients promote lipogenesis and consequently adipogenesis. Growing adipose tissue, especially visceral fat, increases lipolysis and the secretion of free fatty acids. Endogenous and additional free fatty acids from the diet stimulate ectopic fat accumulation in muscle and liver. As a consequence, this can lead to impaired insulin signalling in affected tissues (Curtis et al. 2005; Eckardt et al. 2011) and decreased Glut4 translocation (Nawrocki and Scherer 2004; Boren et al. 2013). Expanding adipose tissue and persistently increased insulin levels divert adipokine secretion towards mediators that lower insulin sensitivity (resistin, leptin). Additionally, low-grade inflammation with macrophage infiltration drives the release of chemoattractants and cytokines (TNFα, Il6), contributing to impaired insulin signaling, both systemically and within adipocytes (Greenberg and Obin 2006; McArdle et al. 2013). Commencing insulin resistance of the peripheral tissue is compensated by enhanced insulin production in the pancreas. Hyperinsulinemia indirectly causes an elevated intrahepatic flux of fatty acids and an increased hepatic glucose output due to reduced inhibition of hepatic

gluconeogenesis (Song et al. 2001; Samuel and Shulman 2016). The already extant intake of a high-fat diet, independent of the development of obesity, can impact glucose and insulin sensitivity (Chisholm and O'Dea 1987; Chiazza et al. 2016). Therefore, composition of the diet, meaning chain length and degree of saturation of fatty acids, mediates different metabolic effects. Diets high in long chain saturated fatty acids are generally considered to exhibit the most deleterious effects favoring lipid accumulation and impairment of insulin sensitivity (Even et al. 2010; Coelho et al. 2011; Geng et al. 2013). Especially high amounts of palmitic acid and stearic acid were shown to promote insulin resistance under certain conditions (Ikemoto et al. 1996; van den Berg et al. 2010). Mono- and polyunsaturated fatty acids have a less negative impact on insulin sensitivity. In numerous studies they even exhibit a beneficial influence on obesity-related comorbidities (Even et al. 2010; Catta-Preta et al. 2012; Salvado et al. 2013).

### 1.3.3. Assessment of glucose homeostasis

For a comprehensive assessment of glucose homeostasis glucose tolerance, insulin sensitivity and insulin secretion need to be measured. Fasting glucose levels are first indicators of glucose handling by the metabolism. Most commonly, a glucose tolerance test is performed in order to measure glucose clearance from the circulation after glucose bolus administration. Glucose can be applied orally or, especially in rodent studies, intraperitoneally and the concentration of glucose in the blood is measured at defined intervals. But this approach gives no information about insulin secretion or the insulin sensitivity of tissues. Similarly to glucose tolerance tests, insulin sensitivity can be assessed using insulin tolerance tests by measuring glycemia after insulin injection. Results are used to evaluate responsiveness of tissues and organs to exogenous insulin. Alternatively, in humans, overnight fasting glucose and insulin levels can be used in mathematical models to calculate indices like HOMA-IR and QUICKI which are surrogate parameters of insulin resistance (Bowe et al. 2014). The gold standard for measuring insulin sensitivity is the hyperinsulinaemic-euglyaemic clamp (Grayson et al. 2013). Thereby, under steady-state conditions of euglycemia, the glucose infusion rate used for maintaining euglycemia equals glucose uptake by all the tissues in the body and is therefore a measure of tissue sensitivity to insulin (DeFronzo et al. 1979). If the test includes infusion of radio- or stable-labelled glucose isotopes, it can also assess glucose turnover in the liver and skeletal muscle (Grayson et al. 2013). Recommendations and considerations for a detailed experimental set-up for testing glucose homeostasis and insulin sensitivity are given in the literature (Stumvoll et al. 2000; Ayala et al. 2010; Bowe et al. 2014; Kowalski and Bruce 2014). Beside the gold standard, the validated method of choice for experimental and clinical practice is the glucose tolerance test as it is cheap and easy to perform (Stumvoll et al. 2000; Gutch et al. 2015)

## 1.4. Mouse strains for studying obesity

For decades animal models offered a fundamental contribution to an understanding of the development of obesity (Speakman et al. 2008; Lutz and Woods 2012). Due to the high reproduction rate, relatively simple and cheap handling and a 99% similarity to the human genome mice are the model organism of choice (Moore 1999; Mouse Genome Sequencing et al. 2002; Carroll et al. 2004; Rosenthal and Brown 2007). For obesity research experiments numerous mouse strains are available. Genetically engineered mouse strains and mice with spontaneous natural mutations are valuable tools for revealing the mechanism and molecules of energy balance regulation (Kennedy et al. 2010). One prominent example is the identification of the appetite controlling hormone, leptin, which was discovered in mice which were extremely obese due to a nonsense mutation in the *ob* gene (Zhang et al. 1994). Especially the influence of a single gene upon targeted manipulation provides fundamental knowledge regarding monogenetic obesity and the mechanisms of energy balance regulation (Nilsson et al. 2012). Secondly, high-fat diet studies in mice can mimic human obesity progression from within days to months (Kennedy et al. 2010). Considering the complexity of human obesity development - which is mostly polygenetic and implicates environmental influence - it is advantageous to study inbred mouse strains showing differential susceptibility to diet-induced obesity (DIO) due to complex gene-environment interaction.

The mouse strain C57BL/6 is the preferred strain for investigation of DIO and related metabolic diseases (Montgomery et al. 2013). Depending on the sub-strain, the comparison strain, exposure time and the composition of used high-fat diet, C57BL/6 mice exhibit obesity accompanied by altered glucose tolerance, hepatic steatosis, insulin resistance and dyslipidemia (West et al. 1992; Surwit et al. 1995; Ikemoto et al. 1996; de Meijer et al. 2010; Fergusson et al. 2014). Two further mouse strains representing extremes of DIO are the SWR/J and the AKR/J strain. It is well documented that AKR/J mice are highly susceptible whereas SWR/J are resistant to DIO (West et al. 1992; Prpic et al. 2002; Hesse et al. 2010). Although quantitative trait locus mapping was performed in the 1990s, gene variants contributing to variation in DIO susceptibility have not yet been identified (West et al. 1994a; West et al. 1994b; York et al. 1997). Both mouse strains have already been characterized and compared regarding feeding patterns and dietary macronutrient preferences (Paigen 1995; West et al. 1995; Smith et al. 1999), spontaneous activity behavior (Lightfoot et al. 2004; Turner et al. 2005) and energy expenditure (Storer 1967; Hesse et al. 2010). Results provided evidence for the contribution of behavior, energy resorption and energy expenditure to differential DIO susceptibility of SWR/J and AKR/J mice and, notably, studies state that the course for response to an administered high-fat diet is set within the first few days (Hesse et al. 2010).

## 1.5. Questions, aims and scope of the study

Studying a complex polygenetic disease such as obesity in humans presents a lot of difficulties due to genetic heterogeneity and variable susceptibility to environmental factors, thus hampering the analysis of causal relationships. To take into account some degree of that complexity this work characterizes high-fat diet (HFD) feeding in mouse strains exhibiting considerable variations in diet-induced obesity (DIO) under controlled conditions.

1. *What is the impact of fat content, fat quality and feeding duration on the induction of obesity and the alteration of glucose tolerance? How do commonly used mouse strains differ in their response?* – To elucidate the importance of quality and quantity of fat and to investigate time-dependent changes in obesity development and glucose tolerance impairment mice of the well-studied C57BL/6 strain receive different HFD for varying periods of time. Depending on the results, 6 mouse strains are fed a defined HFD for a defined period.
2. *What are the proximate causes for DIO? What is mediated by accumulation of fat and what by diet itself?* – Standard protocols for comprehensive metabolic phenotyping of laboratory mice have been published; however, there is a lack of studies applying these state-of-the-art tools for quantification of the relative contribution of energy intake and expenditure to a positive energy balance. This is the first study to identify proximate causes for obesity. DIO susceptible AKR/J mice and DIO resistant SWR/J mice are first subjected to a metabolic phenotyping fed control diet to assess possible predisposing characteristics. Subsequently energy balance during the first few days of HFD feeding is assessed. HFD feeding in strains differing in DIO susceptibility permits discrimination between obesity- and diet-related alterations.
3. *How quickly do metabolic changes emerge during HFD feeding and are they driven by obesity or by diet itself? Are they reversible?* – Kinetic profiling of metabolic changes including glucose tolerance, insulin tolerance and energy expenditure is performed during HFD and refeeding control diet in DIO prone AKR/J and DIO resistant SWR/J mice.
4. *How important is the metabolic status of accumulated adipose tissue? Can an obese mouse be healthy? Does the diet affect the amount and benefit of weight loss?* – Obese AKR/J mice with the same amount of fat mass but an anabolic and catabolic status, are compared. The anabolic status of obese AKR/J mice is achieved by either control diet, or restricted HFD feeding.
5. *Is DIO resistance of SWR/J mice inherited?* – Finally, a crossbreeding experiment with AKR/J and SWR/J mice was performed to examine the heredity of susceptibility to DIO.

# 2. METHODS & MATERIAL

## 2.1. Animal experiments & housing

Animal experiments were performed with permission from the district government of Upper Bavaria (Regierung von Oberbayern, reference number AZ 55.2.-1-54-2532-116-11) and were conducted according to the German guidelines for animal care. Every three months hygienic standards were approved referring to recommendations by the Federation of European Laboratory Animal Science Associations (FELASA).

All mice were bred and maintained in the specified pathogen free mouse facility of TU Munich (TUM Small Animal Research Center Weihenstephan, Freising, Germany). Mice were housed in groups (n = 2-5) in individually ventilated cages (green line type II, long, 540 $cm^2$, Tecniplast, Germany) under controlled temperature, humidity and photoperiod conditions (22 ± 1 °C, humidity of 55 %, 12-h light/dark cycle). Cages were changed weekly. Water and chow food were available *ad libitum*. At the age of 19-21 days mice were weighed and weaned by separating female and male pups respectively from the breeding pair. Male mice only were labeled with ear tags and used for further experiments. Mice received standard chow diet (V1124-3, ssniff, Germany) until assigned to feeding experiments.

## 2.2. Diets

Chow diet is the standard diet after weaning. This plant-based diet contains agricultural byproducts like wheat, corn and oil seed products and is supplemented with minerals and vitamins. All experimental diets were purified and composed of defined nutrients (figure 5). Purified diets were designed to be as comparable as possible and to differ only in the quality and/or quantity of fat. Thus, diet-induced metabolic changes can be traced back to the influence of fat. In high-fat diets corn starch was reduced in order to increase fat. The carbohydrate free lard-based diet with 78 kJ% of fat (lHF $78^{cf}$) was purchased from SAFE diets (Augy, France), all others from Ssniff (Soest, Germany). Due to the high fat content in lHF 75 and lHF $78^{cf}$ it was not possible to produce food pellets. These diets were delivered as pastes and offered to mice in adapted bowls. Numbers in the abbreviations of the diets refer to the energy percentage of fat (table 1). Detailed manufacturer's information on diet composition can be found in the appendix.

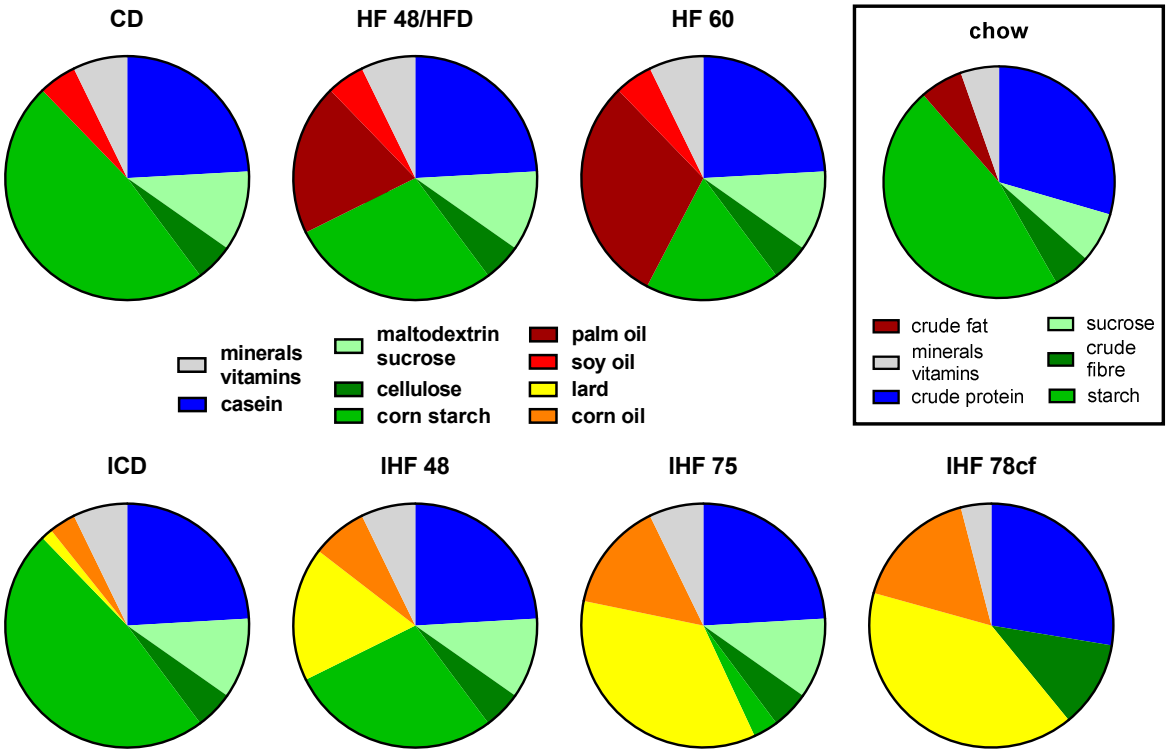


**Figure 5: Weight percentage of nutrient components in chow and experimental diets.** The upper row shows plant-fat-based diets, the lower row lard-based diets (l). Other than chow diet (shown in the box), experimental diets are purified and contain defined nutrients. Data referring to manufacturer's information; CD, control diet; HF, high-fat diet; cf, carbohydrate free.

**Table 1: Energy percentage of nutrients in experimental diets.** Data referring to manufacturer's information. CD, control diet; HF, high-fat diet; cf, carbohydrate free.

| | CD | HF 48/HFD | HF 60 | lCD | lHF 48 | lHF 75 | lHF 78$^{cf}$ |
|---|---|---|---|---|---|---|---|
| Fat [kJ%] | 13 | 48 | 61 | 13 | 48 | 75 | 78 |
| Protein [kJ%] | 23 | 18 | 16 | 23 | 18 | 14 | 22 |
| Carbohydrates [kJ%] | 64 | 34 | 23 | 64 | 34 | 11 | / |
| Metabolizable energy [kJ/g] | 15.3 | 19.7 | 21.8 | 15.3 | 19.6 | 24.9 | 24.8 |

## 2.3. Experimental settings of high-fat diet feeding

### 2.3.1. High-fat diet feeding in C57BL/6J mice

At the age of 8 weeks, all C57BL/6J (BL/6J) mice were fed control diet (CD), and depending on the experimental setting either plant- or lard-based CD, for 4 weeks in order to adapt them to the purified research diet. With 12 weeks of age mice received purified high-fat diet (HFD) or continued CD feeding. During the whole feeding period body mass and body composition were measured regularly.

Plant-based HFD feeding

Feeding intervention with plant-based HFD in BL/6J mice lasted 12 weeks starting at 12 weeks of age. To test the influence of fat quantity mice received either HFD with 48 kJ% or with 60 kJ% fat. One cohort was fed CD continuously. Oral glucose tolerance as a metabolic outcome was measured after 1, 4 and 12 weeks of HFD feeding (figure. 6).

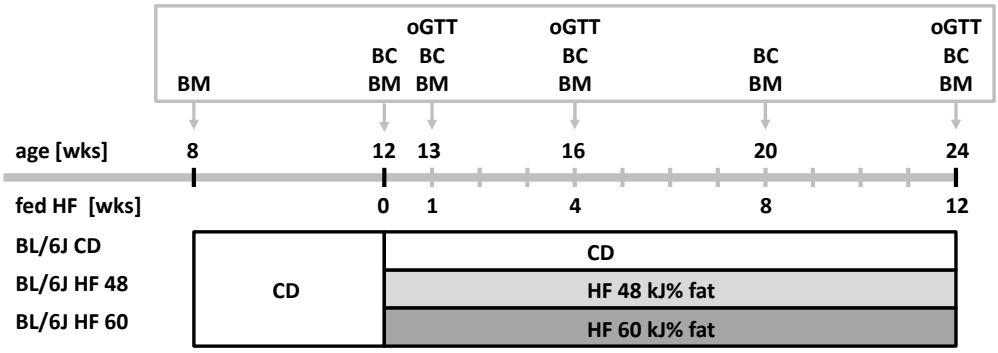


**Figure 6: Experimental setting of plant-based high-fat diet feeding in BL/6J mice.** Two high-fat diets with difference in fat quantity were used [kJ%]. Vertical arrows indicate performance of the oral glucose tolerance test (oGTT), measurement of body composition (BC) and body mass (BM); CD, control diet; HF 48, high-fat diet with 48 kJ% of fat; HF 60, high-fat diet with 60 kJ% of fat; wks, weeks.

Lard-based HFD feeding

BL/6J mice were fed with different lard-based HFD for 4 weeks (figure 7). One cohort was fed CD continuously. Diets differed in the amount of energy derived from fat. Food intake was measured every 3-4 days. Oral glucose tolerance was assessed at the end of 4 weeks of feeding intervention.

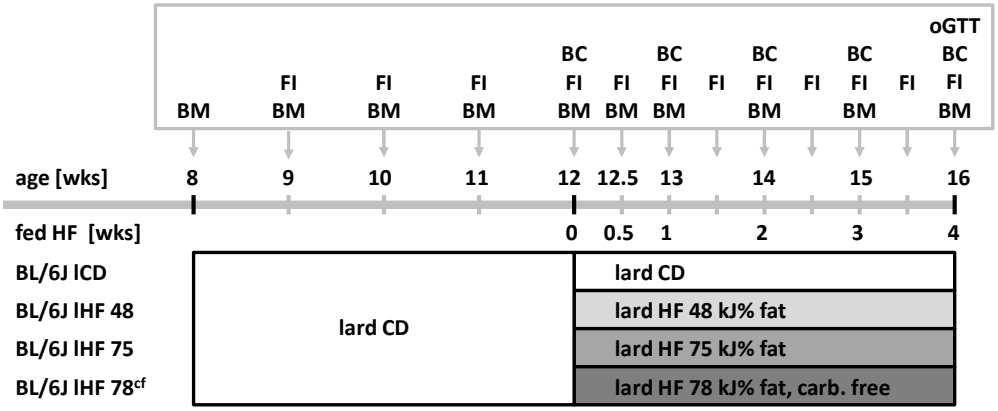


**Figure 7: Experimental setting of lard-based high-fat diet feeding in BL/6J mice.** High-fat diets differed in the quantity of fat: lCD, lard-based control diet; lHF 48, lard-based high-fat diet with 48 kJ% of fat; lHF 75, lard-based high-fat diet with 75 kJ% of fat; lHF 78$^{cf}$, lard-based high-fat diet with 78 kJ% of fat; cf, carbohydrate free. Vertical arrows indicate performance of oral glucose tolerance test (oGTT), measurement of body composition (BC), body mass (BM) and food intake (FI); wks, weeks.

### 2.3.2. High-fat diet feeding in six mouse strains

After 4 weeks of adaptation to purified diet by feeding of plant-based CD, SWR/J, AKR/J, 129sv/evS1, 129sv/evS6, BL/6N and BL/6J mice received HFD plant-based with 48 kJ% of fat for 4 weeks (figure 8). Body mass and body composition were measured at 12 weeks of age before feeding intervention, and at 16 weeks at the end of the study.

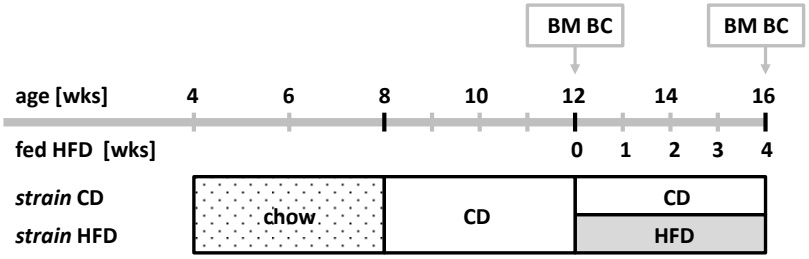


**Figure 8: Experimental setting of high-fat diet feeding in six mouse strains.** SWR/J, AKR/J, 129sv/evS1, 129sv/evS6, BL/6N and BL/6J mice were fed 4 weeks (wks) HFD or CD; CD, control diet; HFD, palm oil-based high-fat diet with 48 kJ% of fat; wks, weeks. Vertical arrows indicate measurement of body composition (BC) and body mass (BM).

### 2.3.3. High-fat diet feeding in AKR/J and SWR/J mice

For the initial AKR/J and SWR/J comparison study, mice were monitored starting at the age of 3 weeks until they were 36 weeks old. At the age of 8 weeks, all AKR/J and SWR/J mice were fed plant-based CD for 4 weeks to adapt them to a purified research diet. During this time a sub-cohort was implanted with telemetry transmitters to assess body core temperature ($T_b$). Twelve weeks old mice received HFD (plant-based, 48 kJ% of fat) for 12 weeks followed by refeeding of CD as a "recovery". One cohort was fed CD continuously. Body mass, body composition, food intake, energy expenditure, $T_b$, activity, glucose and insulin tolerance were measured regularly (figure 9A).

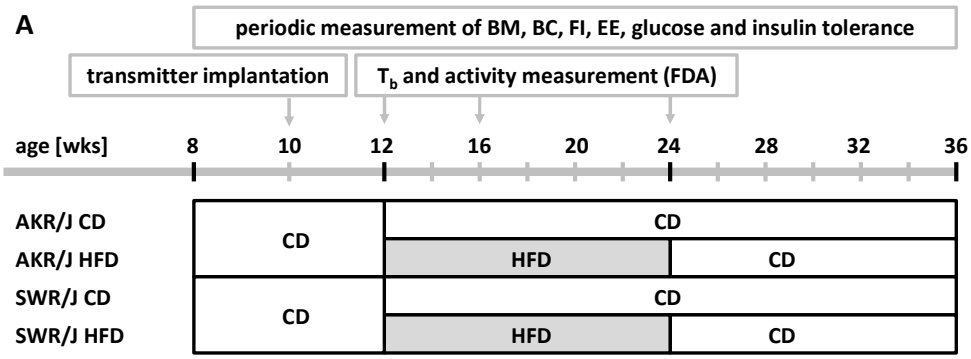

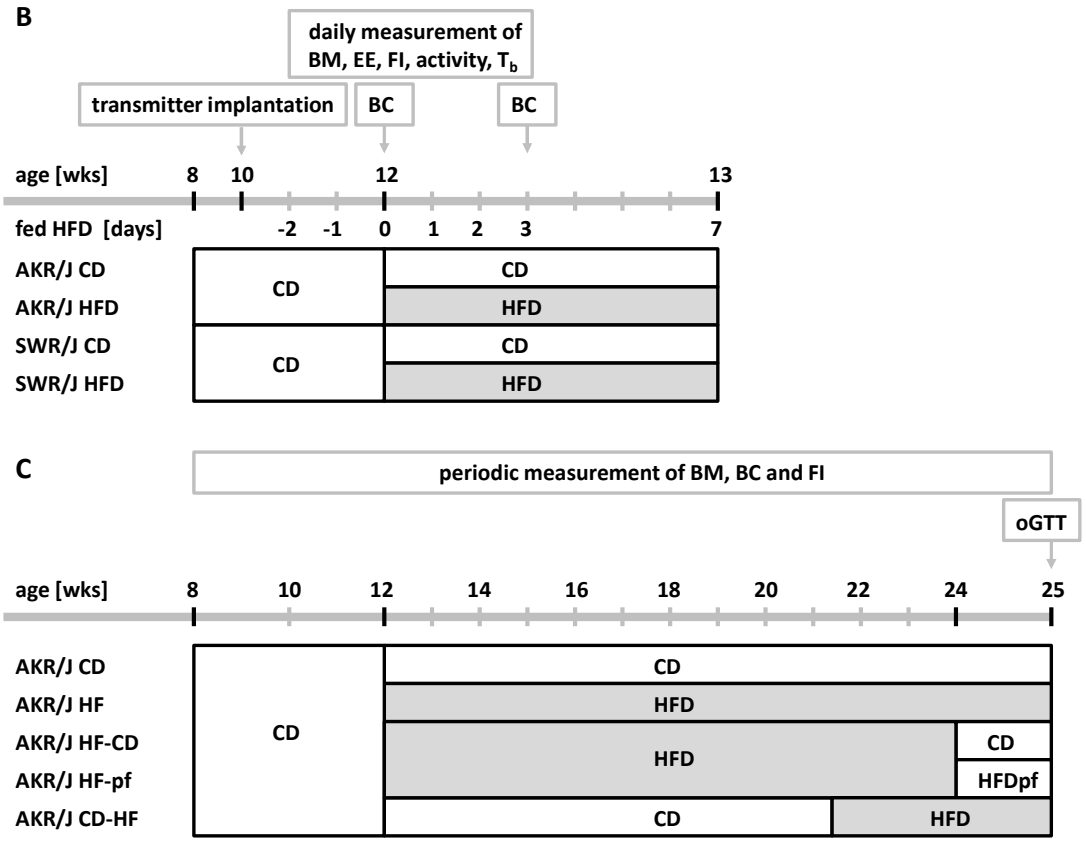


**Figure 9: Experimental setting of high-fat diet feeding in AKR/J and SWR/J mice. (A)** Initial study with 12 weeks (wks) HFD feeding in AKR/J and SWR/J mice followed by refeeding CD. **(B)** Follow-up study with focus on the first days of HFD feeding. **(C)** Follow-up study with focus on reversibility of HFD-induced alterations in AKR/J mice. Energy expenditure (EE) was measured by indirect calorimetry, food intake (FI), activity and body core temperature ($T_b$) in the feeding-drinking-activity device (FDA); CD, control diet; HFD, plant-based high-fat diet with 48 kJ% of fat; pf, pair-feeding; oGTT, oral glucose tolerance test; BC, body composition; BM, body mass.

A second setting focused on the energy balance assessment during the first days of HFD feeding. AKR/J and SWR/J mice were measured using indirect calorimetry and a feeding-drinking-activity device 2 days before and 3 days after onset of HFD feeding at the age of 12 weeks (the first 24 hours were rejected). Energy expenditure, body mass, food intake, activity and body core temperature were monitored every day. Body composition was measured immediately before and 3 days after switching diet from CD to HFD (figure 9B).

In the next study, the duration of the "recovery" refeeding phase was shortened, but extended by three cohorts for AKR/J mice. Beside the CD fed cohort (CD), and the one being re-fed CD after 12 weeks of HFD (HF-CD), one cohort was pair-fed with HFD to the HF-CD group, another cohort received HFD for 13 weeks (HF), and the third additional cohort started HFD feeding at 21-22 weeks of age (CD-HF). Oral glucose tolerance was tested at the age of 25 weeks (figure 9C).

### 2.3.4. Cross-breeding of AKR/J and SWR/J mice

To reveal heredity of diet-induced obesity (DIO), AKR/J and SWR/J mice were crossbred to generate an F1 generation. To account for possible imprinting mechanisms both possible combinations of breeding pairs were considered. The offspring of a male AKR/J and a female SWR/J mouse were named AK-SWR/J mice. Mating male SWR/J with female AKR/J resulted in SW-AKR/J mice. All mice of the F1 generation were weighted at weaning but HFD feeding was only performed in male AK-SWR/J and SW-AKR/J mice. 8 week old mice were fed plant-based CD for 4 weeks to adapt them to purified research diet. At the age of 12 weeks mice were assigned to either CD or HFD (plant-based, 48 kJ% of fat) for 4 weeks. Body mass and body composition were measured regularly and oral glucose tolerance was tested at the age of 16 weeks (figure 10).

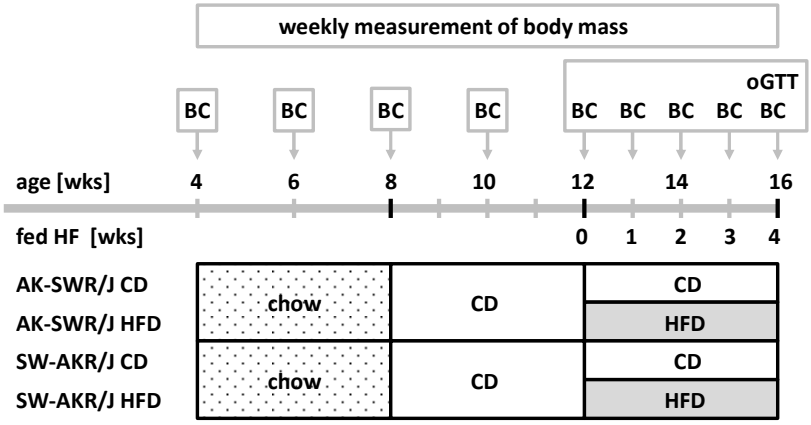


**Figure 10: Experimental setting of high-fat diet feeding in AK-SWR/J and SW-AKR/J mice.** Mice were generated by cross-breeding AKR/ and SWR/J mice. Vertical arrows indicate measurement of body composition (BC) and performance of oral glucose tolerance test (oGTT); CD, control diet; HFD, plant-based high-fat diet with 48 kJ% of fat; wks, weeks.

## 2.4. Tools for energy homeostasis assessment

### 2.4.1. Body mass and body composition

Starting at the age of 8 weeks, body mass was measured at least once weekly using a laboratory balance. Body composition was assessed by nuclear magnetic resonance (NMR) in a minispec TD-NMR analyzer (LF50H, Bruker Optics, USA). Mice with implanted transmitters were excluded from NMR analysis.

### 2.4.2. Food intake and feces collection

During feeding drinking activity (FDA) assessment food intake was measured automatically by the FDA device (2.3.7.). Furthermore, food intake was assessed during the whole mouse lifetime

when mice were group-housed and during indirect calorimetry measurement. Resultantly, the present weight of the food grid was subtracted from the weight of the last measure day. Hence, daily food intake per mouse was calculated by dividing this difference by the days elapsed since the last measure day and the number of mice in the cage.

Feces of a cohort of CD and HFD fed AKR/J and SWR/J mice, respectively, were collected when mice were 15-16 weeks old. Former group-housed mice were housed singly for one week to adapt them to the new conditions. Subsequently, mice were placed in new cages for 4 days. During this time food intake was measured and feces collected and weighed in order to calculate assimilation efficiency (2.3.4.).

### 2.4.3. Bomb (direct) calorimetry

Direct calorimetry in a bomb calorimeter (6300 Calorimeter, Parr, Germany) was used to determine the caloric value of diet and feces samples. Samples were dried at 55 °C until weight constancy was reached. Dried feces were homogenized in a refiner (Tissue Lyser II, Retsch, Germany), portioned in doses of about one gram and pressed into pellets with a press (Typ C21, Janke & Kunkel, Germany). Diet and feces pellets were weighed by an accuracy balance. Burning the pellets completely in the calorimeter under high pressure and oxygen excess leads to heat production in the bomb. The water in the insulating jacket that surrounds the bomb absorbs the resulting heat and the temperature increase ΔT is measured (figure 11). Knowing the energy equivalence value of the calorimeter, following a previous calibration with a substance of defined energy content (benzoic acid: 26.5 kJ/g), the caloric value of the burned sample can be calculated:

$$caloric\ value\ \left[\frac{J}{g}\right] = \frac{W * \Delta T}{m}$$

W = energy equivalent value of the calorimeter [J/K]

ΔT = increase in temperature [K]

m = sample weight [g]

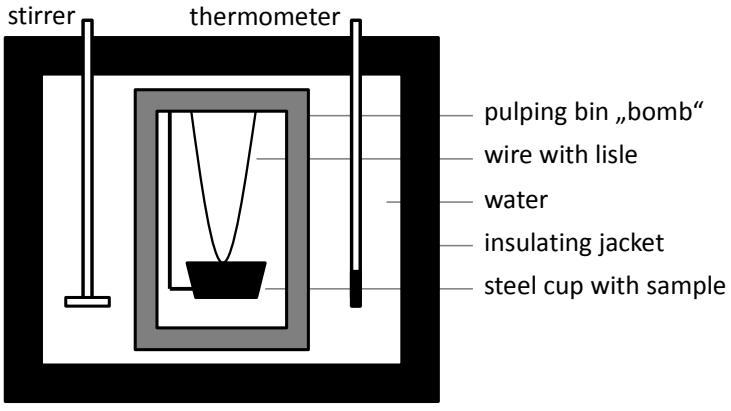


**Figure 11: Setup of a bomb calorimeter.** The sample placed in the steel cup is burned completely under high pressure and excess oxygen. Released heat is detected and translated in the caloric value of the sample.

### 2.4.4. Calculation of assimilation coefficient and metabolizable energy

The energy intake $E_{in}$ and the energy of feces $E_{fec}$ is calculated by multiplying the amount of food intake or the produced mass of feces with the respective caloric value of the sample detected by bomb calorimetry. The assimilation coefficient $EF_{ass}$ is a measure of the efficiency of extraction of energy from the diet. $E_{in}$ multiplied by $EF_{ass}$ results in assimilated energy $E_{ass}$. Metabolizable energy $E_{met}$ is described as the part of ingested energy that remains for metabolism after subtracting not utilizable energy that is excreted via urine (and breath). Two percent of energy were assumed to be dissipated by urine and breath (Street et al. 1964; Schutz 1997; Elvert et al. 2013). Consequently, $E_{met}$ is about 98% of $E_{ass}$.

$$Energy\ intake\ E_{in}\left[\frac{kJ}{d}\right] = food\ intake * caloric\ value\ of\ the\ diet$$

$$Energy\ feces\ E_{fec}\left[\frac{kJ}{d}\right] = feces * caloric\ value\ of\ feces$$

$$Assimilation\ efficiency\ EF_{ass}[\%] = 100 - \left(100 * \frac{E_{fec}}{E_{in}}\right)$$

$$Assimiltated\ energy\ E_{ass}\left[\frac{kJ}{d}\right] = E_{in} * EF_{ass}$$

$$Metabolizable\ energy\ E_{met}\left[\frac{kJ}{d}\right] = E_{ass} - caloric\ value\ of\ urine\ \cong\ E_{ass} * 0.98$$

### 2.4.5. Measurement and calculation of energy expenditure

Energy expenditure was measured by indirect calorimetry in an open respirometric system (TSE systems, Germany) by analyzing $O_2$ consumption ($\dot{V}O_2$) and $CO_2$ production ($\dot{V}CO_2$). Mice were placed individually in home cages (type II, long) especially modified for respirometry in a temperature-controlled climate chamber (TPK 600, Feutron, Germany). Air was drawn out of the cages at a constant flow rate of 0.7 l/min and fresh air sucked in under pressure. Before quantifying gas composition in $O_2$- and $CO_2$-analyzers, air had to pass a filter and was pumped through a heat sink at a flow rate of 0.55 l/min. Differences in gas content were calculated against a mouse-free reference cage with defined gas composition as internal control.

$$\dot{V}\ O_2\left[\frac{ml}{h}\right] = flow\ rate\ \left[\frac{l}{h}\right] * \Delta O_2\,[Vol\%] * 10$$

$$\dot{V}\ CO_2\left[\frac{ml}{h}\right] = flow\ rate\ \left[\frac{l}{h}\right] * \Delta CO_2\,[Vol\%] * 10$$

Every aerobic organism oxidizes nutrients to provide energy for essential and voluntary processes. In this process of conversion of chemical energy, carbon dioxide and water are produced additionally. The amount of generated energy depends on the nutrient:

*Nutrients of the diet* + $O_2$ → $CO_2 + H_2O$ + *energy*

*Glucose:* $C_6H_{12}O_6 + 6\ O_2$ → $6\ CO_2 + 6\ H_2O$ + *2864 kJ*

*Palmitic acid:* $C_{16}H_{32}O_2 + 23\ O_2 \rightarrow 16\ CO_2 + 16\ H_2O + 10042\ kJ$

The respiratory exchange ratio (RER), the quotient of carbon dioxide production and oxygen consumption, give information about the substrate used for production of energy, since it differs between nutrients:

$$RER = \frac{\dot{V}CO_2}{\dot{V}O_2} \qquad RER\ glucose = \frac{6\ CO_2}{6\ O_2} = 1 \qquad RER\ palmic\ acid = \frac{16\ CO_2}{23\ O_2} = 0.7$$

The caloric equivalent, defined as energy produced per liter of oxygen consumed, also differs between nutrients in a range of 19-21 kJ/l $O_2$. To account for the mixture of nutrient in the diet and the dynamics of different fuel oxidation, the caloric equivalent was calculated by the RER, referring to Heldmaier (Heldmaier 1975). Energy expenditure (EE) over a particular period of time is established by multiplying the caloric equivalent with oxygen consumption.

$$caloric\ equivalent\ \left[\frac{kJ}{l\ O_2}\right] = 16 + 5 * RER$$

$$energy\ expenditure\ EE\ \left[\frac{kJ}{time}\right] = caloric\ equivalent\ \left[\frac{kJ}{l\ O_2}\right] * \dot{V}\ O_2\ \left[\frac{l}{time}\right]$$

Standard measuring intervals of $\dot{V}O_2$ and $\dot{V}CO_2$ were 9 minutes. Resting metabolic rate (RMR) and maximal metabolic rate (MMR) were calculated regarding the 27 minutes (3 successive intervals) with the lowest $\dot{V}O_2$ during the day and the highest $\dot{V}O_2$ during the night, respectively. The 3 measure points were verified by the coefficient of variation-method (CV), in order to avoid outliers. The CV indicates variances between measure points and was set so as not to exceed 10 %. RER and EE were calculated for every measure interval separately and summed up or averaged depending on the desired time period, e.g. daily energy expenditure (DEE) was calculated from hourly means of EE added up to 24 h. EE during the night includes values between 5 pm and 5 am, whereas daytime was set between 5 am and 5 pm. Energy expenditure data are expressed in Watt [W] or kilojoule per time [kJ/time].

$$RMR\ [W] = caloric\ equivalent\ \left[\frac{kJ}{l\ O_2}\right] *\ minimal\ \dot{V}\ O_2\ \left[\frac{l}{27\ min}\right]$$

$$MMR\ [W] = caloric\ equivalent\ \left[\frac{kJ}{l\ O_2}\right] *\ maximal\ \dot{V}\ O_2\ \left[\frac{l}{27\ min}\right]$$

$$DEE\ [W]\ or\ \left[\frac{kJ}{24\ h}\right] = caloric\ equivalent\ \left[\frac{kJ}{l\ O_2}\right] *\ \dot{V}\ O_2\ \left[\frac{l}{24\ h}\right]$$

$$EE\ night\ [W] = caloric\ equivalent\ \left[\frac{kJ}{l\ O_2}\right] *\ \dot{V}\ O_2\ of\ 5\ pm\ to\ 5\ am\ \left[\frac{l}{12\ h}\right]$$

$$EE\ day\ [W] = caloric\ equivalent\ \left[\frac{kJ}{l\ O_2}\right] *\ \dot{V}\ O_2\ of\ 5\ am\ to\ 5\ pm\ \left[\frac{l}{12\ h}\right]$$

### 2.4.6. Surgical implantation of telemetry transmitters

For body core temperature measurement, telemetry transmitters (G2 E-Mitter, Starr Life Science Corp., USA) were implanted in 10-weeks-old AKR/J and SWR/J mice. Mice were weighed and anesthetized by combined i.p. injection of medetomidin (0.5 mg/kg Domitor®, Provet AG, Switzerland), midazolam (5 mg/kg Midazolam-ratiopharm®, Ratiopharm, Germany) and fentanyl (0.05 mg/kg Fentanyl®). After confirming anesthesia by reflex triggering, the abdomen was opened with a 6-8 mm incision and the transmitter was placed in the abdominal cavity. The peritoneum and the skin were closed with 3-4 single button sutures of absorbable surgery thread, respectively. The antagonists atipamezole (2.5 mg/kg Antisedan®, Pfizer GmbH, USA), flumazenil (0.5 mg/kg Anexate®, Hoffmann-La Roche, Switzerland) and naloxone (1.2 mg/kg Naloxon®, Ratiopharm, Germany) were injected subcutaneously to terminate anesthesia. Additionally mice received 10 g/kg carprofenum (Rimadyl®, Zoetis Schweiz GmbH, Switzerland). To aid recovery, mice were housed singly at 30 °C and received water soaked CD mash. After 4-5 days mice were reunited in groups under normal housing conditions.

### 2.4.7. Food intake, activity, climbing and body core temperature monitoring

Food intake, activity and $T_b$ were recorded in individually housed mice using an automated monitoring system ("FDA" TSE LabMaster Home Cage Acitivity, type III cages with wire lid, 820 $cm^2$, TSE systems, Germany). Every cage was surrounded by two infrared light beam frames (ActiMot2, TSE systems, Germany), which registered activity in three dimensions. Food baskets were connected to balances which report weight changes to a computer. A receiver plate (ER4000 Energizer/Receiver, Starr Life Science Corp., USA) underneath the cage records body core temperature ($T_b$) signals from the implanted transmitter. All parameters were measured at 5-minute intervals. Additionally, climbing activity (on the grid of the cage lid) by mice with implanted transmitters could be detected, due to periods of interrupted $T_b$ recordings. $T_b$ signal interruption occurred because thee height between cage lid and receiver was greater than the telemetric transmission distance of the transmitters.

### 2.4.8. Adjustment of energy balance parameters

In some settings, metabolizable energy and energy expenditure are compared between mice differing in body mass and body composition. It is known that the energy balance parameter partly depends on body weight and composition. To account for this aspect und for better visualization of possible correlations, energy balance parameters such as RMR, DEE, MMR and energy intake were plotted against body mass, lean mass and fat mass, respectively. In parallel, for statistical analysis, and to find one or more suitable independent variables for adjustment, different linear regression models were calculated by software S+. The best model was chosen (significant correlation and highest $R^2$ value) and the regression formula was used to calculate

the residuals (difference between predicted and measured value). Adding the residual to a defined mean value (e.g. mean of predicted DEE of all mice) resulted in an adjusted energy parameter value.

## 2.5. Assessment of glucose homeostasis

### 2.5.1. Oral glucose tolerance test

To test the reaction in response to an orally administered glucose bolus, oral glucose tolerance tests (oGTT) were performed, based on literature recommendations (Andrikopoulos et al. 2008; Ayala et al. 2010). 6 hours prior to the test, mice were fasted (8 am – 2 pm), single-housed, weighed and body composition was determined. The amount of glucose was calculated with 2.8 mg per g lean mass. This factor was determined in a previous cohort and corresponds to the amount of glucose calculated as 2 mg per g body mass in CD fed, 12 week-old male mice of different strains (BL/6J, BL/6N, sv129evS1, AKR/J, SWR/J, n = 8-12). Before gavage of glucose (Glucose 40 % B.Braun Melsungen AG, Germany), the tail tip of each mouse was scratched superficially with a scalpel to obtain a blood droplet. Blood glucose was measured immediately pre- (basal blood glucose) and at 15, 30, 60 and 120 minutes post-glucose administration, using a commercial hand-held glucometer (Freestyle Lite, Abbott Diabetes Care, USA). To quantify the tolerance to glucose, the total area under the curve (tAUC) of blood glucose levels was calculated. Therefore, the trapezoidal areas between blood glucose measure points were summed up (figure 12). Additionally, the incremental area under the curve (iAUC) was determined, defined as AUC over basal glucose levels. Since this quantification ignores differences in fasting glycemia it gives exclusive information about clearance of glucose in the blood (uptake in the tissue). Generally, a high AUC indicates lower/slower glucose uptake into tissue.

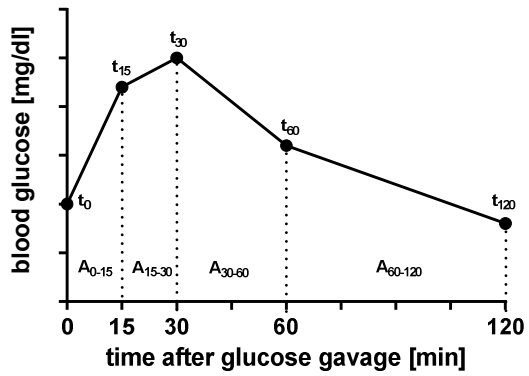


$$A_{0\text{-}15} = 0.5 * 15 * (t_0 + t_{15})$$

$$A_{15\text{-}30} = 0.5 * 15 * (t_{15} + t_{30})$$

$$A_{30\text{-}60} = 0.5 * 30 * (t_{30} + t_{60})$$

$$A_{60\text{-}120} = 0.5 * 60 * (t_{60} + t_{120})$$

$$tAUC = A_{0\text{-}15} + A_{15\text{-}30} + A_{30\text{-}60} + A_{60\text{-}120}$$

$$iAUC = tAUC - (t_0 * 120)$$

**Figure 12: Area under the curve calculation of an oral glucose tolerance test.** Blood glucose levels were measured 0 ($t_0$), 15 ($t_{15}$), 30 ($t_{30}$), 60 ($t_{60}$) and 120 ($t_{120}$) minutes after glucose gavage and total area under the curve (tAUC) and incremental area under the curve (iAUC) were calculated.

### 2.5.2. Oral pyruvate tolerance test

Oral pyruvate tolerance tests (oPTT) were used to assess indirectly hepatic gluconeogenesis. The procedure was similar to the oGTT (2.4.1.). After fasting for 6 hours, singly housed mice received an orally administered pyruvate bolus (pyruvate stock solution 400 mg/ml, Sigma-Aldrich, USA). The recommended concentration of 2 g/kg body mass was converted into 2.8 g pyruvate/g lean mass. Blood glucose levels were measured after 0, 15, 30, 60 and 120 minutes. Total area under the curve and incremental area under the curve were calculated by the trapezoidal method.

### 2.5.3. Intraperitoneal insulin tolerance test

The intraperitoneal insulin tolerance test (ipITT) allows measurement of insulin sensitivity by monitoring glucose clearance in the blood after insulin injection. In the morning of the testing day, mice were singly-housed, weighed and body composition was determined. After 5-6 hours fasting basal blood glucose was measured at the tail tip by means of a superficial incision. Insulin concentration was calculated to lean mass (0.75 U/kg lean mass, insulin stock solution 275 U/ml, Sigma-Aldrich, USA) as recommended by Ayala et al (Ayala et al. 2010). Insulin was injected intraperitoneally and blood glucose was measured after 15, 30, 60 and 120 minutes. A syringe with glucose solution was kept ready to rescue mice showing hypoglycemia. Blood glucose data were expressed as percentage to basal blood glucose levels. Total area under the curve was calculated by the trapezoidal method (figure 13). Generally, a high AUC indicates impaired insulin sensitivity.

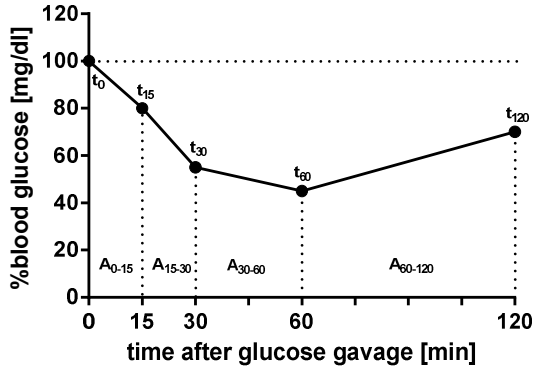


$$A_{0\text{-}15} = 0.5 * 15 * (t_0 + t_{15})$$

$$A_{15\text{-}30} = 0.5 * 15 * (t_{15} + t_{30})$$

$$A_{30\text{-}60} = 0.5 * 30 * (t_{30} + t_{60})$$

$$A_{60\text{-}120} = 0.5 * 60 * (t_{60} + t_{120})$$

$$\%AUC = A_{0\text{-}15} + A_{15\text{-}30} + A_{30\text{-}60} + A_{60\text{-}120}$$

**Figure 13: Area under the curve calculation of an intraperitoneal insulin tolerance test.** Blood glucose levels were measured 0 ($t_0$), 15 ($t_{15}$), 30 ($t_{30}$), 60 ($t_{60}$) and 120 ($t_{120}$) minutes after insulin injection and expressed as % to fasting blood glucose levels. %AUC was calculated summing up trapezoids $A_{0\text{-}15}$ to $A_{60\text{-}120}$.

### 2.5.4. Basal glucose levels

Preparation prior to testing of glucose, pyruvate and insulin tolerance tests was equal. Former group-housed mice were separated and fasted for six hours. Thus, for basal glucose analysis, fasting glucose levels of all 3 set-ups were merged for the corresponding time of feeding intervention.

## 2.6. Post mortem analysis

### 2.6.1. Tissue and plasma collection

Fasted mice (5 – 7 hours) were killed by diaphragm incision after carbon dioxide euthanization. Cardiac blood of the right ventricle was collected in heparin-coated tubes and centrifuged immediately for 10 min at 2000 g. Plasma (supernatant) was stored in aliquots of 20 µl at -80 °C. Furthermore, the following organs and tissues were dissected and weighed: liver, kidneys, spleen, epididymal white adipose tissue (eWAT), retroperitoneal perirenal WAT (rWAT), subcutaneous WAT (sWAT) and intrascapular brown adipose tissue (iBAT) depots. A small piece of the tip of the great liver lobe was fixed in formalin (4 % paraformealdehyde in PBS). The remaining great liver lobe and all other organs and tissues were snap-frozen at -80 °C.

### 2.6.2. Analysis of plasma lipids

Cholesterol (CHOL), high-density lipoprotein cholesterol (HDL), and triglycerides (TRIG) were measured on reagent discs (piccolo Lipid Panel plus, Abaxis, USA) in a fully automated blood chemistry analyzer (Piccolo Xpress, Abaxis, USA). Plasma was diluted (1:2) in dd$H_2O$ and 100 µl were pipetted in the access port of the reagent disc. Plasma was split in compartments where different kinds of chemical reactions for determination of blood parameters were conducted once the reagent disc was inserted into the analyzer.

### 2.6.3. Determination of insulin and leptin

Insulin and leptin were determined by enzyme-linked immunosorbent assay (ELISA). For both parameters a so-called “sandwich ELISA” was used. The principle of this method is to capture the target protein between a solid based antibody and a second antibody that is conjugated with a peroxidase enzyme. Peroxidase catalyzes the oxidation of the added chromogenic substrate TMB (3,3’,5,5’-tetramethylbenzidine) leading to a color change in the reaction solution. The reaction is stopped by sulfuric acid turning the solution yellowish. This colorimetric endpoint is quantified spectrophotometrically at 450 nm (figure 14)

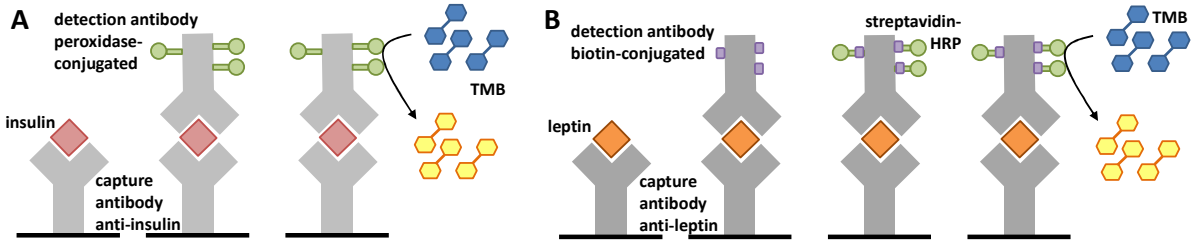


**Figure 14: Schematic test principle of a sandwich ELISA.** The target protein is captured between two antibodies. One antibody is conjugated with peroxidase which mediates a detectable color change reaction of a chromogenic substrate. **(A)** Insulin ELISA with a peroxidase-conjugated detection antibody. **(B)** Leptin ELISA with a biotin-conjugated detection antibody to which streptavidin-HRP binds in a second step. TMB, 3,3',5,5'-tetramethylbenzidine.

For insulin detection, plasma from HFD fed mice was diluted 1:2 in dd$H_2O$, while plasma from all other diet groups was used un-diluted. The assay was performed as referring to manufacturer's instructions (Mercodia, Sweden). Briefly, 25 µl of calibrators and plasma samples were pipetted in duplicates to anti-mouse insulin antibody coated wells. 100 µl of enzyme conjugation solution containing peroxidase-conjugated anti-mouse insulin antibodies were added and incubated for 2 hours (700 rpm, at room temperature (RT). After washing 6 times with 350 µl wash buffer solution, 200 µl substrate TMB were added to each well, followed by 15 min incubation (RT). The reaction was stopped by adding 50 µl acid stop solution. Absorbance at 450 nm was measured. Insulin concentrations of plasma samples were calculated by cubic spline regression with the absorbance results of calibrators.

Leptin ELISA was conducted to manufacturer's instructions (BioVendor, Germany). After diluting the plasma with dilution buffer in a relation of 1:20, 100 µl of the plasma dilution, standard and controls in duplicates were incubated for 1 hour (300 rpm, RT) in anti-mouse leptin antibody coated wells. Samples were washed 3 times. Then 100 µl biotin labelled anti-mouse leptin antibody were added. After incubation (1 h, 300 rpm, RT) and washing (3 times) 100 µl of streptavidin-HRP conjugate were pipetted to the samples, followed by 30 min incubation (300 rpm, RT). Samples were washed 3 times. 100 µl substrate solution containing TMB were added and incubated for 10 min (RT). Pipetting 100 µl stop solution to the samples ended the reaction and absorbance of the yellowish product could be detected at 450 nm. Leptin concentrations of plasma samples were calculated by a standard curve.

### 2.6.4. Measurement of cholesterol and triglycerides in the liver

TRIG and CHOL in the liver were measured using an enzymatic calorimetric endpoint kit (Triglycerides liquicolor and Cholesterol liquicolor, human, Germany). First, 40-60 mg of liver tissue was powdered in liquid nitrogen and weighed exactly. For the extraction of lipids 800 µl chloroform, 400 µl methanol and 100 µl $H_2O$ were added and vortexed, respectively. By centrifugation for 5 min (1200 rpm, 10 °C) the sample separated into 3 phases. The bottom phase containing the lipids was carefully collected and evaporated in the speed vac (SPD111V SpeedVac, Thermo Fisher Scientific USA). Lipids were re-suspended by adding 50 µl pure

ethanol and heating the sample for 5 min to 40 °C (400 rpm). Following the manufacturer's protocol, 3 µl of liver lipid extract were added to 250 µl TRIG reagent and to 250 µl CHOL reagent in duplicates, respectively. For TRIG and CHOL quantification, 3 µl of a TRIG standard and of a CHOL standard were pipetted in the corresponding 250 µl reagent. After 30 min, incubation absorbance (540 nm) was detected in a microplate reader (Varioskan™ Flash Multimode Reader, Thermo Fisher Scientific, USA) and TRIG and CHOL concentrations were calculated referring to the following formula:

$$C\ \left[\frac{mg}{dl}\right] = 200 * \frac{\Delta\ absorbance\ of\ sample}{\Delta\ absorbance\ of\ standard}$$

### 2.6.5. Histology of hepatic tissue

Sample preparation

Pieces of the great liver lobe were fixed in formalin (4 % paraformaldehyde in PBS with 0.0024 % picric acid) for 2-7 days. After fixation, samples were dehydrated with increasing ethanol concentrations up to xylol in a tissue processor (TP1020, Leica Biosystems, Germany) over night and enclosed in paraplast plus. Subsequently, paraffin-embedding was conducted in a tissue embedding system (EG 1150H, Leica Biosystems, Germany). Embedded liver samples were cut in 5 µm slices with a microtome (RM2255, Leica Biosystems, Germany), stretched in a water bath (45 °C), mounted on microscope slides and dried in an incubator (37 °C) for at least 12 hours. Dewaxing of slides in decreasing ethanol concentrations and staining for hematoxylin and eosin was performed automatically in a tissue multi-stainer (ST5020, Leica Biosystems, Germany). Lastly, stained slices on the slides were coated with a mounting medium (Histokitt, Carl Roth, Germany) and protected by a cover glass.

Histological analysis

The grade of hepatic steatosis was analyzed under a light microscope (DMI400B, Leica Microsystems, Germany) using a scoring system that includes lipid infiltration morphology and the amount of affected tissue (figure 15). All slides were blinded and rated by three investigators independently.

The first part of the classification evaluated the morphology of hepatocytes in a 200x magnification. In more detail, the amount and storage form (microvesicles or droplets) of infiltrated lipids in hepatocytes is evaluated: grade 0 = no lipid infiltration visible, grade 1 = small and sparse microvesicular infiltration, grade 2 = small but widespread microvesicular infiltration, grade 3 = besides small microvesicular infiltration, also scattered lipid droplets, grade 4 = predominantly lipid droplets. The second part of the classification of steatosis accounts for the amount and distribution of any kind of lipid infiltration over the whole tissue. A

50x magnitude is used to quantify the percentage of affected tissue: grade 0 = less than 5 % of tissue affected from lipid infiltration, grade 1 = 5-33 % affected, grade 2 = 33-66 % affected and grade 3 = more than 66 % affected tissue.

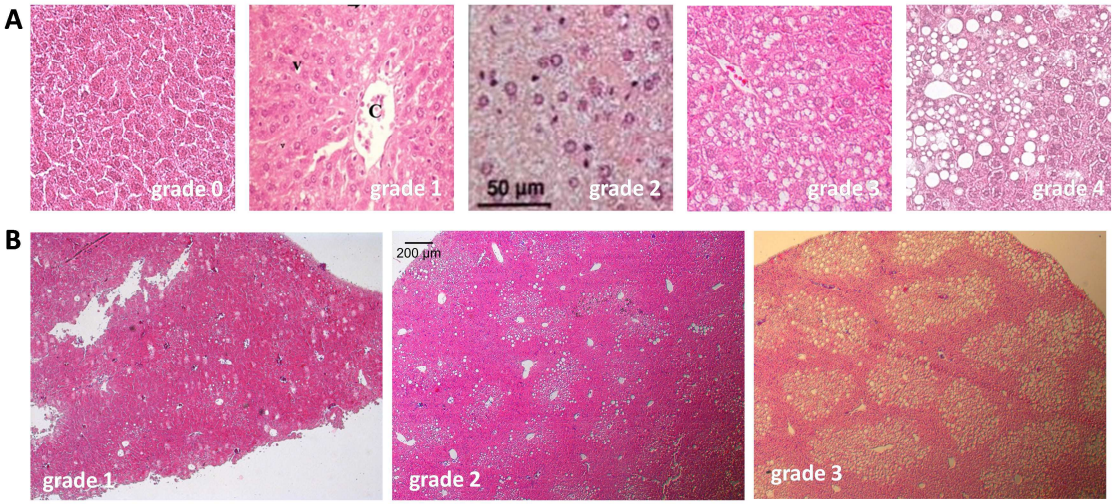


**Figure 15: Classification of hepatic steatosis. (A)** Morphology of lipid infiltrated hepatocytes was rated with grade 0-4, 200x magnitude. **(B)** Amount of affected cells was staged with grade 0-3, 50x magnitude.

## 2.7. Gene expression analysis

### 2.7.1. RNA isolation

Deep-frozen liver and eWAT were ground in liquid nitrogen. RNA was isolated from tissue powder by phenolic extraction and purification with a commercial minicolumn system (SV Total RNA Isolation System, Promega, USA). For liver mRNA isolation, 30 mg frozen and powdered tissue were added to 800 µl phenol containing TRIsure (Bioline, UK). To isolate mRNA from eWAT, 100 µg (frozen and powdered) tissue and 1000 µl TRIsure were used. In both cases the mixture was directly homogenized with a dispersing instrument (Ultra-Turrax D-1, Miccra GmbH, Germany) for 20 sec and incubated for 5 min (RT). For lipid-rich samples, an additional centrifugation step is recommended (5 min, 2500 g, 4 °C). The bottom phase under the fat layer of eWAT samples and the homogenate of liver samples are transferred to 200 µl chloroform, respectively. After intensely shaking, short incubation (2 min, RT) and centrifugation (15 min, 12000 g, 4 °C), the samples separated into three phases. The upper, clear phase was added to 500 µl EtOH (75 % in DEPC treated $H_2O$) and mixed well. Samples were transferred to spin columns of the RNA isolation kit and processed referring to the manufacturer's protocol. After attaching RNA to the columns, degradation of genomic DNA by DNase and washing with EtOH containing buffer, RNA was eluted in 50 µl nuclease-free water.

RNA concentration was measured spectrophotometrically at 260 nm in duplicates with a plate reader (Infinite® 200 PRO NanoQuant, Tecan Group Ltd, Switzerland).

### 2.7.2. RNA integrity

Integrity of RNA was determined by visualizing ribosomal RNA (rRNA) on an agarose-gel. 2 µg of RNA were mixed with nuclease-free water to a final volume of 10 µl. After adding 2 µl 6x loading buffer (Carl Roth, Germany) the mixture was incubated for 10 min at 65 °C and then cooled on ice. The gel contained 1 % agarose (Carl Roth, Germany) in 1x TAE buffer and a dye RNA stain (Roti®-Safe, 5 µl/100 ml). Samples were loaded on the gel, the electrophoresis chamber was filled with 1x TAE running buffer and the system was connected to 110 V. The electrophoretic separation revealed two clear bands (18s rRNA and 28s rRNA) which can be visualized under UV-light due to interaction with the dye.

*Buffer composition:*

TAE buffer (50x stock): 2 M TrisBase, 0.3 M acetic acid, 50 µM EDTA

6x loading dye: 10 mM Tris-HCl (pH 7.6), 60 mM EDTA, 0.2 % OrangeG, 60 % glycerol

### 2.7.3. RNA sequencing and data processing

RNA of epididymal white adipose tissue was isolated and integrity was assured. Transcriptome next generation sequencing (RNA-Seq) was performed on the Illumina HiSeq 2000 platform (Illumina, San Diego, CA, USA). TruSeq RNA Sample Prep kit v2 was used to generate RNA-Seq libraries. Up to 7 libraries were pooled per lane and sequenced 50 nt single-sided (plus barcode) using TruSeq SBS kit v3-HS, resulting in a depth of at least 20 million reads per sample.

Reads were mapped to the mouse genome (Genomatix Mining station; Genomatix, Munich, Germany) using the library version NCBI build 37 and ElDorado Version 08-2011 (seed mapping type 'deep', 92 % minimum alignment quality). Only unique hits were included in differential expression analysis. Two groups were compared using Genomatix software DESeq 1.10.1 and edgeR 3.0.4 algorithms were applied. The 'treated group' versus 'control group' was upregulated when fold change of log2 was > 1 (fold change of > 2.72). Downregulation was indicated at fold change log2 < -1 (fold change of < 0.37). Threshold of p-value was set to 0.05 with the use of a multiple testing correction. For further analysis of transcription data, different criteria were defined for the number of total reads per sample, total reads per group, p-value between groups, fold change between groups and coefficient of variation within one group.

### 2.7.4. cDNA synthesis

RNA was transcribed to complementary deoxyribonucleic acid (cDNA) by viral enzyme reverse transcriptase, using the commercial QuantiTect® Reverse Transcription kit (Qiagen, Germany). 500 ng template RNA were used for reaction, synthesis steps were performed according to the

manufacturer's protocol with adapted volumes to an end-volume of 10 µl. Briefly, genomic DNA was eliminated by a reaction mix that was added to the template RNA and incubated for 2 min at 42 °C. Then a combination of reverse transcriptase, oligonucleotides and random hexamer primer mix was transferred to RNA sample resulting in cDNA transcription during two incubation steps (15 min at 42 °C, 3 min at 95 °C).

### 2.7.5. Quantitative polymerase chain reaction

Measurement of expression of genes of interest was performed by quantitative real-time PCR (qPCR). This method extends the traditional PCR by quantifying target genes using a sensitive optical detection technology. Thereby, SybrGreen intercalates into dsDNA, leading to a photometrically detectable fluorescent signal. With ongoing amplification of DNA templates during every cycle, the fluorometric signal increases until it exceeds background fluorescence (= cycle threshold, Ct-value). The Ct-value gives information about the relative amount of target template in the cDNA when compared to a standard curve. A standard curve was generated for all cDNA samples pooled and diluted $2^n$ in 8 steps. To correct for inter-individual differences, the expression of the gene of interest was normalized to the abundance of two housekeeping genes. Reaction mixture preparation with total volume of 12.5 µl and temperature program are given in table 2. Primer sequences were chosen to generate specific PCR products with up to 250 bp and were validated by in silico PCR (http://genome.ucsc.edu/) (table 3). Quantitative PCR was carried out in a 384-well format and analyzed in in the LightCycler® 480 Instrument II (Roche, Switzerland). Samples for the generation of the standard were measured in duplicates, cDNA samples in triplicates. At the end of the program a melting curve was generated to assure the quality of amplified PCR products and to identify non-specific reaction products.

**Table 2: Quantitative PCR reaction mixture and temperature program.**

| Component | Volume per reaction | Step | Temperature | Time |
|---|---|---|---|---|
| cDNA (1:20 diltution) | 1.00 µl | Denaturation | 95 °C | 420 sec |
| Forward primer (5 nM) | 1.25 µl | Cycle (45x) | 97 °C | 10 sec |
| Reverse primer (5 nM) | 1.25 µl | | 53 °C | 15 sec |
| SensiMix (2x)* | 6.75 µl | | 72 °C | 20 sec |
| Nuclease-free $H_2O$ | 2.25 µl | Melting curve | 60-95 °C | continous |

* SensiMix SYBR No-ROX (Bioline, UK) containing SybrGreen

**Table 3: Primer for qPCR.** All primers were produced by Eurofins MWG Operon, Germany: Fbp (fructose-bisphosphate aldolase B), G6p (glucose-6-phosphatase), housekeeping genes Hprt (hypoxanthine-guanine phosphoribosyl transferase) and Hmbs (hydroxymethylbilane synthase), Insr (insulin receptor), Pck1 (phosphoenolpyruvate carboxykinase 1), Slc2a2 (glucose transporter 2), Slc2a4 (glucose transporter 4), Socs3 (suppressor of cytokine signaling 3).

| Target mRNA | Primer forward | Primer reverse |
|---|---|---|
| Fbp | TCCCTATTGTTGAGCCAGAG | GCCAGGACCTTCTCAGAAAC |
| G6p | CGACTCGCTATCTCCAAGTGA | GTTGAACCAGTCTCCGACCA |
| Hmbs | ACTCTGCTTCGCTGCATTG | AGTTGCCCATCTTTCATCACTG |

| | | |
|---|---|---|
| Hprt | TCAGTCAACGGGGGACATAAA | GGGGCTGTACTGCTTAACCAG |
| Insr | ATCAGAGTGAGTATGACGACTCGG | TCCTGACTTGTGGGCACAATGGTA |
| Pck1 | GTGCCTGTGGGAAGACTAAC | TTGATAGCCCTTAAGTTGCC |
| Slc2a2 | TCAGAAGACAAGATCACCGGA | GCTGGTGTGACTGTAAGTGGG |
| Slc2a4 | GTAACTTCATTGTCGGCATGG | AGCTGAGATCTGGTCAAACG |
| Socs3 | GGGTGGCAAAGAAAAGGAG | GTTGAGCGTCAAGACCCAGT |

## 2.8. Statistics

Data were analyzed using a statistical software package (Excel 2010, Microsoft, USA; SigmaPlot 12.0, Systat Software GmbH, Germany; GraphPad Prism 6, GraphPad Software Inc., USA). Two-sided student's t-test was used for comparisons of one variable between two groups. To test for differences between more than two groups, one-way ANOVA was applied. Two-way (repeated measurement) ANOVA was performed to compare dependent variables within and between two independent variables followed by appropriate post-hoc tests. Significance was approved when p-values of the respective tests were less than 0.05. Analysis of covariance (ANCOVA) was used to adjust dependent variables for independent variables. Therefore, linear regression models to identify covariates and calculations of predicted values of dependent variables referring to regression function were performed using S+ software (Spotfire S+, TIBCO Software Inc., USA). Data in graphs and tables are presented as mean values ± standard deviation. Statistical significance is indicated with asterisks ($p< 0.05$(*), $p< 0.01$(**), or $p< 0.001$(***)), or by using different letters. Graphs were generated with SigmaPlot and GraphPad.

# 3. RESULTS

## 3.1. High-fat diet feeding with different diets and mouse strains

First high-fat diet (HFD) feeding studies addressed the question of whether the degree of diet-induced obesity is dependent on quantity and quality of fat as well as on the duration of feeding intervention. After defining a suitable high-fat diet and feeding period in BL/6J mice, different mouse strains and their response to HFD feeding were investigated.

### 3.1.1. Plant-based high-fat diet feeding in BL/6J mice

In the first setting 12 week-old BL/6J mice were fed palm-based HFD with two different quantities of palm oil for 12 weeks. Within this intervention body composition and oral glucose tolerance were measured regularly to monitor the development over time and to test for effect differences between medium HFD (HF 48, 48 kJ% fat) and high HFD (HF 60, 60 kJ% fat).

The mice did not differ in body, lean and fat mass at the beginning of feeding. Independent of fat quantity, HFD led to a clear increase in body mass due to a gain in fat mass (figure 16A, C). After 1 week, the body mass of HF 60 fed mice was significantly higher than the body mass of control diet (CD) fed mice, whereas the difference between CD fed mice and HF 48 fed mice occurred after 4 weeks. With ongoing feeding, mice on both high-fat diets gained body mass similarly and continuously. Over the entire feeding period, mice fed HF 60 had more lean mass than control diet fed mice (figure 16B). HF 48 fed mice showed an intermediate lean mass development. Fat mass increased significantly with both high-fat diets compared to CD. But after 12 weeks, HF 48 fed mice reached higher a fat mass than HF 60 fed mice.

Summing up, both high-fat diets induced obesity in a time-dependent manner. However, there was no dose-dependent effect regarding fat. HF 60 led to a lean mass increase whereas HF 48 fed mice showed the highest fat mass after 12 weeks of feeding. More fat in the diet did not lead to more body fat accumulation.

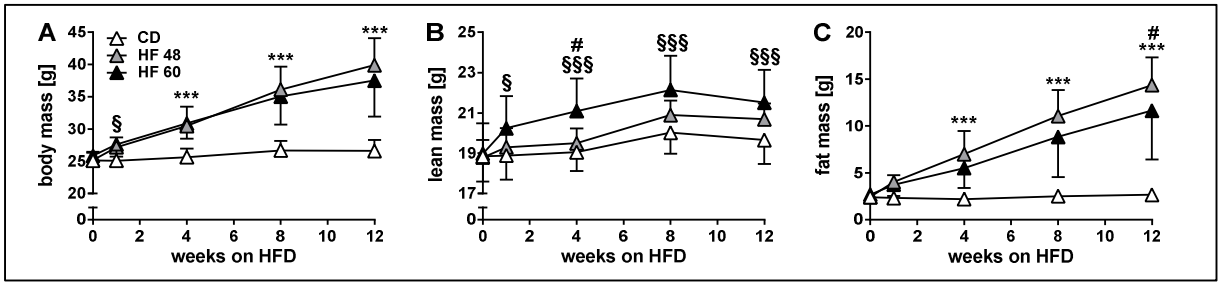


**Figure 16: Body mass and body composition during 12 weeks high-fat diet feeding in BL/6J mice. (A)** Body mass, **(B)** lean mass and **(C)** fat mass development over 12 weeks in BL/6J mice fed control diet (CD, n=18), high-fat diet with 48 kJ% fat (HF 48, n=8) or high-fat diet with 60 kJ% fat (HF 60, n=12). Two-Way ANOVA (diet, time) with repeated measurements reveals differences between diet groups: ***p < 0.001 CD vs. both HF diets; § p < 0.05 CD vs. HF 60; §§§ p < 0.001 CD vs. HF 60; # p < 0.05 HF 48 vs. HF 60.

Oral glucose tolerance was tested after 1, 4 and 12 weeks of high-fat diet feeding. After 6 hours fasting and before administration of glucose, basal blood glucose levels were measured. This parameter did not differ between diet groups after 1 week of intervention (figure 17D). Furthermore, glucose bolus led to a similar increase of blood glucose levels in all groups within the first 15 minutes after glucose gavage (figure 17A). Glucose clearance after 30 minutes was quicker in CD fed mice than in HFD fed mice. The last two measure points after 1 and 2 hours remained higher in mice on HF 48. After 4 weeks of high-fat feeding, at all 5 measure points blood glucose levels were higher in HF 48 fed mice than in CD mice, whereas HF 60 only caused higher blood glucose levels 30 minutes after glucose administration, compared to CD fed mice (figure 17B). The last oral glucose tolerance test after 12 weeks of HFD feeding revealed a similar blood glucose course in both high-fat diets, with partly significant elevated levels compared to CD fed mice (figure 17C).

As a quantifiable measure of oral glucose tolerance, total (tAUC) and the incremental (iAUC) areas under the blood glucose curves were calculated (figure 17E, F). After 1 week, tAUC and iAUC were significantly increased in HF 48 fed mice, compared to control diet and HF 60 fed mice. The difference of tAUC in HF 48 fed mice to the other two diet groups even increased after 4 weeks of intervention. After 12 weeks, HF 48 and HF 60 fed mice showed comparable tAUCs, which were significantly higher than tAUC of control mice.

Consequently, high-fat diet-induced impairment of glucose tolerance seemed neither to be time- nor fat quantity-dependent.

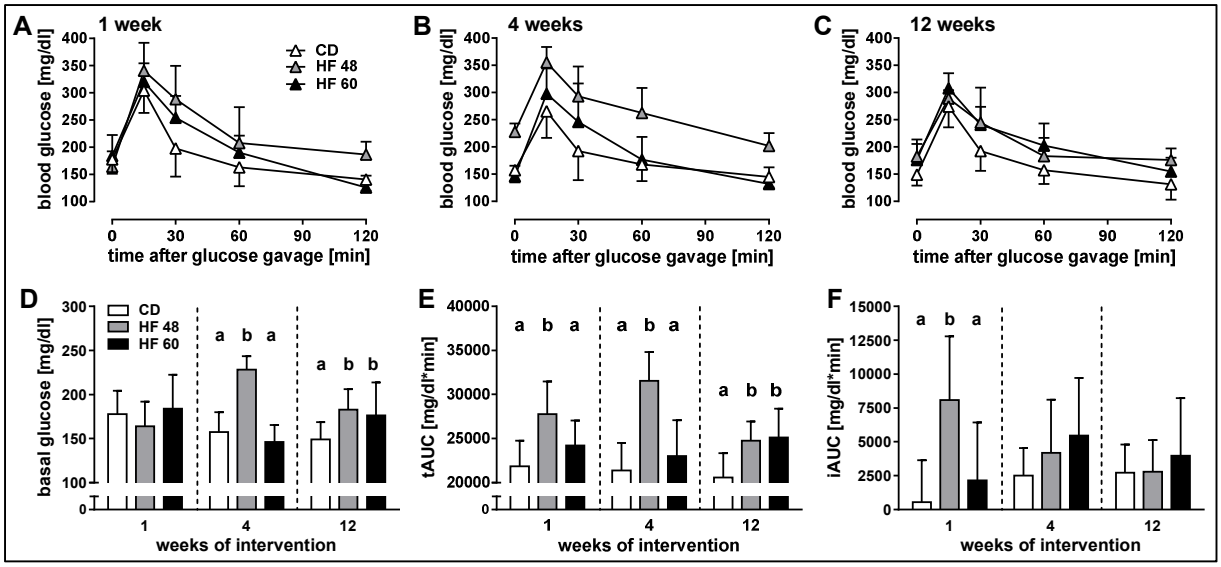


**Figure 17: Glucose tolerance and basal blood glucose during 12 weeks of high-fat diet feeding in BL/6J mice.** Blood glucose curves in response to a glucose gavage (2.8 g glucose/kg lean mass) after **(A)** 1 week, **(B)** 4 weeks and **(C)** 12 weeks high-fat diet feeding. For statistics see appendix. Prior to glucose administration **(D)** basal glucose tolerance was measured. To quantify glucose tolerance **(E)** total (tAUC) and **(F)** incremental (iAUC) areas under the curve were calculated. Different letters indicate significant differences referring to Two-Way ANOVA (time, diet) measurements using Tukey's multiple comparison. CD n=18, HF 48 n=8; HF 60 n=12. For more statistics see appendix.

### 3.1.2. Lard-based high-fat diet feeding in BL/6J mice

Previous feeding study (compare 3.1.1.) of BL/6J mice revealed clear diet and/or obesity mediated alterations of metabolism in response to 4 weeks feeding of plan-based HFD. In a next step, the quality of fat - meaning the source of fat - was on closer examination. Starting at 12 weeks of age, BL/6J mice received lard-based HFD with varying quantities of lard. Besides a medium HFD (lHF 48), two high high-fat diets were fed. One of them was carbohydrate free (lHF 75, lHF 78$^{cf}$). Due to different body mass, lean mass and fat mass at the age of 12 weeks, no absolute masses, but rather mass changes referring to the starting point are shown.

Immediately (0.5 weeks) after starting high-fat diet feeding, mice fed lHF 48 and lHF 75 started to gain weight, mainly due to fat mass increase (figure 18A). This growth of body mass persisted throughout the 4 weeks feeding, resulting in a comparable and significant higher body mass gain than CD fed mice. LHF 78$^{cf}$ feeding led to a delayed gain in body mass. After a slight drop of body mass after 0.5 weeks, lHF 78$^{cf}$ fed mice caught up body mass in parallel to the other two HFD groups. It was not until 3 weeks of intervention that lHF 78$^{cf}$ fed mice showed significant higher body mass than CD fed mice. After 4 weeks of feeding, body mass gain of 2 g in lHF 78$^{cf}$ mice was significantly above controls but likewise significantly below that of mice fed with the other two high-fat diets.

Despite a slight decrease when fed lHF 78$^{cf}$ for one week, lean mass increased continuously in all diet groups during feeding intervention (figure 18B). After 4 weeks, lHF 48 fed mice gained significantly more lean mass than CD fed mice. The course of fat mass gain was comparable to body mass gain (figure 18C). At the end of feeding intervention, all diet groups were significantly different compared to each other with lHF 75, leading to the highest fat mass increase followed by lHF 48. The smallest but still significant effect on fat mass gain was observed in mice fed lHF 78$^{cf}$.

Daily energy intake was measured every half week and calculated per animal per day (figure 18D). LHF 48 and lHF 75 fed mice showed extreme hyperphagia during the first half week of high-fat feeding. Afterwards energy intake was reduced but remained steadily higher in lHF 75 fed mice, compared to CD fed mice. Surprisingly, no typical initial hyperphagia could be observed when mice were offered extreme lHF 78$^{cf}$. Higher energy intake compared to CD was first seen for this diet group after 1 week feeding. Henceforth, energy intake of lHF 78$^{cf}$ fed mice was similar to lHF 75 fed mice. By observing this slowly increasing energy intake, the retarded body/fat mass gain can be explained. Adding up daily energy intake over time resulted in cumulative energy intake (figure 18E). After 2 weeks feeding intervention cumulative energy intake of mice fed any HFD significantly exceeded the energy intake of CD fed mice. No difference in cumulative energy intake between high-fat diets could be found after 4 weeks of feeding.

Comparison of basal glucose levels in fasted mice after 4 weeks feeding intervention revealed elevated glycemia in lHF 48 and lHF 75 fed mice, but not in lHF 78$^{cf}$ fed mice, compared to controls (figure 18G). In response to oral administration of glucose, blood glucose levels increased equally in all diet groups without significant differences (figure 18F). Clearance of blood glucose 30 min and/or 60 min after glucose gavage was reduced in all HFD fed animals. Consequently, any HFD feeding led to a higher total area under blood glucose curves (tAUC) indicating an impaired glucose tolerance, with the highest levels being found in lHF 75 fed mice (figure 18H). Total AUC of lHF 48 fed and lHF 78$^{cf}$ fed mice was increased about 1.2-fold, compared to CD fed mice.

Triglyceride levels measured in the plasma of non-fasted mice after 4 weeks of HFD feeding did not differ between diet groups (figure 18I). However, cholesterol was significantly increased in the plasma of mice fed lHF 48 and lHF 75, compared to controls (figure 18J). In a cooperation project, neither in vivo measurement by PEG urinary recovery rate, nor any ex vivo assessment of intestinal barrier function and inflammation revealed any differences between diet groups (Kless et al. 2015).

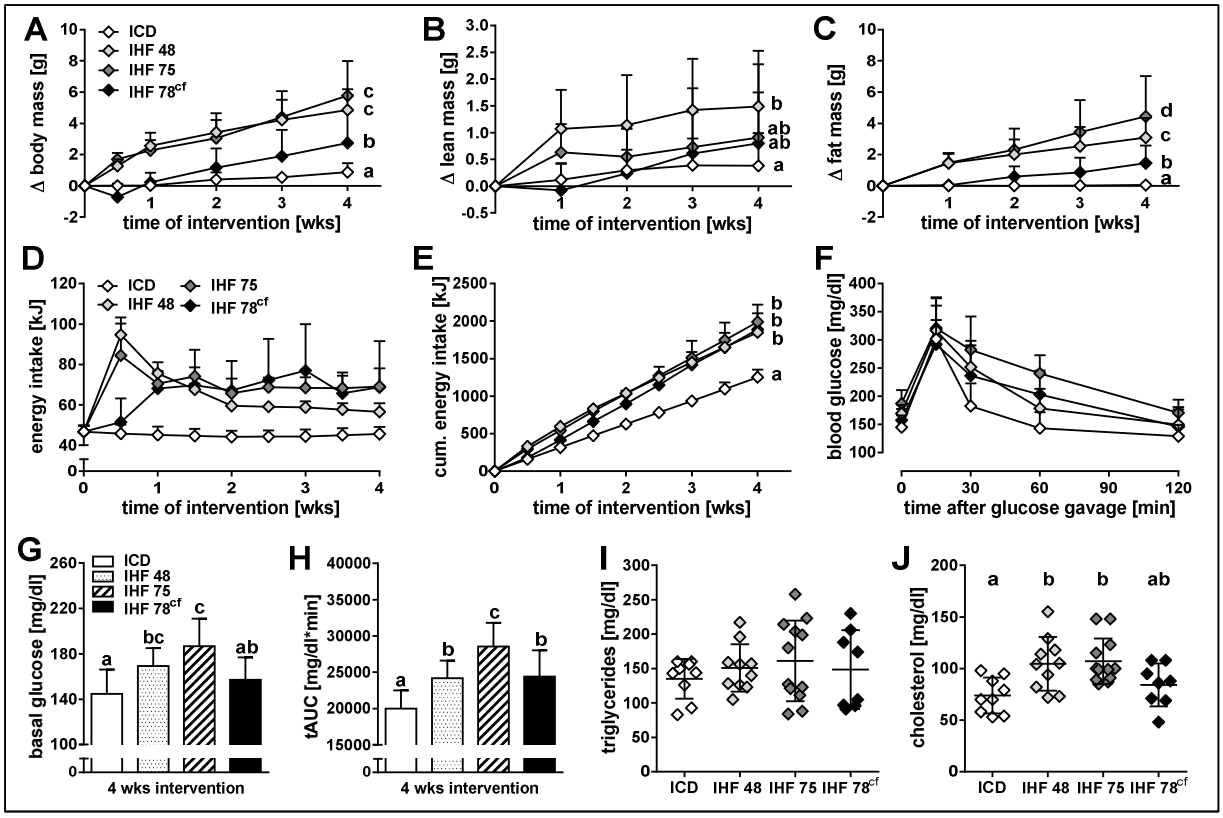


**Figure 18: Metabolic effects of lard-based high-fat diet feeding.** Changes in **(A)** body mass, **(B)** lean mass and **(C)** fat mass referring to the starting point of feeding intervention at 12 weeks of age. Different letters indicate significant differences between diet groups (n=12) after 4 weeks feeding intervention. Energy intake is calculated per animal and displayed **(D)** per day and **(E)** cumulative (n=3-4). **(F)** Blood glucose curves after 4 weeks feeding intervention in response to an oGTT, lCD n=9, lHF 48 n=12, lHF 75 n=10, lHF 78$^{cf}$ n=9, for statistics see appendix. **(G)** Basal glucose levels after 6 hours fasting prior to oGTT and **(H)** total area under the blood glucose curves of oGTT. **(I)** Triglycerides and **(J)** cholesterol were measured in plasma at the end of feeding intervention. For all graphs, different letters present significant differences between diet groups after 4 weeks of high-fat diet feeding calculated by either One-Way ANOVA with Holm-Sidak's multiple comparison or Two-Way ANOVA (time, diet) using Tukey's multiple comparison. For more statistics on (A), (B), (C), (D), (E) and (F), see appendix.

To summarize: feeding lard-based HFD induced a body mass gain due to fat mass gain, and led to impaired glucose tolerance, although metabolic effects were not consequently dependent on fat quantity. In fact, lHF 75 fed mice exhibited the highest fat mass gain, fasting blood glucose levels and tAUC, but lHF 78$^{cf}$ containing nearly equal amounts of fat, showed even less distinct effects on metabolism than HF 48. For further feeding experiments, HFD with 48 kJ% was chosen, since differences to controls were obvious and 48 kJ% fat represents a more physiologically realistic fat amount of the diet than 75 kJ% fat. Besides, HFD with 48 kJ% fat provides better handling because it can be offered in pellets with the same textural form as CD, whereas high HFD is fed as a paste.

### 3.1.3. Comparison of plant- and lard-based high-fat diet-induced effects

So far, HFD with 48 kJ% of fat has been defined as the preferred diet for inducing metabolic alterations, but the source of fat still needed to be determined. Therefore, the effects of 4 weeks lard-based (lCD, lHF 48) and palm-based (pCD, pHF 48) diet feeding were compared. The different fat quality had no influence on CD fed mice (figure 19A): mice receiving pCD and lCD gained similar amounts of body, lean and fat mass and showed no differences in fasting glucose levels and in oral glucose tolerance. Likewise, comparing mice fed the two high-fat diets displayed an increase in body mass and fat mass to the same extent. However, lHF fed mice accumulated significantly more lean mass than mice from the other three diet groups. Compared to lHF fed mice, mice fed pHF had significantly higher glucose levels after fasting, as well as at the 60 min and 120 min measure point during oGTT (figure 19B). Consequently, feeding pHF led to a significantly increased tAUC, compared to lHF, but independent of the fat source, while mice fed HFD exhibited higher tAUCs than any CD. Overall, feeding palm-based HFD over 4 weeks caused more glucose tolerance impairment than lard-based HFD.

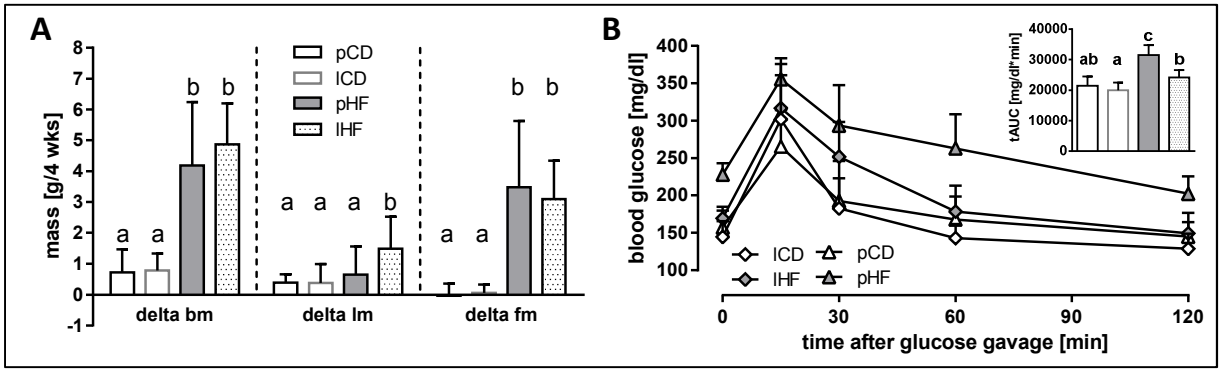


**Figure 19: Comparison of metabolic effects of palm- and lard-based diet feeding in BL/6J mice.** Changes in **(A)** body, lean and fat mass referring to the starting point of feeding intervention at 12 weeks of age; pCD n=38, lCD n=9, pHF n=25, lHF n=12. **(B)** Blood glucose curves after 4 weeks feeding intervention in response to an oGTT, see appendix for statistic; insert: tAUC of the oGTT; pCD n=18, lCD n=9, pHF n=8, lHF n=12. Different letters indicate significant differences between diet groups calculated using One-Way ANOVA with Holm-Sidak's multiple comparison. For more statistics see appendix.

### 3.1.4. Response to high-fat diet feeding in 6 mouse strains

After examining the influence of HFD quality and quantity, the response to HFD in 6 strains was tested. Previously, 4 weeks of feeding intervention with 48 kJ% plant-based HFD was decided to be a suitable setting for strain comparison. Male SWR/J, 129sv/evS1, 129sv/evS6, BL/6J, AKR/J and BL/6N mice were fed CD between 8 and 12 weeks of age. This adaptation phase to purified CD revealed first differences between strains: SWR/J mice had lowest, BL/6N mice the highest body mass (figure 20A). Both 129sv/ev strains were characterized by relatively low lean mass and high fat mass (figure 20C, E), whereas SWR/J and BL/6J mice showed absolutely and relatively little fat mass compared to body mass. AKR/J and BL/6N mice were intermediate regarding fat mass.

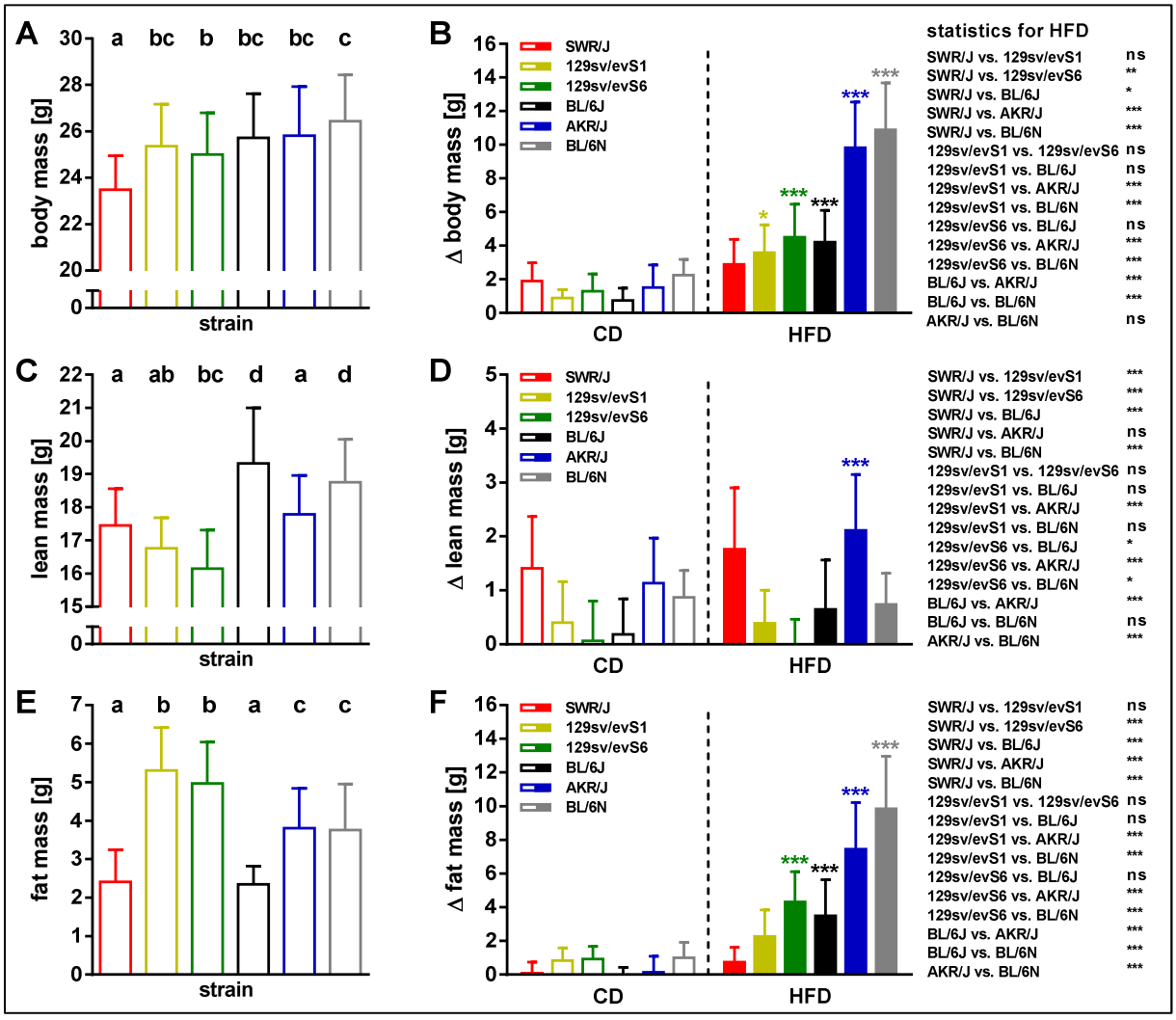


**Figure 20: Body mass and body composition of 6 mouse strains fed CD and HFD.** All mice received control diet (CD) till aged 12 weeks and **(A)** body mass **(C)** lean mass and **(E)** fat mass were measured. Afterwards about half of the mice were fed high-fat diet (HFD, plant-based with 48 kJ% of fat) for four weeks. Changes of **(B)** body mass and **(D)(F)** body composition during feeding intervention were documented for CD and HFD fed mice. Differences between groups were calculated using One- or Two-Way-ANOVA; colored asterisks symbolize intra-strain differences between diet groups, * $p < 0.05$, *** $p < 0.001$; different letters present significant intra-diet group differences between strains; SWR/J n=32-86, 129sv/evS1 n=7-15, 129sv/evS6 n=12-69, BL/6J n=24-104, AKR/ n=33-77, BL/6N n=27-57.

Due to differences in initial body, lean and fat mass, response to HFD and CD was expressed as changes, meaning gain of mass within 4 weeks, compared to a starting mass at 12 weeks of age (figure 20B, D, F). Irrespective of diet, SWR/J mice showed the same increase in body mass, lean mass and fat mass and could therefore defend their status as a DIO resistant strain. 129sv/ev mice of the S1 sub-strain on HFD displayed slightly increased body mass, compared to CD fed mice, whereas mice of the S6 sub-strain clearly gained body and fat mass. A comparable response to HFD was displayed by BL/6J mice, with moderate accumulation of body mass and fat mass. Highest susceptibility to DIO was found in AKR/J and BL/6N mice, with body mass gain of about 10 g within 4 weeks. But only AKR/J mice increased their lean mass when fed HFD, compared to CD fed littermates. BL/6N mice had the highest gain of fat mass, compared to all other strains. For further characterization and investigation of differences in DIO, SWR/J and AKR/J mice were chosen due to their genetic relation but different responses to HFD.

## 3.2. Basal characterization of AKR/J and SWR/J mice

### 3.2.1. Weaning characteristics and development during youth

All AKR/J and SWR/J mice obtained from own breeding were weaned between 18 and 22 days after birth. The relation of females to males was similar in both strains, with a slight majority of males compared to females. In mice of the AKR/J strain 52.5 % were allotted to males (n=1224). Nearly equal: 53.0 % of born SWR/J mice were males (n=1080). Measurement of body weight directly after weaning revealed a lower body mass in females than in males for both strains (figure 21A). Among females, AKR/J mice were heavier than SWR/J mice. A majority of AKR/J mice were born in a litter size of 5 to 7 pubs (figure 21B). Bigger litters with more than 8 pubs were rarely. Most of SWR/J pubs were born in litters with 6 to 8 mice. Thus, SWR/J mice originated from breeding pairs with a higher litter size, and additionally, when weaned were significantly younger than AKR/J mice (appendix). Theoretically, if a linear relation between body weight and litter size, as well as age, were to be assumed, adjustment to these two covariates would reverse significances. Then SWR/J mice would show an adjusted higher body mass then AKR/J mice (appendix).

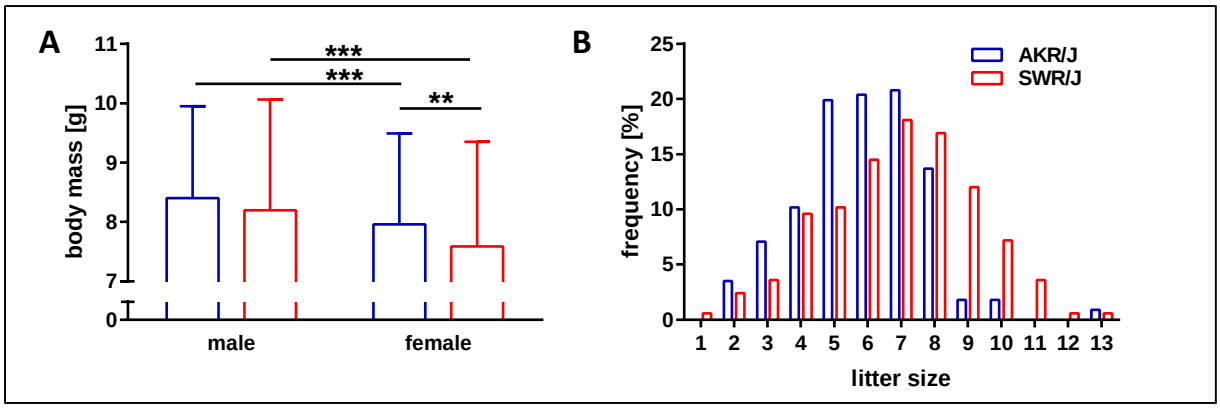


**Figure 21: Body mass and litter size of AKR/J and SWR/J mice at weaning.** Mice were weaned between 18 and 22 days after birth. **(A)** Body mass at weaning of AKR/J and SWR/J mice, separated into males and females, differences were tested using Two-way ANOVA (strain, sex) with Tukey's multiple comparison test; male AKR/J n=538; female AKR/J n=498; male SWR/J n=500, female SWR/J n=446; **p < 0.01, ***p < 0.001. **(B)** Frequency of litter size in percent to all born litters (AKR/J n= 226, SWR/J n=166).

Starting with comparable body mass, one week after weaning at 4 weeks of age, male AKR/J mice were significantly heavier than SWR/J mice (figure 22A). This observation pervaded, except for at 5 weeks of age, throughout the whole youth period. When diet was changed to purified control diet (CD) at the age of 8 weeks, AKR/J reduced body weight by about 1 g within one week. SWR/J mice responded to this diet switch with a one week stagnation in body mass. After one week's adaptation to CD, mice of both strains restarted gaining weight.

Lean mass was continuously higher in AKR/J mice, compared to SWR/J mice during chow feeding (figure 22B). Similar to body mass development, lean mass gain was halted in AKR/J mice when changing diet, whereas lean mass gain in SWR/J mice was not influenced. Feeding CD, no differences between strains were found as regards lean mass. AKR/J mice exhibited significantly more fat mass than SWR/J mice at 6 weeks of age (figure 22C). At 8 weeks of age and again at 12 weeks, AKR/J mice displayed about 3.5 g fat mass. SWR/J mice reduced fat mass after a peak at 6 weeks of age of 2.8 g, to levels of about 2.3 g fat mass at the age of 12 weeks.

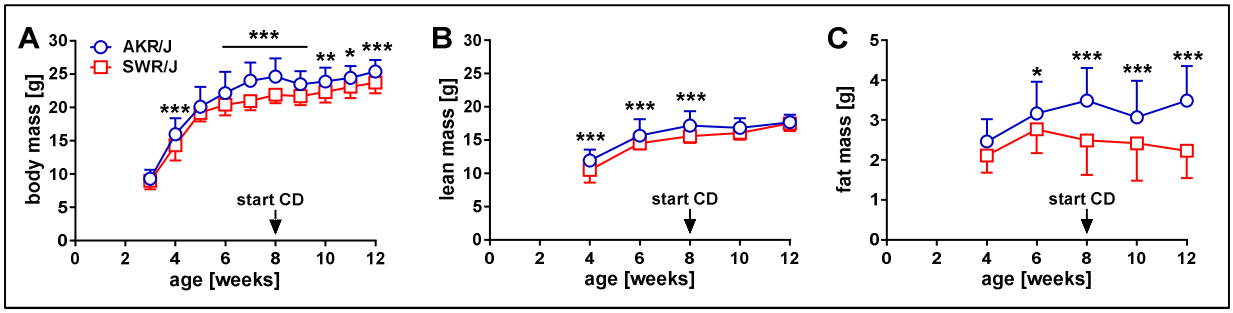


**Figure 22: Body mass and body composition of AKR/J and SWR/J mice with 3 to 12 weeks of age.** Mice were fed chow diet until 8 weeks of age, afterwards mice had ad libitum access to purified control diet. **(A)** Body mass, **(B)** lean mass and **(C)** fat mass development of AKR/J and SWR/J male mice starting at weaning till 12 weeks of age. Differences between strains were calculated using Two-Way-ANOVA (time, strain) repeated measurement with Bonferroni's multiple comparison test; *p < 0.05; **p < 0.01; ***p < 0.001; CD, control diet; AKR/J n=52-56, SWR/J n=45-56.

### 3.2.2. Baseline characteristics during control diet feeding

Prior to the start of high-fat diet feeding, body mass, body composition, food intake and energy expenditure of AKR/J and SWR/J mice on CD were analyzed. At the age of 12 weeks AKR/J mice weighed about 2.2 g more than SWR/J mice, due to a significantly higher fat mass and a trend towards higher lean mass (figure 23A).

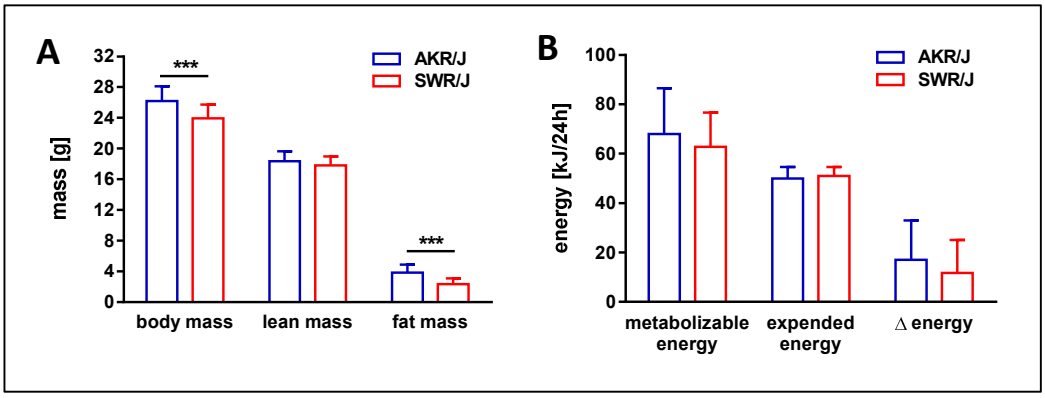


**Figure 23: Body mass, body composition and energy budget parameter of 12 weeks old AKR/J and SWR/J mice fed control diet. (A)** Body mass, lean mass and fat mass after 4 weeks control diet feeding. **(B)** Metabolizable energy was calculated by multiplying energy intake with assimilation efficiency and subtracting assumed caloric value of urine. Expended energy was assessed using indirect calorimetry. Difference between metabolizable and expended energy resulted in Δenergy. Differences between strains were calculated using student's t-test, ***$p < 0.001$; AKR/J n=29, SWR/J n=30.

Mean energy intake during 24 h tended to be higher in AKR/J (78.3 ± 21.3 kJ) than in SWR/J mice (71.0 ± 15.7 kJ). Calculation of metabolizable energy with nearly similar assimilation efficiency (calculation see 3.4.2.) did not reveal differences between strains (figure 23B). Expended energy over 24 h (DEE), measured by indirect calorimetry, was almost identical in AKR/J (50.0 ± 4.7 kJ) and SWR/J mice (51.1. ± 3.7 kJ). Both mouse strains revealed an energy surplus when expended energy was subtracted from that metabolizable energy which was not different between strains. Furthermore, measured maximal metabolic rate (MMR) was comparable between strains (AKR/J: 67.2 ± 6.1 kJ/24h; SWR/J: 67.5 ± 5.7 kJ/24h), whereas resting metabolic rate (RMR) was significantly higher in SWR/J mice (AKR/J: 34.8 ± 4.4 kJ/24h; SWR/J: 38.4 ± 2.7 kJ/24h).

As variations in body weight and body composition may impact on energy balance parameters different linear regression models were calculated in order to find suitable independent variables for the adjustment of energy balance parameters (table 4). Based on the power of correlations ($R^2$) and p-values, body mass, lean mass or a combination of lean and fat mass (lean mass + 0.2*fat mass) would be most suitable for adjustment of DEE and MMR, whereas body mass was the only covariate with significant correlation to metabolizable energy. Fat mass turned out to correlate not at all to any parameter.

**Table 4: Linear regression models to identify covariates for adjustment of energy balance parameters.** Models were calculated by S+ software; AKR/J n=28, SWR/J n=30. RMR, resting metabolic rate; DEE, daily energy expenditure; MMR, maximal metabolic rate; $E_{met}$, metabolizable energy.

| Covariates | Statistics | Energy balance parameter | | | |
|---|---|---|---|---|---|
| | | RMR | DEE | MMR | $E_{met}$ |
| body mass | $R^2$ | 0.017 | 0.121 | 0.083 | 0.087 |
| | p-value | 0.325 | **0.008** | **0.028** | **0.023** |
| lean mass | $R^2$ | 0.056 | 0.316 | 0.236 | 0.046 |
| | p-value | 0.073 | **<0.001** | **<0.001** | 0.105 |
| fat mass | $R^2$ | 0.013 | 0.007 | 0.012 | 0.037 |
| | p-value | 0.396 | 0.532 | 0.405 | 0.145 |
| lean mass, fat mass | $R^2$ | 0.072 | 0.328 | 0.255 | 0.080 |
| | p-value | 0.128 | **<0.001** | **<0.001** | 0.102 |

For all significant correlations, adjustment of energy balance parameter to the corresponding covariate was performed and differences between strains were calculated (table 5). Finally, body mass was chosen for adjustment as it is the only covariate applicable to all energy balance parameters. Adjustment for body mass revealed higher DEE in SWR/J mice than in AKR/J mice (figure 24A, AKR/J: 49.2 ± 3.9 kJ/24h; SWR/J: 51.8 ± 3.6 kJ/24h).

**Table 5: Differences between strains of measured and adjusted energy budget parameters.** P-values were determined using Student's t-test, AKR/J n=28, SWR/J n=30. RMR, resting metabolic rate; DEE, daily energy expenditure; MMR, maximal metabolic rate; $E_{met}$, metabolizable energy; n.a., not applicable.

| | Differences between strains (p-value) | | | | |
|---|---|---|---|---|---|
| | RMR | DEE | MMR | $E_{met}$ | Δenergy |
| Measured raw data | **<0.001** | 0.344 | 0.871 | 0.227 | 0.175 |
| Adjusted to body mass | n.a. | **0.011** | 0.169 | 0.986 | 0.645 |
| Adjusted to lean mass | n.a. | **0.020** | 0.265 | n.a. | n.a. |
| Adjusted to fat mass | n.a. | n.a. | n.a. | n.a. | n.a. |
| Adjusted to lean and fat mass | n.a. | 0.580 | 0.698 | n.a. | n.a. |

Just as without adjustment, delta energy calculated with adjusted values was positive and did not differ between strains (figure 24A). Correspondingly, nearly all mice gained body mass during 24 h measurement. In fact, a significant correlation of delta energy with changes in body mass was observed (adjusted delta energy = 12.2 * Δ body mass + 4.3; figure 24B).

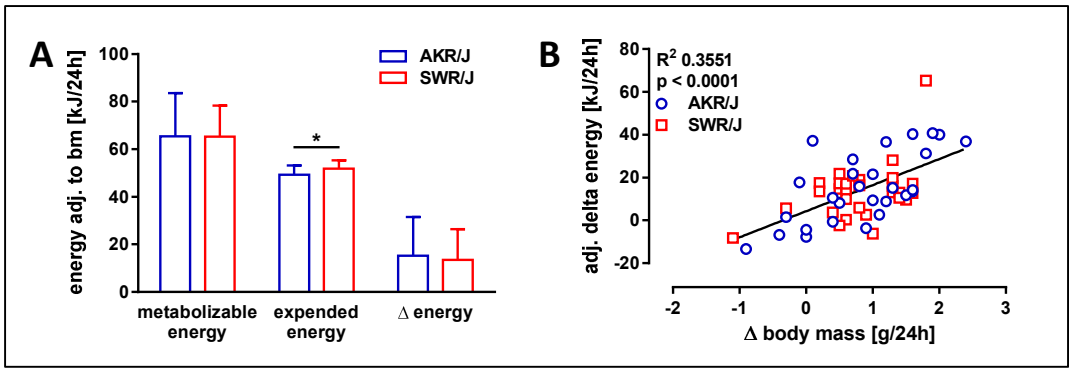


**Figure 24: Energy balance parameter and correlation of energy balance to body mass changes. (A)** Metabolizable and expended energy were adjusted to body mass as suitable covariate for both parameters. Difference between adjusted metabolizable and expended energy resulted in Δenergy. Differences between strains were calculated using Student's t-test, *p < 0.01; AKR/J n=28, SWR/J n=30. **(B)** For each animal adjusted Δenergy is plotted against change of body mass within 24 h; statistics calculated by linear regression.

In both strains energy expenditure was higher during the nocturnal activity phase (scotophase) than during photophase, but the pattern differed between strains (figure 25A). AKR/J mice exhibited elevated energy expenditure during the entire scotophase with highest values manifesting during the second half of the scotophase. In SWR/J mice, similar nocturnal energy expenditure levels as those in AKR/J mice were observed during the first half of the scotophase. Starting at midnight, however, energy expenditure started to drop continuously until it attained minimal nocturnal levels at 3 am. Thereafter, energy expenditure rose rather steeply and peaked at around 7 am, 2 hours after lights on. Measured RMR was significantly higher in SWR/J mice than in AKR/J mice (figure 25B). As described above, DEE and MMR were adjusted to body mass, indicating increased DEE in SWR/J mice, compared to AKR/J mice, whereas no strain difference for MMR was found. In conclusion, during CD feeding SWR/J mice display higher DEE due to elevation of RMR compared to AKR/J mice.

Next, respiratory exchange ratio (RER) was inspected as an indicator for metabolic substrate utilization. Overall, the pattern of higher and lower RER corresponded to energy expenditure in both strains (figure 25C). Additionally, RER over 24 h showed the same progression as food intake delayed by about 1-2 hours (appendix, notably food intake was not assessed with the same mice as RER). During scotophase, also over 24 h, SWR/J mice attained lower RER than AKR/J mice (figure 25D). As no strain difference in RER was detectable during photophase, this suggests a higher rate of lipid oxidation in SWR/J mice during nocturnal activity phase. To further pinpoint strain differences in metabolic substrate preferences, the association of RER and oxygen consumption on a 24 hour basis was analyzed in a 3D frequency distribution plot (figure 25E, F). The graphical illustration reveals that high RER values typically accompany high oxygen consumption. Low RERs were mostly restricted to resting metabolic rates. In AKR/J mice

these two conditions seemed to be definite, whereas in SWR/J mice the transition was less distinct.

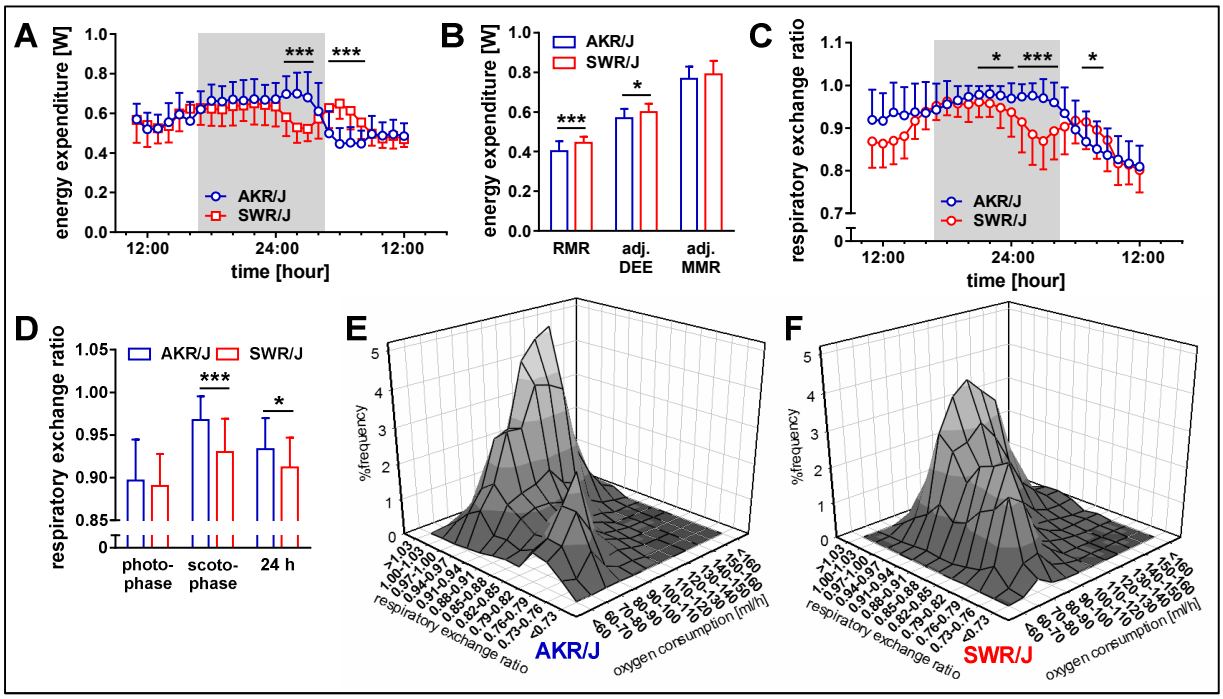


**Figure 25: Indirect calorimetry measurements in AKR/J and SWR/J mice fed control diet.** 11-12 weeks old AKR/J (n=29) and SWR/J mice (n=30) fed CD were measured by indirect calorimetry for 24 h. **(A)** Energy expenditure was measured in 9 min intervals and expressed per hour, shaded column symbolizes scotophase. **(B)** Daily energy expenditure (DEE) was calculated over 24 h. Based on lowest and on highest oxygen consumption levels, resting metabolic rate (RMR) and maximal metabolic rate (MMR) were calculated, respectively. DEE and MMR were adjusted to body mass. **(C)** Respiratory exchange ratio (RER) data were pooled for photophase, scotophase and 24 h based on **(D)** measurements of RER per hour. RER and oxygen consumption of **(E)** AKR/J mice and **(F)** SWR/J mice were sectioned in categories, respectively and plotted against the frequency of combined occurrences. Differences between strains were calculated using Student's t-test and Two-Way-ANOVA repeated measurement with Bonferroni's multiple comparison test, *p < 0.05, ***p < 0.001.

In summary, baseline characterization on CD revealed the indispensability of adjustment of energy balance parameters (metabolizable and expended energy). Appropriate adjustment showed no differences of metabolizable energy between AKR/J and SWR/J, but rather higher energy expenditure in SWR/J mice. Additionally, SWR/J mice exhibited higher RMR and lower RER, compared to AKR/J mice. Diurnal and metabolic flexibility patterns were specific for each strain.

## 3.3. Proximate causes for diet-induced obesity in AKR/J and SWR/J mice

At the age of 12 weeks, diet of AKR/J and SWR/J mice was switched from CD to HFD (48 kJ% of fat based on palm oil). The aim was to reveal proximate causes for differences in diet-induced obesity between strains using measurements of body mass, body composition, energy intake, energy expenditure, activity and body core temperature meaning key parameters of energy balance.

### 3.3.1. Body mass, body composition and energy expenditure

At the beginning of HFD feeding, AKR/J and SWR/J mice were body weight matched. One day, after onset of HFD feeding, AKR/J mice weighed significantly more than SWR/J mice (figure 26A). During the following days, this distinct difference in body weight proceeded. After 3 days on HFD mean body mass gain was 3.3 ± 1.0 g in AKR/J, compared to 1.6 ± 0.5 g in SWR/J (figure 26B).

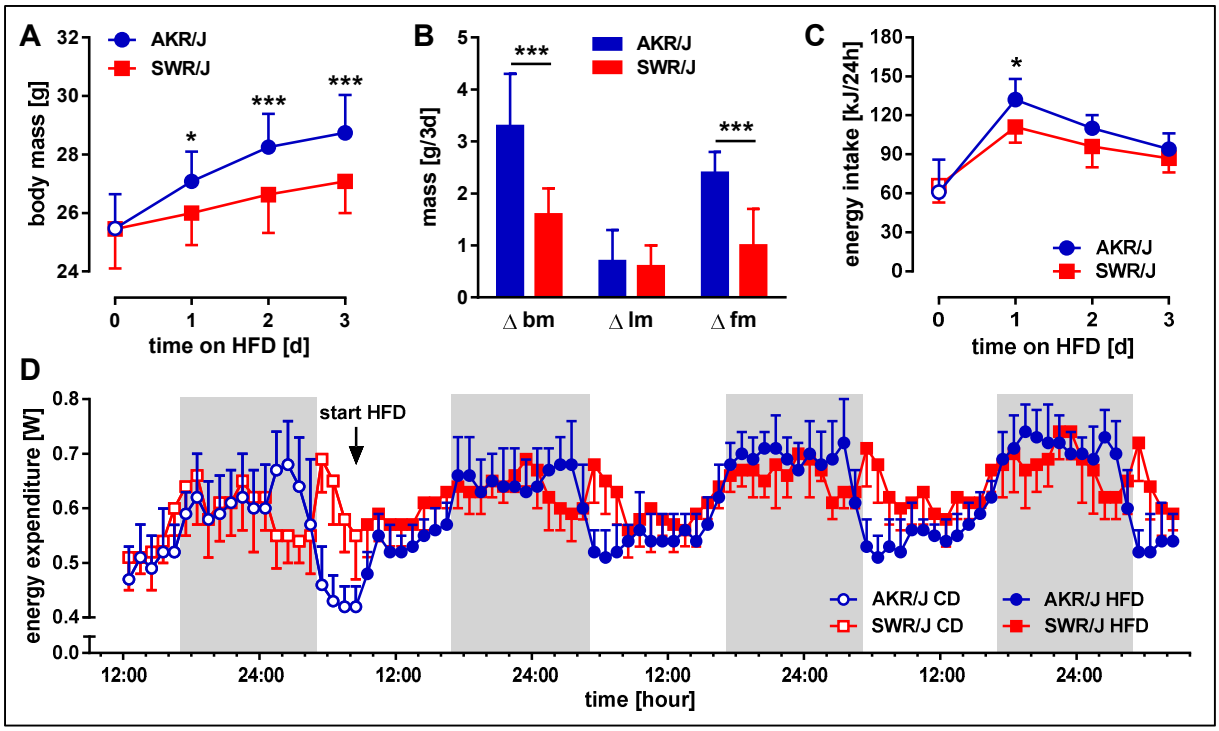


**Figure 26: Body mass, body composition, energy intake and energy expenditure in AKR/J and SWR/J mice one day before and during first 3 days of high-fat diet feeding.** After 4 weeks of adaptation to purified control diet (CD), body mass matched AKR/J and SWR/J mice were fed high-fat diet (HFD, plant-based with 48 kJ% of fat). **(A)** Body mass was measured daily. **(B)** Changes in body mass (bm), lean mass (lm) and fat mass (fm) during the first three days on high-fat diet were highlighted. Body composition was determined before and three days after start of high-fat diet feeding. **(C)** Energy intake was monitored daily in the feeding-drinking device. **(D)** Energy expenditure was measured by indirect calorimetry, shaded columns symbolize scotophase. Differences between strains were calculated using Student's t-test and One-Way-ANOVA repeated measurement; *p < 0.05, ***p < 0.001; n=8-24.

Body mass gain in AKR/J mice was mainly caused by an expansion of fat mass, whereas in SWR/J mice both lean and fat masses accounted for moderate body mass gain. Both mouse strains exhibited hyperphagia on HFD, with the most pronounced effect being evident after one day on HFD (figure 26C). Afterwards, elevated energy intake waned but had not reached CD levels after three days of HFD feeding. Differences between strains were only first observed one day after onset of HFD, with AKR/J mice (132 ± 16 kJ) showing higher energy intake than SWR/J mice (111 ± 12 kJ).

At the onset of HFD feeding, an instantaneous increase of energy expenditure during day and night was recorded for both strains (figure 26D). Differences in the diurnal pattern of energy expenditure between strains observed on CD (figure 21A) were maintained on HFD. AKR/J mice continued with a clear day-night-rhythm, whereas SWR/J mice showed a distinct peak in energy expenditure at the start of photophase. Therefore, despite a HFD induced increase in both strains, energy expenditure during photophase was higher in SWR/J mice than in AKR/J mice (figure 27A).

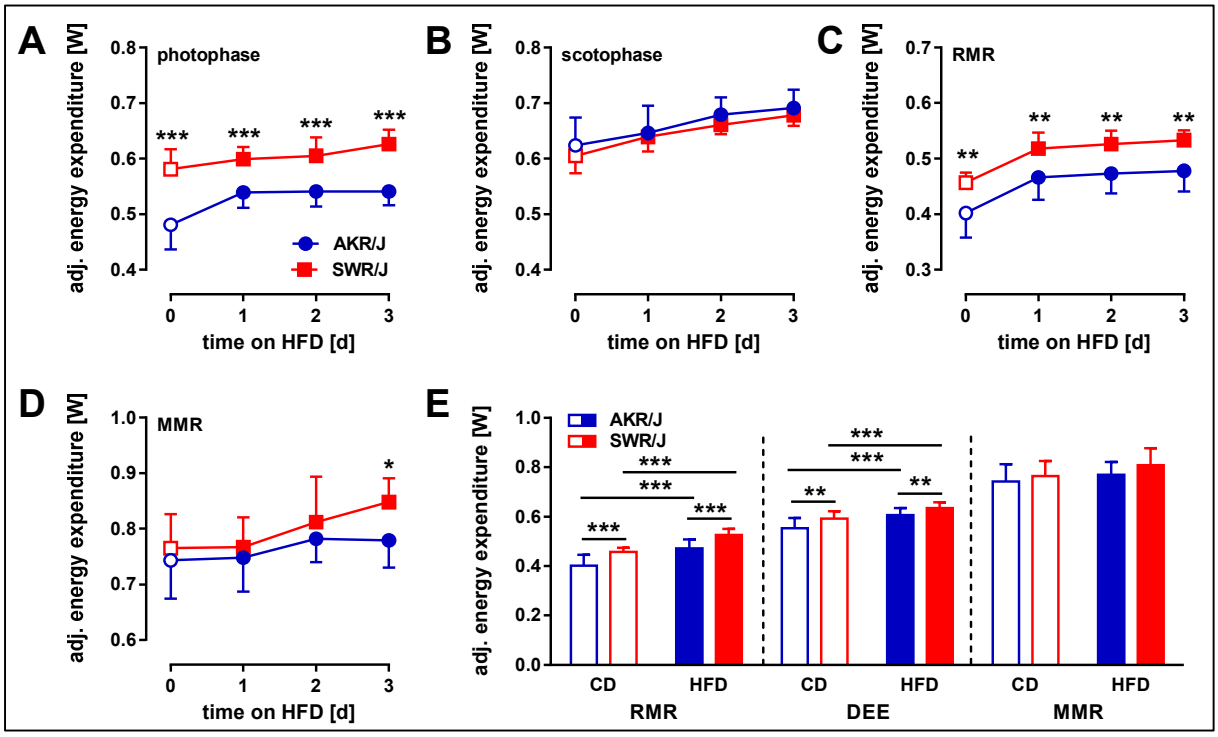


**Figure 27: Measurement of energy expenditure in AKR/J and SWR/J mice one day before and during first 3 days of high-fat diet feeding.** Energy expenditure was measured by indirect calorimetry in AKR/J and SWR/J mice (n=8). Daily energy expenditure (DEE) was divided in **(A)** photophase and **(B)** scotophase contribution. Based on measurement intervals with the lowest and highest oxygen consumption, respectively **(C)** resting metabolic rate (RMR) and **(D)** maximal metabolic rate (MMR) were calculated. **(E)** Mean of adjusted RMR, DEE and MMR of 24 h on control diet (CD) and of 3 days on high-fat diet (HFD) were calculated for both mouse strains, respectively. All energy expenditure data were adjusted to baseline regression (energy expenditure of control diet fed animals normalized to body mass). Differences between strains were calculated using Two-Way ANOVA and One-Way-ANOVA repeated measurement; *p < 0.05, **p < 0.01, ***p < 0.001, for statistics over time see appendix.

Continuously rising energy expenditure during scotophase did not differ between strains (figure 27B). Independent of strain, RMR increased due to HFD feeding (figure 27C). AKR/J and SWR/J mice elevated RMR immediately after onset of HFD. On the following two days on HFD increasing RMR stagnated. Since the progress of RMR proceeded in parallel in both strains, elevation of RMR observed in CD fed SWR/J, compared to AKR/J mice (figure 25B), also persisted on HFD feeding. MMR was unaffected by diet change in AKR/J mice (figure 27D). SWR/J mice increased MMR with ongoing HFD feeding, resulting in higher MMR compared to AKR/J mice on the third day on HFD. Building the mean of all three days on HFD, and comparing it to CD revealed an HFD-mediated elevation of DEE, due to an increased RMR independent in the strain (figure 27E). Higher RMR and DEE in SWR/J mice, compared to those in AKR/J mice on CD remained on HFD. MMR tended to increase more in SWR/J mice than in AKR/J mice.

### 3.3.2. Energy balance

To point out proximate causes of obesity, energy balance during the first three days of HFD feeding was assessed by analyzing the contributions of energy intake, energy expenditure and energy accumulation. Feeding HFD to body mass matched AKR/J and SWR/ mice led to body mass gain in both strains. Nevertheless, AKR/J mice fed HFD diet were always heavier than SWR/J mice and gained significantly more body mass, mainly due to fat mass expansion. HFD-induced hyperphagia occurred in both mouse strains, although the increased energy intake was more pronounced in AKR/J than in SWR/J mice (compare figure 26). Due to equally high assimilation efficiency on HFD for both strains (figure 33D), levels of adjusted metabolizable energy reflect those of energy intake (figure 28A). In the subset of mice used for indirect calorimetry measurements, adjusted energy expenditure before feeding HFD was significantly higher in SWR/J mice than in AKR/J mice (figure 28B). Mice of both strains increased energy expenditure continuously during HFD feeding. For a daily energy balance equation the difference of metabolizable energy and energy expenditure was calculated (figure 28C). Both mouse strains revealed a positive energy balance during high-fat diet feeding, which peaked on the first day of HFD. Adding together all three days of positive energy balance, AKR/J reached a surplus of 139.9 ± 11.5 kJ/3d and SWR/J of 104.3 ± 11.4 kJ/3d. The difference of excess energy between strains of about 36 kJ matched the body mass gain perfectly. Additionally, correlation of body mass increase and positive energy balance was highly significant (figure 28D). A simple calculation comparing energy balance and mass gain can explain differences in susceptibility to DIO in AKR/J and SWR/J mice: it is estimated that building up 1 g of fat mass corresponds to the storage of about 30 kJ (Wishnofsky 1958; Thomas 1962). Body mass gain can be divided into lean and fat mass increases. Since lean mass gain is similar in both strains, only the variance in

fat mass gain needs to be considered. The difference between strains of 1.4 g reflects approximately 42 kJ. Consequently, between AKR/J and SWR/J the difference of accumulation of fat mass (42 kJ) is almost equivalent to the difference of accumulated energy (36 kJ).

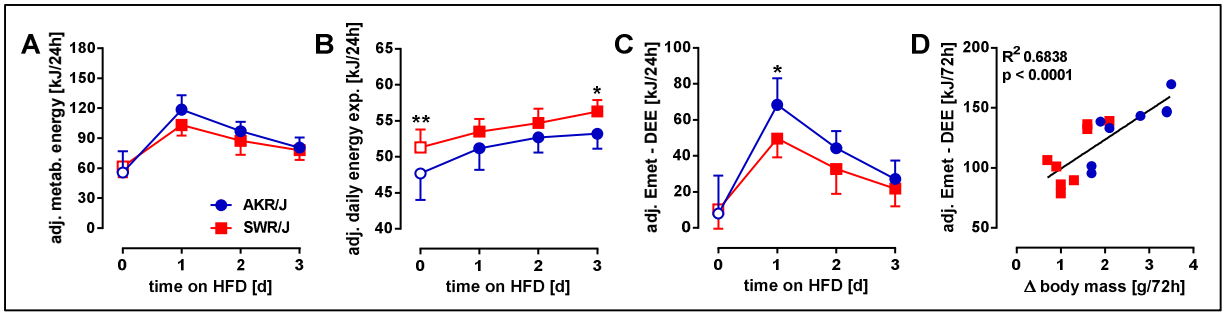


**Figure 28: Metabolizable and expended energy during diet change.** Food intake and energy expenditure were measured daily one day before and three days after changing diet from control to high-fat diet (HFD). Energy intake was calculated by multiplying food intake with the energy density of the respective diet. Energy intake reduced by the resorption efficiency and energy loss via urine resulted in **(A)** metabolizable energy. **(B)** Energy expenditure was measured by indirect calorimetry. **(C)** Energy balance is the result of the difference between metabolizable energy (Emet) and energy expenditure (DEE). Emet and DEE were adjusted to baseline regression. **(D)** Sum of positive energy during 3 days HFD is plotted against change of body mass within 3 days HFD. Differences between strains were calculated using One-Way-ANOVA repeated measurement; *p < 0.05, **p < 0.01.

### 3.3.3. Body core temperature and activity

Detected by implanted body core temperature ($T_b$) sensors, AKR/J mice showed a clear diurnal $T_b$-cycle with amplitude of about 1.5 °C prior to HFD feeding. This 24-hour cycle of $T_b$ was maintained after onset of HFD feeding, but characterized by a striking reduction in amplitude due to elevation of $T_b$ during photophase (figure 29A). In SWR/J mice on CD, the diurnal $T_b$-rhythm, equal to energy expenditure and RER, was not as distinct as in AKR/J mice. At the start of HFD feeding, SWR/J mice raised $T_b$ in the scoto- and photophase (figure 29B). Comparing strains on CD revealed elevated $T_b$ during photophase in SWR/J mice, whereas AKR/J showed higher $T_b$ during scotophase (figure 29C, D). Independent of strain HFD, feeding induced an increase in $T_b$ and attenuated strain differences. In general, despite HFD-induced changes in $T_b$, there were no strain differences in mean 24 h $T_b$, neither on HFD nor on CD (figure 29E).

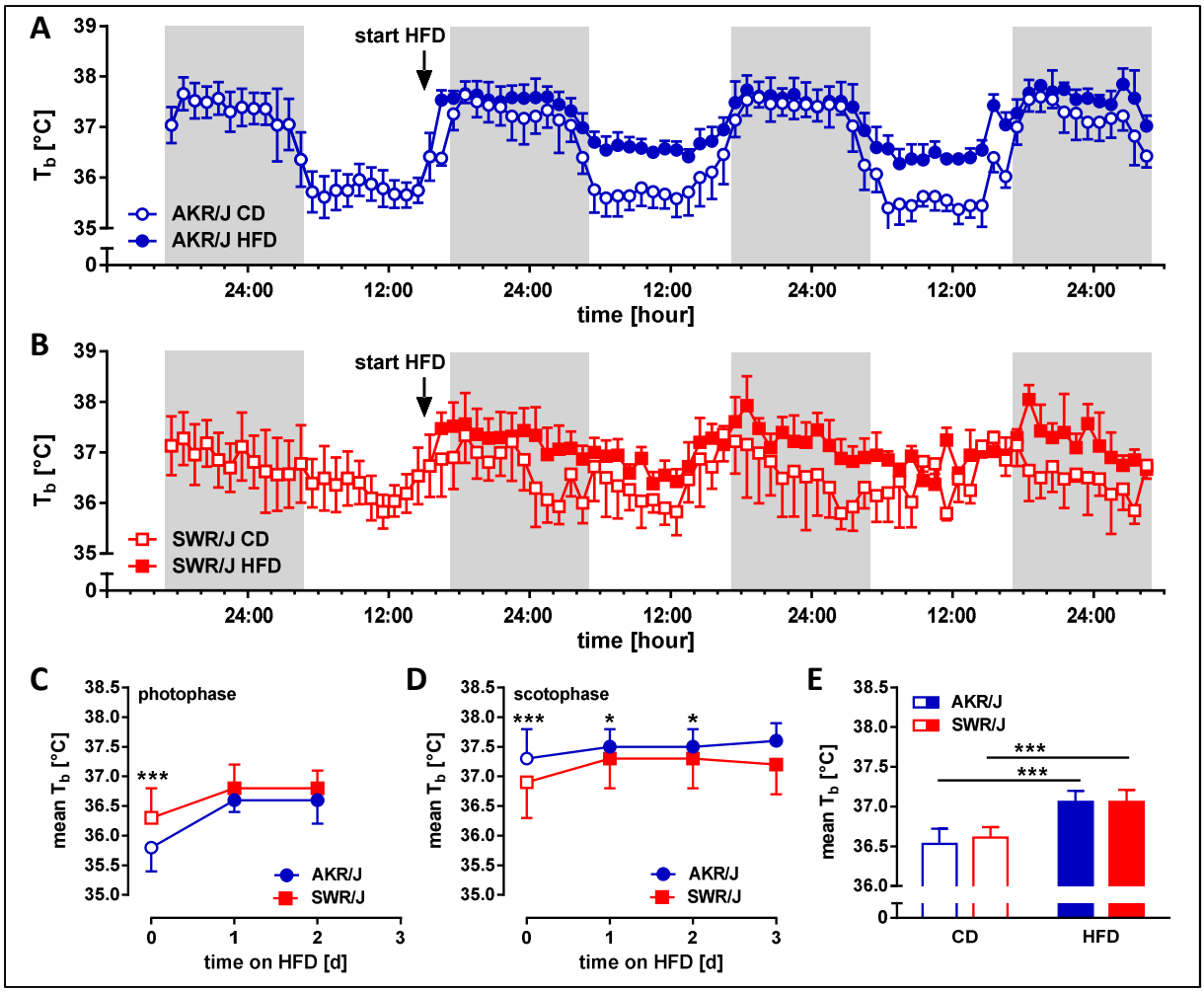


**Figure 29: Body core temperature ($T_b$) in AKR/J and SWR/J mice one day before and during first 3 days of high-fat diet feeding.** $T_b$ was reported in 5 min intervals from the implanted minimitter and mean values per hour were calculated for **(A)** AKR/J and **(B)** SWR/J mice (n=8), shaded columns indicate scotophase. Mean $T_b$ during diet change in **(C)** photophase and **(D)** scotophase was measured. **(E)** Mean of $T_b$ of 24 h on control diet (CD) and of 3 days on high-fat diet (HFD) were calculated for each strain, respectively. Differences between strains were calculated using Two-Way ANOVA and One-Way-ANOVA repeated measurement; *p < 0.05, ***p < 0.001.

As expected for night active animals, both mouse strains show largely increased activity during scotophase, compared to photophase (figure 30A, B). Irrespective of diet, SWR/J mice were more active than AKR/J mice during photophase, whereas AKR/J mice were more active during scotophase. Overall, on CD AKR/J mice showed more activity counts than SWR/J mice (figure 30C). This strain difference resolved when mice were fed the HFD. In general, rearing activity was more pronounced in SWR/J than in AKR/J mice (figure 30D, E). During HFD feeding, AKR/J, but not SWR/J mice, reduced rearing significantly (figure 30F). Notably, SWR/J mice spent approximately one hour during the night clinging to or climbing at the cage lid, whereas this behavior was rarely observed at all in AKR/J mice. This kind of exercise was independent of diet (figure 30G, H, I).

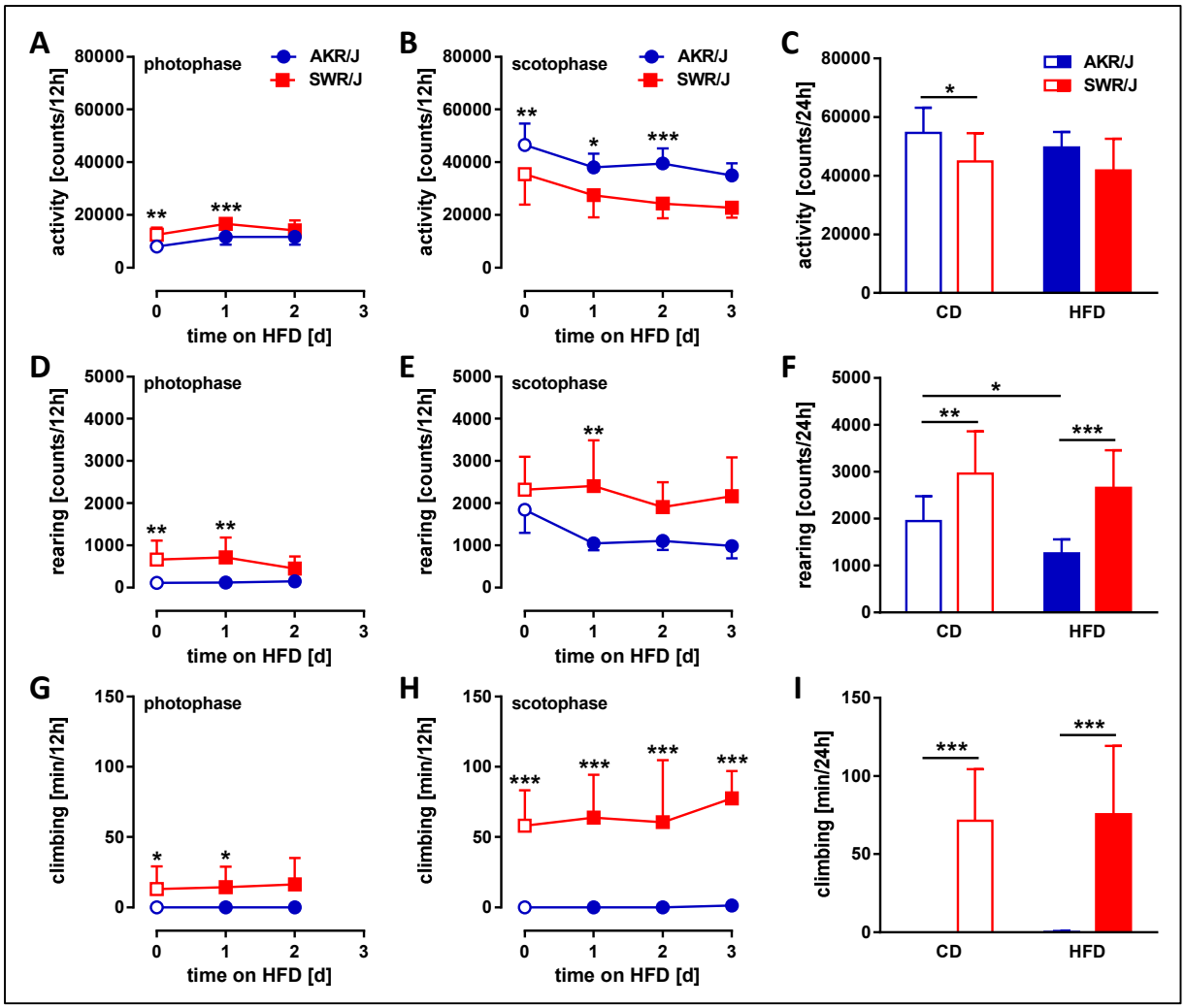


**Figure 30: Activity in AKR/J and SWR/J mice one day before and during first 3 days of high-fat diet feeding.** In a feeding-drinking-activity device total activity was measured during **(A)** photophase and **(B)** scotophase in 12 weeks old AKR/J and SWR/J mice (n=8). **(C)** Mean of total activity of 24 h on control diet (CD) and of 3 days on high-fat diet (HFD) was calculated for both mouse strains, respectively. Additionally **(D-F)** rearing activity and **(G-I)** climbing were monitored. Differences between strains were calculated using Two-Way ANOVA and One-Way-ANOVA repeated measurement; *p < 0.05, **p < 0.01, ***p < 0.001.

### 3.3.4. Summary of proximate causes of obesity

In response to HFD AKR/J mice clearly gained more fat mass than SWR/J mice. HFD led to an overall equal increase in energy expenditure and body core temperature in both strains. But SWR/J mice started on higher levels of RMR and DEE. Further SWR/J mice showed a more extreme exercise rate, in the form of rearing and climbing, with a tendency to higher MMR levels. On the other side of the energy balance, hyperphagia occurred in both strains but, compared to SWR/J mice, AKR/J mice resorbed more energy. Consequently the proximate cause for DIO in AKR/J mice was an increase in metabolizable energy that is not contra-regulated sufficiently by increasing energy expenditure.

## 3.4. Metabolic effects of 12 week high-fat diet feeding and their reversibility

In a further step - after characterization of the first days of HFD feeding - the response to HFD over 12 weeks was analyzed in AKR/J and SWR/J mice. The aim was to detect possible late-term effects in SWR/J, to discriminate between HFD- and obesity-induced effects and to monitor time-dependent changes in such effects. Moreover, reversibility of HFD-induced effects was tested by refeeding the control diet after 12 weeks HFD.

### 3.4.1. Body mass and body composition

Since the first measure point after half a week of HFD feeding, AKR/J mice increased steadily in body mass with significant differences to CD fed AKR/J mice, as well as to SWR/J mice fed HFD (figure 31A). Body mass of AKR/J mice after 12 weeks HFD feeding peaked at 43.4 ± 3.6 g. Refeeding *ad libitum* CD decreased body weight nearly exponentially. Differences in body mass between continuously fed CD AKR/J and refed AKR/J mice vanished after 5 weeks with refed AKR/J mice stabilizing body mass at about 33 g. SWR/J mice fed CD and SWR/J mice on HFD did not differ in body mass at any time during feeding intervention. But nevertheless, body mass increase was higher in HFD fed SWR/J mice than in CD fed mice (figure 31A, D). Lean mass gain could be observed throughout the entire feeding period of 24 weeks, except for AKR/J mice refed CD (figure 31B). Especially in the second half of the feeding period, SWR/J mice on CD exhibited more lean mass than all other groups. Accumulation of fat mass is the main cause for body mass gain in AKR/J mice, as it increased in the same progression (figure 31C). AKR/J mice built up nearly 13 g of fat mass when fed HFD resulting in 16.2 ± 1.9 g total fat mass (figure 31C, D). During the refeeding phase former HFD fed AKR/J mice lost fat mass dramatically and approached with a steady 6 g of fat mass CD fed AKR/J mice after 5 weeks. In SWR/J mice fat mass of HFD mice had significantly exceeded the fat mass of CD fed mice just after 12 weeks of feeding (figure 31C). At this time point, SWR/J HFD mice had almost doubled fat mass compared to CD fed SWR/J mice. Nevertheless fat mass levels in SWR/J mice on HFD are quite low and do not represent the main contributor to body mass gain in SWR/J mice since lean mass gain had more impact (figure 31E, F).

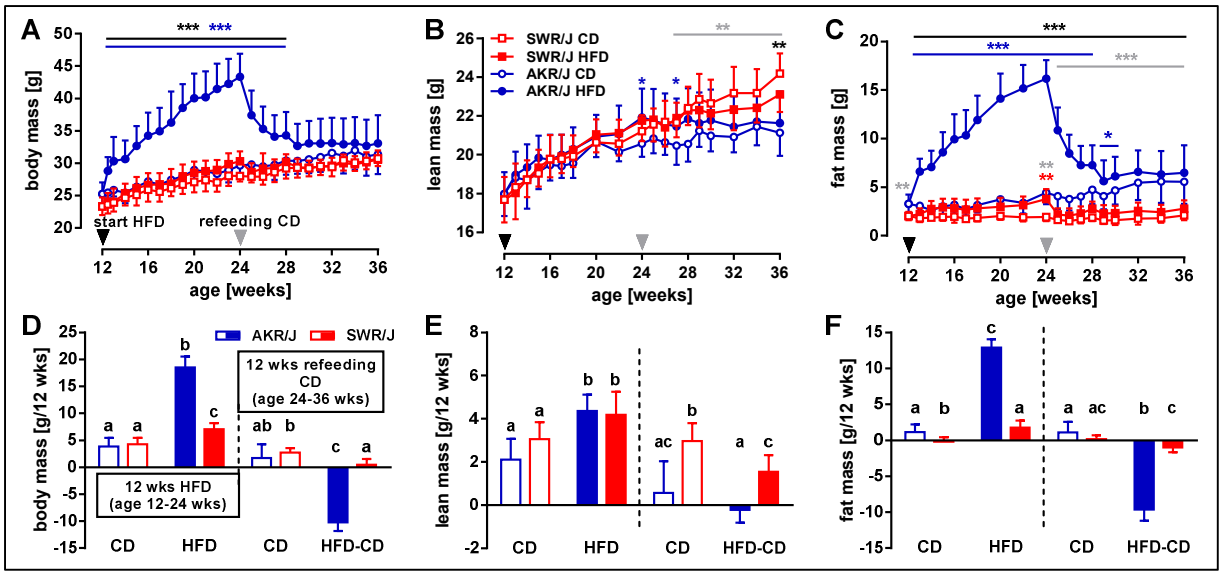


**Figure 31: Body mass and body composition of AKR/J and SWR/J mice during high-fat diet feeding followed by refeeding control diet. (A)** Body mass, **(B)** lean mass and **(C)** fat mass were measured regularly during high-fat diet (HFD) feeding and refeeding control diet (CD). Black triangles indicate start of HFD feeding and grey triangles symbolize the onset of refeeding CD in the HFD fed mice. Differences between strains and diet groups were calculated by Two-Way ANOVA; *p < 0.05, **p < 0.01, ***p < 0.001; black asterisk AKR/J HFD(-CD) vs. SWR/J HFD(-CD), grey asterisk AKR/J CD vs. SWR/J CD, blue asterisk AKR/J CD vs. AKR/J HFD(-CD), red asterisk SWR/J CD vs. SWR/J HFD(-CD). Gain or loss of **(D)** body mass, **(E)** lean mass and **(F)** fat mass were calculated for the HFD feeding and for the refeeding CD period. Differences between strains and diet groups were calculated separately for feeding periods using Two-Way ANOVA with Holm-Sidak's multiple comparison; different letters indicate significant differences; n=10-14.

### 3.4.2. Energy intake and assimilated energy

A subset of mice was monitored in the feeding drinking activity device (FDA) three times during feeding intervention: the first time for 4 days when starting HFD, then at the age of 16 weeks for three days when HFD feeding lasted 4 weeks and the last time was for 4 days when HFD fed mice were refed CD. As observed in a previous experiment (figure 26), mice of both strains showed hyperphagia starting HFD having a more pronounced effect in AKR/J mice (figure 32A). This effect is extreme for the first day of HFD and declined during the next two days. Regarding the diurnal proportion of energy intake AKR/J mice fed CD ate only during scotophase (figure 32B, C). Starting HFD food was also consumed during photophase. SWR/J mice at 12 weeks of age consume about one third of the food during day and two thirds in the night. On HFD, eating behavior during photophase remained unchanged whereas energy intake was increased during scotophase. After four weeks of HFD, the energy intake of all groups was stable. Independent of strain, HFD mice consumed more than the respective CD fed mice. Further on, AKR/J ate about one fourth and SWR/J mice about one third of the HFD during photophase. At the end of the 12 weeks HFD feeding intervention, there were no differences in energy intake between CD and HFD fed mice within strains. Switching HFD fed mice to CD led to a drastic and continuing drop in energy intake in AKR/J mice, whereas SWR/J mice only showed a slight

reduction during photophase. At 24 weeks of age SWR/J mice ate equal amounts of food during day and night. AKR/J persisted on distinct scotophase food consumption.

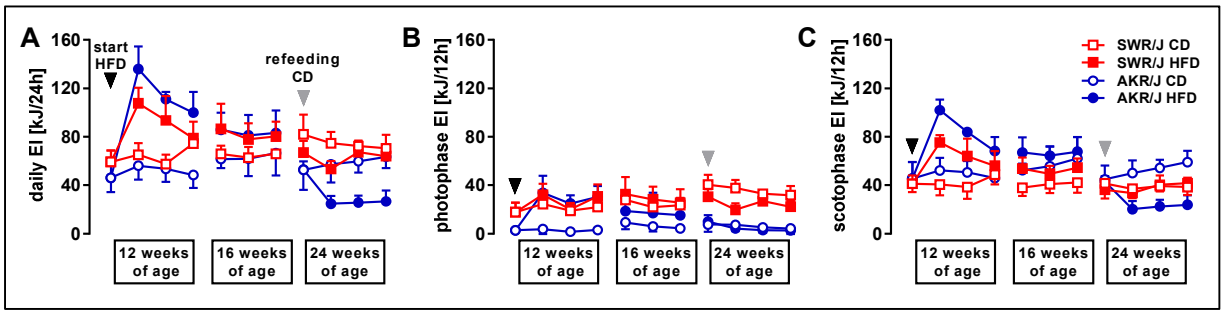


**Figure 32: Energy intake of AKR/J and SWR/J mice during FDA measurement.** Energy intake (EI) was calculated by multiplying food intake by energy content of the diet. Data are expressed for **(A)** 24 hours, for **(B)** photophase and **(C)** scotophase. Measurements were conducted at the age of 12 weeks when AKR/J and SWR/J mice received either control diet (CD) or high-fat diet (HFD) for 4 days, at the age of 16 weeks for 3 days and at the age of 24 weeks for 4 days when HFD fed mice were refed with CD ad libitum. For statistical differences see appendix; n=7-8.

The stable condition attained after 4 weeks HFD feeding was used to calculate assimilation efficiency - which is needed to calculate metabolizable energy for other experiments (e.g. 3.3.2.). After adaptation to single housing, food intake and feces production were measured in AKR/J and SWR/J mice on CD and on HFD. No differences between diet groups and strains could be detected regarding energy intake (figure 33A). Energy lost by feces was significantly higher in SWR/J mice fed CD, compared to AKR/J mice on CD (figure 33B). Calculating the difference between ingested energy and energy lost by feces (= assimilated energy) merely revealed higher assimilated energy in SWR/J mice fed HFD compared to AKR/J mice on CD (figure 33C). Finally, assimilation efficiency was significantly increased in HFD fed mice independent of strain (AKR/J CD: 88.6 ± 2.1 %; AKR/J HFD: 92.8 ± 2.3 g; SWR/J CD: 90.3 ± 0.7 %; SWR/J HFD: 93.4 ± 1.4 %) (figure 33D).

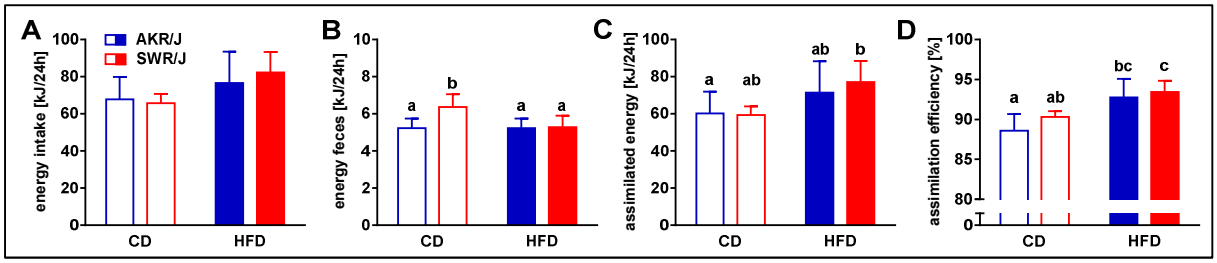


**Figure 33: Parameters and calculation of assimaltion efficency.** After adaptation to single housing food intake and feces production were measured for 3 days. With this data and the determination of energy content **(A)** energy intake and **(B)** energy of feces and **(C)** assimilated energy were calculated for 24 h. The relation of assimilated energy to energy intake results in **(D)** assimilation efficiency. Differences between diet groups were determined using Two-Way ANOVA with Tukey's multiple comparison test; different letters indicate significant differences; n=6-9.

### 3.4.3. Body core temperature and activity

Prior to HFD feeding, AKR/J and SWR/J mice showed no differences over 24 hours $T_b$ (figure 34A), but separation in day and night revealed significantly higher $T_b$ in SWR/J during photophase and in AKR/J during scotophase (figure 34B, C). HFD feeding induced a strain independent $T_b$ increase, although in AKR/J mice temperature rose notably during the day and in SWR/J especially during the night. After 4 weeks, HFD feeding had not led to $T_b$ differences in AKR/J mice. Over 24 hours temperature was increased in HFD fed SWR/J mice, due to clearly higher $T_b$ during scotophase. This observation was maintained until 12 weeks of HFD feeding yielded a tendency to higher photophase $T_b$ in AKR/J mice fed HFD, compared to CD. In AKR/J mice, refeeding CD caused temperature decrease but without any influence on 24 hours $T_b$. SWR/J mice stayed rather unaffected by switching HFD to CD. $T_b$ remained higher in the former HFD fed group during the night, but over 24 hours no difference between any of the groups was detected within the first two days of refeeding.

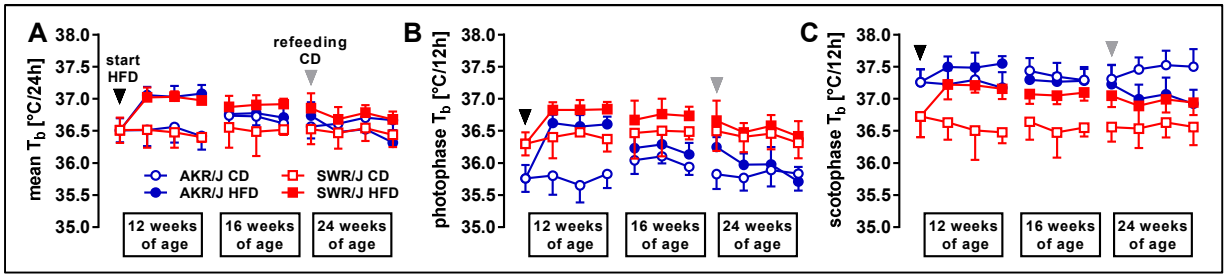


**Figure 34: Body core temperature ($T_b$) of AKR/J and SWR/J mice during FDA measurement.** $T_b$ was detected by implanted transmitters and expressed **(A)** as mean over 24 hours and separately for **(B)** photophase and **(C)** scotophase. Measurements were conducted at the age of 12 weeks when AKR/J and SWR/J mice received either control diet (CD) or high-fat diet (HFD) for 4 days, at the age of 16 weeks for 3 days and at the age of 24 weeks for 4 days when HFD fed mice were re-fed with CD ad libitum. For statistical differences see appendix; n=7-8.

Total activity counts did not differ between any strain or diet groups throughout the whole 24 weeks feeding intervention (figure 35A). Regarding activity extremes, SWR/J mice tended to spend more time rearing than AKR/J mice (figure 35B), with significance emerging solely between AKR/J and SWR/J mice fed CD. AKR/J mice did not show climbing activity, whereas SWR/J mice spend one hour climbing on average (figure 35C). Climbing was not significantly different between diet groups or over time.

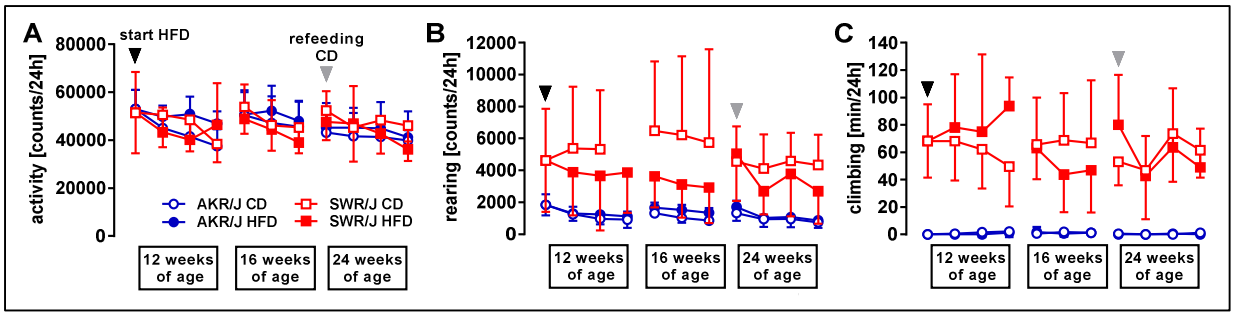


**Figure 35: Activity counts of AKR/J and SWR/J mice during FDA measurement. (A)** Activity was detected in three dimensions and **(B)** separately for vertical z-direction. Caused by temperature transmitter interruptions **(C)** climbing activity was measured. Measurements were conducted at the age of 12 weeks when AKR/J and SWR/J mice received either control diet (CD) or high-fat diet (HFD) for 4 days, at the age of 16 weeks for 3 days and at the age of 24 weeks for 4 days when HFD fed mice were re-fed with CD ad libitum. For statistical differences see appendix; n=7-8.

### 3.4.4. Energy expenditure

Indirect calorimetry measurements were conducted at eight time points during feeding intervention to assess resting metabolic rate (RMR), daily energy expenditure (DEE), maximal metabolic rate (MMR) and respiratory exchange ratio (RER). As observed in baseline characterization, fed CD RMR was higher in SWR/J mice, compared to AKR/J mice (figure 36A). HFD feeding induced RMR increase in both strains, but differences between diet groups were only seen in AKR/J mice. RMR of SWR/J mice was unaffected by diet and by time. During the first 4 weeks of HFD feeding, RMR of AKR/J mice rose further and stayed on elevated levels for the duration of ongoing HFD feeding. Refeeding CD declined RMR immediately to levels of AKR/J mice continuously fed CD. The trajectory of DEE and MMR during feeding intervention over eight measure points behaved in a comparable way to RMR (figure 36B, C). SWR/J mice augmented DEE and MMR after one week HFD feeding and remained on these, mostly not significantly higher levels for additional 11 weeks. A slight, not significant drop in energy expenditure was caused by refeeding CD. AKR/J on HFD diet increased DEE and MMR continuously, which was interrupted by refeeding CD at the age of 24 weeks. Then energy expenditure declined and remained on levels of CD fed animals. Irrespective of strain and feeding duration, RER showed levels of about 0.94 when mice were fed CD, and of about 0.85 with HFD feeding (figure 36D). Immediately after one week refeeding CD, refed SWR/J mice increased RER to CD levels whereas refed AKR/J mice needed more time in reaching RER of continuously CD fed mice.

Plotting DEE against the corresponding body mass showed a significant positive correlation of these two parameters for AKR/J and SWR/J mice fed CD at the age of 12 weeks (figure 36E, appendix). When fed HFD, AKR/J increased body mass, but DEE did not increase proportionally. Significance of correlation vanished for AKR/J mice in both diet groups for the rest of the intervention, except for the CD group at 32 weeks of age. RMR was not correlated significantly to body mass at any measure point for any diet group (appendix). Generally, the correlation plots

of DEE/RMR and body mass for SWR/J mice were significant for CD groups at the age of 12 and 16 weeks and appeared diffusely for the other correlations (appendix).

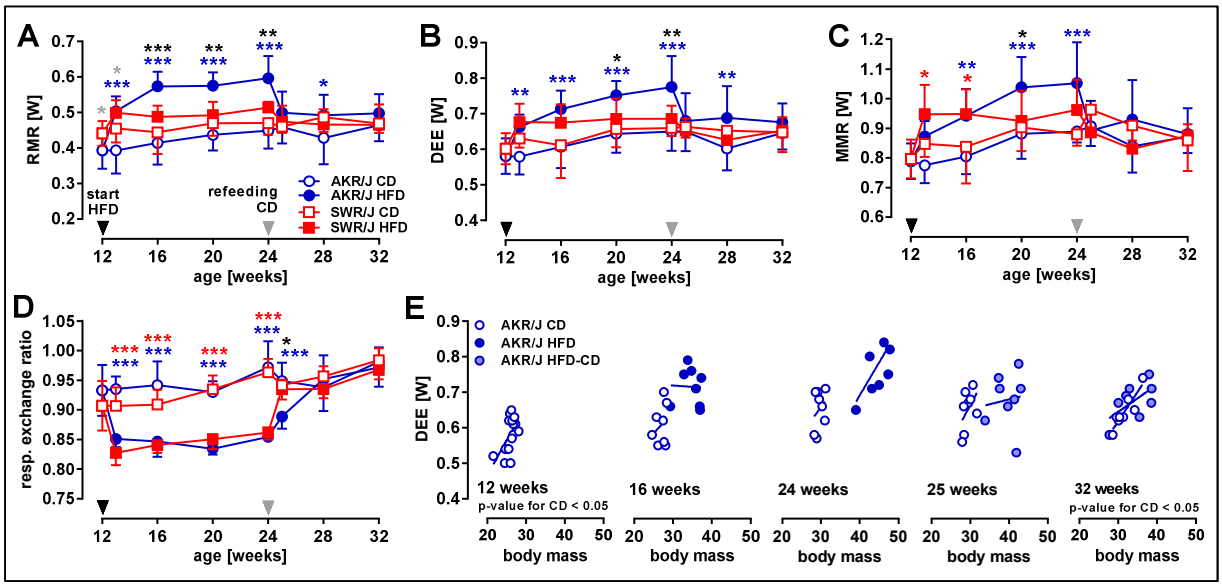


**Figure 36: Indirect calorimetry of AKR/J and SWR/J mice during high-fat diet feeding and refeeding control diet. (A)** Resting metabolic rate (RMR), **(B)** daily energy expenditure (DEE), **(C)** maximal metabolic rate (MMR) and **(D)** respiratory exchange ratio (RER) were calculated 8 times during feeding intervention. **(E)** For the measurements with 12, 16, 24, 25 and 32 weeks of age, DEE of individual AKR/J mice was plotted against corresponding body mass. Differences were calculated using Two-Way ANOVA with Tukey's multiple comparison test; n=7-9; * $p < 0.05$; ** $p < 0.01$; *** $p < 0.001$. black asterisk AKR/J HFD(-CD) vs. SWR/J HFD(-CD), grey asterisk AKR/J CD vs. SWR/J CD, blue asterisk AKR/J CD vs. AKR/J HFD(-CD), red asterisk SWR/J CD vs. SWR/J HFD(-CD); for more correlation plots an statistics see appendix; CD, control diet; HFD, high-fat diet.

### 3.4.5. Glucose, insulin and pyruvate tolerance

To assess the influence of HFD and obesity on glucose metabolism glucose, insulin and pyruvate tolerance tests were conducted. Within strains basal blood glucose levels after 1.5 days of HFD feeding did not differ (figure 37A, B). Comparing strains revealed higher glucose concentrations in AKR/J than in SWR/J mice, independent of diet (statistics see appendix). Throughout the whole feeding intervention, SWR/J mice showed no differences between diet groups. With ongoing age there was a tendency towards lower basal glucose levels. In AKR/J mice, one week of HFD feeding increased basal glucose to levels of about 160 mg/dl, revealing significant differences, compared to CD fed animals. Higher levels in HFD fed AKR/J mice persisted with ongoing HFD feeding. CD fed mice had fasting glucose levels of about 130 mg/dl, which were reached by former HFD fed mice after one week refeeding CD.

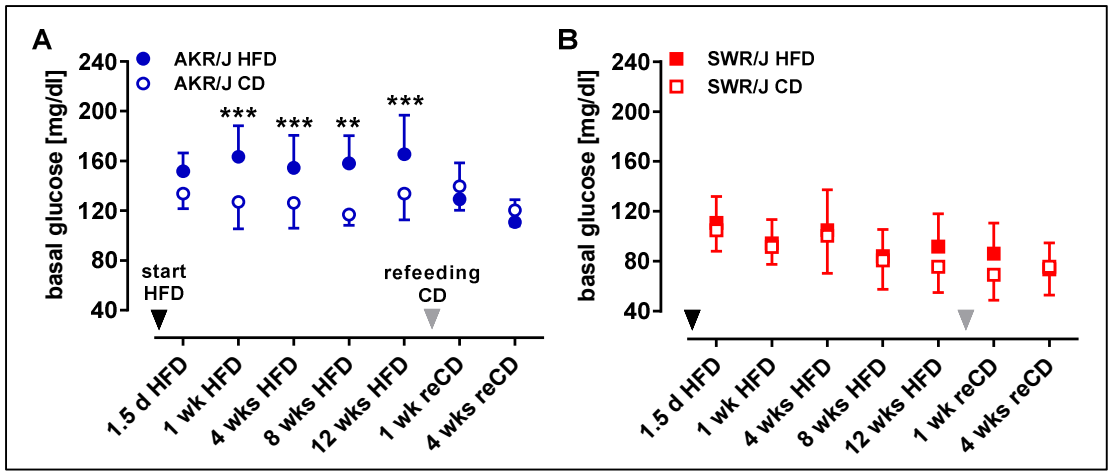


**Figure 37: Basal glucose levels of AKR/J and SWR/J mice during high-fat diet feeding and refeeding control diet.** In advance of glucose, insulin and pyruvate tolerance test basal glucose levels after 6 hours fasting were measured. Data were collected for every time point during feeding intervention and expressed for **(A)** AKR/J and **(B)** SWR/J mice. Differences were calculated using Two-Way ANOVA with Sidak multiple comparison test; n=7-38; ** $p < 0.01$; *** $p < 0.001$; statistic for comparison of strain see appendix; CD, control diet; HFD, high-fat diet.

Immediately after 1.5 days, HFD feeding led to altered oral glucose tolerance (figure 38A, D). Independent of strain, mice fed HFD responded to an orally administered glucose bolus by increasing blood glucose levels higher than corresponding CD fed mice. Due to higher glycemia peak at 15 min, the first glucose clearance point 30 min after gavage was increased in HFD fed mice. Further measure points did not differ between diet groups, neither did the total area under the curve (tAUC) (figure 38A, B).

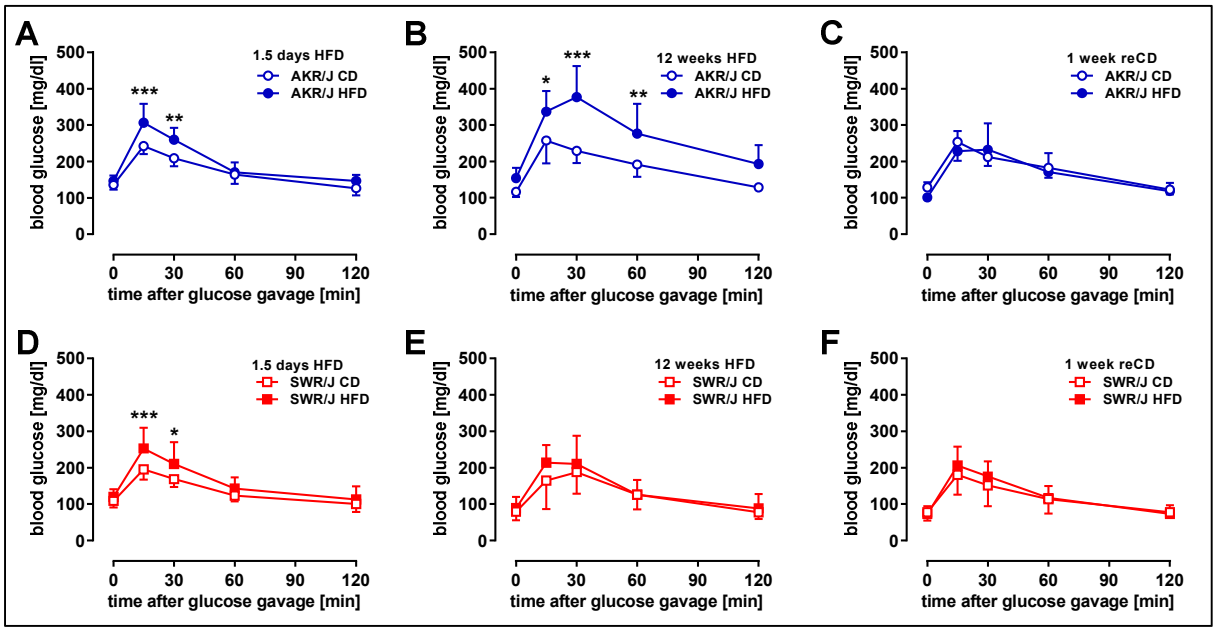


**Figure 38: Glucose tolerance in AKR/J and SWR/J mice during high-fat diet feeding and refeeding control diet.** Blood glucose curves in response to glucose gavage after **(A, D)** 1.5 days and **(B, E)** 12 weeks of high-fat diet (HFD) feeding and after **(C, F)** 1 week refeeding control diet (CD) in AKR/J and SWR/J mice (2.8 g glucose/kg lean mass). Differences were calculated using Two-Way ANOVA with Tukey's multiple comparison test; n=7-9; *$p < 0.05$; ** $p < 0.01$; *** $p < 0.001$; statistic for comparison of strain see appendix.

During HFD feeding, glucose tolerance was additionally measured after 1, 4, 8 (see appendix for blood glucose curves) and 12 weeks. After 1 week, impaired glucose tolerance in AKR/J mice on HFD was clearly obvious due to elevated glucose levels during the oral glucose tolerance test and by calculation of tAUC (figure 38A). Glucose tolerance improved after 4 weeks, marked by no differences in tAUC, but worsened with ongoing HFD feeding for 8 and 12 weeks. At the endpoint of HFD feeding after 12 weeks, still fasting glycemia did not differ between diet groups of AKR/J mice. But blood glucose levels increased dramatically after glucose gavage in HFD fed AKR/J mice, peaking after 30 min and leading to a significantly enhanced tAUC and iAUC (figure 38B, appendix). Impaired glucose tolerance vanished completely after 1 week of refeeding CD to former HFD fed AKR/J mice (figure 38C). SWR/J mice showed altered glucose tolerance in early stages of HFD feeding (after 1.5 days and 1 week, figure 38D, appendix,), but subsequently CD and HFD fed mice showed equal glycemia during oral glucose tolerance tests (figure 38E, F, appendix). Therefore, neither tAUC nor iAUC differed at any time between diet groups of SWR/J mice (figure 39B, appendix). Comparing tAUC of both strains within diet groups revealed significantly higher tAUC in AKR/J mice since 13 weeks of age onwards, respectively (appendix).

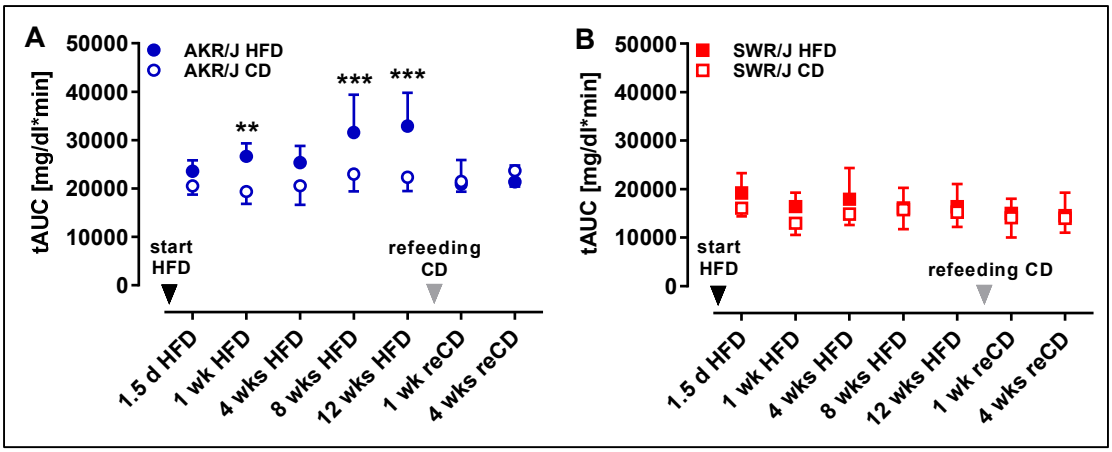


**Figure 39: Total area under the curve of glucose tolerance test in AKR/J and SWR/J mice.** Total area under the curve was calculated of oral glucose tolerance tests during high-fat diet (HFD) feeding and refeeding control diet (CD) of **(A)** AKR/J and **(B)** SWR/J mice. Differences were calculated using Two-Way ANOVA with Tukey's multiple comparison test; n=7-9; ** $p < 0.01$; *** $p < 0.001$, statistic for comparison of strain see appendix.

Furthermore, insulin tolerance was assessed during feeding intervention. Reaction to insulin was altered neither in AKR/J nor in SWR/J mice after 1.5 days HFD feeding, compared to respective CD groups (figure 40A, D). Nevertheless, between strains the glucose-decreasing effect of insulin differs dramatically. AKR/J mice lowered blood glucose to levels of about 65 % basal glucose, whereas in SWR/J mice glycemia dropped to levels of about 20 % basal glucose. After 1 and 4 weeks HFD feeding (see appendix), SWR/J mice responded highly sensitively to insulin, independent of diet. AKR/J mice fed HFD displayed more and more resistance to insulin, marked by a glucose decline of about 85 % of basal levels (4 weeks HFD). Likewise, insulin had

almost no effect on blood glucose levels in AKR/J mice on CD after 12 weeks feeding intervention (figure 40B). HFD fed AKR/J mice of the same age even responded to insulin injection with a significant blood glucose elevation. Refeeding CD for 1 week normalized insulin reaction to CD fed AKR/J mice, but both groups showed insulin resistance (figure 40C). With a 15 min delayed effect on blood glucose, SWR/J mice remained insulin sensitive at the end of 12 weeks HFD feeding and after refeeding CD (figure 40E, F).

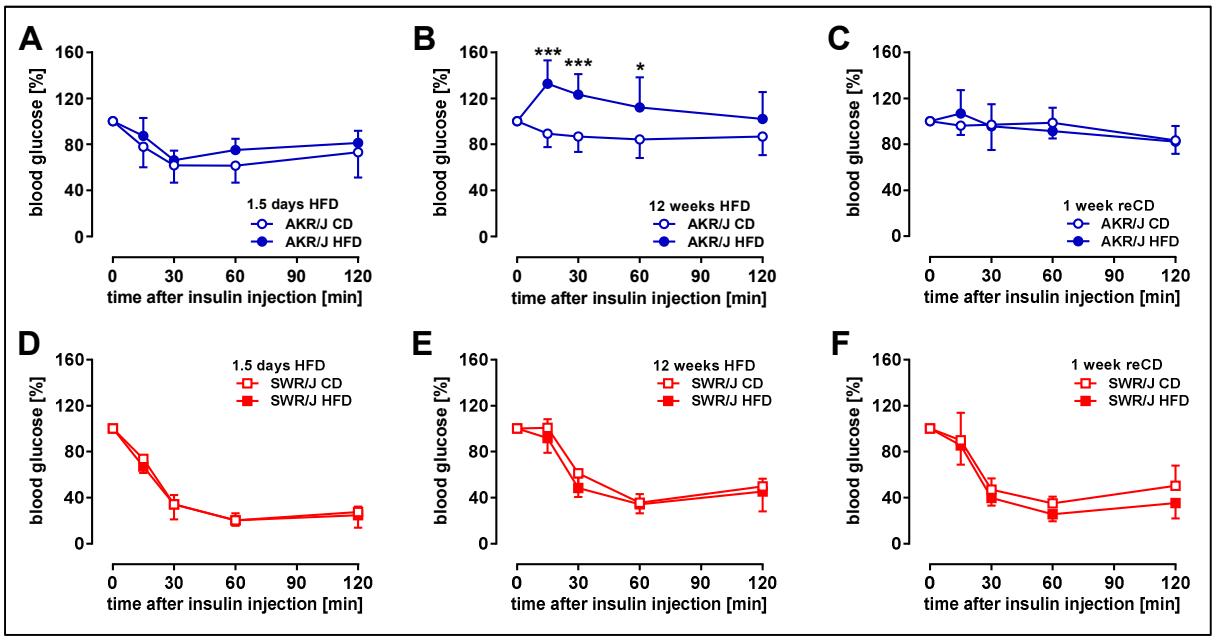


**Figure 40: Insulin tolerance of AKR/J and SWR/J mice during high-fat diet feeding and refeeding control diet.** Blood glucose curves in response to insulin injection (0.75 U/kg lean mass) after **(A, D)** 1.5 days and **(B, E)** 12 weeks of high-fat diet (HFD) feeding and after **(C, F)** 1 week refeeding control diet (CD) in AKR/J and SWR/J mice. Blood glucose levels 15, 30, 60 and 120 minutes after injection were calculated as %change to basal blood glucose levels. Differences were calculated using Two-Way ANOVA with Tukey's multiple comparison test; n=5-8; *p < 0.05; ** p < 0.01; *** p < 0.001; statistic for comparison of strain see appendix.

Due to higher basal blood glucose levels in AKR/J mice fed HFD, compared to CD fed mice, the area under the curve, as quantification of insulin tolerance, was significantly elevated throughout the whole HFD feeding (see appendix). Calculation of the area under the curve with values of %change blood glucose to basal glucose levels revealed no differences between diet groups within one strain except after 12 weeks of feeding intervention, when HFD fed AKR/J mice had higher tAUC [%] than CD fed AKR/J mice (figure 41A, B). AKR/J and SWR/J mice tended to increase tAUC [%] with age. Independent of diet, AKR/J mice exhibited higher tAUC [%] than SWR/J mice.

For an indirect assessment of hepatic gluconeogenesis pyruvate tolerance tests were conducted in AKR/J mice. In response to oral pyruvate administration blood glucose levels in mice fed HFD diet for 1 week rose higher than that in CD fed mice (figure 42A).

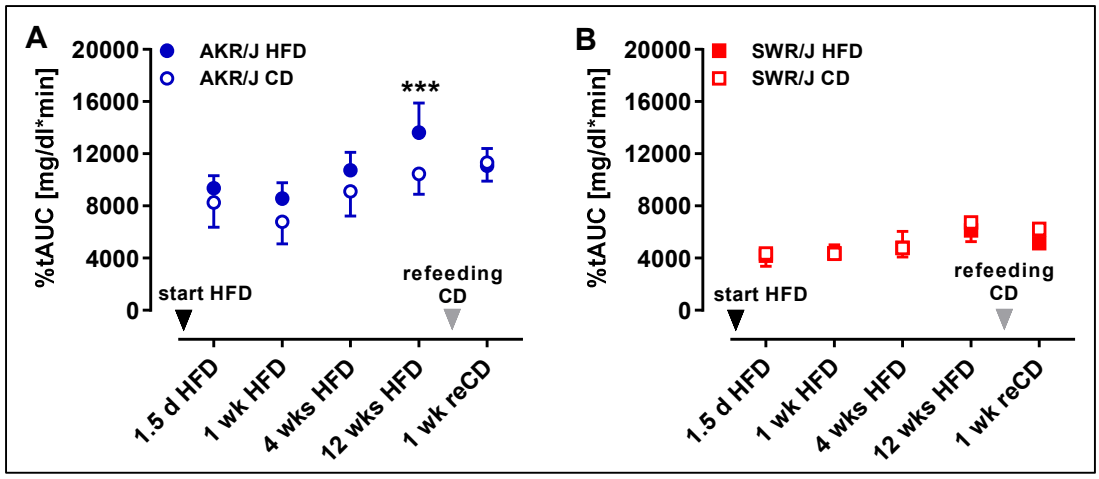


**Figure 41: Total area under the curve of insulin tolerance test in AKR/J and SWR/J mice.** Total area under the curve was calculated of %change of blood glucose to basal glucose levels after insulin injection over time (data of figure 41) for **(A)** AKR/J and **(B)** SWR/J mice. Differences were calculated using Two-Way ANOVA with Tukey's multiple comparison test; n=5-8; *** p < 0.001; CD, control diet; HFD, high-fat diet.

Comparing different feeding durations showed the most pronounced response to pyruvate in mice fed HFD for 4 weeks, as indicated by significantly elevated blood glucose levels at every measure point after pyruvate gavage (figure 42B), a higher tAUC and iAUC (figure 42C, F). After 12 weeks HFD, increased blood glucose levels after pyruvate bolus were mainly due to higher basal glucose levels (figure 42D). Refeeding CD for 1 week reversed elevated glucose levels prior to and during the pyruvate tolerance test in former HFD fed mice (figure 42E).

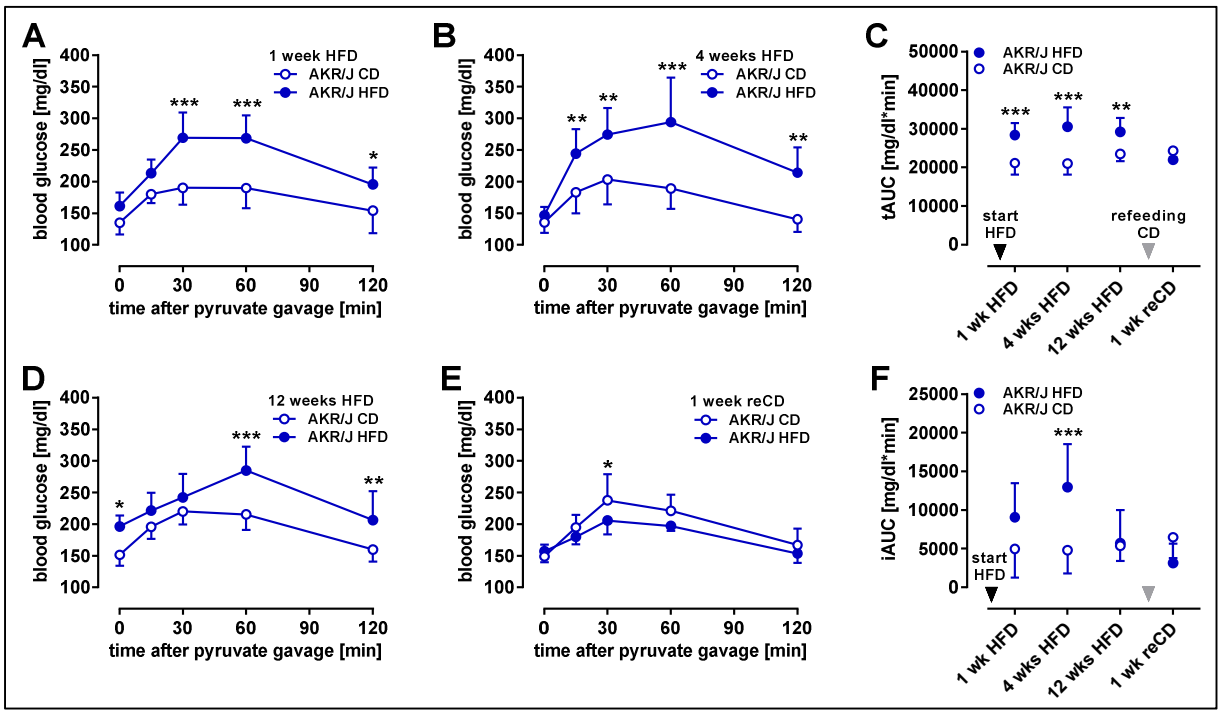


**Figure 42: Pyruvate tolerance of AKR/J mice during high-fat diet feeding and refeeding control diet.** Blood glucose curves in response to pyruvate gavage (2.8 g/kg lean mass) after **(A)** 1 week, **(B)** 4 weeks and **(D)** 12 weeks high-fat diet (HFD) feeding and after **(E)** refeeding control diet (CD) in AKR/J mice. **(C)** Total and **(F)** incremental area under the curve were calculated based on blood glucose progression after pyruvate bolus. Differences were calculated using Two-Way ANOVA with Tukey's multiple comparison test; n=7-8; *p < 0.05; ** p < 0.01; *** p < 0.001.

## 3.5. Effects of anabolic and catabolic status in AKR/J mice

Prior observations in AKR/J mice demonstrated that alterations in glucose metabolism caused by 12 weeks of HFD feeding were reversible within one week of refeeding CD. At the same time, mice were still obese, leading to the conclusion that not the amount of fat per se, but the status of adipose tissue is crucial for metabolism regulation. The question arose as to whether amelioration of HFD induced effects can also be achieved through restricted HFD feeding. Therefore, AKR/J mice were assigned to 5 feeding regimes (see 2.2.2.), generating different metabolic statuses for the characterization of body composition, glucose tolerance, plasma parameters, hepatic morphology, liver and adipose tissue transcripts.

### 3.5.1. Body mass, body composition and oral glucose tolerance

AKR/J mice received 5 different diet regimes for 13 weeks, starting at 12 weeks of age: one group was fed the control diet (CD), one the high-fat diet (HF-HF) throughout the whole intervention phase. To induce obese but simultaneously catabolic statuses, some mice that were fed for 12 weeks with HFD received either CD for one week (HF-CD), or were pair-fed with HFD to the energy amount of the HF-CD group (HF-pf). The fifth group started with HFD at the age of about 22 weeks in order to match the two catabolic groups (CD-HF). At the end of feeding intervention at the age of 25 weeks, the body mass of AKR/J mice in the anabolic CD-HF, catabolic HF-CD and HF-pf groups was not distinguishable (figure 43A). CD mice weighed about 5 g less and HF-HF mice about 5 g more than the three moderately obese diet groups. Lean mass was comparable in groups of CD, HF-CD, HF-pf and CD-HF, whereas lean mass was increased in HF-HF mice (figure 43B). Final fat mass showed the same pattern as body mass, with significantly lowest fat mass in CD mice, the highest fat mass in HF-HF mice and intermediate fat mass for CD-HF, HF-CD and HF-pf mice (figure 43C).

Glucose tolerance was tested at the end of feeding intervention. Prior measured basal glucose levels differed depending on diet groups. Despite moderate obesity, mice of both catabolic diet groups (HF-CD, HF-pf) had lower glycemia than CD fed animals (figure 43E). Furthermore, independent of duration (HF-HF 13 weeks, CD-HF 3-4- weeks), HFD fed AKR/J mice showed higher basal glucose levels than other groups. In response to glucose gavage, increase and clearance of glucose was equal in CD and catabolic mice, also being marked by no differences in area under the curve (figure 43D, F). HF-HF mice reacted to glucose bolus with the highest blood glucose elevation after 30 minutes. Consequently, the area under the curve was greater than in all other diet groups (figure 43F). Oral glucose tolerance as indicated by blood glucose levels, as

well as by the area under the curve of CD-HF mice, was intermediate, lying between HFD and CD fed animals.

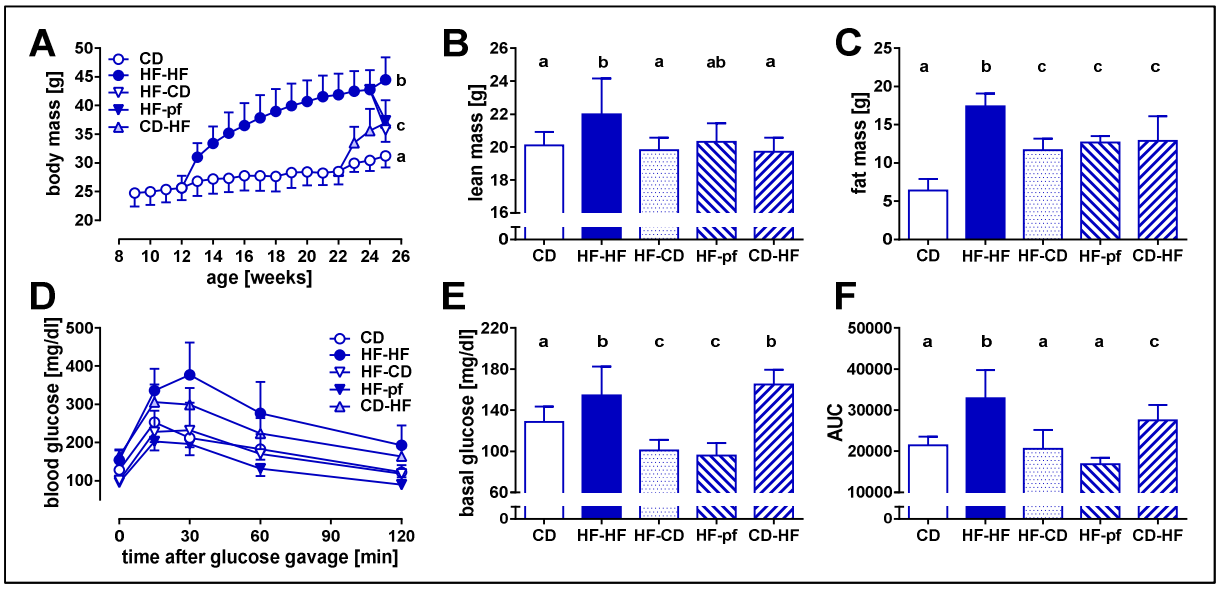


**Figure 43: Body mass, body composition and glucose tolerance parameters of AKR/J mice fed 5 different diet regimes. (A)** Body mass development during feeding intervention. **(B)** Lean mass and **(C)** fat mass at the end of feeding intervention with 25 weeks of age. **(D)** Blood glucose curves at the age of 25 weeks during oGTT. **(E)** Basal glucose levels after 6 hours fasting prior to oGTT and **(F)** total area under the blood glucose curves of oGTT. For all graphs, different letters present significant differences between diet groups at the end of feeding intervention calculated using One-Way ANOVA with Tukey's multiple comparison (n=8-13); CD, control diet; HF, high-fat diet (plant-based with 48 kJ% of fat); pf, pair-fed; oGTT, oral glucose tolerance test.

### 3.5.2. Plasma and liver parameter

Plasma concentrations of insulin and leptin, hormones crucial for glucose metabolism, were detected at the end of feeding intervention in fasted mice. Insulin concentrations in mice of CD, HF-CD and HF-pf groups were comparable, whereas levels in mice fed 3-4 weeks HFD (CD-HF) were almost doubled and levels in mice after 13 weeks on HFD (HF-HF) showed a nearly 5fold increase, compared to CD (figure 44A). Leptin levels in obese mice with catabolic metabolism were slightly elevated in HF-CD mice and significantly increased when fed restricted high-fat diet (HF-pf), compared to CD mice. Likewise, depending on duration, HFD feeding led to 5fold (CD-HF) and 10fold (HF-HF) higher leptin levels than CD feeding (figure 44D). Moderately anabolic status caused by 3-4 weeks HFD feeding did not affect plasma levels of cholesterol and triglycerides (figure 44B, E). Catabolic metabolism led to a decrease in cholesterol of about 35 % and in triglycerides of about 20 %, compared to CD and CD-HF mice. On the other hand, prolonged HFD feeding initiated a 30 % rise of cholesterol and triglycerides levels in plasma. Comparison of diet groups regarding hepatic cholesterol and hepatic triglycerides levels revealed no significant variations in CD, HF-pf and CD-HF mice (figure 44C, F). But levels of both parameters were elevated in the livers of HF-HF and HF-CD mice compared to CD fed animals.

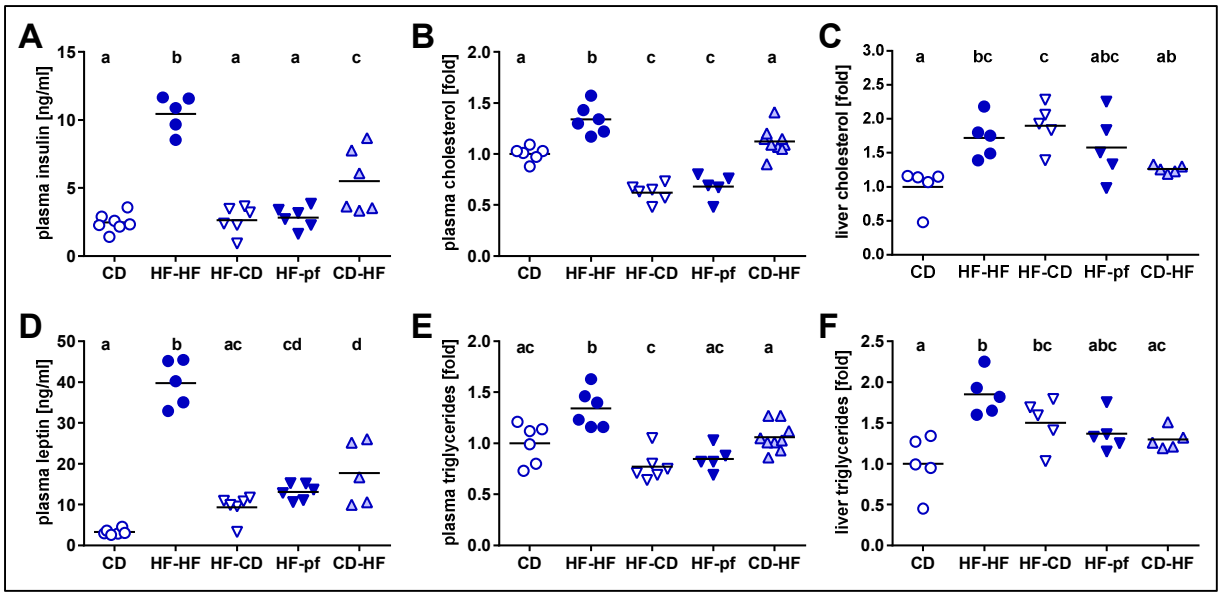


**Figure 44: Plasma and liver parameters of AKR/J mice fed 5 different diet regimes.** After feeding intervention AKR/J mice and fasting for about 6 hours, plasma and liver were collected and analyzed. **(A)** Insulin and **(D)** leptin concentrations in plasma were detected by enzyme-linked immunosorbent assay (ELISA), **(B)** cholesterol and **(E)** triglycerides in plasma were measured on reaction discs in a fully automated blood chemistry analyzer and values normalized to the mean of CD mice, **(C)** hepatic cholesterol and **(F)** triglycerides were analyzed using an enzymatic calorimetric endpoint kit and values normalized to the mean of CD mice. For all graphs, different letters present significant differences between diet groups at the end of feeding intervention calculated using One-Way ANOVA with Tukey's multiple comparison (n=5-9); CD, control diet; HF, high-fat diet; pf, pair-fed.

Besides oral glucose tolerance testing, glucose metabolism was additionally analyzed using gene expression analysis of relevant genes in the liver. The only difference in the abundance of genes of gluconeogenesis (G6p, Pck1) and glycolysis (Fbp) was seen for HF-pf mice displaying about 4fold upregulated G6p expression (figure 45A, B, C). Glucose transporter 4 expression (Slc2a4) was downregulated in all HFD containing groups to less than 50 % of levels of CD fed animals (figure 45D). Transcript abundance was unchanged between diet groups for insulin signaling genes Slc2a2, Insr and Socs3 (figure 45E, F, G).

Fatty liver status was assessed by a histological staging system. Initially, morphology of the hepatocytes was investigated and infiltration of fat per hepatocyte evaluated. Pronounced lipidosis, marked by distinct fat droplet inclusions between and within hepatocytes could be observed in HF-HF and HF-pf livers (figure 45H). Hepatocytes of HF-CD and CD-HF mice are characterized by small microvesicular fat infiltrations and scattered lipid droplets. Furthermore, the spread of lipidosis means that the grade of affected tissue was estimated (figure 45I). There was a wide range of individual differences within diet groups. Overall in HF-HF mice about 33-66 % of liver tissue was affected by fat infiltration (grade 2), whereas the grade in HF-CD, HF-pf and CD-HF was comparable with about 25 % affected tissue on average. Since two CD fed mice showed small indications of fatty liver, there was no statistical difference.

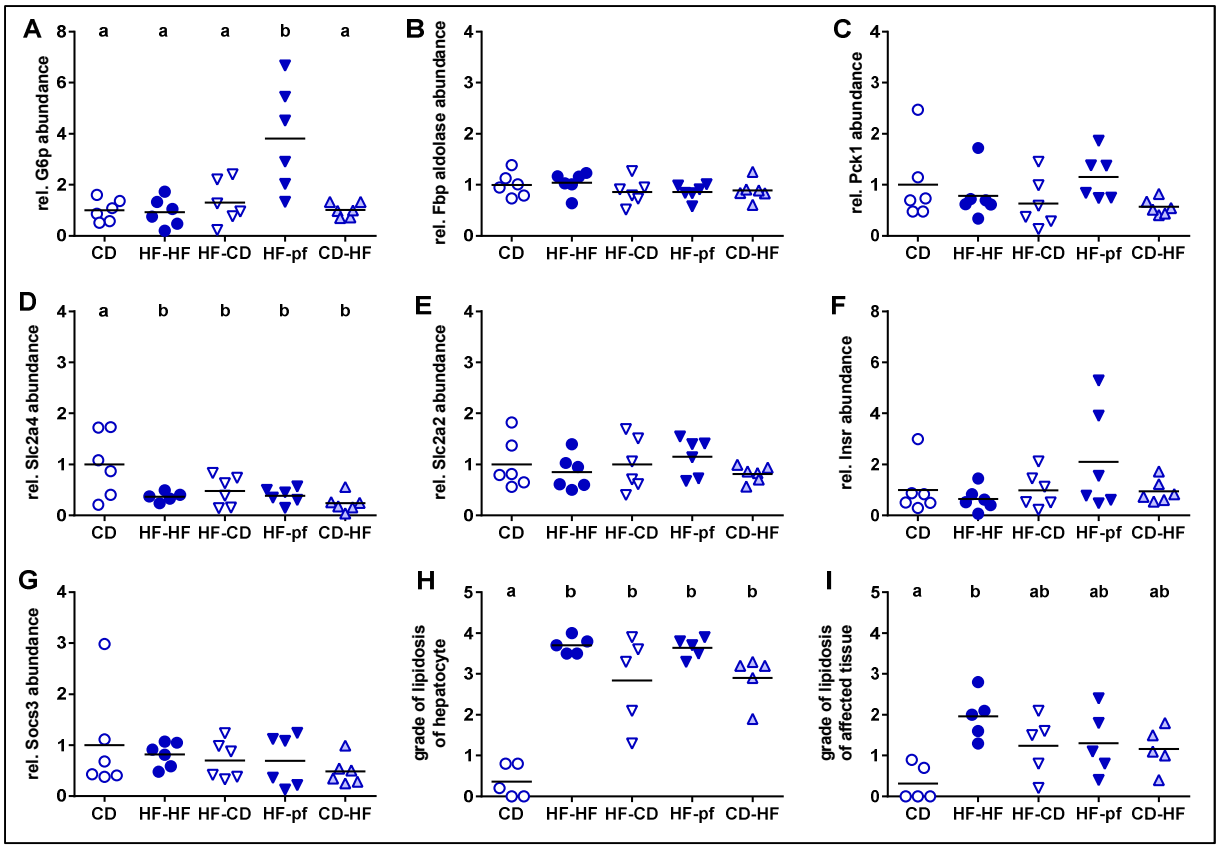


**Figure 45: Hepatic gene expression and grade of lipidosis of AKR/J mice fed 5 different diet regimes.** Abundance of genes of hepatic glucose metabolism was measured by qPCR related to housekeeping genes (Hprt, Hmbs): **(A)** G6p (glucose-6-phosphatase), **(B)** Fbp (fructose-bisphosphate aldolase B), **(C)** Pck1 (phosphoenolpyruvate carboxykinase 1), **(D)** Slc2a4 (glucose transporter 4), **(E)** Slc2a2 (glucose transporter 2), **(F)** Insr (insulin receptor), **(G)** Socs3 (suppressor of cytokine signaling 4); abundances were normalized to the mean of CD mice. Hepatic steatosis was classified by a histological staging system including **(H)** morphology/lipidosis of hepatocytes and **(I)** amount/grade of affected hepatic tissue. For all graphs, different letters present significant differences between diet groups at the end of feeding intervention calculated using One-Way ANOVA with Tukey's multiple comparison (n=5-6).

### 3.5.3. Adipose tissue

White adipose tissue depots were weighed at the end of feeding intervention. Independent of location, white adipose tissue depots of HF-HF mice showed about 3fold enlargement, compared to CD fed mice (figure 46A, B, C). Although total fat mass detected by NMR was unchanged between HF-CD, HF-pf and CD-HF (compare figure 43C) on depot levels, the anabolic CD-HF group showed larger eWAT and rWAT depots, compared to one or both catabolic groups. SWAT seemed to be quite stable in body mass decreasing conditions, as there are no differences between HF-HF and HF-pf groups. Nevertheless, between body mass matched HF-CD, HF-pf and CD-HF groups, sWAT mass was unaltered. For further investigation on transcript levels between these groups, eWAT was chosen, due to weight variation as a first hint to differences between catabolic and anabolic status.

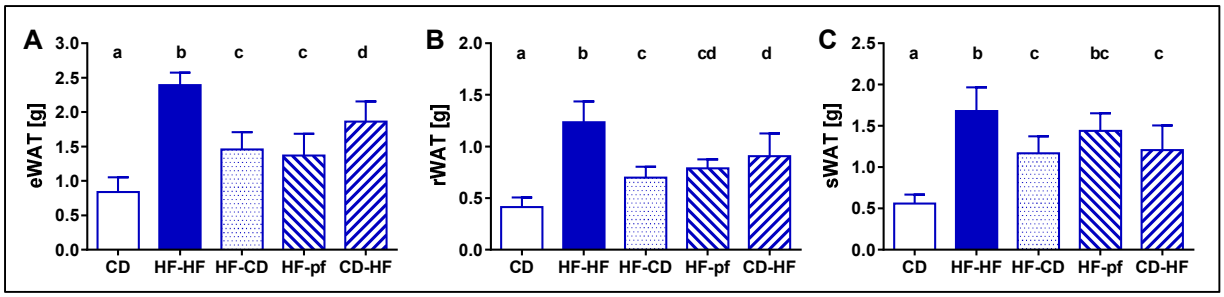


**Figure 46: White adipose tissue depots of AKR/J mice fed 5 different diet regimes**. **(A)** Epididymal, **(B)** pooled retroperitoneal perirenal and **(C)** subcutaneous white adipose tissue were prepared and weighed at the age of 25 weeks. For all graphs, different letters present significant differences between diet groups at the end of feeding intervention calculated using One-Way ANOVA with Tukey's multiple comparison (n=8-10); CD, control diet; HF, high-fat diet; pf, pair-fed.

Using transcriptome next generation sequencing and subsequent evaluation of results by genomatix software, eWAT RNA samples of 3 animals per HF-CD, HF-pf and CD-HF group were analyzed, respectively. Mass of eWAT was matched and did not differ between groups. First gene expression data of all groups was opposed to each other group (table 6). This exposed little difference within the catabolic groups HF-CD and HF-pf with only three regulated genes (Prph: mean log2 1.17, Abp1: mean log2 -2.07, Kctd14: mean log2 -1.87). Therefore, the type of diet for energy intake reduction after HFD feeding is nearly irrelevant for transcriptome differences. Gene expression of the anabolic group differed to HF-CD group in 543 genes and to HF-pf group in 992 genes. In both cases more genes were down regulated rather than up regulated in the anabolic status.

**Table 6: Regulated genes in eWAT of AKR/J mice with different metabolic status.** Catabolic status was initiated by caloric restriction after high-fat diet feeding either by ad libitum feeding of control diet (HF-CD) or by restricted high-fat diet feeding in a pair-fed manner to HF-CD energy intake (HF-pf). The third group was fed with high-fat diet for 3-4 weeks (CD-HF). EWAT transcriptomics were performed at the age of 25 weeks (n=3). Differences in expression were calculated using genomatix software.

| **Comparision** | **Regulated genes** | | |
|---|---|---|---|
| | n | up | down |
| HF-pf versus HF-CD | 3 | 1 | 2 |
| CD-HF versus HF-CD | 543 | 203 | 340 |
| CD-HF versus HF-pf | 992 | 392 | 600 |

Secondly, three combination set-ups were built to account for any possible arrangement, comparing gene expression of one group against the combination of the other two groups (figure 47). Most differences in gene expression revealed comparison of catabolic group (HF-CD, HF-pf) versus anabolic group, showing 314 up regulated and 549 down regulated genes. Pooling transcripts of the two groups that received high-fat diet either by restricted pair-feeding, or for 3-4 weeks ad libitum and opposing them to the control diet fed HF-CD group, revealed no

significant gene expression results. Pair-fed animals differed to the group combination of ad libitum fed mice in 9 genes (2 up regulated, 7 down regulated).

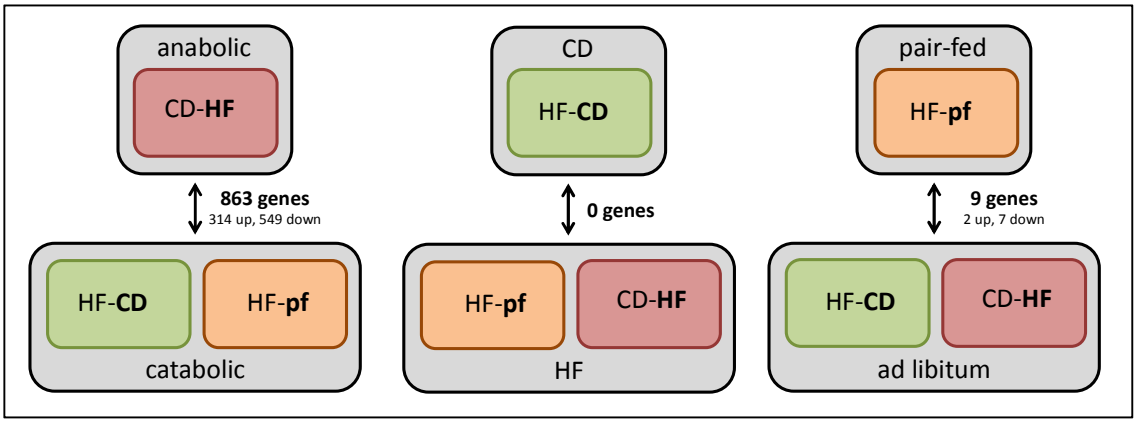


**Figure 47: Gene expression differences between combined groups.** Results of two groups with one similarity regarding metabolic status, diet and feeding type were compared to the third group, respectively. EWAT transcriptomics were performed at the age of 25 weeks (n=3). Differences in expression were calculated using genomatix analysis software; CD, control diet; HF, high-fat diet; pf, pair-fed.

Since analysis results pointed out that differences in eWAT gene expression between HF-CD and HF-pf groups were negligible, both groups were united and named as a catabolic group. Additionally, because analysis revealed most differences between transcripts of anabolic and catabolic eWAT, further investigations focussed on the comparison of these two groups. In total, 18.701 transcripts were identified with 10 or more total reads (mean per group) and assigned to known genes.

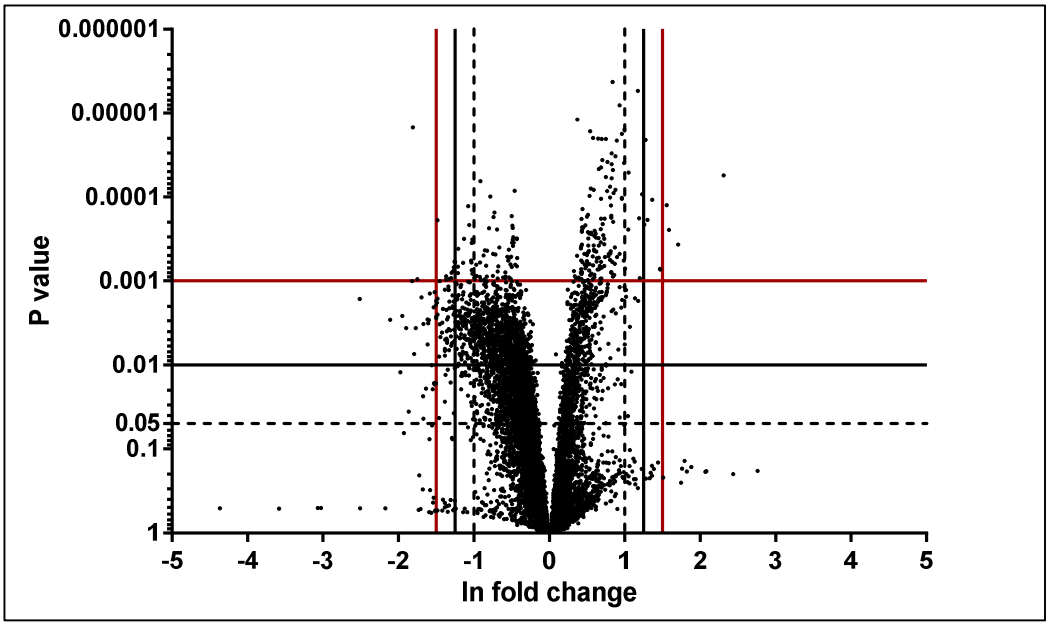


**Figure 48: Volcano plot of gene expression differences of anabolic and catabolic eWAT.** All mapped genes (black dots) are represented in dependence of p-value to ln fold change between groups. Different lines define low, middle and high criteria (table 7).

To find differences of gene expression between the anabolic and the catabolic groups, ln-fold change and p-values were calculated manually for every gene. Results were displayed in a volcano plot to visualize distribution of p-value to ln fold change (figure 48). In accordance with the results of table 5, more genes were down than up regulated in the anabolic status, compared to catabolic status. For identification of the most regulated genes, low, middle and high criteria were determined (table 7). Lowest criteria revealed 242 regulated genes. 83 genes were regulated by applying middle criteria and, under the strictest conditions, 9 genes were differently expressed between groups.

**Table 7: Number of genes differing in expression between anabolic and catabolic status of eWAT referring to varying criteria.** RNA of eWAT of 9 AKR/J mice was analyzed by NGS. Gene expression results were compared between catabolic (n=6) and anabolic (n=3) groups by a combination of ln fold change and p-value.

| Criteria | Line in figure 48 | Anabolic up regulation | | Anabolic down regulation | | p-value |
|---|---|---|---|---|---|---|
| | | Ln change | n | Ln change | n | |
| low | dotted | ≥ 1.0 | 23 | ≤ -1.0 | 219 | ≤ 0.05 |
| middle | black | ≥ 1.2 | 9 | ≤ -1.2 | 74 | ≤ 0.01 |
| high | dark red | ≥ 1.5 | 4 | ≤ -1.5 | 5 | ≤ 0.001 |

In more detail: the 5 most down regulated genes in anabolic eWAT were Gpr50, Fabp3, Gpnmb, Nptx1 and Lair1. The list of 4 up regulated genes consisted of Trhade, Pnpla3, Orm3 and Ear11 (table 8). Using InCroMAP transcript analysis, regulated genes were classified and annotated to KEGG pathways. For the short list of 9 genes matching the high criteria pathway of glycerolipid metabolism and PPAR signaling pathway were found to be significantly regulated. However, this result is only based on two genes namely Pnpla3, a lipase that mediates triacylglycerol hydrolysis, and fatty acid binding protein (Fabp3).

**Table 8: 9 genes with most differences in expression between anabolic and catabolic of eWAT according to high criteria.** Gene expression is displayed as total reads of the transcript. Criteria for differences were ln change ≥ 1.5 or ≤ -1.5 and p-value 0.001; anabolic: n=3, catabolic: n=6. Identified genes: G-protein-coupled receptor 50 (Gpr50), fatty acid binding protein 3 (Fabp3), glycoprotein nmb (Gpnmb), neuronal pentraxin 1 (Nptx1), leukocyte-associated Ig-like receptor 1 (Lair1), TRH-degrading enzyme (Trhde), patatin-like phospholipase domain containing 3 (Pnpla3), orosomucoid 3 (Orm3), eosinophil-associated, ribonuclease A family, member 11 (Ear11); SD, standard deviation, CV, coefficient of variation.

| Gene | Anabolic total reads | | | Catabolic total reads | | | ln fold change | p-value |
|---|---|---|---|---|---|---|---|---|
| | mean | SD | CV | mean | SD | CV | | |
| Gpr50 | 19 | 14 | 72 | 117 | 29 | 25 | -1.819 | 0.001 |
| Fabp3 | 11 | 6 | 57 | 67 | 8 | 11 | -1.809 | 0.000 |
| Gpnmb | 2,470 | 1,530 | 62 | 14,181 | 3,458 | 24 | -1.748 | 0.001 |
| Nptx1 | 46 | 31 | 66 | 224 | 55 | 25 | -1.583 | 0.001 |
| Lair1 | 218 | 109 | 50 | 998 | 245 | 25 | -1.521 | 0.001 |
| Trhde | 142 | 33 | 24 | 30 | 13 | 43 | 1.555 | 0.000 |
| Pnpla3 | 6,571 | 1,909 | 29 | 1,344 | 423 | 31 | 1.587 | 0.000 |
| Orm3 | 99 | 31 | 32 | 18 | 8 | 45 | 1.705 | 0.000 |
| Ear11 | 1,241 | 319 | 26 | 123 | 77 | 63 | 2.311 | 0.000 |

Notably, the coefficient of variation (CV) was very high for this high criteria gene list, thus standing for big individual differences within one diet group. Therefore, further possible evaluations were applied to compare anabolic and catabolic gene expression. Taking the 83 genes matching middle criteria and reducing CV to less than 33 %, resulted in 10 down regulated genes (Slc6a7, Trpc4, Pou2f2, Rasgrf1, Prrx2, Hpca, Stac2, Bsn, Speg, Fyb) and 2 upregulated genes (Retnla, Pnpla3) in anabolic eWAT (appendix). Merely the identification of Pnpla3 overlapped with previous results in the high criteria list. The only assigned pathway for this list was glycerolipid metabolism.

After searching the biggest differences in single gene expression, pathways were analyzed showing significant differences between anabolic and catabolic eWAT. Therefore, 236 of 242 regulated genes matching low criteria were evaluated by InCroMAP, taking account of ln-change and p-value. As a result, 20 pathways were identified that vary between anabolic and catabolic groups. The most differently regulated pathway was phagosome, with 11 regulated genes of 93 known to be involved in this pathway. Further pathways were characterized by involvement in infections and the immune system, such as natural killer cell mediated cytotoxicity or B cell receptor signaling pathway (table 9).

**Table 9: 20 pathways with differences in regulation between anabolic and catabolic eWAT.** Based on 236 genes differing in gene expression between anabolic and catabolic eWAT InCroMAP analysis tool determines regulated pathways. BG ratio presents the amount of genes attributed to respective pathway out of 14623 documented genes in the InCroMAP library.

| Pathway name | List ratio | BG ratio | p-value | genes |
|---|---|---|---|---|
| Phagosome | 11/236 | 93/14623 | < 0.001 | Olr1, Cd14, Cd209c, Ctss, Fcgr1, Msr1, Itgb2, Clec7a, Ncf4, Cybb, Fcgr4 |
| Osteoclast differentiation | 10/236 | 98/14623 | < 0.001 | Tnfrsf11a, Fhl2, Fcgr1, Trem2, Ncf4, Blnk, Tyrobp, Ctsk, Cybb, Fcgr4 |
| Natural killer cell mediated cytotoxicity | 8/236 | 71/14623 | < 0.001 | Lat, Ptpn6, Rac2, Vav1, Itgb2, Hcst, Tyrobp, Fcgr4 |
| B cell receptor signaling pathway | 7/236 | 54/14623 | < 0.001 | Ptpn6, Pik3ap1, Rac2, Card11, Vav1, Cd22, Blnk |
| Tuberculosis | 9/236 | 120/14623 | < 0.001 | Cd14, Cd209c, Ctss, Fcgr1, Itgb2, Clec7a, Itgax, Tlr1, Fcgr4 |
| Hematopoietic cell lineage | 7/236 | 77/14623 | < 0.001 | Cd4, Cd14, Cd5, Fcgr1, Il7r, Cd22, Anpep |
| Staphylococcus aureus infection | 5/236 | 37/14623 | < 0.001 | Cfd, Fcgr1, C3ar1, Itgb2, Fcgr4 |
| Cell adhesion molecules (CAMs) | 7/236 | 95/14623 | 0.001 | Siglec1, Nfasc, Cd4, Nrcam, Cadm1, Itgb2, Cd22 |
| Leukocyte transendothelial migration | 6/236 | 72/14623 | 0.001 | Mmp2, Rac2, Vav1, Itgb2, Ncf4, Cybb |
| Toll-like receptor signaling pathway | 6/236 | 75/14623 | 0.001 | Spp1, Cd14, Tlr8, Cd3, Ctsk, Tlr1 |

| | | | | |
|---|---|---|---|---|
| Leishmaniasis | 5/236 | 52/14623 | 0.001 | Ptpn6, Fcgr1, Itgb2, Ncf4, Fcgr4 |
| Fc gamma R-mediated phagocytosis | 5/236 | 53/14623 | 0.001 | Hck, Lat, Rac2, Fcgr1, Vav1 |
| Regulation of actin cytoskeleton | 8/236 | 147/14623 | 0.002 | Fgd3, Cd14, Rac2, Vav1, Itgad, Itgb2, Itgax, Nckap1l |
| Rheumatoid arthritis | 5/236 | 62/14623 | 0.003 | Tnfrsf11a, Itgb2, Cd3, Mmp3, Ctsk |
| T cell receptor signaling pathway | 5/236 | 81/14623 | 0.008 | Lat, Ptpn6, Cd4, Card11, Vav1 |
| NF-kappa B signaling pathway | 5/236 | 81/14623 | 0.008 | Tnfrsf11a, Lat, Cd14, Card11, Blnk |
| Primary immunodeficiency | 3/236 | 35/14623 | 0.016 | Cd4, Il7r, Blnk |
| Chemokine signaling pathway | 6/236 | 137/14623 | 0.017 | Hck, Ccr5, Cxcl14, Rac2, Vav1, Cd3 |
| Systemic lupus erythematosus | 3/236 | 42/14623 | 0.025 | Fcgr1, C7, Fcgr4 |
| Fc epsilon RI signaling pathway | 3/236 | 44/14623 | 0.028 | Lat, Rac2, Vav1 |

Besides random gene expression comparisions, and searching for most up and down regulated genes or pathways in catabolic and anabolic eWAT, targeted genes were also compared between feeding groups. Expression of genes in the adipose tissue derived hormones leptin, adiponektin and resistin was higher in anabolic CD-HF fed mice, compared to both catabolic groups, respectively (figure 49A, B, C). Expression patterns of hormone receptor genes were not defined clearly: leptin receptor RNA was higher expressed in eWAT of HF-CD fed mice, compared to both HFD fed groups (figure 49D). Adiponectin receptor 2 RNA was most abundant in anabolic mice, but was only significantly differently expressed between HF-pf and CD-HF groups (figure 49E). As for Adiponectin receptor2, lowest expression of insulin receptor was detected in the HF-pf group (figure 49F). HF-CD and CD-HF fed mice had similar Insulin receptor abundance.

Further expression of adipose tissue derived peptides with endocine function, as regarding adiposity, insulin resistance and inflammation, were compared between groups. Tumor necrosis factor α was significantly and interleukin 6 tendentially, down regulated in CD-HF mice (figure 50A, B). Apelin and retinol binding protein 4 was at a higher abundance in anabolic eWAT, compared to catabolic eWAT (figure 50C, F). Chemerin expression was increased in CD-HF mice, but only significantly to the pf-HF group (figure 50D). No differences, but a tendency to decreased abundance in the CD-HF group, could be found for monocyte chemotactic protein 1 and the serine peptidase inhibitor (figure 50E, G). Interferon gamma-induced protein 10 showed significantly lower expression in CD-HF mice than in HF-CD mice (figure 50H), whereas expression in HF-pf mice was intermediate to the other groups.

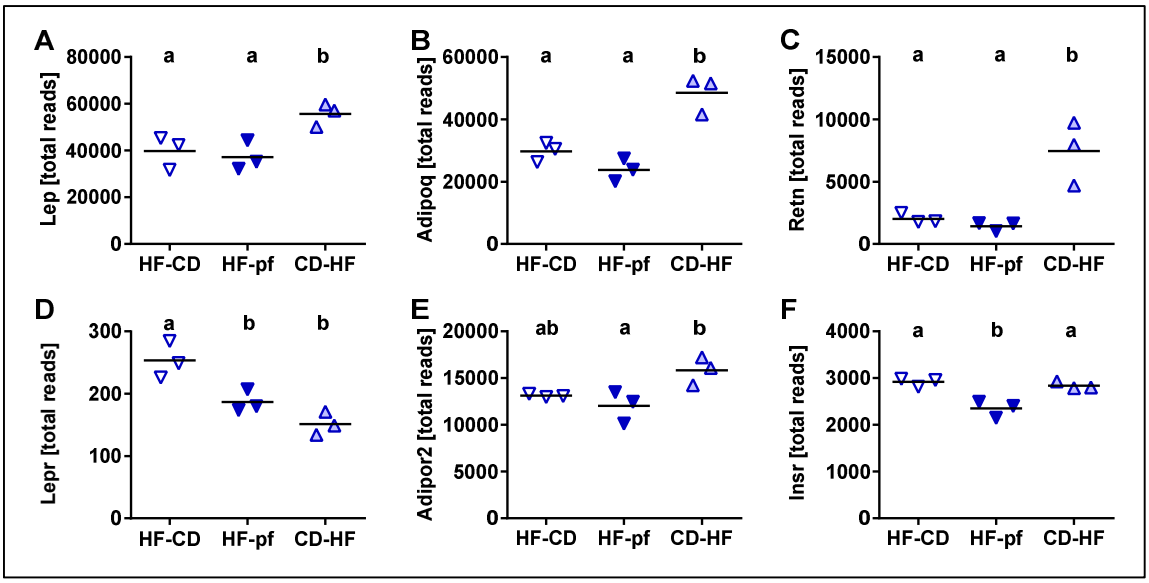


**Figure 49: Gene expression of adipose tissue derived hormones and receptors in eWAT.** RNA of eWAT of AKR/J mice with different feeding regimes was analyzed using next generation sequencing. **(A)** Leptin (Lep), **(B)** adiponectin (Adipoq), **(C)** resistin (Retn), **(D)** leptin receptor (Lepr), **(E)** adiponectin receptor 2 (Adipor2), **(F)** insulin receptor (Insr); different letters present significant differences between diet groups calculated using One-Way ANOVA with Tukey's multiple comparison (n=3); CD, control diet; HF, high-fat diet; pf, pair-fed.

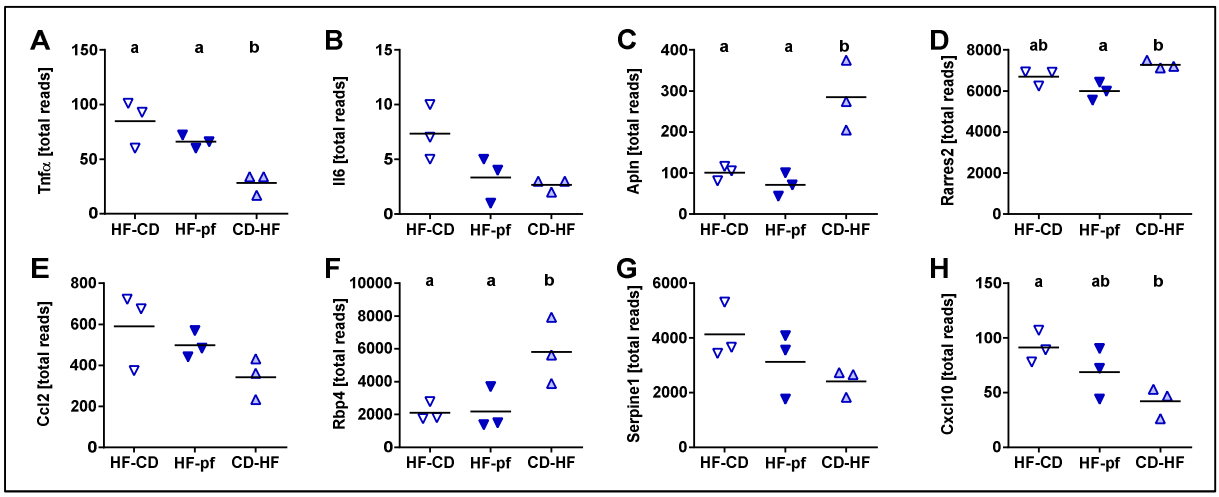


**Figure 50: Gene expression of adipokines in eWAT.** RNA of eWAT of AKR/J mice with different feeding regimes was analyzed by next generation sequencing. **(A)** Tumor necrosis factor alpha (Tnfα), **(B)** interleukin 6 (Il6), **(C)** apelin (Apln), **(D)** retinoic acid receptor responder or chemerin (Rarres2), **(E)** chemokine (C-C motif) ligand 2 or monocyte chemotactic protein 1 (Ccl2), **(F)** retinol binding protein 4 (Rbp4), **(G)** serine (or cysteine) peptidase inhibitor, clade E, member 1 (Serpine1), **(H)** C-X-C motif chemokine 10 or interferon gamma-induced protein 10 (Cxcl10); different letters present significant differences between diet groups calculated using One-Way ANOVA with Tukey's multiple comparison (n=3); CD, control diet; HF, high-fat diet; pf, pair-fed.

Genes involved in lipogensis, such as fatty acid synthase and Pnpla3 were obviously up regulated in the anabolic group, compared to both catabolic groups (figure 51B, D). Acaca and Tpi1 showed a clear trend to up-regulation in anabolic status, but abundance of genes was only significantly different between mice of the CD-HF and HF-pf group (figure 51A, C). On the other hand, Srebf2, Acacb and Cpt1b, all involved in fatty acid oxidation, were in significantly or at least tendentially higher abundance in both catabolic groups, compared to the anabolic group

(figure 51E, F, G). Only hormone-sensitive lipase had significantly higher expression levels in eWAT of CD-HF mice, compared to eWAT of HF-pf mice (figure 51H). Gene abundance in both catabolic groups was comparable in this analyzed expression set of 8 genes.

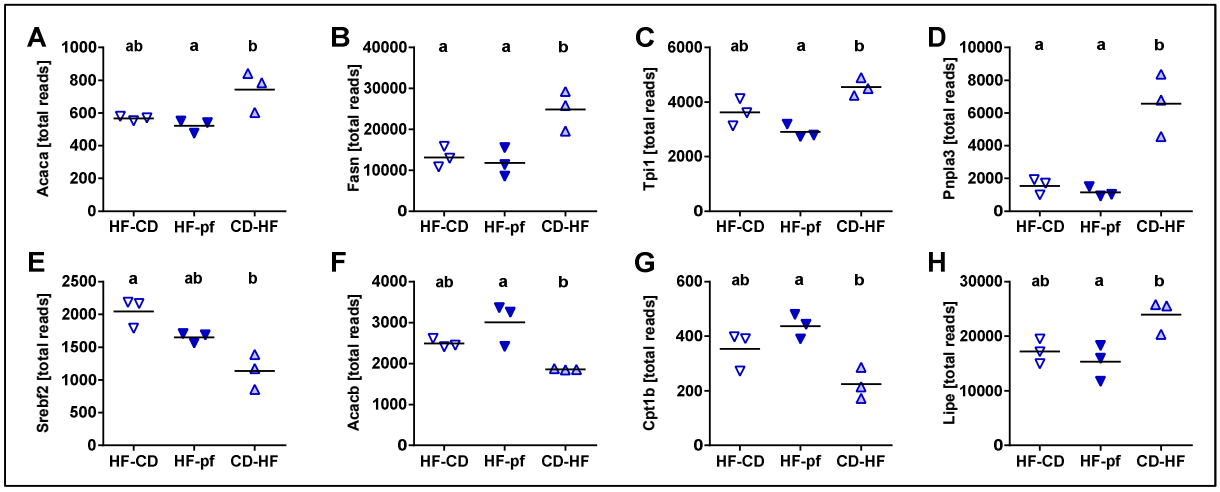


**Figure 51: Expression of genes involved in lipogenesis and fatty acid oxidation in eWAT.** RNA of eWAT of AKR/J mice with different feeding regimes was analyzed by next generation sequencing. Lipogenesis: **(A)** acetyl-Coenzyme A carboxylase alpha (Acaca), **(B)** fatty acid synthase (Fasn), **(C)** triosephosphate isomerase 1 (Tpi1), **(D)** patatin-like phospholipase domain containing 3 (Pnpla3); fatty acid oxidation: **(E)** sterol regulatory element binding factor 2 (Srebf2), **(F)** acetyl-Coenzyme A carboxylase beta (Acacb), **(G)** carnitine palmitoyltransferase 1b (Cpt1b), **(H)** hormone-sensitive lipase (Lipe); different letters present significant differences between diet groups calculated using One-Way ANOVA with Tukey's multiple comparison (n=3); CD, control diet; HF, high-fat diet; pf, pair-fed.

## 3.6. Heredity of diet-induced obesity – crossbreeding of AKR/J and SWR/J mice

### 3.6.1. Body mass and body composition

Cross breeding of obesity prone AKR/J and obesity resistant SWR/J mice strains was performed to investigate the heredity of characteristic traits. At weaning, offspring of F1 generation, bred by crossing male AKR/J and female SWR/J mice (AK-SWR/J), had similar body weights as AKR/J and SWR/J mice (figure 52A). Whereas SW-AKR/J pubs, the cross combination of male SWR/J and female AKR/J mice, weighed markedly more than the other three strains. These differences between strains were found in male and female mice (figure 52B, C). Notably, generally more than 8 pubs per litter were born in breeding pairs of male AKR/J and female SWR/J mice. SWR/J breeding pairs had a mean litter size of nearly 7, and the smallest litter size was observed in pairs with AKR/J females (AKR/J: 5.9 ± 1.9, SWR/J: 6.9 ± 2.3, AK-SWR/J: 8.2 ± 1.4, SW-AKR/J: 5.5 ± 2.1) (appendix). To eliminate the influence of different litter size and slight differences in weaning age (appendix) on weaning body mass, a linear relation was assumed. This resulted in

normalized body weight at weaning and changed differences between strains: all four strains differed significantly in body mass within the four strains. AKR/J mice had slightest adjustment in body weight, followed by SWR/J mice. The recombinant offspring AK-SWR/J weighed significantly more than AKR/J and SWR/J mice, but less than SW-AKR/J mice, and showed the highest body mass (appendix).

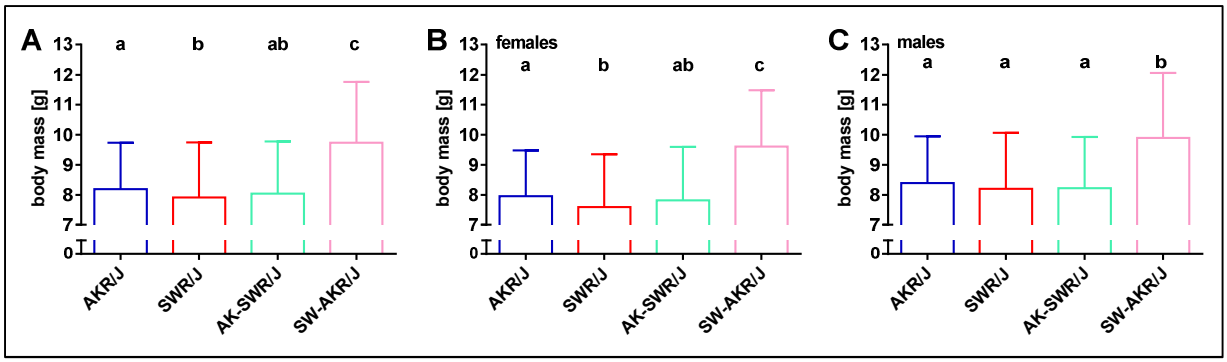


**Figure 52: Weaning body mass of AKR/J, SWR/J, AK-SWR/J and SW-AKR/J mice.** Mice were weighed at weaning with 18-22 days of age. Results are displayed for **(A)** all mice and separately for **(B)** female and **(C)** male mice. AKR/J: n=1036 (538 males, 498 females), SWR/J: n=946 (500 males, 446 females), AK-SWR/J: n=131 (72 males, 59 females), SW-AKR/J: n=70 (33 males, 37 females); different letters present significant differences between strains calculated using One-Way ANOVA with Tukey's multiple comparison test.

After weaning, male mice of all four strains had ad libitum access to chow diet before they were fed CD, starting at 8 weeks of age. During chow diet feeding AKR/J, AK-SWR/J and SW-AKR/J mice gained more body mass than the SWR/J mice. Feeding CD led to a temporary decline of body mass in AKR/J and SWR/J mice for one week (compare 3.2.1.), whereas mice of both recombinant strains gained weight continuously (figure 53A). Lean mass growth was identical in AK-SWR/J and SW-AKR/J mice and independent of diet change (figure 53B). SWR/J mice showed similar lean mass progression to the recombinant strains but consistently had about 2 g less total lean mass. During chow feeding, comparable lean mass gain of AKR/J, AK-SWR/J and SW-AKR/J was observed. But AKR/J mice lost lean mass when fed CD and approached the lean mass of SWR/J mice. Fat mass maximum was reached in SWR/J, AK-SWR/J and SW-AKR/J mice with 6 weeks of age (figure 53C). AKR/J had increased fat mass until 8 weeks of age. Recombinant strains kept fat mass stable with ongoing age, whereas SWR/J mice decreased fat mass after 6 weeks of age. Likewise, AKR/J lost fat mass due to diet change at the age of 8 weeks. Unlike body mass and lean mass, recombinant strains differed in fat mass. SW-AKR/J mice had more fat mass than AK-SWR/J mice.

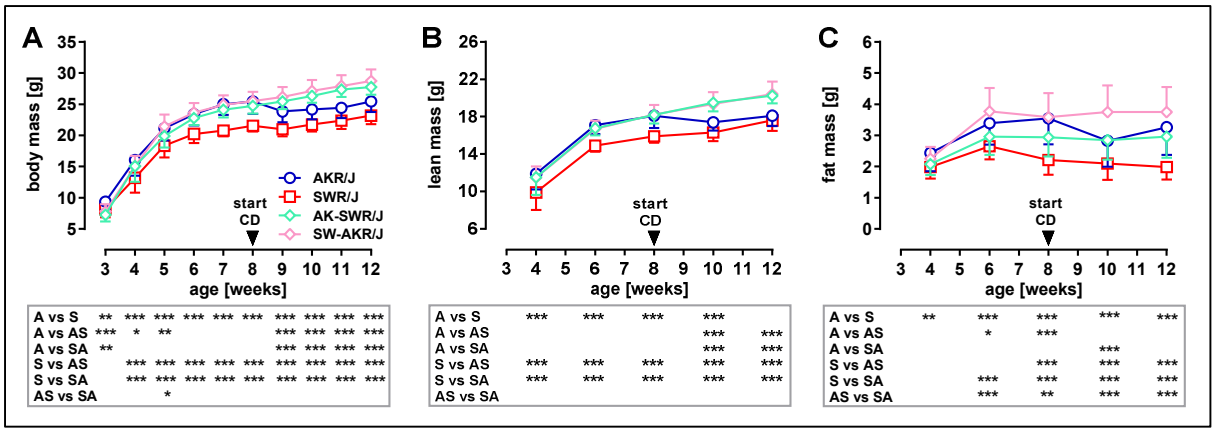


**Figure 53: Body mass and body composition of AKR/J, SWR/J, AK-SWR/J and SW-AKR/J mice with 3 to 12 weeks of age.** Mice were fed chow diet until 8 weeks of age, afterwards mice had ad libitum access to purified control diet (CD). **(A)** Body mass, **(B)** lean mass and **(C)** fat mass development of mouse strains. Differences between mouse strains for every time point were calculated using Two-Way-ANOVA and indicated below graphs in grey boxes; AKR/J (A): n=36, SWR/J (S): n=39, AK-SWR/J (AS): n=38, SW-AKR/J (SA): n=14; *p < 0.05; ** p < 0.01; *** p < 0.001.

With 12 weeks of age half of the mice received HFD. Initially, intra-strain differences between diet groups were analyzed. In accordance with previous results (compare 3.3.1, 3.4.1.), AKR/J mice fed HFD weighed significantly more than CD fed mice after one week (figure 54A). Differences between diet groups within recombinant strains were obvious in SW-AKR/J mice after 3 weeks and in AK-SWR/J mice after 4 weeks HFD feeding. In SWR/J mice, body mass and fat mass did not differ between diet groups at any time (figure 54A, C). For all four strains no differences in lean mass were observed between diet groups (figure 54B). Mice of both recombinant strains fed HFD for two weeks had higher fat mass than CD fed mice, respectively.

Comparing strains fed CD revealed no differences between recombinant strains AK-SWR/J and SW-AKR/J regarding body mass, lean mass and fat mass except slightly higher fat mass in SW-AKR/J mice at 12 weeks of age (figure 54D, E, F). AKR/J mice weighed less compared to both recombinant strains, due to less lean mass in combination with similar fat mass. Within CD groups, SWR/J mice had lowest body mass, lean mass and fat mass compared to all three other strains. Likewise, during HFD feeding, SWR/J mice showed lower body mass and fat mass than the three other strains and lower lean mass than recombinant strains (figure 54G, H, I). Feeding HFD to both recombinant strains exhibited the same progression of moderate body mass, lean mass and fat mass increase. Starting with lower body mass, AKR/J mice caught up with SW-AKR/J and AK-SWR/J mice and even overtook both recombinant strains in fat mass after one week HFD feeding. After four weeks of HFD feeding, recombinant strains ended up with fat mass in-between AKR/J and SWR/J mice. Regarding body mass, AK-SWR/J and SW-AKR/J mice resembled AKR/J mice.

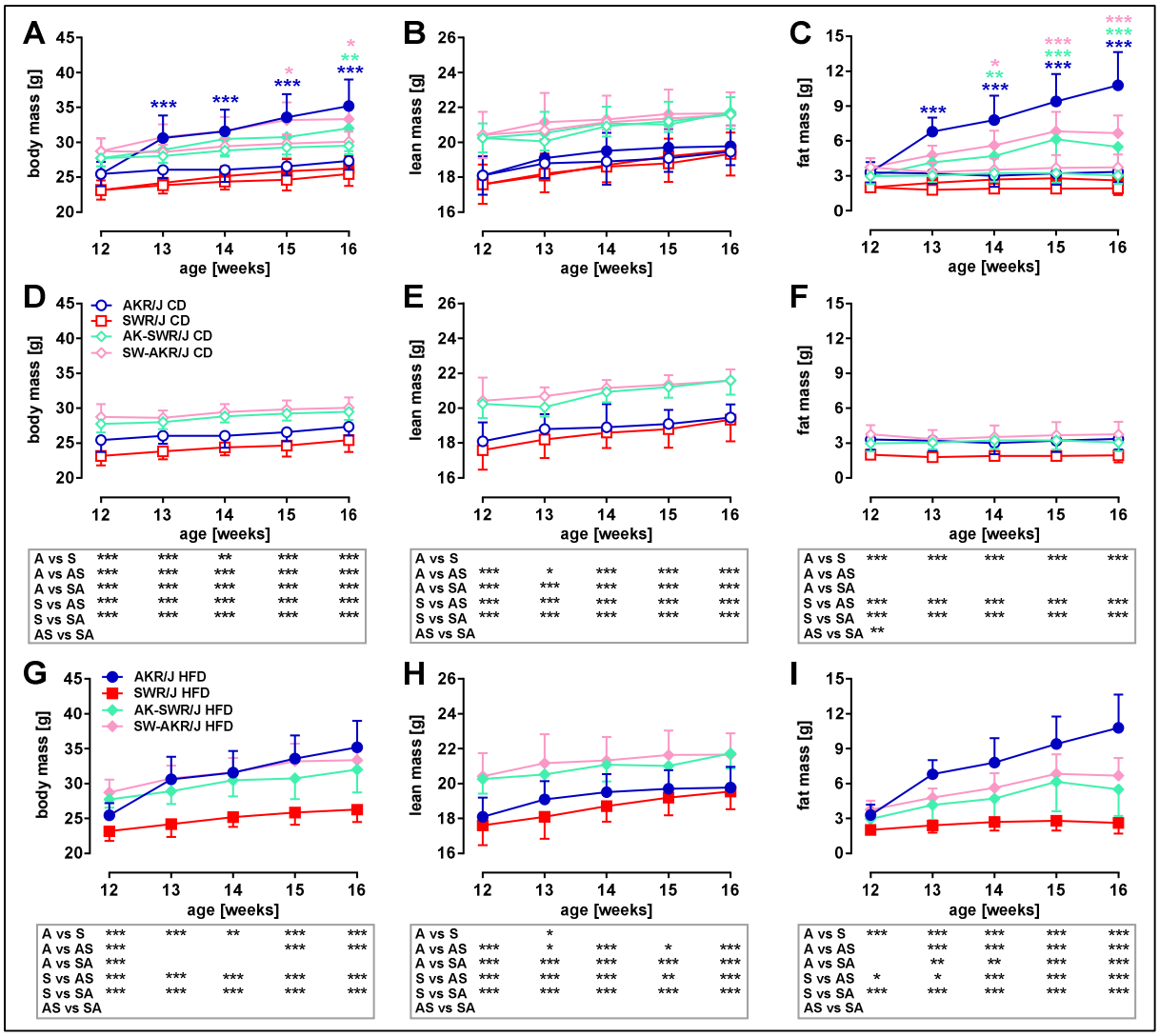


**Figure 54: Body mass and body composition of AKR/J, SWR/J, AK-SWR/J and SW-AKR/J mice with 12 to 16 weeks of age.** With 12 weeks of age mice were fed either continuing control diet (CD) or high-fat diet (HFD) chow diet for four weeks. Masses are shown in three ways: **(A)** body mass **(B)** lean mass and **(C)** fat mass of all groups to highlight differences between diet groups within one strain and separately for **(D, E, F)** control diet and **(G, H, I)** and high-fat diet to illustrate inter-strain differences. Differences between groups for every time point were calculated using Two-Way-ANOVA; *p < 0.05; ** p < 0.01; *** p < 0.001; body mass: AKR/J (n=36, 17 CD, 19 HFD), SWR/J (n=39, 18 CD, 21 HFD), AK-SWR/J (n=38, 19 CD, 19 HFD), SW-AKR/J (n=14, 6 CD, 8 HFD); body composition: AKR/J (A; n=36, 17 CD, 19 HFD), SWR/J (S; n=39, 18 CD, 21 HFD), AK-SWR/J (AS; n=38, 8-19 CD, 7-19 HFD), SW-AKR/J (SA; n=14, 6 CD, 8 HFD).

Additionally, changes in body mass, lean mass and fat mass within four weeks feeding intervention were calculated, due to different starting points between strains' weights at 12 weeks of age (figure 55). In the CD fed group, mice gained about 1.5 to 2.5 g body mass, 0.9 to 1.6 g lean mass and nearly no fat mass; there were no differences between strains. Compared to respective controls, AKR/J mice on HFD increased body mass, lean mass and fat mass significantly. Additionally, AK-SWR/J mice fed HFD showed higher fat mass gain than CD fed mice. Comparing strains within the HFD group revealed that AKR/J mice gained more body mass than the other three strains, which had a comparable body mass gain. Fed HFD, the slight lean mass increase was higher in AKR/J and SWR/J, compared to recombinant strains. AKR/J

accumulated most fat mass, whereas SWR/J mice gained nearly no fat and recombinant strains increased fat mass intermediately.

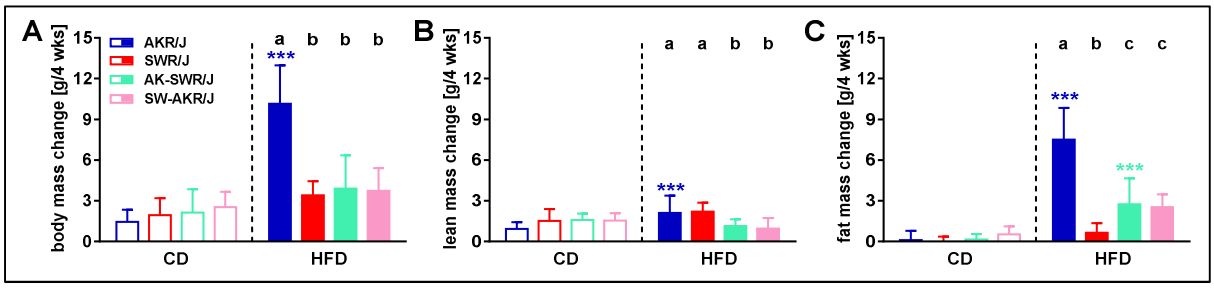


**Figure 55: Body mass and body composition changes of AKR/J, SWR/J, AK-SWR/J and SW-AKR/J mice during 4 weeks feeding intervention.** Mice were fed control diet (CD) or high-fat diet (HFD) for four weeks. Changes of **(A)** body mass **(B)** lean mass and **(C)** fat mass between start and end of feeding intervention. Differences between groups were calculated using Two-Way-ANOVA; asterisks symbolize intra-strain differences between diet groups, *** $p < 0.001$; different letters present significant intra-diet group differences between strains; body mass: AKR/J (n=36, 17 CD, 19 HFD), SWR/J (n=39, 18 CD, 21 HFD), AK-SWR/J (n=38, 19 CD, 19 HFD), SW-AKR/J (n=14, 6 CD, 8 HFD); body composition: AKR/J (n=36, 17 CD, 19 HFD), SWR/J (n=39, 18 CD, 21 HFD), AK-SWR/J (n=27, 15 CD, 12 HFD), SW-AKR/J (n=14, 6 CD, 8 HFD).

In summary, changes in body mass and body composition after 4 weeks HFD feeding were comparable in AK-SWR/J and SW-AKR/J mice. Recombinant strains are characterized by a higher and more stable lean mass in response to diet change than AKR/J and SWR/J mice. Except for measured fat mass, recombinant strains did not show a clear intermediate phenotype after 4 weeks HFD feeding. Measured body mass was similar to AKR/J mice, but gain of body mass and fat mass was more like that in SWR/J mice.

### 3.6.2. Glucose tolerance

Since AKR/J and SWR/J mice react differently to glucose when fed HFD, glucose tolerance in recombinant strains after 4 weeks HFD feeding was tested to check for the possible dominant heredity of a parental strain.

In accordance to previous investigations (compare 3.4.6.), AKR/J mice that had been 4 weeks on HFD had higher blood glucose levels after glucose gavage, compared to CD fed mice. Neither SWR/J nor both recombinant strains showed intra-strain differences between diet groups (appendix). Comparing strains fed CD revealed significant higher blood glucose levels in AK-SWR/J mice, compared to the three other strains (figure 56A). Relating to this observation, when additionally fed HFD, AK-SWR/J mice and AKR/J mice both displayed increased blood glucose at higher levels than SW-AKR/J and SWR/J mice (figure 56B). Therefore, glucose curves of HFD fed mice in response to glucose bolus were comparable for AKR/J and AK-SWR/J mice and for SWR/J and SW-AKR/J mice.

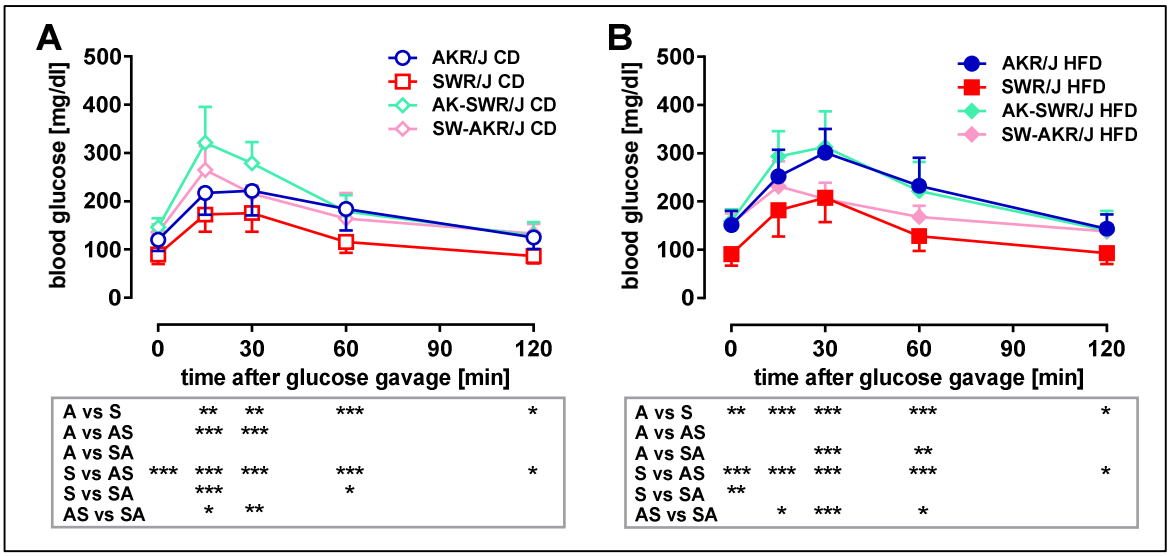


**Figure 56: Glucose tolerance of AKR/J, AK-SWR/J, SW-AKR/J and SWR/J mice.** Blood glucose curves in response to glucose gavage (2.8 g glucose/kg lean mass) after 4 weeks feeding intervention for **(A)** control diet (CD) and **(B)** high-fat diet (HFD) fed mice. Differences were calculated using Two-Way ANOVA with Tukey's multiple comparison test; *p < 0.05; ** p < 0.01; *** p < 0.001; AKR/J (n=27, 14 CD, 13 HFD), SWR/J (n=28, 14 CD, 14 HFD), AK-SWR/J (n=27, 15 CD, 12 HFD), SW-AKR/J (n=14, 6 CD, 8 HFD).

It was solely in AKR/J mice that basal blood glucose levels were increased due to HFD (figure 57A). CD fed, as well as HFD fed recombinant strains had comparable basal glycemia to AKR/J mice. Dependent on lean mass and independent on diet, AKR/J and SWR/J received less glucose than recombinant AK-SWR/J and SW-AKR/J mice (figure 57B). AKR/J mice showed elevated total area under the blood glucose curve (tAUC) when fed HFD, compared to CD (figure 57C). Comparing strains, SWR/J and SW-AKR/J mice had lower tAUC than AKR/J and AK-SWR/J mice. Incremental area under the curve (iAUC) was not affected by HFD feeding for any strain (data not shown).

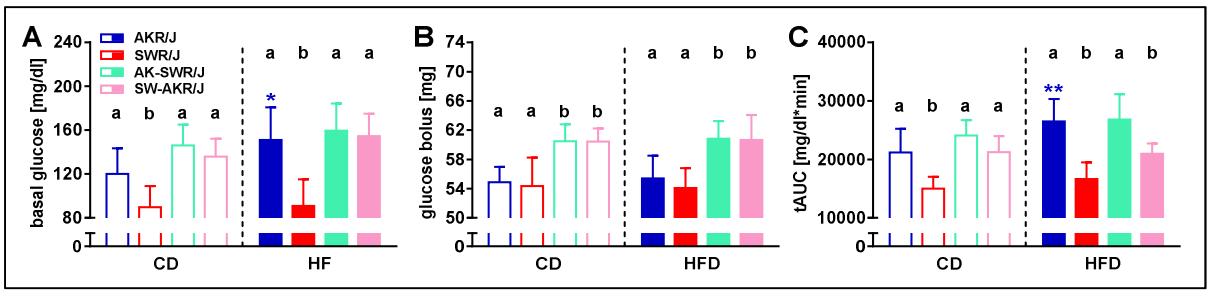


**Figure 57: Basal glucose levels, glucose bolus and tAUC of AKR/J, AK-SWR/J, SW-AKR/J and SWR/J mice. (A)** Basal blood glucose levels were measured after 6 hours fasting. **(B)** Glucose bolus was calculated by lean mass. **(C)** Total area under the curve was calculated based on blood glucose development after glucose bolus. Differences between groups were calculated using Two-Way-ANOVA; asterisks symbolize intra-strain differences between diet groups, ** p < 0.01; different letters present significant intra-diet group differences between strains; AKR/J (n=27, 14 CD, 13 HFD), SWR/J (n=28, 14 CD, 14 HFD), AK-SWR/J (n=27, 15 CD, 12 HFD), SW-AKR/J (n=14, 6 CD, 8 HFD); CD, control diet; HFD, high-fat diet.

In summary, glucose tolerance of the F1 generation originating from AKR/J and SWR/J cross-breeding showed no uniform phenotype. On the one hand, comparing glucose curves of the oral glucose tolerance test after 4 weeks HFD feeding, offspring with AKR/J dams (SW-AKR/J) resembled SWR/J mice and, the other way round offspring with SWR/J dams (AK-SWR/J) showed similar glucose tolerance to AKR/J mice. On the other hand, there were no differences between recombinant strains on HFD and on CD being indicative of a SWR/J phenotype.

### 3.6.3. Organ and adipose tissue weight

Weighing of organs and adipose tissue after 4 weeks HFD feeding was chosen as demonstrating a further distinct difference between AKR/J and SWR/J mice and, consequently as a possible classification of F1 generation to a parental trait.
CD fed AK-SWR/J and SW-AKR/J mice had heavier livers than AKR/J and SWR/J mice (figure 58A). HFD feeding led to an increase in liver weight in AKR/J mice. To the contrary, in both recombinant strains, liver weight decreased due to HFD feeding. Liver weight of SWR/J mice was not influenced by diet. Although HFD liver weights of recombinant strains were intermediate compared to purebred strains, AK-SWR/J showed more similarity to SWR/J and SW-AKR/J to AKR/J. Since body mass was different between strains and organ weight is, in a way, dependent on body weight, liver weight results were adjusted to body mass (appendix). This underlined the liver shrinkage in recombinant strains when fed HFD and relativized increased liver weight in AKR/J mice. Fed CD, the spleen of SWR/J mice weighed twice as much as the spleen of AKR/J mice (figure 58B). AK-SWR/J and SW-AKR/J spleens lay exactly in-between. HFD feeding caused a slight increase in spleen weight, which was only significant for AK-SWR/J mice. The relation of spleen weight between strains was maintained on HFD. Adjustment of spleen weight to body mass revealed a HFD-caused increase of spleen weight for AKR/J mice and, secondly, led to it approaching that of SWR/J and AK-SWR/J spleen weight. On HFD, AKR/J mice gained intrascapular brown adipose tissue mass (iBAT) (figure 58C). This effect vanished after adjustment (appendix). Nevertheless, AKR/J mice had significantly more iBAT when fed HFD, compared to the other three strains.

As pointed out previously, when fed HFD AKR/J gained the most fat mass, SWR/J nearly nothing and both recombinant strains roughly intermediately (figure 54I). For a more precise definition of the location of fat mass accumulation, three white adipose tissue depots were dissected and weighed after feeding intervention. Mass of fat depots did not differ between strains when mice were fed CD (figure 59).

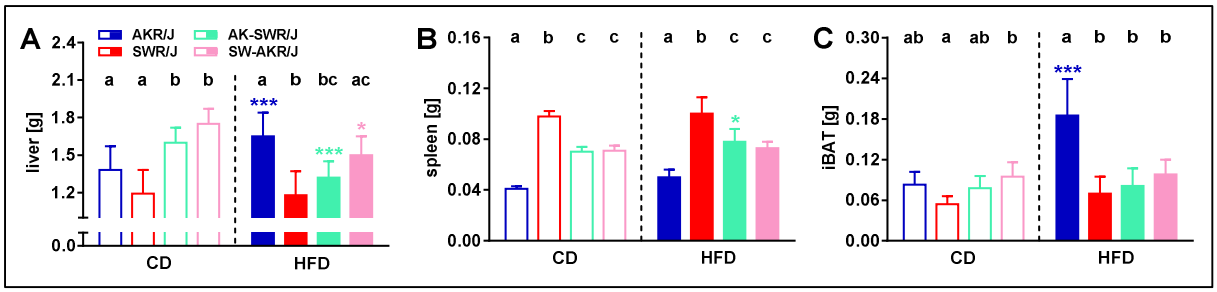


**Figure 58: Organ weight of AKR/J, AK-SWR/J, SW-AKR/J and SWR/J mice. (A)** Liver, **(B)** spleen and **(C)** intrascapular brown adipose tissue (iBAT) were weighed after dissection. Differences between groups were calculated using Two-Way-ANOVA; asterisks symbolize intra-strain differences between diet groups, * $p < 0.05$; *** $p < 0.001$; different letters present significant intra-diet group differences between strains; liver and iBAT: AKR/J (n=28, 14 CD, 14 HFD), SWR/J (n=29, 14 CD, 15 HFD), AK-SWR/J (n=38, 19 CD, 19 HFD), SW-AKR/J (n=17, 9 CD, 8 HFD); spleen: AKR/J (n=12, 6 CD, 6 HFD), SWR/J (n=12, 6 CD, 6 HFD), AK-SWR/J (n=38, 19 CD, 19 HFD), SW-AKR/J (n=17,9 CD, 8 HFD); CD, control diet; HFD, high-fat diet.

HFD fed AKR/J mice had more than four times as much visceral adipose tissue (eWAT, rWAT) und about 3.5 times more subcutaneous fat than CD. Due to HFD feeding, eWAT was increased by 80-90 % in both recombinant strains and rWAT was slightly increased in AK-SWR/J mice, compared to CD fed littermates, respectively. SWR/J mice were resistant to adipose tissue accumulation. Thus, regarding visceral adipose tissue gain, recombinant strains showed an intermediate phenotype. Since subcutaneous fat was merely increased in AKR/J mice, recombinant strains reflected SWR/J mice, as characterized by no sWAT increase through HFD.

Taken together, and compared to both extremes of DIO susceptibility (AKR/J and SWR/J mice), organ and adipose tissue weights of AK-SWR/J and SW-AKR/J mice fed HFD did not differ between both recombinant combinations. Regarding visceral adiposity, the phenotype of recombinant strains was intermediate to parental strains and regarding subcutaneous fat, AK-SWR/J and SW-AKR/J mice showed more relation to SWR/J mice.

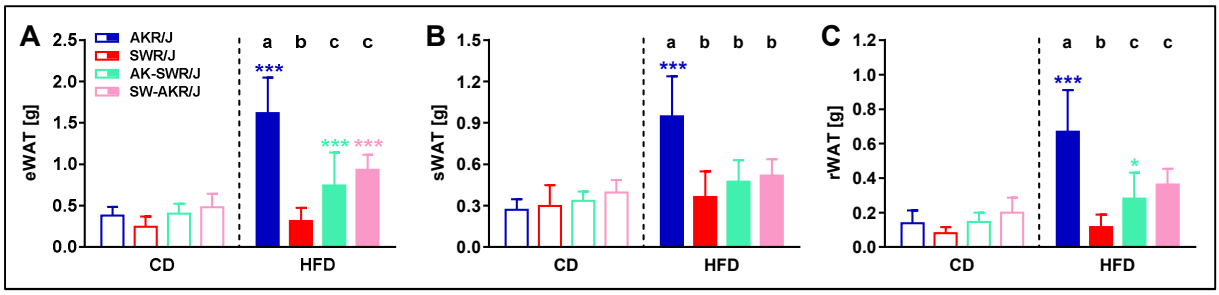


**Figure 59: Adipose tissue weight of AKR/J, AK-SWR/J, SW-AKR/J and SWR/J mice. (A)** Epididymal **(B)** subcutaneous and **(C)** retroperitoneal white adipose tissues were weighed after dissection. Differences between groups were calculated using Two-Way-ANOVA; asterisks symbolize intra-strain differences between diet groups, * $p < 0.05$; *** $p < 0.001$; different letters present significant intra-diet group differences between strains; AKR/J (n=25, 12 CD, 13 HFD), SWR/J (n=27, 13 CD, 14 HFD), AK-SWR/J (n=38, 19 CD, 19 HFD), SW-AKR/J (n=17, 9 CD, 8 HFD); CD, control diet; HFD, high-fat diet.

# 4. DISCUSSION

## 4.1. Challenges planning high-fat diet feeding studies

**Choice of diet and duration of intervention**

In preparation to address hypothesis of cause and consequence of high-fat diet-induced obesity, it is crucial to compile a suitable study design with appropriate diets and intervention duration. For all diet intervention studies, high-fat diet (HFD) feeding started at the age of 12 weeks. Mice of this age are stable in lean mass and fat mass and fully sexual mature. Consequently, changes in body weigh in response to HFD are influenced more by diet than by growth during adolescence. In general, HFD-induced effects are generally evaluated by comparing mice fed HFD with mice, ideally littermates, fed a low-fat control diet. Generally, HFD are compositionally defined diets, whereas respectively, for low-fat diet, rodent chow is often used. Chow diets containing plant-derived ingredients like wheat, corn and vegetable oil may be closer to wild-life food consumption but, therefore, components are not well defined and vary by batch, season and vendor (Chassaing et al. 2015). Fibers and plant-derived phytoestrogens are ingredients known to especially influence the progression of metabolic diseases (Sasidharan et al. 2013; Chassaing et al. 2015). In studies with a focus on HFD-induced obesity and related comorbidities, all possible confounding and endocrine-modulating ingredients should be eliminated (Lephart et al. 2004; Thigpen et al. 2004). Only 5 from 35 papers published in 2007 in 5 high-impact journals with the keyword “mouse high-fat” compared defined HFD and CD as merely differing in amounts of fat and carbohydrate (Warden and Fisler 2008). Consequently, for the present HFD interventions it was crucial to compare mice on semi-purified diets that only differed in fat quantity. Due to the different texture and taste of chow, the switch to a semi-purified diet can itself have an influence on food intake and body mass. Therefore, an adaptation period to CD was set 4 weeks prior to HFD feeding. Especially in 8-weeks old AKR/J mice, feeding CD caused a decrease in body mass which was recovered within the following three weeks (compare 3.2.1.). If this adaptation had been omitted and mice had received HFD/CD immediately after chow feeding at the age of 12 weeks, HFD-induced body mass gain would have been overrated due to unstable body mass in the CD fed group.

Firstly, two plant-based high-fat diets varying in fat quantity were fed to male 12 weeks old C57BL/6J mice for 12 weeks (compare 3.1.1.). Unexpectedly, the effects of HFD were not strictly dose dependent. After one week, mice fed “the fatter” HFD, with 60 kJ% of fat (HF 60), had higher body mass than CD fed mice. But this body mass increase was not due to fat mass accumulation, but rather to lean mass gain (figure 16). Short-term HF 60 feeding did not

influence glucose tolerance, whereas mice on the moderate HFD, with 48 kJ% of fat (HF 48), developed impaired glucose clearance, despite normal body composition (figure 17). Mice on both high-fat diets had comparable elevated body and fat mass, compared to the controls after four weeks of HFD. Still, glucose tolerance, especially basal glucose levels were markedly impaired in those fed HF 48. Intervention extension to 12 weeks did not aggravate glucose tolerance, but led instead to more fat accumulation in HF 48 mice than in 60 HF mice. These findings led to the conclusion that 4 weeks of HFD feeding are sufficient to induce metabolic alterations in fat mass and glucose tolerance which are main read-outs for the next experiments. Furthermore, effects are more pronounced on HF 48. This diet has the additional benefit that it is available in pelleted dosage form, so that food intake is quantifiable. Measurement of food intake may also have been of importance in explaining differences between both high-fat diets. Unfortunately, the texture of pellets of HF 60 was quite crumby, so that spillage of food was spread all over the cage, making it impossible to assess energy intake. Additionally, fatty food spillage in the nesting material may have caused discomfort for mice, hampering pair grooming and eventually leading to a reduced food intake, as compared to HF 48.

In the literature, few experiments can be found that compare the influence of high-fat diets, varying solely fat quantity, for metabolic outcomes over time. Krishna et al. fed a 60 kJ% HFD to C57Bl/6 mice for 5 or 20 weeks, starting at 6 weeks of age. As observed and expected in the present approach, body mass increased with prolonged HFD intake. Likewise, glucose tolerance was impaired, with areas under the curve being 78% and 43% greater in mice fed HFD for 5 and 20 weeks, respectively (Krishna et al. 2016). Although neither the age of the mice, nor diet, nor feeding duration was equal in the present study and that of Krishna et al., in both experiments an amelioration of impaired glucose tolerance over time was observed. It is possible that metabolism of mice adapts to enduring fat intake. In respect of the impact of fat quantity of HFD, Benoit et al. were unable to observe clear dose-dependent effects. They fed 6 weeks old male C57BL/6J mice with either low-fat diet (8 kJ% fat), a moderate HFD (48 kJ% fat), or a very HFD (74 kJ% fat) for 12 weeks. The inconsistent outcome was that mice on the very HFD were obese and displayed significantly increased plasma concentrations of triglycerides, leptin and adiponectin, and liver lipids. This was not shown in mice fed moderate HFD, although they developed metabolic endotoxemia and inflammation (Benoit et al. 2015). Consequently, more fat in the diet does not necessarily lead to more body fat accumulation and more metabolic impairments. A feeding intervention in rats came to a similar conclusion in which HFD of 45 kJ% to 60 kJ% of fat (additionally differing in soy oil and lard content) was fed for 84 days. Development of obesity was comparable for all HFD groups, but accompanied by unchanged serum glucose levels, compared to controls (Sasidharan et al. 2013). Additionally, they observed that adiposity index, serum triglycerides and cholesterol tended to be higher in diet groups with

greater lard amount. This leads to the assumption that lard containing HFD might challenge metabolism more than plant-based HFD.

For the second study-design, lard containing high-fat diets were chosen (compare 3.1.2., figure 18). The feeding period was set to 4 weeks, as was shown to be sufficient for the induction of metabolic impairments in the previous experiment. Body mass increase was comparable in mice fed lard HFD with 48 kJ% fat (lHF 48) and with 75 kJ% fat (lHF 75) after 4 weeks. But fat mass increase and basal glucose levels were clearly dependent on fat quantity, since feeding lHF 75 showed the greatest effects. High basal glycemia can be explained by an upregulated hepatic gluconeogenesis (DeFronzo et al. 1989; Cano et al. 2003; Brons et al. 2009), since extreme fat-rich diets are low in carbohydrates. Impaired glucose tolerance in HFD fed mice is mainly due to delayed clearance of glucose. Maybe peripheral tissues start developing insulin resistance when struggling with the uptake of sudden increases in glucose (DeFronzo et al. 1989; Cano et al. 2003; DeFronzo and Abdul-Ghani 2011). Interestingly, mice fed the most extreme of the high-fat diets, which were carbohydrate free and with 78 kJ% fat (lHF 78$^{cf}$), gained less body mass and fat mass, compared to lHF 48 fed mice. Glucose tolerance and basal glucose levels of lHF 78$^{cf}$ and lHF 48 fed mice were similar. The reason for this mild phenotype can be ascribed to food intake. During the first week of feeding intervention, mice ate sparsely of lHF 78$^{cf}$, probably because of the butter-like texture. The calculated energy intake was comparable to CD fed mice. Consequently, mice did not gain weight yet decreased body mass. Within the next few weeks they caught up in body mass, due to fat mass increase, but at the end of the study, lHF 78$^{cf}$ mice only reached weights below the other two high-fat diets. This experiment shows a positive correlation between fat quantity to a certain degree and fat mass accumulation and impairment of glucose tolerance. But it also illustrated the limitations of high-fat diets. The higher the fat amount is, the more other macronutrients have to be replaced. The loss of carbohydrates in the diet provoked the metabolism to ketogenesis (Robinson and Williamson 1980; Sussman et al. 2013). Ketone bodies influence metabolism and are known to be helpful in the treatment of disorders of the central nervous system (Veech 2004; Van der Auwera et al. 2005; Hartman et al. 2007). But due to their high impact, they may bias the analysis of obesity-induced alterations. A further disadvantage of extreme high-fat diets already mentioned above is the problem of administration. The diet can only be offered as paste. Interestingly, food-texture has a high impact on the development of obesity as it was shown by Desmarchelier et al. (Desmarchelier et al. 2013). They were able to reveal that, independent of macronutrient composition (control and HFD), mice receiving diet in powder form became obese whereas in the group with pellet diet only HFD fed mice gained weight. This result underlines the importance of a similar food-texture when effects of different diets are compared in feeding studies.

Furthermore, for lard-based high-fat diets 48 kJ% of fat was sufficient to induce effects on glucose tolerance. After settling fat quantity to 48 kJ% of fat, the question was which source of fat (plant or lard) to use. Due to identical study design, mice in the first study, fed plant-based HF 48, and mice in the second experiment, fed lard-based lHF 48, can be compared (compare 3.1.3., figure 19). Both high-fat diets led to the same gain of body mass and fat mass after a 4 week feeding period. But plant-based HF 48 had a higher impact on basal hyperglycemia and impairment of glucose tolerance. Thus, for the development of obesity in this mouse model, the pure surplus of energy provided by an increased fat quantity in the diet is crucial, whereas for impact on glucose metabolism, the kind of fat or fat quality has an additional influence. Depending on the source of fat, namely lard and palm oil, the contained fatty acids vary in chain-length and saturation level. These variations lead to different biochemical properties and consequently to the induction of distinct metabolic effects (Wilkes et al. 1998; Buettner et al. 2006; Catta-Preta et al. 2012). Various similar conclusions are found in the literature. For example, feeding three different high-fat diets based on milk fat, lard and safflower oil (all 37.5 kJ% of fat) for 4 weeks to male C57BL/6 mice caused similar body weight gain, but an altered microbiota and adipose tissue inflammatory profile between HFD groups (Huang et al. 2013). Catta-Preta et al. investigated the influence of 4 high-fat diets with 60 kJ% fat, containing lard, olive oil, sunflower oil, or canola oil on adipokines and glucose tolerance. After 10 weeks, mice fed lard HFD had accumulated the most subcutaneous and visceral adipose tissue. Additionally, they exhibited, together with mice fed olive oil HFD, the highest levels of resistin, leptin, insulin and basal glucose. The authors explained these striking effects by the high amount of saturated (SFAs) and monounsaturated fatty acids (MUFAs) in lard and olive oil, compared to the other diets high in polyunsaturated fatty acids (PUFAs) (Catta-Preta et al. 2012). Direct comparisons of lard- and palm oil-based high-fat diets in the literature revealed the same gain in body mass for both diets in Wistar rats after 10 weeks feeding (45 kJ% fat) (Janssens et al. 2015), and in C57BL/6J mice after a 19 weeks feeding period (60 kJ%) (Ikemoto et al. 1996). In both studies, both high-fat diets led to impaired glucose tolerance. But only in lard fed rats was hepatic glucose tolerance altered (Janssens et al. 2015). 30 minutes after administering the glucose bolus, glucose levels in C57BL/6J mice were clearly higher in the lard fed mice than in those mice receiving palm HFD, whereas hyperinsulinemia occurred only in palm fed mice (Ikemoto et al. 1996). The main difference between lard and palm-based diet lies in the dominating saturated fatty acid. Palm HFD contains more palmitic acid (C16:0), whereas lard is richer in stearic acid (C18:0). It has been well studied that efficiency of oxidation declines with the increasing chain length of the saturated fatty acids (Leyton et al. 1987; Pai and Yeh 1996; DeLany et al. 2000). Therefore, stearic acid containing HFD should be less efficiently oxidized than palmitic acid and, in contrast, should be more readily stored in fat depots, causing higher grade of obesity. This hypothesis was proven by Van den Berg et al.. C57BL/6 mice were fed

with either palm HFD (4.4 % stearate) or lard HFD (15 % stearate), or palm HFD supplemented with stearate (13.9 % stearate). Fat accounted for 45 kJ% in all diets. After a 5 week feeding period, mice receiving HFD rich in stearate had decreased hepatic insulin sensitivity and displayed more body mass due to lower energy expenditure and higher food intake, than palm HFD fed mice. Nevertheless, all high-fat diets decreased insulin-stimulated glucose uptake by peripheral tissues (van den Berg et al. 2010). To sum up, publications reveal induction of obesity and impairment of insulin/glucose tolerance for palm- and lard-based high-fat diets. Lard HFD, however, tended to provoke more drastic alterations in metabolism, probably due to higher amounts of stearic acid. Differing from the literature, the present study shows that, in addition to equal induction of obesity, hyperglycemia was more pronounced in palm HFD fed mice.

**Mouse strains and housing conditions**

The repertory of mouse strains available for the investigation of questions of interest is quite large. In first experiments when defining a suitable diet and feeding period, C57BL/6J mice were used, as being one of the best studied mouse strains for diet-induced obesity (DIO), since they show solid weight gain when fed HFD (Surwit et al. 1988; West et al. 1992; Winzell and Ahren 2004). But for the following experiments, not only the consequences of DIO should be analyzed but, additionally, the obesity independent effects of HFD and reasons for differences in DIO. Therefore, two mouse strains had to be identified as representing extremes of DIO. In a 4 week HFD feeding intervention (48 kJ% of fat), six inbred mouse strains from our mouse facility were compared as regarding body, lean and fat mass gain (compare 3.1.4., figure 20). Comparing fat mass accumulation to CD fed littermates, mouse strains were divided into three groups of DIO: SWR/J and 129sv/evS1 mice were resistant, 129sv/evS6 and C57BL/6J mice became moderately obese and AKR/J and C57BL/6N mice showed the highest propensity to DIO. Interestingly, within one mouse strain such, as 129sv/ev, sub-strains could not be classified into the same DIO group. In the literature, especially for BL/6 mice, many differences among sub-strains in behavior, metabolism and genetics are reported (Sluyter et al. 1999; Bothe et al. 2004; Toye et al. 2005; Bryant et al. 2008; Fergusson et al. 2014; Heiker et al. 2014). Overall, the response of mouse strains to HFD is in accordance with published studies comparing different strains (West et al. 1992; Montgomery et al. 2013). For comparisons of a DIO prone and resistant strain, the combination of BL/6J and A/J mice is often investigated (Surwit et al. 1988; Surwit et al. 1995; Black et al. 1998; Prpic et al. 2003). This pairing was ineligible for this study because A/J mice bred poorly in our facility, generating insufficient number of animals for convincing experiments. For further experiments, mice of the SWR/J strain were chosen, as developing identical body, lean and fat mass when fed CD and when fed HFD. AKR/J mice served as DIO susceptible counterparts, although fat mass increase was higher in BL/6N mice. AKR/J mice were favored, due to a lean mass increase comparable to SWR/J mice. Consequently, HFD

induced differences in body mass between strains can be related to fat mass gain. Furthermore, AKR/J and SWR/J mice are more closely related than BL/6J and SWR/J mice, as revealed by phylogenetic analyses (Petkov et al. 2004; Tsang et al. 2005). Moreover, the literature offers helpful references in comparing AKR/J and SWR/J mice as regards genetics (West et al. 1994a; West et al. 1994b; York et al. 1997; Wittenburg et al. 2002), behavior (Smith et al. 1999; Lightfoot et al. 2004; Milner and Crabbe 2008; Hesse et al. 2010) and HFD feeding effects (Eberhart et al. 1994; Paigen 1995; Prpic et al. 2002). It is of great importance to choose the correct strains and, if necessary, sub-strains fitted to the tackled physiologic phenomenon, since strains vary in susceptibility to develop specific behavioral, biochemical or metabolic characteristics (Crawley et al. 1997; Champy et al. 2008). Additionally, if the choice of strain is merely based on literature research, the first question will be if mouse strains will exhibit the expected phenotype. Although the wish for standardization is great (Champy et al. 2004), mouse facilities differ in housing conditions and mouse handling, with some factors directly influencing DIO, for example temperature (Stemmer et al. 2015) and hygienic status (Muller et al. 2016). The microbial environment is particularly crucial for the development of obesity and/or metabolic diseases (Ley et al. 2005; Ridaura et al. 2013) and the outcome of experiments (Ma et al. 2012; Kless et al. 2015).

**Adjustment of metabolic data**

To find explanations for the differences in DIO between SWR/J and AKR/J mice, energy balance was itemized. Feeding CD revealed no differences between strains in terms of measured energy expenditure and metabolizable energy (figure 23). But since these two energy budget parameters are dependent on body mass and body composition, and show the differences between strains, an adjustment of energy expenditure and metabolizable energy was reasonable. Adjustment and interpretation of energy expenditure data has a long history in research. Kleiber's law is one of the first approaches in describing an interspecies allometric relationship between body mass and metabolism (Kleiber 1932). Organs and tissues in the body differ in their metabolic activity (Elia 1992; Muller et al. 2013). Consequently, the best means for making an adjustment would include knowledge of the exact mass and metabolic rate of tissues and organs. Since this method is invasive and laborious and therefore unfeasible, normalization of physiological data to one or more covariates by the generalized linear model ANCOVA was applied, as recommended in the literature (Allison et al. 1995; Packard 1999; Even and Nadkarni 2012; Tschop et al. 2012). With this approach Even et al. proposed the sum of lean mass and 20 % fat mass as an adequate correction factor for energy expenditure (Even and Nadkarni 2012) in low sample sizes. This suggestion fits with the estimation that the activity of fat mass is about 20 % of fat-free mass (Ravussin et al. 1986; Speakman and Johnson 2000; Selman et al. 2001; Arch et al. 2006). It is important to bear in mind that measuring energy balance has two

sides (metabolizable and expanded energy), and when comparing both sides, energy expenditure and metabolizable energy must be adjusted in the same way (Arch et al. 2006; Tschop et al. 2012). Regarding this fact, and calculating linear regression models for different variables for the present data, body mass was chosen as the most appropriate adjustment factor for energy expenditure and metabolizable energy.

## 4.2. Proximate causes of differences in diet-induced obesity of AKR/J and SWR/J mice

**Weaning characteristics and predispositions in energy expenditure and substrate oxidation on control diet**

In search of first indications for differences in DIO, the weaning characteristics of SWR/J and AKR/J mice were compared (compare 3.2.1.). Independent of gender, AKR/J mice were heavier than SWR/J mice (figure 21). An explanation could be that AKR/J mice were born in smaller litters, with the result that fewer pubs compete for nursing. In respect of litter size, dependent susceptibility to weight gain, published rodent studies offer hints towards obesity in smaller litters. Neonatal over-nutrition, induced by reducing litters to 4 pubs, led to increased post-weaning body weight and fat mass, compared to pubs of normal sized litters (Rodrigues et al. 2007; Mozes et al. 2014). Additionally, over-nourishment during the suckling period caused changes in the energy circuitry in the hypothalamus of the offspring, predisposing them to the onset of obesity later in life (Rodrigues et al. 2007; Patel and Srinivasan 2011), accompanied by impaired glucose tolerance, insulin resistance and hyperleptinemia in response to HFD (Glavas et al. 2010; Ye et al. 2012). Although AKR/J and SWR/J mice merely differ by about one pub per litter, this fact could be a piece of the puzzle regarding differences in DIO.

Furthermore, 12 week old mice of both strains fed CD were analyzed in order to assess predispositions that render SWR/J mice less susceptible to DIO (compare 3.2.2.). Due to an increased resting metabolic rate, SWR/J mice displayed higher daily energy expenditure than AKR/J mice (figure 25B). This result confirms previous findings (Storer 1967; Hesse et al. 2010) and can explain baseline differences in body mass between strains in combination with unaltered metabolizable energy. SWR/J mice are more flexible in their energy substrate oxidation since they cover the whole physiological range of respiratory exchange ratio (RER) under low and normal oxygen consumption conditions (figure 25E, F). Additionally, lower RER in SWR/J mice, as compared to AKR/J mice, indicates a higher fatty acid oxidation capacity in SWR/J mice, which might be a protective benefit in resistance to DIO. SJL mice, which are closely related to SWR/J mice (Petkov et al. 2004; Kirby et al. 2010), lack the TBC Rab-GTPase-activating

protein domain, due to a mutation in the tbc1d1 gene (Chadt et al. 2008). Genome-wide scans linked this gene region to DIO (Kluge et al. 2000; Giesen et al. 2003). Mice lacking the TBC1D1 gene showed a lean phenotype and reduced RER (Chadt et al. 2008). Furthermore, human studies show evidences that lean trained men have lower RER than untrained man (Ramos-Jimenez et al. 2008) and, on the other hand, that a higher respiratory quotient is associated with weight gain (Zurlo et al. 1990).

Further discussed possibilities for DIO resistance in SWR/J mice are: reduced expression of the muscle growth inhibitor of myostatin (Lyons et al. 2010), exhibited increased capacity of skeletal muscle to metabolize fat (Leibowitz et al. 2005), and high sensitivity to negative feedback signals, with reduced neuropeptide Y expression (Smith et al. 2000; Leibowitz et al. 2005). On the other hand, the increased sensitivity of AKR/J adipocytes to insulin might indicate a predisposition to improved adipose tissue lipid storage (Eberhart et al. 1994).

**Climbing as diet-induced obesity protective activity characteristic**

All through the literature, SWR/J mice are characterized as highly-active (Lightfoot et al. 2001; Lightfoot et al. 2004; Jung et al. 2010), less anxious mice (Milner and Crabbe 2008) with a high sympathetic tonus (Prpic et al. 2002), whereas AKR/J are claimed to be sedentary, with rather low physical activity (Lightfoot et al. 2001; Turner et al. 2005). Surprisingly, the present investigations revealed more ground activity counts in AKR/J than in SWR/J mice (figure 30C). Nevertheless, the data fitted to the literature, as SWR/J mice showed more vertical activity in the form of rearing and climbing (figure 30F, I). These two forms of extreme exercise cannot be detected at the same time with commercially available activity monitoring devices. In combination with implanted minimitters, however, it was possible to detect both activities in parallel: rearing and climbing activity. As rearing was far more pronounced, with climbing even occurring exclusively in SWR/J mice, this strain can be regarded as “exercised”. Publications analyzing the influence of substances on behavior in different mouse strains, support this observation. Baseline results revealed higher rearing activity in SWR/J mice, compared to AKR/J mice (Crabbe et al. 1998; Wiltshire et al. 2015). For climbing activity observations, no published study could be found. But alternatively as voluntary exercise activity, SWR/J mice spend more time and/or distance in a running wheel than the comparable strain (Lightfoot et al. 2004; Turner et al. 2005; Jung et al. 2010). Energy consuming, voluntary exercise phenomena may additionally contribute to DIO resistance, as climbing also tends to increase with ongoing HFD feeding.

**Atypical diurnal rhythm of SWR/J mice**

Comparing night-day pattern of energy expenditure, RER and body core temperature ($T_b$) between AKR/J and SWR/J mice revealed a clear active scoto- and an inactive photophase in AKR/J mice, whereas DIO protected SWR/J mice showed a less pronounced night-day-rhythm (figure 26, 29). On the one hand, this is in contrast to the literature, where a disruption of the circadian rhythm, leading to altered activity and eating patterns increased the risk of obesity in mice and humans (Antunes et al. 2010; Froy 2010; Yoshida et al. 2012). But the circadian rhythm in SWR/J mice may not be regarded as disrupted, more preferably as atypical in mice with a still existing, though less distinct rhythm. This argument regarding a changed circadian rhythm may even, to a degree, be true for AKR/J mice fed HFD. AKR/J mice modified their activity pattern and increased $T_b$ and energy expenditure solely during photophase. Whereas, feeding HFD to SWR/J mice increased $T_b$ and energy expenditure moderately and equally during photo- and scotophase. Responsibility for the altered night-day rhythm in SWR/J mice might be attributed to a mutation in the rd gene, which causes degeneration of the rods in the retina and is associated with night blindness (Carter-Dawson et al. 1978; Bowes et al. 1993; Dalke et al. 2004). Due to a possibly reduced ability to see at night, SWR/J mice are hampered in being fully active in the dark. They therefore spread their food consumption and energy expenditure evenly over 24 hours. Such increased activity during the day could also explain the subjective impression that SWR/J mice are more aggressive and active than AKR/J mice. This impression is backed by a study investigating wildness and ease of handling in different mouse strains (Wahlsten et al. 2003). SWR/J mice are counted among those mouse strains with the highest number of tests with bites and the highest rating for wildness. With the knowledge that SWR/J mice are in general more active during the day, the suitable timeframe for conducting experiments is confounding. For practical reasons, nearly all studies are performed by day, during the inactive phase of most mouse strains. In the case of experiments done by night, results for mouse handling would turn out to be different.

**Disequilibrium of energy balance during HFD exposure**

Accumulating excess energy as fat during HFD feeding can be traced back to a reduced energy expenditure and/or increased energy intake. Hesse et al. postulated that SWR/J mice fed HFD defend their body mass by adjusting energy intake, increasing activity levels and energy consuming thermoregulatory behavior (Hesse et al. 2010). In the present study energy balance in the first three days of HFD feeding was investigated to unravel the contributions of energy intake and energy expenditure to DIO in body mass-matched AKR/J and SWR/J mice. Particularly in the first 24 hours, hyperphagia and, consequently, a gain in metabolizable energy occurred in both strains, but it was more pronounced in AKR/J mice (figure 28). Published

studies confirmed that the peak of overeating is reached within the first 24 h after offering HFD (DeRuisseau et al. 2004; Bjursell et al. 2008; Hesse et al. 2010). Feeding HFD leads to an equal elevation of energy expenditure in both mouse strains which is driven by rising resting metabolic rate (figure 27). A partial explanation is provided by the thermogenic effect of the diet because digestion, absorption and disposal of the excessive calories consume more energy. Additionally, a diet-dependent and strain-independent increase of body core temperature was observed (figure 29). This adaptive thermogenesis contributes to the increased energy expenditure and can be regarded as contra-regulation of the metabolism to store energy by dissipating excess energy as heat. The key player in this process is the uncoupling protein 1 (Ucp1), whose role in feeding high-fat diets was outlined previously (Fromme and Klingenspor 2011). Briefly, this review demonstrated that brown adipose tissue Ucp1 mRNA and protein levels increase in the large majority of studies when feeding rodents a HFD. One study analyzing Ucp1 expression in different fat depots reported an increase in SWR/J mice, but a drastic decrease in AKR/J mice when fed HFD (Prpic et al. 2002). The authors concluded that limited capacity in energy dissipating mechanisms might be the reason for DIO in AKR/J mice. In the present study this hypothesis could not be confirmed because adaptive thermogenesis, measured by increased daily energy expenditure and $T_b$ as an acute response to HFD, was observed in both mouse strains equally.

Firstly, to demonstrate the correctness of the present energy balance calculation, the energy equation of the 24-h baseline measurement on CD was calculated. The difference between metabolized and expended energy exhibited a positive energy balance in both strains (figure 24). As body weight also increases proportionally during this time, this demonstrates that present methods of measurement are precise enough to assess energy balance. Summing up the first three days of HFD feeding showed, on the one side hyperphagia in both mouse strains, with more metabolizable energy available in AKR/J mice (figure 28). On the other side, a strain-independent increase in expended energy was observed with higher levels in SWR/J mice than in AKR/J mice. Calculating the difference of both sides of energy input and output reveals a positive energy balance matching the observed weight gain, although comparing the surplus energy between strains over three days of HFD feeding uncovers a difference that meets perfectly the difference in accumulated body fat. In contrast to other studies which claim lower activity/energy expenditure (Bjursell et al. 2008) or hyperphagia (DeRuisseau et al. 2004; Hariri and Thibault 2010) as major contributors to DIO, here it is clearly demonstrated that DIO in AKR/J mice results from an acutely imbalanced interaction between these two factors. In contrast to SWR/J mice, the elevation of energy expenditure in AKR/J mice is not sufficient to contra-regulate the anyhow higher metabolizable energy.

In conclusion, there is no single genetic, behavioral or metabolic modification between AKR/J and SWR/J mice that could account for the critical differences in DIO. In fact, a variety of

characteristics combine to play a part in solve this puzzling question. Through CD feeding, SWR/J mice show higher energy expenditure and lower RER, indicating better fatty acid oxidation than AKR/J mice. Less pronounced night-day-rhythm, transferring SWR/J mice into steady activity and more vertical/climbing activity, may predispose SWR/J mice to handle HFD and burn excess energy better than AKR/J mice. The first days of HFD feeding determine susceptibility to DIO. Independent of the strain, resting metabolic rate and body core temperature increased in response to HFD. AKR/J mice become obese due to higher metabolizable energy that cannot be defended sufficiently by rising energy expenditure. The difference in positive energy balance between strains correlates with accumulated fat mass.

## 4.3. Diet-induced and obesity-induced alterations of glucose tolerance

Comparing HFD experiments with mouse strains differing in susceptibility of DIO presents the possibility to distinguish between the effects of diet and obesity. Here, glucose, insulin and pyruvate tolerance were tested several times during 12 weeks of HFD feeding in AKR/J and SWR/J mice (compare 3.4.6.). At the first measure point, precisely 1.5 days after the onset of HFD feeding, both mouse strains exhibited impaired glucose tolerance, compared to the respective control strains (figure 38A, D). Basal blood glucose was unchanged, but glycemia levels 15 and 30 minutes after glucose administration were elevated in mice when fed HFD. This strain and obesity independent observation indicates a quick metabolic reaction to energy substrate provided by the diet. During the first days of HFD, hyperphagia occurred in both strains and metabolic pathways were mainly activated to deal with the huge fat load. A quick elimination of glucose from the blood by uptake in the periphery seems not to have priority since enough energy is available from the fat. The fact that at the same time insulin tolerance was normal indicates that the principle mechanism of insulin mediated uptake of glucose is still intact (figure 40A, D).

After one week of HFD feeding diet-induced altered glucose tolerance changed to obesity-induced impaired glucose tolerance. In obese AKR/J mice, fasting blood glucose was elevated, response to glucose bolus and consequently AUC of glucose curves was altered, compared to CD fed mice. Additionally, sensitivity to insulin decreased. On the other hand, lean SWR/J mice fed HFD for one week exhibited normal basal glycemia and insulin tolerance. But due to very low blood glucose levels in CD fed mice during oral glucose tolerance test, HFD mice showed significantly higher levels. Nevertheless, at this time point SWR/J mice seemed to adapt their metabolism to the new substrate, whereas developing obesity in AKR/J mice led to an

aggravation of glucose and insulin sensitivity. With ongoing HFD feeding, this divergent progression persisted, resulting in obese insulin resistant AKR/J mice and highly insulin sensitive lean SWR/J mice.

Besides insulin and glucose tolerance tests on AKR/J mice, pyruvate tolerance tests were also performed in order to test hepatic gluconeogenesis (figure 42). Decreased glucose uptake of tissue due to increased hepatic glucose production can be a reason for elevated fasting blood glucose (DeFronzo et al. 1989; Brons et al. 2009). Glucose production after pyruvate bolus was consistently higher in HFD fed mice indicating elevated gluconeogenesis. Since glucose availability through diet is diminished in HFD, the metabolism is dependent on hepatic glucose production. Upregulated gluconeogenesis might contribute to elevated basal glycemia, but the main reason lies in deteriorated insulin sensitivity.

Starting at one week of HFD feeding, injected insulin was not able to lower glucose levels in AKR/J mice. Additionally, 24 week old CD fed AKR/J mice were resistant to exogenous insulin. Age-dependent loss of insulin sensitivity was also reported for BL/6J mice (Krishna et al. 2016). The fact that long-term HFD feeding for weeks, or even months, leads to obesity and that especially visceral/ectopic fat accumulation and chronic inflammation are associated with insulin resistance, has been published often (Hotamisligil et al. 1993; Weisberg et al. 2003; Xu et al. 2003; Bergman et al. 2007; Suganami et al. 2012; Ye 2013; Castro et al. 2014).

No study has measured either glucose or insulin tolerance after 1.5 days of HFD feeding. But a few publications analyzed the short-term effects of HFD feeding within 3 to 7 days. In this early periode, they agreed about alterations in glucose/insulin sensitivity and offered a wide range of contributing mechanisms, depending on the investigated focus. The onset of HFD feeding leads to adipocyte hypoxia, due to increased uncoupled respiration (Lee et al. 2014), elevated emission of reactive oxygen species of mitochondria (Paglialunga et al. 2015), inflammatory processes in the liver (Radonjic et al. 2009; Kleemann et al. 2010; Lanthier et al. 2010), hypothalamus (Thaler et al. 2012) and/or adipose tissue (Ji et al. 2012; Hadad et al. 2013; Wiedemann et al. 2013), as well as altered production of adipose-tissue derived cytokines (Lee et al. 2011; Williams et al. 2014). Considered individually, every mechanism can lead to insulin resistance sooner or later, but in every metabolism all processes interact and it is nearly impossible to find the crucial pathway. Besides this, it was not feasible to perform all required experiments to cover all metabolic possibilities. Moreover, metabolism is not a steady system and is keen to adapt to the environment. More precisely, returning to the first days of HFD feeding, the similarity of all above published results is an unusual lipid overload caused by hyperphagia of HFD.

The development of HFD-induced impairments of glucose homeostasis needs to be divided into two parts: firstly, the diet-dependent and, secondly, the obesity-related phase. In the present study, AKR/J and SWR/J mice showed impaired glucose tolerance and normal insulin tolerance

in response to acute over-eating of HFD, independent of obesity. As opposed to this, a moderate intake of HFD in a pair-fed group resulted in normal glucose tolerance (Williams et al. 2014). Further evidence comes from studies working with intravenous infusions of lipids. Spontaneous lipid-overload induced systemic insulin resistance in rodents and humans (Ferrannini et al. 1983; Roden et al. 1996; Holland et al. 2007; Frangioudakis and Cooney 2008). The second phase of impaired glucose and insulin tolerance during HFD feeding is characterized by obesity. SWR/J mice resistant to obesity normalized glucose tolerance during continuing HFD feeding. Adipose tissue accumulation in AKR/J mice seems to be critical in inducing insulin resistance, possibly due to chronic inflammatory processes in adipose tissue and liver. Studies comparing short- and long-term HFD feeding related acute effects on glucose/insulin tolerance to lipid overload but manifest, chronic insulin resistance as being developed by adipose tissue inflammation (Kleemann et al. 2010; Lee et al. 2011; Turner et al. 2013; Wiedemann et al. 2013; Cummins et al. 2014; Williams et al. 2014).

In summary, the early-onset strain- and obesity-independent impairment of glucose tolerance is induced by acute lipid overload die to HFD hyperphagia. This observation is accompanied by normal insulin sensitivity and – reviewed in the literature - independent of inflammation. Whereas, development of obesity through continuing HFD feeding is responsible for chronically reduced glucose and insulin tolerance.

## 4.4. Reversibility of diet-induced obesity effects

**Body mass**

In AKR/J mice, HFD feeding for 12 weeks led to a drastic body mass increase due to fat mass gain and impaired glucose and insulin tolerance. Changing the diet and giving the mice ad libitum access to CD, initiated an instantaneous decrease in body and fat mass (figure 31). After about 5 weeks of refeeding CD, formerly obese mice and steadily CD fed mice did not differ in body mass and fat mass levels any more. Although not significantly, refed mice maintained higher body and fat mass levels. Similar observations were made for C57BL/6 mice refeeding ad libitum chow diet after 7 weeks of HFD feeding (Guo et al. 2009). An attained body mass plateau in AKR/J mice of about 32 g and fat mass of about 6 g, seemed to be a genetically determined set or settling point for AKR/J mice, since CD fed mice continuously increased in weight during the next weeks to finally approach and hold those levels.

Especially in human weight management research, the set point theory is often cited to explain body weight gain after body weight loss (Hoevenaars et al. 2013). Maintenance of a lower body weight is hard to obtain, as it contradicts the evolutionary view of building energy depots in

good times, in order to survive bad times. In a meta-analysis merely half of the patients observed over 2 years (Franz et al. 2007), and in the National Health and Nutrition Examination Survey (NHANES) study only about two thirds, succeeded in holding reduced body mass (Weiss et al. 2007). Factors determining the achievement are genetic predisposition, consciousness of controlling energy balance and, more particularly, resisting western lifestyle and diet temptations (Kramer et al. 1989; Bouchard et al. 1996; Anderson et al. 2001; Vogels et al. 2005). In the present study with AKR/J mice in a controlled environment, reversibility of DIO and maintenance of weight loss were clearly shown, extending till the end of the observational period.

**Energy expenditure**

In the literature, conflicting results relating to the reversibility of DIO in rodent studies have been reported (Guo et al. 2009). Depending on the obesity induction period, as well as on the reversal time, some studies found persistent obesity (Rolls et al. 1980; Rogers 1985; Harris and Martin 1989; Hill et al. 1989; Levin and Dunn-Meynell 2002), whereas others have observed more or less complete obesity reversibility (Bartness et al. 1992; Parekh et al. 1998; Enriori et al. 2007). Despite some degree of remaining obesity, refeeding chow diet normalized metabolic abnormalities, such as serum hormones or energy expenditure (Guo et al. 2009). Interestingly, in humans, energy expenditure during weight loss maintenance is reduced by about 10 % relative to appropriate values for the new body mass (Leibel et al. 1995; Doucet et al. 2003; Rosenbaum et al. 2003). Accordingly, a follow-up study that recently investigated contestants of the TV show "The Biggest Loser", revealed that 6 years after successfully losing weight, most of the participants had regained weight. Additionally, resting metabolic rate which decreased during weight loss, was found to be further reduced after 6 years (Fothergill et al. 2016). Likewise, body mass loss induced reduction of energy expenditure was observed in the present mouse study (figure 36). One week of refeeding CD in AKR/J mice decreased energy expenditure, mainly resting metabolic rate, at about 15-20 % compared to measured values with 12 weeks of HFD feeding. But, as opposed to from the case in humans, energy expenditure did not drop further. Compared to CD fed mice, no differences in energy expenditure were detected in formerly HFD fed AKR/J mice after refeeding the CD for 1, 4 and 8 weeks. RER ratio adapted to the offered diet. One week after switching diet from HFD to CD, RER of refed AKR/J mice was still significantly lower, due to upregulated metabolization of excessive fat mass. But, after 4 weeks RER was comparable to that in CD fed mice. Present end-point results are in accordance with the publication of Guo et al., reporting similar RER and 24 h energy expenditure for BL/6 mice fed chow diet and mice being refed chow diet for 7 weeks after the same time and previously on HFD (Guo et al. 2009).

**Glucose and insulin tolerance**

Hyperinsulinemia and hyperglycemia developed by 4 months HFD feeding in BL/6J mice were completely reversed after 4 months of low-fat diet feeding (Parekh et al. 1998). Further reports supporting the reversibility of impaired glucose metabolism, as induced by the HFD feeding of BL/6J mice, were published after 6 weeks (Schmitz et al. 2016) and 45 days (Kirchner et al. 2012) of caloric restriction. In all three studies, fasting glucose and/or glucose tolerance was measured when previously obese mice reached the body mass of CD fed mice. Thus, through reversibility of obesity, obesity-induced alterations also vanished. The present study broadens these findings by revising how quickly impaired glucose tolerance is ameliorated. After feeding HFD in AKR/J mice for 12 weeks, one week ad libitum CD was sufficient to normalize impaired glucose tolerance. At this time-point, mice still have significantly more fat mass than constantly CD fed mice. Consequently, improvement of glucose tolerance is independent of obesity, instead, the metabolic status of the metabolism - whether it is anabolic or catabolic - is important. Additionally, glycemia in response to an insulin bolus showed the same progression in CD and refed AKR/J mice. But, for both diet groups, this does not imply recovery of insulin tolerance, because injection of insulin did not lead to a decrease in blood glucose. Insulin intolerance seems to be an AKR/J strain specific trait; developing with age and independent of obesity or provided diet. But, as was also seen in BL/6J mice, compared to a fast improvement of glucose tolerance, insulin tolerance required a longer period of caloric restriction (16 weeks) for recovery after 18 weeks HFD feeding (Schmitz et al. 2016).

**Impact of the macronutrient composition and dosage form of the diet during weight loss**

So far, one week of weight loss through refeeding CD was sufficient to normalize impaired glucose tolerance. In the next step, a pair-feeding experiment should clarify if the type of diet is responsible for glucose tolerance amelioration, or if caloric restriction per se leads to improvements. The “new” pair-feeding group received, after 12 weeks ad libitum HFD feeding, restricted amounts of HFD containing the same quantity of energy as the ad libitum refeeding CD group. Loss of fat mass and recovery of glucose tolerance were nearly identical in both weight loss groups (figure 43). For quick reversibility of obesity-induced metabolic alterations the fact that body mass is reduced has more impact than the way in which the reduction is achieved. Interestingly, whereas AUC of the oral glucose tolerance test was comparable for CD, refed and pair-fed mice, fasting glucose levels in the two catabolic diet groups were even lower than levels of CD fed mice. This beneficial effect of caloric intake reduction on glucose tolerance was additionally observed in two studies working with caloric restriction after HFD feeding. Schmitz et al. showed lower glycemia during glucose tolerance tests on formerly obese BL/6J mice that lost weight by receiving 60 % of energy in the form of a low-fat diet, as compared to CD fed mice

(Schmitz et al. 2016). Kirchner et al. performed caloric restriction with 50 % of the calories, as compared to standard diet fed mice with low- and with high-fat diet. Independent of diet, both groups exhibited lower glucose excursion and AUC than the controls. Furthermore, this could underline the importance of the quantity and not the source of calories by a fat mass clamped group. These mice were constantly kept lean on HFD, matching the fat mass of mice fed a low-fat standard diet. Glucose and insulin tolerance of the clamped mice was better than in the controls. This improvement can be explained by a reduced sucrose intake, since HFD contained less sucrose than the standard diet (Kirchner et al. 2012). Sucrose was shown to play a crucial role in the development of insulin resistance (Jurgens et al. 2007), and a high intake is correlated with the pathogenesis of diabetes, obesity and inflammation in humans (Schulze et al. 2004; Stanhope et al. 2009; Malik et al. 2010). All diets in the present work have the same percentual amount of sucrose (5 %). But, with a decrease of food intake in the refed and pair-fed groups, reduced sucrose consumption might contribute to glucose metabolism improvements.

As regards the enduring reversibility of obesity and impaired glucose tolerance, the present study differs from other publications. Here, ad libitum refeeding of CD was the method used to reverse obesity and impaired glucose tolerance. Until the end of the investigation period, no reversion of metabolic improvements was observed. Both studies mentioned above used caloric restriction, with a defined amount of calories being offered to mice once a day. In fact, this forced reduced energy intake led also to beneficial health results, but when caloric restriction ended and mice had ad libitum access to low-fat diet (Schmitz et al. 2016), or high-fat diet (Kirchner et al. 2012), weight regain started quickly. Both state that post-obese individuals are programmed to favor hyperphagia and regaining weight. To maintain prevention of chronically altered metabolic programming, livelong caloric restriction is crucial (Kirchner et al. 2012).

**Plasma parameter and hepatic triglycerides, cholesterol and lipidosis**

Further beneficial effects of one week of refeeding CD, or pair-feeding of restricted HFD, were normalization of several plasma parameters (figure 44). In accordance with the literature (Parekh et al. 1998; Kirchner et al. 2012; Hoevenaars et al. 2014; Schmitz et al. 2016), formerly elevated insulin and leptin levels decreased in response to weight loss. Fasting insulin in both catabolic groups was equal to CD fed mice, whereas leptin was still slightly increased in the pair-fed group. Additionally, lipid metabolism parameters measured in plasma like triglycerides and cholesterol were completely reversed after one week reduced feeding intervention. But, the period of one week was not sufficient to normalize hepatic triglycerides and cholesterol amounts. Likewise, the histological assessment of lipidosis of hepatocytes and hepatic tissue revealed a minor subjective amelioration, but no quick reversibility of ectopic fat accumulation (figure 45). One study showed that liver triglycerides were significantly reduced after 5 weeks of refeeding ad libitum low-fat diet or, after the same time, restricted amounts of HFD in the same

range, compared to HFD fed BL/6J mice (Hoevenaars et al. 2014). In contradiction to this, Wang et al. found differences in the improvement of hepatic inflammation and steatosis between obese BL/6J mice that lost weight either by ad libitum low-fat diet feeding, or restricted HFD feeding. After 4 weeks, intervention with low-fat diet was superior in reducing liver triglycerides and expression of chemokines and macrophage markers in the liver (Wang et al. 2011). Similar results were published by de Meijer et al., showing that HFD induced hepatic steatosis is made reversible (measured after 9 weeks) through caloric restriction, but to a greater extend, yet more sustainable through low-fat diet feeding, than by restricted HFD feeding (de Meijer et al. 2010).

Finally, HFD induced alterations of metabolism, namely impaired glucose tolerance and plasma parameters were reversible within one week of refeeding CD, or pair-feeding HFD, to an equal caloric quantity. The complete reversibility of obesity and hepatic steatosis needs more time. Short-time metabolic ameliorations are achieved independently of the source of calories, but most essential is the reduction itself. But, for maintaining long-lasting weight reduction success and benefits, low-fat diets are superior, as referred to in the literature. Furthermore, some publications found evidence that formerly obese individuals are programmed to favor regaining weight, for example through the slowing down of metabolism. Analysis of energy expenditure in the present study does not give hints towards this hypothesis.

## 4.5. Influence of metabolic status of adipose tissue

After HFD feeding, one week of reduced energy intake, independent of the diet's macronutrient composition, was sufficient to normalize impaired metabolic parameters, such as glucose tolerance. Obesity, however, was not totally reversible at this time-point, but clearly retrogressive. To give an appropriate comparison for these still obese AKR/J mice with catabolic metabolism, a further group of AKR/J mice started HFD later and reached equal body mass after 3 weeks of HFD feeding. At the age of 25 weeks, mice of both the catabolic and anabolic groups had the same lean mass, fat mass, hepatic lipidosis and nearly equal gene expression of glucose-metabolism related genes in the liver (figure 43, 45). But mice of the anabolic group exhibited elevated fasting glycemia, impaired glucose tolerance and higher plasma levels of insulin, leptin and cholesterol (figure 43, 44). Since the liver, as the key organ in glucose metabolism, was inconspicuous, adipose tissue was investigated in more detail.

In human studies of weight reduction, visceral adipose tissue is preferentially reduced, as compared to subcutaneous fat (Ross and Rissanen 1994; Janssen and Ross 1999) and may contribute to the advantages of modest weight loss (Chaston and Dixon 2008). Furthermore, in

obese rats responsiveness of lipid metabolism-related genes to fasting is more sensitive in visceral fat than in subcutaneous fat (Li et al. 2003). In the present study, fat depot weighing after dissection revealed higher visceral fat mass, as represented by epididymal and retroperitoneal fat in anabolic AKR/J mice, than in catabolic AKR/J mice (figure 46). Apparently, the abdominal region is, on the one hand, most susceptible to accumulate fat in times of excess energy and, on the other hand, it is the fat depot that can be quickly mobilized when energy is needed. For further characterization of visceral epididymal white adipose tissue (eWAT) on the gene expression level, next-generation sequencing was performed.
The catabolic group consists of mice losing weight either through refeeding CD (HF-CD) or through restricted feeding of HFD (HF-pf). First expression analysis of eWAT revealed distinct similarities in both catabolic groups. Merely three genes were differentially regulated in eWAT between HF-CD and HF-pf mice (table 6). Peripherin (Prph) was upregulated in eWAT of HF-pf mice, Abp1 and Kctd14 were upregulated in HF-CD eWAT. Since abundance of all three genes is rather low in adipose tissue - in the present study namely 6-166 total reads - expression differences as a discrimination characteristic of HF-pf and HF-CD groups, can be neglected.

Taken together, in vivo data, plasma levels and gene transcripts of adipose tissue did not differ between obese AKR/J mice losing weight by ad libitum CD feeding, and AKR/J mice on restricted HFD. In the literature, gene expression of eWAT was different between caloric restriction through low-fat diet and restricted HFD. Hoevenaars et al. showed activation of genes involved in mitochondrial carbohydrate and fatty acid metabolism as well as reduction of inflammation markers and macrophage infiltration in the white adipose tissue of mice fed restricted HFD (Hoevenaars et al. 2014). Reasons for the superiority of restricted HFD feeding may be found in a higher caloric restriction (70 % of previous HFD consumption) and, consequently, more body mass loss, as compared to the group of mice receiving low-fat diet ad libitum after obesity induction (Hoevenaars et al. 2014). These findings are supported by the publication of Wang et al., describing greater improvements in adipose tissue inflammation in mice losing weight by restricted HFD feeding than in mice losing weight through normal diet feeding (Wang et al. 2011). Contrary to the studies of Hoevenaars and Wang, weight-reduction experiments of Schmitz and colleagues in obese mice indeed showing slightly improved insulin sensitivity, but did not achieve amelioration of macrophage infiltration and inflammatory gene expression in white adipose tissue (Schmitz et al. 2016). The most striking difference between the studies might be that Schmitz et al. used a low-fat diet for the reduction of energy intake. This summary of the literature stresses the importance of the method of caloric restriction. More positive effects in adipose tissue are generated by body weight reduction through restricted HFD feeding, than by refeeding (ad libitum) low-fat diet. One possible explanation could be an additional fasting period, occurring inevitably in experiments with energy restriction, and that has an

impact on metabolic parameters and gene expression (Mizuno et al. 1996; Ahren et al. 1997; Zhang et al. 2002). Normally, pair-fed mice receive their food bolus immediately before lights off. Based on experience, they eat up food within the first hours. Consequently, the fasting period begins within the second half of the night. When experiments are performed in the midday after a 6 hour fast starting in the morning, pair-fed mice would have been without food longer than their fasted control littermates after ad libitum feeding. In the present analysis, gene expression in adipose tissue did not differ considerately between both catabolic diet groups after a one week intervention.

Because of the great similarity of regulated genes in the HF-CD and HF-pf both groups can be merged into one catabolic group. The next step focused on RNA expression differences in eWAT in the catabolic AKR/J mice, and in fat mass matched anabolic AKR/J mice, with the aim to find promising candidates or activated pathways which might help to explain differences in glucose metabolism. Resulting genes lists failed to bring forth salient and convincing candidate genes (table 8). The challenge was that less is known or has been published in the literature about most of the assigned genes. Further numbers of total reads varied a lot between genes and raise the question as to whether transcripts with more than 1000 total reads have more impact than transcripts with less than 100 reads. Generally, it is debatable as to how much can be concluded from transcript level to protein expression, or even to whole metabolism. Nevertheless, for some genes, the relation of expression in anabolic and catabolic eWAT underlines the processes taking place in adipose tissue. For example, fatty acid binding protein 3, involved in fatty acid uptake, transport and targeting (Nakamura et al. 2013) is more expressed in catabolic eWAT, where tissue is undergoing a break-down process and fatty acids from adipose tissue are required as an energy substrate. Another interesting gene clearly overexpressed in anabolic eWAT, is Pnpla3. Normally Pnpla3, also known as adiponutrin, plays a role in lipid droplet formation (Chamoun et al. 2013) and is expressed in liver and adipose tissue (Li et al. 2012). In the literature it was shown that adiponutrin expression was highly nutritional, regulated depending on energy status. In humans, low-calorie intake for two days reduced adiponutrin expression in adipose tissue by about one third, whereas refeeding increased abundance by about the same range over the baseline (Liu et al. 2004). Likewise, in adipose tissue of mice during fasting, adiponutrin expression was nearly undetectable, whereas it increased dramatically through feeding a high carbohydrate diet (Baulande et al. 2001). Hints towards metabolic interference of adiponutrin and glucose metabolism are provided by in vitro experiments, detecting an insulin-mediated upregulation of expression in a dose- and time-dependent manner (Kershaw et al. 2006). Further influence of adiponutrin expression on fat accumulation and glucose metabolism are discussed controversially. Overexpression of Pnpla3 in mouse liver increased serum triglyceride levels and altered glucose tolerance (Qiao et al. 2011), whereas, in contrast, overexpression in adipose tissue (Li et al. 2012) and a global deletion and experimental intervention to increase

Pnpla3 expression did not affect metabolic phenotypes of energy, glucose, lipid homoeostasis or hepatic steatosis (Basantani et al. 2011). In the present study, impaired glucose tolerance and increased plasma cholesterol and insulin were associated with high Pnpla3 abundance. Certainly, more research needs to be done but, adiponutrin expression is one possible contributor to explaining differences in glucose tolerance between anabolic and catabolic AKR/J mice.

Analysis of pathways identified 20 differentially regulated pathways between eWAT of catabolic and anabolic AKR/J mice (table 9). Greatest variations were found for the phagosome, followed by osteoclast differentiation and a broad range of infectious and immune system-related processes. This list looks at first glance atypical. However, here the first week of caloric restriction goes hand-in-hand with a massive breakdown of adipose tissue that mobilizes fatty acid for energy supply. Besides lipolysis of accumulated fat, adipocytes along with all of their surrounding environment and incorporations are degraded. All metabolic breakdown products have to be recycled or removed and cleared away. The high ranking of phagosome action within regulated pathways can be explained by the fact that phagocytosis is a main player in these degrading processes. A relative of the phagocytes is to be found at position two of the regulated pathways: osteoclasts, responsible for breakdown of bone tissue, derived from the monocyte/macrophage haematopoietic lineage (Boyle et al. 2003). It has been shown that caloric restriction has a high impact on bone integrity. Experiments examining caloric restriction in obese female rats for 4 months (Shen et al. 2013), in male rats for 2 weeks (Turner and Iwaniec 2011), in male adult mice for 10 weeks (Hamrick et al. 2008) and in young mice for 12 weeks (Devlin et al. 2010) revealed decreased bone mass and formation. Possibly, this progression starts already within the first week of caloric restriction, accompanied by upregulation of pathways in adipose tissue that influence osteoclast differentiation. Published comparable transcriptomic analysis of adipose tissue is currently quite rare. In the mouse study of Kim et al. caloric restriction effects transcriptome of epididymal fat through the down-regulation of genes influencing extracellular matrix structure, cell adhesion, cytoskeleton, cell cycle and adipogenesis. Whereas on the other hand, genes involved in tricarboxylic acid cycle and the electron transport chain were up-regulated (Kim et al. 2016). In the present study these groups of genes were not among the top-regulated pathways. However, the transcriptome analysis of Kim et al. was conducted in lean mice after 10 weeks of caloric restriction and therefore presented results of a rather steady state that limit comparability to the list of regulated pathways in the present study.

Generally, results of this analysis do not reveal for which metabolic status the pathway is up- or down-regulated. Only 236 differentially expressed genes that match low criteria are clustered and assigned to a suitable pathway. With this selection of genes, the biggest differences are seen for pathways with influence on the immune system. This does not mean that other metabolic

processes are unchanged between anabolic and catabolic eWAT, but that this approach may not be appropriate in detecting differences. For example, the fact that mice were fasted for at least 6 hours before tissue withdrawal could have covered possible changes between pathways of energy substrate oxidation, whereas gene expression involving pathways of the immune system is rather independent of fasting or feeding status. Further small insignificant differences between both catabolic groups may lead to an increase in variation within the catabolic group and conceal differences that could exist between expression levels of anabolic and one of the catabolic groups. Therefore, in the last step of RNA sequencing data analysis, expression of defined genes was compared between all three groups (figure 51). Selecting 4 representative genes for lipogenesis (Acaca, Fasn, Tpi1, Pnpla3) and for fatty acid oxidation (Srebf2, Acacb, Cpt1b, Lipa), respectively, revealed increased expression of lipogenic genes in the anabolic HFD group and a trend towards up-regulated fatty acid oxidation in both catabolic groups. Furthermore, this approach of targeted comparison of expression gives hints that may help to explain different glucose tolerance in mice with the same fat mass. Indeed, expression of adipose tissue derived hormones, leptin and resistin, known to be associated with obesity and insulin resistance (Steppan and Lazar 2002; Kershaw and Flier 2004) are upregulated in the anabolic group, as compared to both catabolic groups (figure 49). Interestingly, adiponectin expression, as assumed protector of insulin resistance (Yamauchi et al. 2001), showed the same expression pattern as leptin and resistin. In respect of pro- and anti-inflammatory adipokines, it was not possible to show a clear classification into diet groups (figure 50). For example, highest expression of retinol binding protein 4, discussed as contributing to insulin resistance and obesity (Yang et al. 2005) in the anabolic group, fits to expectations. But expression of pro-inflammatory adipokines TNFα and Il6 was significantly, or tended to be downregulated in eWAT of HFD fed mice.

To sum up, expression of adipokines such as adiponutrin, leptin and resistin contribute to partly explain differences in glucose tolerance in obese AKR/J with catabolic and anabolic metabolism. Identification of most regulated pathways of phagosome, osteoclast and immune response helped to characterize dominant processes. Limitations of applied comparison of expression data are the low number of total reads of some transcripts and the investigation of tissue of only 9 mice (n=3 anabolic, n=6 catabolic). And ultimately, gene expression does not reflect levels of active circulating proteins due to post-translational modifications and complex molecule interaction.

## 4.6. Heredity of diet-induced obesity

Based on clear differences in susceptibility to DIO of AKR/J and SWR/J mice, a cross-breeding experiment of these two strains could offer insights into the heredity of resistance or propensity to DIO. Progeny of the F1-generation are heterozygous regarding every gene, receiving one AKR/J allele and one SWR/J allele of every other gene. Based on fundamental genetic rules, phenotypes of monogenetic traits of the F1 progeny can be attributed to a dominant-recessive, co-dominant or intermediate inheritance. To account for possible allosome heredity, and more likely for uterine and weaning influences of the dams, both parental combinations of F1-generation offspring were bred. Male AKR/J and female SWR/J mice gave birth to AK-SWR/J mice. The other way round, breeding male SWR/J and female AKR/J mice resulted in SW-AKR/J mice. Size of the litter was dependent on the strain of the mother (table 10, appendix). As observed in our own breeding facility (figure 21), as well as in inbred experiments in the Jackson Laboratories (Laboratory 1991), female SWR/J mice bear more pubs per litter than AKR/J mice. This fact is transferable to cross-breeding since AK-SWR/J mice were born in larger litters than SW-AKR/J mice.

**Table 10: Comparative summary of weaning parameters and post-weaning development of body mass and composition in recombinant strains.** Recombinant strains AK-SWR/J and SW-AKR/J were compared to their parental strains AKR/J (A) and SWR/J (S). Results were classified as similar (=), greater (>) or smaller (<) to a parental strain or intermediate (int.) within both strains.

| basics | litter size | body mass | | | lean mass | | fat mass | |
|---|---|---|---|---|---|---|---|---|
| | | Weaning | 3-8 wks | 8-12 wks | 3-8 wks | 8-12 wks | 3-8 wks | 8-12 wks |
| AK-SWR/J | =S | int. | =A | >A, >S | =A | >A, >S | =S | =A, >S |
| SW-AKR/J | =A | >A, >S | =A | >A, >S | =A | >A, >S | =A | >A |

Due to the inverse correlation of litter size and birth weight (Crozier and Enzmann 1935; Reading 1966; Funk-Keenan 2005), AK-SWR/J mice weighed less than SW-AKR/J mice. Notably, despite the comparable litter size of AKR/J and SW-AKR/J mice, pubs of the recombinant strain weighed significantly more at weaning than inbred AKR/J mice. Generally, in smaller litters more nursing care and mother's milk remains for pubs. Maybe SWR/J mice, usually born in greater litters, have developed mechanisms for a more effective nourishment utilization to catch up with growth quickly. These SWR/J related influences, together with small litter sizes might contribute to the high weaning weight in SW-AKR/J mice. Further gain of body mass and lean mass during chow and CD feeding proceeded absolutely identically for both recombinant strains (figure 53). Even changing diet to purified CD did not interrupt the gain of body mass, due to increasing lean mass. The ability to quickly adaptat to diet may be attributed to SWR/J influence since, in contrast to AKR/J mice, SWR/J mice have a stable body mass in response to diet change. Initially, in respect of fat mass, both recombinant strains resembled their maternal strain,

respectively. They reached a critical fat mass at the age of 6 weeks where they leveled out for the next few weeks. This was a unique characteristic of recombinant strains since inbred AKR/J and SWR/J decreased in fat mass. This beneficial capability for stability and adaptation can be the result of cross-breeding, the first step towards outbreeding. Increased genetic variability, with presence of two possibly different alleles for one gene, may not only express the mean of traits but also a symbiotic reinforcement that was previously reduced, due to inbreeding (Brockmann 2005). Although AK-SWR/J and SW-AKR/J mice mostly showed the same phenotype, development of fat mass does not proceed similarly, but in parallel (figure 53). Between 6 and 12 weeks of age, SW-AKR/J mice had about 30 % (1 g) more fat than AK-SWR/J mice. Higher fat mass in SW-AKR/J can be an imprinting phenomenon which is characterized by a parent-of-origin dependent expression of genes (Bartolomei and Ferguson-Smith 2011; Lawson et al. 2013). It is however more likely that the mother's intrauterine environment and nursing care might have long-term effects on recombinant strains, so that fat mass gain is more related to the respective maternal strain (Funk-Keenan 2005). Additionally, higher body mass at weaning of SW-AKR/J mice can contribute to a higher increase in fat mass.

In respect of body mass and body composition, 4 weeks HFD feeding led to an identical response in AK-SWR/J and SW-AKR/J mice (table 11, figure 54). No differences between maternal and paternal combination were found to be indicative of an imprinting independent progress. On first sight, both recombinant strains seemed to be comparable to AKR/J mice, since measured body mass during HFD feeding resembles that of AKR/J mice on HFD. But, differently to AKR/J mice, whose increase in body mass is mainly caused by fat mass accumulation, in AK-SWR/J and SW-AKR/J mice, high lean mass has distinct impact on body mass, whereas fat mass developed intermediately, related to parental strains.

**Table 11: Comparative summary of body mass and body composition in recombinant strains during high-fat diet feeding intervention.** Recombinant strains AK-SWR/J and SW-AKR/J fed HFD were compared to their parental strains AKR/J (A) and SWR/J (S). Results were classified as similar (=), greater (>) or smaller (<) to a parental strain or intermediate (int.) within both strains.

| Strain | Measured data | | | Delta values | | |
|---|---|---|---|---|---|---|
| | body mass | lean mass | fat mass | body mass | lean mass | fat mass |
| AK-SWR/J | =A | >A, >S | int. | =S | <A, <S | int. |
| SW-AKR/J | =A | >A, >S | int. | =S | <A, <S | int. |

Moreover, calculation of delta values, reflecting the difference between mass at the beginning and the end of intervention, revealed comparable body mass gain in AK-SWR/J, SW-AKR/J and SWR/J mice (figure 55). For recombinant strains, the accumulation of fat mass within 4 weeks of HFD feeding ranged between AKR/J and SWR/J mice, with more tendency towards SWR/J mice. On balance, it is not that simple to assign the response to HFD of AK-SWR/J and SW-AKR/J mice

to a parental strain. Depending on the readout, recombinant strains resemble in their susceptibility to DIO either AKR/J mice (measured body mass), or SWR/J mice (body mass changes), or have phenotype in-between strains (fat mass).

In the 1990s, West at al. performed cross-breeding experiments with AKR/J and SWR/J mice to investigate the genetics of dietary obesity (West et al. 1994b). After feeding mice of the F1-generation with condensed milk containing HFD (32.6 kJ% of fat) for 12 weeks, body mass of the intercross progeny was intermediate relating to parental strains, with trends towards AKR/J body mass. Following that they analyzed DIO in the F2-generation and in the F1 back-cross (F1 X AKR/J, F1 X SWR/J), and came to the conclusion that the AKR/J genotype significantly dominates the SWR/J phenotype. Unfortunately, West et al. gave no further information about body mass changes or body composition. Additionally, due to a different study-design (diet, intervention duration, age of mice), comparison of the present data to the West study is limited. Nevertheless, one important aim of West et al. was to discover genes that differ between AKR/J and SWR/J mice, and could therefore be crucial for DIO. With QTL analysis, several loci could be defined as having a certain impact on obesity progression (West et al. 1994a). But below the line, HFD induced obesity is a polygenetic progression. Since differences between AKR/J and SWR/J mice cannot be traced back to classical genes known for monogenetic obesity, extreme phenotypes of these two mouse strains are the interaction of the expression of different genes. The findings of West et al. support the results in the present study that reason that differences in DIO are found on both sides of the energy balance. West et al. did not observe a significant correlation of cumulative caloric intake and adiposity (West et al. 1994b). Recombinant progeny of the F2-generation were lighter than AKR/J mice, but tended to have a higher food intake. Consequently, the adiposity driving trait is not solely located on the side of energy intake regulation. For that recombinant progeny are able to counteract the AKR/J-like hyperphagia, the energy expenditure side needing to be activated in a more SWR/J similar manner. For a more exact statement of the heredity of energy balance regulation, further experiments need to be done. As for AKR/J and SWR/J mice, a comprehensive energy balance breakdown featuring assimilated energy, activity, body core temperature and indirect caloric measurement would be necessary.

The next evaluated distinguishing characteristic between AKR/J and SWR/J for identifying the heredity of obesity-induced metabolic alterations was the analysis of glucose tolerance in AK-SWR/J and SW-AKR/J mice after 4 weeks of HFD feeding (figure 56, 57). As shown above, AKR/J mice fed HFD developed an impaired glucose tolerance, whereas basal glucose, oral glucose tolerance and tAUC were unaffected by diet in SWR/J mice. In recombinant strains on CD basal blood, glucose was relatively high and comparable to that of AKR/J mice (table 12). With this higher reference value, and differing from AKR/J mice, basal glycemia was not increased due to HFD in recombinant strains.

**Table 12: Comparative summary of glucose parameters in recombinant strains during high-fat diet feeding intervention.** Recombinant strains AK-SWR/J and SW-AKR/J were compared to their parental strains AKR/J (A) and SWR/J (S). Results were classified as similar (=), greater (>) or smaller (<) to a parental strain or intermediate (int.) within both strains.

| Glucose | basal | | oGTT | | tAUC | |
|---|---|---|---|---|---|---|
| | CD | HF | CD | HF | CD | HF |
| AK-SWR/J | =A | =A | >A, >S | =A | =A | =A |
| SW-AKR/J | =A | =A | >A, >S | =S | =A | =S |

To evaluate whether HFD induces changes in glucose tolerance in recombinant strains, and to which parental strain possible changes may be attributed, once more it is important to find the suitable reference. First, when response to oral glucose administration in HFD fed AKR/J mice is defined as impaired, then AK-SWR/J mice, with comparable glucose curves and tAUC to AKR/J, will show impaired glucose tolerance as well. But at a second glance, and more suitably for interpretation, comparing recombinant mice on CD with respective HFD fed mice reveals no differences between diet groups (appendix). Thus, AK-SWR/J and SW-AKR/J mice have neither HFD-induced impaired glucose tolerance, nor altered basal glucose levels. Reasons for that may be the already relatively high levels on CD. With higher amounts of lean mass, as compared to parental strains there might be more need for glucose as an energy substrate. Therefore, the gluconeogenesis rate can be increased and can lead to higher basal glucose levels. Additionally, gained through a combination of AKR/J and SWR/J alleles, recombinant strains are more flexible in dealing with changing energy substrates. This assumption addresses once more Brockmann's explanation that inbreeding caused metabolic restrictions can be improved by increased genetic variability (Brockmann 2005). Moreover, as shown in the long-term HFD feeding of AKR/J and SWR/J mice, impaired glucose tolerance is rather a consequence of obesity, than of diet per se. This is supported by the literature, where visceral adiposity is strongly correlated with glucose metabolism impairments, namely insulin resistance (Bergman et al. 2007; Ye 2013). For recombinant strains, a feeding period of 4 weeks might be too short for the accumulation of fat mass amounts to cause impaired glucose tolerance. The 6 g of fat mass that were reached on average in HFD fed recombinant mice are standard levels for other age-matched inbred mouse strains (129X1, DBA/2) on CD with normal glucose tolerance (Montgomery et al. 2013).

Glucose tolerance is unchanged by 4 weeks of HFD feeding in recombinant strains but, however, blood glucose curves during glucose tolerance tests differ clearly between AK-SWR/J and SW-AKR/J mice. At younger ages, and in respect of fat mass development recombinant strains were more associated with respective maternal strains. For glucose levels in response to glucose bolus, this relation turns around and recombinant strains resemble more respective paternal strains. Once more, besides obesity regulation of glucose metabolism is also polygenic and not dominantly inherited by a parental strain. Furthermore, imprinting plays a role since

recombinant strains show differences. A broad range of studies examined imprinting genes of obesity (Vrang et al. 2010; Weinstein et al. 2010; Cheverud et al. 2011; Morita et al. 2014), insulin resistance (Hines et al. 2011) and type 2 diabetes (Kong et al. 2009). By methylation of DNA, the expression of either the maternal or paternal allele is promoted, which can be influenced by environmental factors. During intrauterine development and nursing time, influence of the mother dominates clearly, so that expression might be in favor of maternal alleles. With ongoing age, sexual maturity and independence from parental care, paternal alleles may become more pronounced.

On CD, AK-SWR/J and SW-AKR/J mice had heavier livers than AKR/J and SWR/J mice (figure 59). In fact, the observation can be partly explained by higher body mass in recombinant strains. Adjustment of liver weight to body mass rendered AK-SWR/J mice comparable to AKR/J mice (appendix). Nevertheless, liver weight in SW-AKR/J mice remained higher than the weight in the other strains. HFD feeding led to an increase in liver mass in AKR/J mice. Liver mass in SWR/J mice was unchanged. On the one hand, liver mass gain can be interpreted as ectopic fat accumulation, or on the other hand, as necessary organ enlargement for adaptation to more body mass. After adjustment of data to body mass for AKR/J mice, the HFD-induced increase vanished. Although the second interpretation might give a mathematical explanation, findings in other experiments should not be ignored. Considering that histological analysis of AKR/J mice fed HFD for 3-4 weeks revealed fat droplet inclusions between and within hepatocytes (figure 45H, I), the assumption that increased liver weight is based on ectopic fat accumulation was supported. Liver mass of HFD fed AK-SWR/J and SW-AKR/J mice weighed intermediately, compared to parental strains and matched perfectly the results of West et al. (West et al. 1994b). But compared to respective intra-strain CD fed mice it was quite astonishing that recombinant mice decreased liver weight on HFD. Unfortunately, West et al. did not present any results for liver weights in CD fed F1-generation mice. In the literature there is no hint of HFD-induced reduction in liver weight. The only unlikely possibility may be organ destroying liver cirrhosis. But visual inspection during dissection was unsuspicious and 4 weeks of HFD feeding was too short for this chronic disease. Thus comparably high liver weight on CD and the reduction on HFD are unique characteristics of recombinant strains which cannot be explained by any parental strain. Certainly, when solely concerned with existing liver weights, no conclusions for functionality and histology of the liver can be drawn.

The spleen functions as a blood filter and the initiator of immune reactions, which enlarges during infections (Lucia and Booss 1981; Cesta 2006; Tarantino et al. 2011). The difference of spleen weight between parental strains is significantly different (figure 58). Independent of diet, spleen mass in SWR/J mice is twice that in AKR/J mice. Mice of the intercross fed CD and HFD, showed a spleen mass in-between that of AKR/J and SWR/J mice. Adjustment to body mass

revealed a HFD-related increase in spleen mass in AKR/J and AK-SWR/J mice. This might be an indicator for a challenged immune system. Numerous studies state a close relation between obesity, inflammation and insulin resistance (Hotamisligil et al. 1993; Xu et al. 2003; Pedersen et al. 2015). Matching these results, increased spleen weight occurred in the two mouse strains with highest glycemia during the oral glucose tolerance test. But for more than speculative associations, further functional and histological studies need to be done. Besides that, mostly (visceral) white adipose tissue inflammation is related to HFD induced impaired glucose tolerance or insulin resistance (Shoelson et al. 2006; Bergman et al. 2007; Xu et al. 2012; Ye 2013). Solely in AKR/J mice, HFD led to extension of all weighed fat depots. Compared to respective intra-strain CD fed mice, AKR/J is the only strain with impaired glucose tolerance. Consequently white adipose tissue accumulation might have the bigger impact on glucose metabolism alterations than spleen mass. Additionally, the highest spleen mass is measured in lean, HFD fed SWR/J mice with normal glucose tolerance. In general, determined spleen masses in SWR/J mice fit to the published data with inbred mouse strains of about the same age who show spleen masses of about 100 mg (Welch and Welch 1969; Tsai et al. 2002; Laboratory 2006). Taking this into account draws the attention to the abnormally light AKR/J spleens, rather than to “big” spleens in SWR/J mice. Besides for obesity research, AKR/J mice are often used in the study of leukemia. AKR/J mice possess an endogenous ectopic murine leukemia virus which causes leukemia at the age of 6 to 7 months (Hays and Vredevoe 1977; Rowe 1978; Cloyd et al. 1980). 90 % of AKR/J mice die due to leukemia within 200 to 400 days of age (Storer 1966; Yun et al. 2010). The presence of the virus, and possible multiple proviral DNA expressions which prepare the onset of cancer genesis, may cause small spleen weight to suppress immune function.

Liver and spleen weight as well as the mass change during HFD, is inherited neither with the dominance of one parental strain, nor intermediately. Unique characteristics in strains were first thought to simplify relationships but, in fact, demonstrate a polygenetic interplay.

So far obesity was discussed in respect of the results of fat mass assessment by NMR. Briefly, measured fat mass of recombinant strains was intermediate compared to parenteral strains, whereas absolute gain in fat mass during intervention was still in-between strains, but more closely related to SWR/J mice (figure 54, 55). Weighing different adipose tissues supported these results (figure 59). After HFD feeding, intrascapular brown adipose tissue, whose increase in AKR/J mice was most likely due to ectopic white fat infiltration, and subcutaneous inguinal white adipose tissue, were comparable between SWR/J, AK-SWR/J and SW-AKR/J mice (table 13). Visceral fat, dissected from the epididymal and retroperitoneal region, was moderately but significantly increased in recombinant strains fed HFD, and therefore in-between parental strains. Differences for CD fed mice were negligible. For humans it is well reviewed that body fat

distribution is crucial for the development of obesity-related comorbidities, like impaired glucose tolerance with a higher prevalence of abdominal fat accumulation, than for subcutaneous fat accumulation (Kahn et al. 2001; Bergman et al. 2007; Booth et al. 2014). In more in detail: a good metabolic status with healthy adipokine secretion is more important than fat mass and location per se, and leads to metabolically healthy obese men and mice (Denis and Obin 2013; Gunawardana 2014). This may also be the case for AK-SWR/J and SW-AKR/J mice, which are moderately abdominally obese, but with no differences in oral glucose tolerance tests between mice fed CD and mice on HFD. After 4 weeks of HFD, fat mass extension had not reached a threshold that caused glucose metabolism alterations.

**Table 13: Comparative summary of white adipose tissue weights after high-fat diet feeding in recombinant strains.** Recombinant strains AK-SWR/J and SW-AKR/J fed HFD were compared to their parental strains AKR/J (A) and SWR/J (S). Results were classified as similar (=), greater (>) or smaller (<) to a parental strain or intermediate (int.) within both strains.

| Adipose tissue | iBAT | eWAT | sWAT | rWAT |
|---|---|---|---|---|
| AK-SWR/J | =S | int. | =S | int. |
| SW-AKR/J | =S | int. | =S | int. |

In summary, mice of the F1-generation of an intercross of AKR/J, and SWR/J mice, display both complexity of polygenetic heredity of DIO and glucose tolerance. For characterization, selected traits were used with clear differences between parental strains, aiming at a distinct attribution of the progeny. The offspring from the cross-breeding could neither be associated with one parental strain, nor was the phenotype intermediate. Depending on the observed trait, the F1-generation was like AKR/J (e.g. body mass after 4 weeks HFD), like SWR/J (e.g. body mass change during 4 weeks HFD), intermediate (e.g. fat mass), or developed recombinant specific features, such as high lean mass and basal glucose levels. To account for the different origin of Y-/ X-chromosomes, mitochondrial DNA, the influence of uterine and nursing environment and imprinting in general, offspring of both parental combinations were bred (Brockmann 2005; Funk-Keenan 2005). Generally, both recombinant strains exhibited the same phenotype. But in early development (week 3-12), maternal strain impact concerning fat mass was observed, whereas oral glucose tolerance after 4 weeks of HFD was influenced by the paternal strain. This assessable study set-up gives first results about heredity and thought-provoking impulses for a better characterization of the F1 generation. It would be interesting to conduct indirect calorimetry, to assess energy intake, activity and body-core temperature, to extend HFD feeding and to repeat experiments on female progeny also. Furthermore, to collect more information about heredity, a F2-generation with back-cross to parental strains needs to be bred and analysis of the genome done. The latter was done more than 20 years ago by West et al., who found indications of AKR/J dominance and identifying quantitative trait loci (QTL) involved in

the development of DIO (West et al. 1994a; West et al. 1994b). Additionally, today's bioinformatical tools and growing databases that share information about SNPs, QTLs and gene expression offer possibilities to substantiate phenotype observations with descriptive results.

## 4.7. Conclusion and Perspectives

The first part of this work emphasized the importance of planning a well-considered study. Depending on the question addressed to the HFD feeding intervention study, the choice of diet, mouse strain, start and duration of feeding are crucial to the outcome. In the present study, impaired glucose tolerance and the fat mass accumulation of C57BL/6J mice, as main read-outs for HFD-induced metabolic changes, did not develop in a strict time- and fat quantity-dependent manner. Partly controversially, as regards the literature, feeding HFD based on palm oil impaired glucose tolerance more than feeding lard-based HFD. Furthermore, besides all efforts at standardization, it is challenging to compare one's own gathered results with those in the literature, due to differences in housing conditions, mouse handling and hygienic status.

Basically, obesity develops because more energy is taken up by food and remains in the body, than the energy that is extended. This study is the first to examine both sides of energy balance and to unravel the proximate causes that lead to diet-induced obesity. DIO resistant SWR/J and DIO prone AKR/J mice were precisely compared regarding metabolizable energy and energy expenditure before HFD feeding. Higher energy expenditure, lower RER, less pronounced night-day-rhythm and more vertical/climbing activity may predispose SWR/J mice to burn excess energy better than AKR/J mice do. Both strains showed hyperphagia, increased RMR and $T_b$ immediately after starting HFD feeding. AKR/J mice become obese due to higher metabolizable energy that cannot be defended sufficiently by rising energy expenditure. The difference in positive energy balance between strains correlates with accumulated fat mass. Additionally, as recommended by the literature, linear regression models and ANCOVA were used to adjust the data of energy balance. This method should be state-of-the-art and applied for energy expenditure and metabolizable energy in all future experiments that investigate energy balance in individuals differing in body mass/composition.

HFD experiments with mouse strains that differ in susceptibility to DIO, make it possible to distinguish between the effects of diet and obesity. Therefore, development of HFD-induced impairments of glucose homeostasis could be divided into two parts. Firstly, the diet- dependent phase during the initial days of HFD, in which AKR/J and SWR/J mice showed impaired glucose tolerance in response to acute over-eating of HFD (1.5 days). The second phase is characterized by obesity. Adipose tissue accumulation in AKR/J mice seemed to be critical for the progression

of impaired glucose and insulin tolerance, since SWR/J mice normalized glucose tolerance during continuing HFD feeding. After HFD feeding for 12 weeks, one week of reduced energy intake independent of the diet's macronutrient composition was sufficient to normalize impaired metabolic parameters, such as glucose tolerance. However, obesity was not totally reversed at this time point. It remained on a level similar to AKR/J mice fed HFD for about 3 weeks that exhibited impaired glucose tolerance. Investigated expression of adipokines, such as adiponutrin, leptin and resistin in eWAT, could partly explain differences in glucose tolerance in obese AKR/J with catabolic and anabolic metabolism. Furthermore, analysis of examples of other tissues, as well as proteomics and metabolomics would be helpful to find metabolites and pathways causing differences in glucose tolerance. Continuing weight loss in formerly obese HFD fed AKR/J mice decreased energy expenditure. But, other than in human weight reduction observations, energy expenditure did not decrease beneath values that were expected for the respective body mass. Moreover, this might be a crucial factor for the success of AKR/J mice in maintaining reduced body mass. More investigations of energy balance, similar to the assessment during the first days of HFD, during continuing HFD feeding and during subsequent weight loss would be valuable for a better understanding of energy balance regulation.

In the last section the F1-generation of an intercross of AKR/J and SWR/J mice was characterized in order to clarify the heredity of DIO susceptibility. To account for imprinting influence, offspring from both parental combinations was bred. The progeny displayed the complexity of polygenetic heredity of DIO and glucose tolerance, as it could neither be associated to one parental strain, nor was the phenotype intermediate. It would be interesting to conduct indirect calorimetry, to assess energy intake, activity and body-core temperature, to extend HFD feeding and to repeat experiments in female progeny also. Additionally, today's bioinformatical tools and growing databases share information about SNPs, QTLs and gene expression and offer possibilities for substantiating phenotype observations with descriptive results, and might help to unravel DIO heredity.

# 5. LITERATURE

**Aberle, J.; Flitsch, J.; Beck, N.A.; Mann, O.; Busch, P.; Peitsmeier, P.; and Beil, F.U.** (2008). Genetic variation may influence obesity only under conditions of diet: analysis of three candidate genes. Mol Genet Metab *95*, 188-191.

**Ahren, B.; Mansson, S.; Gingerich, R.L.; and Havel, P.J.** (1997). Regulation of plasma leptin in mice: influence of age, high-fat diet, and fasting. Am J Physiol *273*, R113-120.

**Allison, D.B.; Paultre, F.; Goran, M.I.; Poehlman, E.T.; and Heymsfield, S.B.** (1995). Statistical considerations regarding the use of ratios to adjust data. Int J Obes Relat Metab Disord *19*, 644-652.

**Anderson, J.W.; Konz, E.C.; Frederich, R.C.; and Wood, C.L.** (2001). Long-term weight-loss maintenance: a meta-analysis of US studies. Am J Clin Nutr *74*, 579-584.

**Andrikopoulos, S.; Blair, A.R.; Deluca, N.; Fam, B.C.; and Proietto, J.** (2008). Evaluating the glucose tolerance test in mice. Am J Physiol Endocrinol Metab *295*, E1323-1332.

**Antunes, L.C.; Levandovski, R.; Dantas, G.; Caumo, W.; and Hidalgo, M.P.** (2010). Obesity and shift work: chronobiological aspects. Nutr Res Rev *23*, 155-168.

**Arch, J.R.; Hislop, D.; Wang, S.J.; and Speakman, J.R.** (2006). Some mathematical and technical issues in the measurement and interpretation of open-circuit indirect calorimetry in small animals. Int J Obes (Lond) *30*, 1322-1331.

Atwater, W.O.; and Benedict, F.G. (1903). Experiments on the metabolism of matter and energy in the human body, 1900-1902., U.S.D.o.A.O.o.E. Stations, ed. (Washington, D.C.: United States Government Printing Office).

**Atwater, W.O.; and Rosa, E.B.** (1899). A New Respiration Calorimeter and Experiments on the Conservation of Energy in the Human Body. Physical Review *9*, 214-251.

**Ayala, J.E.; Samuel, V.T.; Morton, G.J.; Obici, S.; Croniger, C.M.; Shulman, G.I., . . . Consortium, N.I.H.M.M.P.C.** (2010). Standard operating procedures for describing and performing metabolic tests of glucose homeostasis in mice. Dis Model Mech *3*, 525-534.

**Ayub, Q.; Moutsianas, L.; Chen, Y.; Panoutsopoulou, K.; Colonna, V.; Pagani, L., . . . Xue, Y.** (2014). Revisiting the thrifty gene hypothesis via 65 loci associated with susceptibility to type 2 diabetes. Am J Hum Genet *94*, 176-185.

**Barsh, G.S.; Farooqi, I.S.; and O'Rahilly, S.** (2000). Genetics of body-weight regulation. Nature *404*, 644-651.

**Bartness, T.J.; Polk, D.R.; McGriff, W.R.; Youngstrom, T.G.; and DiGirolamo, M.** (1992). Reversal of high-fat diet-induced obesity in female rats. Am J Physiol *263*, R790-797.

**Bartolomei, M.S.; and Ferguson-Smith, A.C.** (2011). Mammalian genomic imprinting. Cold Spring Harb Perspect Biol *3*.

**Basantani, M.K.; Sitnick, M.T.; Cai, L.; Brenner, D.S.; Gardner, N.P.; Li, J.Z., . . . Kershaw, E.E.** (2011). Pnpla3/Adiponutrin deficiency in mice does not contribute to fatty liver disease or metabolic syndrome. J Lipid Res *52*, 318-329.

**Baulande, S.; Lasnier, F.; Lucas, M.; and Pairault, J.** (2001). Adiponutrin, a transmembrane protein corresponding to a novel dietary- and obesity-linked mRNA specifically expressed in the adipose lineage. J Biol Chem *276*, 33336-33344.

**Bell, J.T.; and Spector, T.D.** (2011). A twin approach to unraveling epigenetics. Trends Genet *27*, 116-125.

**Benoit, B.; Laugerette, F.; Plaisancie, P.; Geloen, A.; Bodennec, J.; Estienne, M., . . . Michalski, M.C.** (2015). Increasing fat content from 20 to 45 wt% in a complex diet induces lower endotoxemia in parallel with an increased number of intestinal goblet cells in mice. Nutr Res.

**Bergman, R.N.; Kim, S.P.; Hsu, I.R.; Catalano, K.J.; Chiu, J.D.; Kabir, M., . . . Ader, M.** (2007). Abdominal obesity: role in the pathophysiology of metabolic disease and cardiovascular risk. Am J Med *120*, S3-8; discussion S29-32.

**Bjursell, M.; Gerdin, A.K.; Lelliott, C.J.; Egecioglu, E.; Elmgren, A.; Tornell, J., . . . Bohlooly, Y.M.** (2008). Acutely reduced locomotor activity is a major contributor to Western diet-induced obesity in mice. Am J Physiol Endocrinol Metab *294*, E251-260.

**Black, B.L.; Croom, J.; Eisen, E.J.; Petro, A.E.; Edwards, C.L.; and Surwit, R.S.** (1998). Differential effects of fat and sucrose on body composition in A/J and C57BL/6 mice. Metabolism *47*, 1354-1359.
**Blaxter, K.L.** (1978). Adair Crawford and calorimetry. Proc Nutr Soc *37*, 1-3.
**Booth, A.; Magnuson, A.; and Foster, M.** (2014). Detrimental and protective fat: body fat distribution and its relation to metabolic disease. Horm Mol Biol Clin Investig *17*, 13-27.
**Boren, J.; Taskinen, M.R.; Olofsson, S.O.; and Levin, M.** (2013). Ectopic lipid storage and insulin resistance: a harmful relationship. J Intern Med *274*, 25-40.
**Bothe, G.W.; Bolivar, V.J.; Vedder, M.J.; and Geistfeld, J.G.** (2004). Genetic and behavioral differences among five inbred mouse strains commonly used in the production of transgenic and knockout mice. Genes Brain Behav *3*, 149-157.
**Bouchard, C.; Tremblay, A.; Despres, J.P.; Nadeau, A.; Lupien, P.J.; Moorjani, S., . . . Kim, S.Y.** (1996). Overfeeding in identical twins: 5-year postoverfeeding results. Metabolism *45*, 1042-1050.
**Bowe, J.E.; Franklin, Z.J.; Hauge-Evans, A.C.; King, A.J.; Persaud, S.J.; and Jones, P.M.** (2014). Metabolic phenotyping guidelines: assessing glucose homeostasis in rodent models. J Endocrinol *222*, G13-25.
**Bowes, C.; Li, T.; Frankel, W.N.; Danciger, M.; Coffin, J.M.; Applebury, M.L.; and Farber, D.B.** (1993). Localization of a retroviral element within the rd gene coding for the beta subunit of cGMP phosphodiesterase. Proc Natl Acad Sci U S A *90*, 2955-2959.
**Boyle, W.J.; Simonet, W.S.; and Lacey, D.L.** (2003). Osteoclast differentiation and activation. Nature *423*, 337-342.
**Bray, G.A.** (1996). Health hazards of obesity. Endocrinol Metab Clin North Am *25*, 907-919.
Brockmann, G.A. (2005). Inbreeding and Crossbreeding. In The Mouse in Animal Genetics and Breeding Research, E.J. Eisen, ed. (London: Imperial College Press), pp. 57-83.
**Brons, C.; Jensen, C.B.; Storgaard, H.; Hiscock, N.J.; White, A.; Appel, J.S., . . . Vaag, A.** (2009). Impact of short-term high-fat feeding on glucose and insulin metabolism in young healthy men. J Physiol *587*, 2387-2397.
**Bryant, C.D.; Zhang, N.N.; Sokoloff, G.; Fanselow, M.S.; Ennes, H.S.; Palmer, A.A.; and McRoberts, J.A.** (2008). Behavioral differences among C57BL/6 substrains: implications for transgenic and knockout studies. J Neurogenet *22*, 315-331.
**Buettner, R.; Parhofer, K.G.; Woenckhaus, M.; Wrede, C.E.; Kunz-Schughart, L.A.; Scholmerich, J.; and Bollheimer, L.C.** (2006). Defining high-fat-diet rat models: metabolic and molecular effects of different fat types. J Mol Endocrinol *36*, 485-501.
**Cano, C.; Bermudez, V.J.; Medina, M.T.; Bermudez, F.A.; Ambard, M.J.; Souki, A.J., . . . Velasco, M.** (2003). Trimetazidine diminishes fasting glucose in rats with fasting hyperglycemia: a preliminary study. Am J Ther *10*, 444-446.
**Carroll, L.; Voisey, J.; and van Daal, A.** (2004). Mouse models of obesity. Clin Dermatol *22*, 345-349.
**Carter-Dawson, L.D.; LaVail, M.M.; and Sidman, R.L.** (1978). Differential effect of the rd mutation on rods and cones in the mouse retina. Invest Ophthalmol Vis Sci *17*, 489-498.
**Castillo-Fernandez, J.E.; Spector, T.D.; and Bell, J.T.** (2014). Epigenetics of discordant monozygotic twins: implications for disease. Genome Med *6*, 60.
**Castro, A.V.; Kolka, C.M.; Kim, S.P.; and Bergman, R.N.** (2014). Obesity, insulin resistance and comorbidities? Mechanisms of association. Arq Bras Endocrinol Metabol *58*, 600-609.
**Catta-Preta, M.; Martins, M.A.; Cunha Brunini, T.M.; Mendes-Ribeiro, A.C.; Mandarim-de-Lacerda, C.A.; and Aguila, M.B.** (2012). Modulation of cytokines, resistin, and distribution of adipose tissue in C57BL/6 mice by different high-fat diets. Nutrition *28*, 212-219.
**Cesta, M.F.** (2006). Normal structure, function, and histology of the spleen. Toxicol Pathol *34*, 455-465.
**Chadt, A.; Leicht, K.; Deshmukh, A.; Jiang, L.Q.; Scherneck, S.; Bernhardt, U., . . . Al-Hasani, H.** (2008). Tbc1d1 mutation in lean mouse strain confers leanness and protects from diet-induced obesity. Nat Genet *40*, 1354-1359.

**Chakravarthy, M.V.; and Booth, F.W.** (2004). Eating, exercise, and "thrifty" genotypes: connecting the dots toward an evolutionary understanding of modern chronic diseases. J Appl Physiol (1985) *96*, 3-10.
**Chamoun, Z.; Vacca, F.; Parton, R.G.; and Gruenberg, J.** (2013). PNPLA3/adiponutrin functions in lipid droplet formation. Biol Cell *105*, 219-233.
**Champy, M.F.; Selloum, M.; Piard, L.; Zeitler, V.; Caradec, C.; Chambon, P.; and Auwerx, J.** (2004). Mouse functional genomics requires standardization of mouse handling and housing conditions. Mamm Genome *15*, 768-783.
**Champy, M.F.; Selloum, M.; Zeitler, V.; Caradec, C.; Jung, B.; Rousseau, S., . . . Auwerx, J.** (2008). Genetic background determines metabolic phenotypes in the mouse. Mamm Genome *19*, 318-331.
**Chassaing, B.; Miles-Brown, J.; Pellizzon, M.; Ulman, E.; Ricci, M.; Zhang, L., . . . Gewirtz, A.T.** (2015). Lack of soluble fiber drives diet-induced adiposity in mice. Am J Physiol Gastrointest Liver Physiol *309*, G528-541.
**Chaston, T.B.; and Dixon, J.B.** (2008). Factors associated with percent change in visceral versus subcutaneous abdominal fat during weight loss: findings from a systematic review. Int J Obes (Lond) *32*, 619-628.
**Cheverud, J.M.; Lawson, H.A.; Fawcett, G.L.; Wang, B.; Pletscher, L.S.; A, R.F., . . . Semenkovich, C.F.** (2011). Diet-dependent genetic and genomic imprinting effects on obesity in mice. Obesity (Silver Spring) *19*, 160-170.
**Chiazza, F.; Challa, T.D.; Lucchini, F.C.; Konrad, D.; and Wueest, S.** (2016). A short bout of HFD promotes long-lasting hepatic lipid accumulation. Adipocyte *5*, 88-92.
**Chisholm, K.W.; and O'Dea, K.** (1987). Effect of short-term consumption of a high fat diet on glucose tolerance and insulin sensitivity in the rat. J Nutr Sci Vitaminol (Tokyo) *33*, 377-390.
**Cloyd, M.W.; Hartley, J.W.; and Rowe, W.P.** (1980). Lymphomagenicity of recombinant mink cell focus-inducing murine leukemia viruses. J Exp Med *151*, 542-552.
**Coelho, D.F.; Pereira-Lancha, L.O.; Chaves, D.S.; Diwan, D.; Ferraz, R.; Campos-Ferraz, P.L., . . . Lancha Junior, A.H.** (2011). Effect of high-fat diets on body composition, lipid metabolism and insulin sensitivity, and the role of exercise on these parameters. Braz J Med Biol Res *44*, 966-972.
**Comuzzie, A.G.; and Allison, D.B.** (1998). The search for human obesity genes. Science *280*, 1374-1377.
**Crabbe, J.C.; Gallaher, E.J.; Cross, S.J.; and Belknap, J.K.** (1998). Genetic determinants of sensitivity to diazepam in inbred mice. Behav Neurosci *112*, 668-677.
**Crawley, J.N.; Belknap, J.K.; Collins, A.; Crabbe, J.C.; Frankel, W.; Henderson, N., . . . Paylor, R.** (1997). Behavioral phenotypes of inbred mouse strains: implications and recommendations for molecular studies. Psychopharmacology (Berl) *132*, 107-124.
**Crozier, W.J.; and Enzmann, E.V.** (1935). On the Relation between Litter Size, Birth Weight, and Rate of Growth, in Mice. J Gen Physiol *19*, 249-263.
**Cummins, T.D.; Holden, C.R.; Sansbury, B.E.; Gibb, A.A.; Shah, J.; Zafar, N., . . . Hill, B.G.** (2014). Metabolic remodeling of white adipose tissue in obesity. Am J Physiol Endocrinol Metab *307*, E262-277.
**Curtis, R.; Geesaman, B.J.; and DiStefano, P.S.** (2005). Ageing and metabolism: drug discovery opportunities. Nat Rev Drug Discov *4*, 569-580.
**Dalke, C.; Loster, J.; Fuchs, H.; Gailus-Durner, V.; Soewarto, D.; Favor, J., . . . Graw, J.** (2004). Electroretinography as a screening method for mutations causing retinal dysfunction in mice. Invest Ophthalmol Vis Sci *45*, 601-609.
**de Meijer, V.E.; Le, H.D.; Meisel, J.A.; Akhavan Sharif, M.R.; Pan, A.; Nose, V.; and Puder, M.** (2010). Dietary fat intake promotes the development of hepatic steatosis independently from excess caloric consumption in a murine model. Metabolism *59*, 1092-1105.
**DeFronzo, R.A.; and Abdul-Ghani, M.** (2011). Assessment and treatment of cardiovascular risk in prediabetes: impaired glucose tolerance and impaired fasting glucose. Am J Cardiol *108*, 3B-24B.

**DeFronzo, R.A.; Ferrannini, E.; and Simonson, D.C.** (1989). Fasting hyperglycemia in non-insulin-dependent diabetes mellitus: contributions of excessive hepatic glucose production and impaired tissue glucose uptake. Metabolism *38*, 387-395.
**DeFronzo, R.A.; Tobin, J.D.; and Andres, R.** (1979). Glucose clamp technique: a method for quantifying insulin secretion and resistance. Am J Physiol *237*, E214-223.
**DeLany, J.P.; Windhauser, M.M.; Champagne, C.M.; and Bray, G.A.** (2000). Differential oxidation of individual dietary fatty acids in humans. Am J Clin Nutr *72*, 905-911.
**Denis, G.V.; and Obin, M.S.** (2013). 'Metabolically healthy obesity': origins and implications. Mol Aspects Med *34*, 59-70.
**DeRuisseau, L.R.; Parsons, A.D.; and Overton, J.M.** (2004). Adaptive thermogenesis is intact in B6 and A/J mice studied at thermoneutrality. Metabolism *53*, 1417-1423.
**Desmarchelier, C.; Ludwig, T.; Scheundel, R.; Rink, N.; Bader, B.L.; Klingenspor, M.; and Daniel, H.** (2013). Diet-induced obesity in ad libitum-fed mice: food texture overrides the effect of macronutrient composition. Br J Nutr *109*, 1518-1527.
**Devlin, M.J.; Cloutier, A.M.; Thomas, N.A.; Panus, D.A.; Lotinun, S.; Pinz, I., . . . Bouxsein, M.L.** (2010). Caloric restriction leads to high marrow adiposity and low bone mass in growing mice. J Bone Miner Res *25*, 2078-2088.
**Doucet, E.; Imbeault, P.; St-Pierre, S.; Almeras, N.; Mauriege, P.; Despres, J.P., . . . Tremblay, A.** (2003). Greater than predicted decrease in energy expenditure during exercise after body weight loss in obese men. Clin Sci (Lond) *105*, 89-95.
**Eberhart, G.P.; West, D.B.; Boozer, C.N.; and Atkinson, R.L.** (1994). Insulin sensitivity of adipocytes from inbred mouse strains resistant or sensitive to diet-induced obesity. Am J Physiol *266*, R1423-1428.
**Eckardt, K.; Taube, A.; and Eckel, J.** (2011). Obesity-associated insulin resistance in skeletal muscle: role of lipid accumulation and physical inactivity. Rev Endocr Metab Disord *12*, 163-172.
Elia, M. (1992). Organ and tissue contribution to metabolic rate. In Energy Metabolism: Tissue Determinants and Cellular Corollaries, J.M. Kinney, and H.N. Tucker, eds. (New York: Raven Press), pp. 61-77.
**Elvert, R.; Wille, A.; Wandschneider, J.; Werner, U.; Glombik, H.; and Herling, A.W.** (2013). Energy loss via urine and faeces--a combustive analysis in diabetic rats and the impact of antidiabetic treatment on body weight. Diabetes Obes Metab *15*, 324-334.
**Enriori, P.J.; Evans, A.E.; Sinnayah, P.; Jobst, E.E.; Tonelli-Lemos, L.; Billes, S.K., . . . Cowley, M.A.** (2007). Diet-induced obesity causes severe but reversible leptin resistance in arcuate melanocortin neurons. Cell Metab *5*, 181-194.
**Even, P.; Mariotti, F.; and Hermier, D.** (2010). Postprandial effects of a lipid-rich meal in the rat are modulated by the degree of unsaturation of 18C fatty acids. Metabolism *59*, 231-240.
**Even, P.C.; and Nadkarni, N.A.** (2012). Indirect calorimetry in laboratory mice and rats: principles, practical considerations, interpretation and perspectives. Am J Physiol Regul Integr Comp Physiol *303*, R459-476.
**Farooqi, I.S.; and O'Rahilly, S.** (2005). Monogenic obesity in humans. Annu Rev Med *56*, 443-458.
**Fergusson, G.; Ethier, M.; Guevremont, M.; Chretien, C.; Attane, C.; Joly, E., . . . Alquier, T.** (2014). Defective insulin secretory response to intravenous glucose in C57Bl/6J compared to C57Bl/6N mice. Mol Metab *3*, 848-854.
**Ferrannini, E.; Barrett, E.J.; Bevilacqua, S.; and DeFronzo, R.A.** (1983). Effect of fatty acids on glucose production and utilization in man. J Clin Invest *72*, 1737-1747.
**Fothergill, E.; Guo, J.; Howard, L.; Kerns, J.C.; Knuth, N.D.; Brychta, R., . . . Hall, K.D.** (2016). Persistent metabolic adaptation 6 years after "The Biggest Loser" competition. Obesity (Silver Spring).
**Frangioudakis, G.; and Cooney, G.J.** (2008). Acute elevation of circulating fatty acids impairs downstream insulin signalling in rat skeletal muscle in vivo independent of effects on stress signalling. J Endocrinol *197*, 277-285.
**Franz, M.J.; Boucher, J.L.; Rutten-Ramos, S.; and VanWormer, J.J.** (2015). Lifestyle weight-loss intervention outcomes in overweight and obese adults with type 2 diabetes: a

systematic review and meta-analysis of randomized clinical trials. J Acad Nutr Diet *115*, 1447-1463.
**Franz, M.J.; VanWormer, J.J.; Crain, A.L.; Boucher, J.L.; Histon, T.; Caplan, W., . . . Pronk, N.P.** (2007). Weight-loss outcomes: a systematic review and meta-analysis of weight-loss clinical trials with a minimum 1-year follow-up. J Am Diet Assoc *107*, 1755-1767.
**Fromme, T.; and Klingenspor, M.** (2011). Uncoupling protein 1 expression and high-fat diets. Am J Physiol Regul Integr Comp Physiol *300*, R1-8.
**Froy, O.** (2010). Metabolism and circadian rhythms--implications for obesity. Endocr Rev *31*, 1-24.
Funk-Keenan, J.A., W. R. (2005). Maternal Effects, Genomic Imprinting and Evolution. In The Mouse in Animal Genetics and Breeding Research, E.J. Eisen, ed. (London: Imperial College Press), pp. 29-56.
**Geng, T.; Hu, W.; Broadwater, M.H.; Snider, J.M.; Bielawski, J.; Russo, S.B., . . . Cowart, L.A.** (2013). Fatty acids differentially regulate insulin resistance through endoplasm reticulum stress-mediated induction of tribbles homologue 3: a potential link between dietary fat composition and the pathophysiological outcomes of obesity. Diabetologia *56*, 2078-2087.
**Giesen, K.; Plum, L.; Kluge, R.; Ortlepp, J.; and Joost, H.G.** (2003). Diet-dependent obesity and hypercholesterolemia in the New Zealand obese mouse: identification of a quantitative trait locus for elevated serum cholesterol on the distal mouse chromosome 5. Biochem Biophys Res Commun *304*, 812-817.
**Glavas, M.M.; Kirigiti, M.A.; Xiao, X.Q.; Enriori, P.J.; Fisher, S.K.; Evans, A.E., . . . Grove, K.L.** (2010). Early overnutrition results in early-onset arcuate leptin resistance and increased sensitivity to high-fat diet. Endocrinology *151*, 1598-1610.
**Grayson, B.E.; Seeley, R.J.; and Sandoval, D.A.** (2013). Wired on sugar: the role of the CNS in the regulation of glucose homeostasis. Nat Rev Neurosci *14*, 24-37.
**Greenberg, A.S.; and Obin, M.S.** (2006). Obesity and the role of adipose tissue in inflammation and metabolism. Am J Clin Nutr *83*, 461S-465S.
**Greenfield, J.R.; and Campbell, L.V.** (2006). Relationship between inflammation, insulin resistance and type 2 diabetes: 'cause or effect'? Curr Diabetes Rev *2*, 195-211.
**Grundy, S.M.** (2004). Obesity, metabolic syndrome, and cardiovascular disease. J Clin Endocrinol Metab *89*, 2595-2600.
**Gunawardana, S.C.** (2014). Benefits of healthy adipose tissue in the treatment of diabetes. World J Diabetes *5*, 420-430.
**Guo, J.; Jou, W.; Gavrilova, O.; and Hall, K.D.** (2009). Persistent diet-induced obesity in male C57BL/6 mice resulting from temporary obesigenic diets. PLoS One *4*, e5370.
**Gutch, M.; Kumar, S.; Razi, S.M.; Gupta, K.K.; and Gupta, A.** (2015). Assessment of insulin sensitivity/resistance. Indian J Endocrinol Metab *19*, 160-164.
**Hadad, N.; Burgazliev, O.; Elgazar-Carmon, V.; Solomonov, Y.; Wueest, S.; Item, F., . . . Levy, R.** (2013). Induction of cytosolic phospholipase a2alpha is required for adipose neutrophil infiltration and hepatic insulin resistance early in the course of high-fat feeding. Diabetes *62*, 3053-3063.
**Hamrick, M.W.; Ding, K.H.; Ponnala, S.; Ferrari, S.L.; and Isales, C.M.** (2008). Caloric restriction decreases cortical bone mass but spares trabecular bone in the mouse skeleton: implications for the regulation of bone mass by body weight. J Bone Miner Res *23*, 870-878.
**Hariri, N.; and Thibault, L.** (2010). High-fat diet-induced obesity in animal models. Nutr Res Rev *23*, 270-299.
**Harris, R.B.; and Martin, R.J.** (1989). Changes in lipogenesis and lipolysis associated with recovery from reversible obesity in mature female rats. Proc Soc Exp Biol Med *191*, 82-89.
**Hartman, A.L.; Gasior, M.; Vining, E.P.; and Rogawski, M.A.** (2007). The neuropharmacology of the ketogenic diet. Pediatr Neurol *36*, 281-292.
**Hays, E.F.; and Vredevoe, D.L.** (1977). A discrepancy in XC and oncogenicity assays for murine leukemia virus in AKR mice. Cancer Res *37*, 726-730.
**Heiker, J.T.; Kunath, A.; Kosacka, J.; Flehmig, G.; Knigge, A.; Kern, M., . . . Kloting, N.** (2014). Identification of genetic loci associated with different responses to high-fat diet-induced obesity in C57BL/6N and C57BL/6J substrains. Physiol Genomics *46*, 377-384.

**Heldmaier, G.** (1975). The influence of the social thermoregulation on the cold-adaptive growth of BAT in hairless and furred mice. Pflugers Arch *355*, 261-266.
**Hesse, D.; Dunn, M.; Heldmaier, G.; Klingenspor, M.; and Rozman, J.** (2010). Behavioural mechanisms affecting energy regulation in mice prone or resistant to diet-induced obesity. Physiol Behav *99*, 370-380.
**Hill, J.O.; Dorton, J.; Sykes, M.N.; and Digirolamo, M.** (1989). Reversal of dietary obesity is influenced by its duration and severity. Int J Obes *13*, 711-722.
**Hill, J.O.; and Peters, J.C.** (1998). Environmental contributions to the obesity epidemic. Science *280*, 1371-1374.
**Hines, I.N.; Hartwell, H.J.; Feng, Y.; Theve, E.J.; Hall, G.A.; Hashway, S., . . . Rogers, A.B.** (2011). Insulin resistance and metabolic hepatocarcinogenesis with parent-of-origin effects in AxB mice. Am J Pathol *179*, 2855-2865.
**Hoevenaars, F.P.; Keijer, J.; Herreman, L.; Palm, I.; Hegeman, M.A.; Swarts, H.J.; and van Schothorst, E.M.** (2014). Adipose tissue metabolism and inflammation are differently affected by weight loss in obese mice due to either a high-fat diet restriction or change to a low-fat diet. Genes Nutr *9*, 391.
**Hoevenaars, F.P.; Keijer, J.; Swarts, H.J.; Snaas-Alders, S.; Bekkenkamp-Grovenstein, M.; and van Schothorst, E.M.** (2013). Effects of dietary history on energy metabolism and physiological parameters in C57BL/6J mice. Exp Physiol *98*, 1053-1062.
**Holland, W.L.; Brozinick, J.T.; Wang, L.P.; Hawkins, E.D.; Sargent, K.M.; Liu, Y., . . . Summers, S.A.** (2007). Inhibition of ceramide synthesis ameliorates glucocorticoid-, saturated-fat-, and obesity-induced insulin resistance. Cell Metab *5*, 167-179.
**Hotamisligil, G.S.; Shargill, N.S.; and Spiegelman, B.M.** (1993). Adipose expression of tumor necrosis factor-alpha: direct role in obesity-linked insulin resistance. Science *259*, 87-91.
**Huang, E.Y.; Leone, V.A.; Devkota, S.; Wang, Y.; Brady, M.J.; and Chang, E.B.** (2013). Composition of dietary fat source shapes gut microbiota architecture and alters host inflammatory mediators in mouse adipose tissue. JPEN J Parenter Enteral Nutr *37*, 746-754.
**Ikemoto, S.; Takahashi, M.; Tsunoda, N.; Maruyama, K.; Itakura, H.; and Ezaki, O.** (1996). High-fat diet-induced hyperglycemia and obesity in mice: differential effects of dietary oils. Metabolism *45*, 1539-1546.
**Janssen, I.; and Ross, R.** (1999). Effects of sex on the change in visceral, subcutaneous adipose tissue and skeletal muscle in response to weight loss. Int J Obes Relat Metab Disord *23*, 1035-1046.
**Janssens, S.; Heemskerk, M.M.; van den Berg, S.A.; van Riel, N.A.; Nicolay, K.; Willems van Dijk, K.; and Prompers, J.J.** (2015). Effects of low-stearate palm oil and high-stearate lard high-fat diets on rat liver lipid metabolism and glucose tolerance. Nutr Metab (Lond) *12*, 57.
**Ji, Y.; Sun, S.; Xia, S.; Yang, L.; Li, X.; and Qi, L.** (2012). Short term high fat diet challenge promotes alternative macrophage polarization in adipose tissue via natural killer T cells and interleukin-4. J Biol Chem *287*, 24378-24386.
**Johnson, A.M.; and Olefsky, J.M.** (2013). The origins and drivers of insulin resistance. Cell *152*, 673-684.
**Jung, A.P.; Curtis, T.S.; Turner, M.J.; and Lightfoot, J.T.** (2010). Physical activity and food consumption in high- and low-active inbred mouse strains. Med Sci Sports Exerc *42*, 1826-1833.
**Jurgens, H.S.; Neschen, S.; Ortmann, S.; Scherneck, S.; Schmolz, K.; Schuler, G., . . . Joost, H.G.** (2007). Development of diabetes in obese, insulin-resistant mice: essential role of dietary carbohydrate in beta cell destruction. Diabetologia *50*, 1481-1489.
**Kahn, S.E.; Hull, R.L.; and Utzschneider, K.M.** (2006). Mechanisms linking obesity to insulin resistance and type 2 diabetes. Nature *444*, 840-846.
**Kahn, S.E.; Prigeon, R.L.; Schwartz, R.S.; Fujimoto, W.Y.; Knopp, R.H.; Brunzell, J.D.; and Porte, D., Jr.** (2001). Obesity, body fat distribution, insulin sensitivity and Islet beta-cell function as explanations for metabolic diversity. J Nutr *131*, 354S-360S.

**Kaiyala, K.J.; Morton, G.J.; Leroux, B.G.; Ogimoto, K.; Wisse, B.; and Schwartz, M.W.** (2010). Identification of body fat mass as a major determinant of metabolic rate in mice. Diabetes *59*, 1657-1666.
**Kaiyala, K.J.; and Ramsay, D.S.** (2011). Direct animal calorimetry, the underused gold standard for quantifying the fire of life. Comp Biochem Physiol A Mol Integr Physiol *158*, 252-264.
**Kaiyala, K.J.; and Schwartz, M.W.** (2011). Toward a more complete (and less controversial) understanding of energy expenditure and its role in obesity pathogenesis. Diabetes *60*, 17-23.
**Keller, U.** (2006). From obesity to diabetes. Int J Vitam Nutr Res *76*, 172-177.
**Kennedy, A.J.; Ellacott, K.L.; King, V.L.; and Hasty, A.H.** (2010). Mouse models of the metabolic syndrome. Dis Model Mech *3*, 156-166.
**Kershaw, E.E.; and Flier, J.S.** (2004). Adipose tissue as an endocrine organ. J Clin Endocrinol Metab *89*, 2548-2556.
**Kershaw, E.E.; Hamm, J.K.; Verhagen, L.A.; Peroni, O.; Katic, M.; and Flier, J.S.** (2006). Adipose triglyceride lipase: function, regulation by insulin, and comparison with adiponutrin. Diabetes *55*, 148-157.
**Khaodhiar, L.; McCowen, K.C.; and Blackburn, G.L.** (1999). Obesity and its comorbid conditions. Clin Cornerstone *2*, 17-31.
**Kim, S.S.; Choi, K.M.; Kim, S.; Park, T.; Cho, I.C.; Lee, J.W.; and Lee, C.K.** (2016). Whole-transcriptome analysis of mouse adipose tissue in response to short-term caloric restriction. Mol Genet Genomics *291*, 831-847.
**Kirby, A.; Kang, H.M.; Wade, C.M.; Cotsapas, C.; Kostem, E.; Han, B., . . . Daly, M.J.** (2010). Fine mapping in 94 inbred mouse strains using a high-density haplotype resource. Genetics *185*, 1081-1095.
**Kirchner, H.; Hofmann, S.M.; Fischer-Rosinsky, A.; Hembree, J.; Abplanalp, W.; Ottaway, N., . . . Habegger, K.M.** (2012). Caloric restriction chronically impairs metabolic programming in mice. Diabetes *61*, 2734-2742.
**Kleemann, R.; van Erk, M.; Verschuren, L.; van den Hoek, A.M.; Koek, M.; Wielinga, P.Y., . . . Kooistra, T.** (2010). Time-resolved and tissue-specific systems analysis of the pathogenesis of insulin resistance. PLoS One *5*, e8817.
**Kleiber, M.** (1932). Body size and metabolism. Hilgardia *6*, 315-353.
**Kless, C.; Muller, V.M.; Schuppel, V.L.; Lichtenegger, M.; Rychlik, M.; Daniel, H., . . . Haller, D.** (2015). Diet-induced obesity causes metabolic impairment independent of alterations in gut barrier integrity. Mol Nutr Food Res *59*, 968-978.
**Klop, B.; Elte, J.W.; and Cabezas, M.C.** (2013). Dyslipidemia in obesity: mechanisms and potential targets. Nutrients *5*, 1218-1240.
**Kluge, R.; Giesen, K.; Bahrenberg, G.; Plum, L.; Ortlepp, J.R.; and Joost, H.G.** (2000). Quantitative trait loci for obesity and insulin resistance (Nob1, Nob2) and their interaction with the leptin receptor allele (LeprA720T/T1044I) in New Zealand obese mice. Diabetologia *43*, 1565-1572.
**Kong, A.; Steinthorsdottir, V.; Masson, G.; Thorleifsson, G.; Sulem, P.; Besenbacher, S., . . . Stefansson, K.** (2009). Parental origin of sequence variants associated with complex diseases. Nature *462*, 868-874.
**Kowalski, G.M.; and Bruce, C.R.** (2014). The regulation of glucose metabolism: implications and considerations for the assessment of glucose homeostasis in rodents. Am J Physiol Endocrinol Metab *307*, E859-871.
**Kramer, F.M.; Jeffery, R.W.; Forster, J.L.; and Snell, M.K.** (1989). Long-term follow-up of behavioral treatment for obesity: patterns of weight regain among men and women. Int J Obes *13*, 123-136.
**Krishna, S.; Lin, Z.; de La Serre, C.B.; Wagner, J.J.; Harn, D.H.; Pepples, L.M., . . . Filipov, N.M.** (2016). Time-dependent behavioral, neurochemical, and metabolic dysregulation in female C57BL/6 mice caused by chronic high-fat diet intake. Physiol Behav *157*, 196-208.

**Kroes, M.; Osei-Assibey, G.; Baker-Searle, R.; and Huang, J.** (2016). Impact of weight change on quality of life in adults with overweight/obesity in the United States: a systematic review. Curr Med Res Opin *32*, 485-508.
Laboratory, T.J. (1991). Reproductive performance survey, females of 33 inbred strains of mice. In Jaxpheno2 (Mouse Phenome Database web site: The Jackson Laboratory).
Laboratory, T.J. (2006). Morphometric (organ weight) survey of 11 strains of mice, J. Denegre, ed. (Mouse Phenome Database web site: The Jackson Laboratory).
**Lam, Y.Y.; and Ravussin, E.** (2016). Analysis of energy metabolism in humans: A review of methodologies. Mol Metab *5*, 1057-1071.
**Lanthier, N.; Molendi-Coste, O.; Horsmans, Y.; van Rooijen, N.; Cani, P.D.; and Leclercq, I.A.** (2010). Kupffer cell activation is a causal factor for hepatic insulin resistance. Am J Physiol Gastrointest Liver Physiol *298*, G107-116.
**Lawson, H.A.; Cheverud, J.M.; and Wolf, J.B.** (2013). Genomic imprinting and parent-of-origin effects on complex traits. Nat Rev Genet *14*, 609-617.
**Lee, S.Y.; and Gallagher, D.** (2008). Assessment methods in human body composition. Curr Opin Clin Nutr Metab Care *11*, 566-572.
**Lee, Y.S.; Kim, J.W.; Osborne, O.; Oh da, Y.; Sasik, R.; Schenk, S., . . . Olefsky, J.M.** (2014). Increased adipocyte O2 consumption triggers HIF-1alpha, causing inflammation and insulin resistance in obesity. Cell *157*, 1339-1352.
**Lee, Y.S.; Li, P.; Huh, J.Y.; Hwang, I.J.; Lu, M.; Kim, J.I., . . . Kim, J.B.** (2011). Inflammation is necessary for long-term but not short-term high-fat diet-induced insulin resistance. Diabetes *60*, 2474-2483.
**Leibel, R.L.; Rosenbaum, M.; and Hirsch, J.** (1995). Changes in energy expenditure resulting from altered body weight. N Engl J Med *332*, 621-628.
**Leibowitz, S.F.; Alexander, J.; Dourmashkin, J.T.; Hill, J.O.; Gayles, E.C.; and Chang, G.Q.** (2005). Phenotypic profile of SWR/J and A/J mice compared to control strains: possible mechanisms underlying resistance to obesity on a high-fat diet. Brain Res *1047*, 137-147.
**Lephart, E.D.; Setchell, K.D.; Handa, R.J.; and Lund, T.D.** (2004). Behavioral effects of endocrine-disrupting substances: phytoestrogens. ILAR J *45*, 443-454.
**Leto, D.; and Saltiel, A.R.** (2012). Regulation of glucose transport by insulin: traffic control of GLUT4. Nat Rev Mol Cell Biol *13*, 383-396.
**Levin, B.E.; and Dunn-Meynell, A.A.** (2002). Defense of body weight depends on dietary composition and palatability in rats with diet-induced obesity. Am J Physiol Regul Integr Comp Physiol *282*, R46-54.
**Levine, J.A.** (2005). Measurement of energy expenditure. Public Health Nutr *8*, 1123-1132.
**Ley, R.E.; Backhed, F.; Turnbaugh, P.; Lozupone, C.A.; Knight, R.D.; and Gordon, J.I.** (2005). Obesity alters gut microbial ecology. Proc Natl Acad Sci U S A *102*, 11070-11075.
**Leyton, J.; Drury, P.J.; and Crawford, M.A.** (1987). Differential oxidation of saturated and unsaturated fatty acids in vivo in the rat. Br J Nutr *57*, 383-393.
**Li, J.Z.; Huang, Y.; Karaman, R.; Ivanova, P.T.; Brown, H.A.; Roddy, T., . . . Hobbs, H.H.** (2012). Chronic overexpression of PNPLA3I148M in mouse liver causes hepatic steatosis. J Clin Invest *122*, 4130-4144.
**Li, Y.; Bujo, H.; Takahashi, K.; Shibasaki, M.; Zhu, Y.; Yoshida, Y., . . . Saito, Y.** (2003). Visceral fat: higher responsiveness of fat mass and gene expression to calorie restriction than subcutaneous fat. Exp Biol Med (Maywood) *228*, 1118-1123.
**Lightfoot, J.T.; Turner, M.J.; Daves, M.; Vordermark, A.; and Kleeberger, S.R.** (2004). Genetic influence on daily wheel running activity level. Physiol Genomics *19*, 270-276.
**Lightfoot, J.T.; Turner, M.J.; Debate, K.A.; and Kleeberger, S.R.** (2001). Interstrain variation in murine aerobic capacity. Med Sci Sports Exerc *33*, 2053-2057.
**Liu, Y.M.; Moldes, M.; Bastard, J.P.; Bruckert, E.; Viguerie, N.; Hainque, B., . . . Clement, K.** (2004). Adiponutrin: A new gene regulated by energy balance in human adipose tissue. J Clin Endocrinol Metab *89*, 2684-2689.
**Lucia, H.L.; and Booss, J.** (1981). Immune stimulation, inflammation, and changes in hematopoiesis. Host responses of the murine spleen to infection with cytomegalovirus. Am J Pathol *104*, 90-97.

**Lutz, T.A.; and Woods, S.C.** (2012). Overview of animal models of obesity. Curr Protoc Pharmacol *Chapter 5*, Unit5 61.
**Lyons, J.A.; Haring, J.S.; and Biga, P.R.** (2010). Myostatin expression, lymphocyte population, and potential cytokine production correlate with predisposition to high-fat diet induced obesity in mice. PLoS One *5*, e12928.
**Ma, B.W.; Bokulich, N.A.; Castillo, P.A.; Kananurak, A.; Underwood, M.A.; Mills, D.A.; and Bevins, C.L.** (2012). Routine habitat change: a source of unrecognized transient alteration of intestinal microbiota in laboratory mice. PLoS One *7*, e47416.
**Maes, H.H.; Neale, M.C.; and Eaves, L.J.** (1997). Genetic and environmental factors in relative body weight and human adiposity. Behav Genet *27*, 325-351.
**Malik, V.S.; Popkin, B.M.; Bray, G.A.; Despres, J.P.; Willett, W.C.; and Hu, F.B.** (2010). Sugar-sweetened beverages and risk of metabolic syndrome and type 2 diabetes: a meta-analysis. Diabetes Care *33*, 2477-2483.
**McArdle, M.A.; Finucane, O.M.; Connaughton, R.M.; McMorrow, A.M.; and Roche, H.M.** (2013). Mechanisms of obesity-induced inflammation and insulin resistance: insights into the emerging role of nutritional strategies. Front Endocrinol (Lausanne) *4*, 52.
**Milner, L.C.; and Crabbe, J.C.** (2008). Three murine anxiety models: results from multiple inbred strain comparisons. Genes Brain Behav *7*, 496-505.
**Mizuno, T.M.; Bergen, H.; Funabashi, T.; Kleopoulos, S.P.; Zhong, Y.G.; Bauman, W.A.; and Mobbs, C.V.** (1996). Obese gene expression: reduction by fasting and stimulation by insulin and glucose in lean mice, and persistent elevation in acquired (diet-induced) and genetic (yellow agouti) obesity. Proc Natl Acad Sci U S A *93*, 3434-3438.
**Montgomery, M.K.; Hallahan, N.L.; Brown, S.H.; Liu, M.; Mitchell, T.W.; Cooney, G.J.; and Turner, N.** (2013). Mouse strain-dependent variation in obesity and glucose homeostasis in response to high-fat feeding. Diabetologia *56*, 1129-1139.
**Moore, K.J.** (1999). Utilization of mouse models in the discovery of human disease genes. Drug Discov Today *4*, 123-128.
**Morita, S.; Horii, T.; Kimura, M.; Arai, Y.; Kamei, Y.; Ogawa, Y.; and Hatada, I.** (2014). Paternal allele influences high fat diet-induced obesity. PLoS One *9*, e85477.
**Mouse Genome Sequencing, C.; Waterston, R.H.; Lindblad-Toh, K.; Birney, E.; Rogers, J.; Abril, J.F., . . . Lander, E.S.** (2002). Initial sequencing and comparative analysis of the mouse genome. Nature *420*, 520-562.
**Mozes, S.; Sefcikova, Z.; and Racek, L.** (2014). Long-term effect of altered nutrition induced by litter size manipulation and cross-fostering in suckling male rats on development of obesity risk and health complications. Eur J Nutr *53*, 1273-1280.
**Muller, M.J.; Wang, Z.; Heymsfield, S.B.; Schautz, B.; and Bosy-Westphal, A.** (2013). Advances in the understanding of specific metabolic rates of major organs and tissues in humans. Curr Opin Clin Nutr Metab Care *16*, 501-508.
**Muller, V.M.; Zietek, T.; Rohm, F.; Fiamoncini, J.; Lagkouvardos, I.; Haller, D., . . . Daniel, H.** (2016). Gut barrier impairment by high-fat diet in mice depends on housing conditions. Mol Nutr Food Res *60*, 897-908.
**Mutch, D.M.; and Clement, K.** (2006). Unraveling the genetics of human obesity. PLoS Genet *2*, e188.
**Nakamura, Y.; Sato, T.; Shiimura, Y.; Miura, Y.; and Kojima, M.** (2013). FABP3 and brown adipocyte-characteristic mitochondrial fatty acid oxidation enzymes are induced in beige cells in a different pathway from UCP1. Biochem Biophys Res Commun *441*, 42-46.
**Nakatsuji, H.; Kishida, K.; Kitamura, T.; Nakajima, C.; Funahashi, T.; and Shimomura, I.** (2010). Dysregulation of glucose, insulin, triglyceride, blood pressure, and oxidative stress after an oral glucose tolerance test in men with abdominal obesity. Metabolism *59*, 520-526.
**Nawrocki, A.R.; and Scherer, P.E.** (2004). The delicate balance between fat and muscle: adipokines in metabolic disease and musculoskeletal inflammation. Curr Opin Pharmacol *4*, 281-289.
**Neel, J.V.** (1962). Diabetes mellitus: a "thrifty" genotype rendered detrimental by "progress"? Am J Hum Genet *14*, 353-362.
**Nilsson, C.; Raun, K.; Yan, F.F.; Larsen, M.O.; and Tang-Christensen, M.** (2012). Laboratory animals as surrogate models of human obesity. Acta Pharmacol Sin *33*, 173-181.

**Packard, G.C.B., T.J.** (1999). The use of percentages and size-specific indices to normalize physiological data for variation in body size: wasted time, wasted effort? Comparative Biochemistry and Physiology Part A *122*, 37-44.
**Paglialunga, S.; Ludzki, A.; Root-McCaig, J.; and Holloway, G.P.** (2015). In adipose tissue, increased mitochondrial emission of reactive oxygen species is important for short-term high-fat diet-induced insulin resistance in mice. Diabetologia *58*, 1071-1080.
**Pai, T.; and Yeh, Y.Y.** (1996). Stearic acid unlike shorter-chain saturated fatty acids is poorly utilized for triacylglycerol synthesis and beta-oxidation in cultured rat hepatocytes. Lipids *31*, 159-164.
**Paigen, B.** (1995). Genetics of responsiveness to high-fat and high-cholesterol diets in the mouse. Am J Clin Nutr *62*, 458S-462S.
**Parekh, P.I.; Petro, A.E.; Tiller, J.M.; Feinglos, M.N.; and Surwit, R.S.** (1998). Reversal of diet-induced obesity and diabetes in C57BL/6J mice. Metabolism *47*, 1089-1096.
**Patel, M.S.; and Srinivasan, M.** (2011). Metabolic programming in the immediate postnatal life. Ann Nutr Metab *58 Suppl 2*, 18-28.
**Pedersen, D.J.; Guilherme, A.; Danai, L.V.; Heyda, L.; Matevossian, A.; Cohen, J., . . . Czech, M.P.** (2015). A major role of insulin in promoting obesity-associated adipose tissue inflammation. Mol Metab *4*, 507-518.
**Petkov, P.M.; Ding, Y.; Cassell, M.A.; Zhang, W.; Wagner, G.; Sargent, E.E., . . . Wiles, M.V.** (2004). An efficient SNP system for mouse genome scanning and elucidating strain relationships. Genome Res *14*, 1806-1811.
**Prentice, A.M.** (2001). Obesity and its potential mechanistic basis. Br Med Bull *60*, 51-67.
**Prentice, A.M.; Hennig, B.J.; and Fulford, A.J.** (2008). Evolutionary origins of the obesity epidemic: natural selection of thrifty genes or genetic drift following predation release? Int J Obes (Lond) *32*, 1607-1610.
**Prpic, V.; Watson, P.M.; Frampton, I.C.; Sabol, M.A.; Jezek, G.E.; and Gettys, T.W.** (2002). Adaptive changes in adipocyte gene expression differ in AKR/J and SWR/J mice during diet-induced obesity. J Nutr *132*, 3325-3332.
**Prpic, V.; Watson, P.M.; Frampton, I.C.; Sabol, M.A.; Jezek, G.E.; and Gettys, T.W.** (2003). Differential mechanisms and development of leptin resistance in A/J versus C57BL/6J mice during diet-induced obesity. Endocrinology *144*, 1155-1163.
**Qiao, A.; Liang, J.; Ke, Y.; Li, C.; Cui, Y.; Shen, L., . . . Chang, Y.** (2011). Mouse patatin-like phospholipase domain-containing 3 influences systemic lipid and glucose homeostasis. Hepatology *54*, 509-521.
**Radonjic, M.; de Haan, J.R.; van Erk, M.J.; van Dijk, K.W.; van den Berg, S.A.; de Groot, P.J., . . . van Ommen, B.** (2009). Genome-wide mRNA expression analysis of hepatic adaptation to high-fat diets reveals switch from an inflammatory to steatotic transcriptional program. PLoS One *4*, e6646.
**Ramos-Jimenez, A.; Hernandez-Torres, R.P.; Torres-Duran, P.V.; Romero-Gonzalez, J.; Mascher, D.; Posadas-Romero, C.; and Juarez-Oropeza, M.A.** (2008). The Respiratory Exchange Ratio is Associated with Fitness Indicators Both in Trained and Untrained Men: A Possible Application for People with Reduced Exercise Tolerance. Clin Med Circ Respirat Pulm Med *2*, 1-9.
**Ravussin, E.; Lillioja, S.; Anderson, T.E.; Christin, L.; and Bogardus, C.** (1986). Determinants of 24-hour energy expenditure in man. Methods and results using a respiratory chamber. J Clin Invest *78*, 1568-1578.
**Reading, A.J.** (1966). Effects of parity and litter size on the birth weight of inbred mice. J Mammal *47*, 111-114.
**Ridaura, V.K.; Faith, J.J.; Rey, F.E.; Cheng, J.; Duncan, A.E.; Kau, A.L., . . . Gordon, J.I.** (2013). Gut microbiota from twins discordant for obesity modulate metabolism in mice. Science *341*, 1241214.
**Robinson, A.M.; and Williamson, D.H.** (1980). Physiological roles of ketone bodies as substrates and signals in mammalian tissues. Physiol Rev *60*, 143-187.
**Roden, M.; Price, T.B.; Perseghin, G.; Petersen, K.F.; Rothman, D.L.; Cline, G.W.; and Shulman, G.I.** (1996). Mechanism of free fatty acid-induced insulin resistance in humans. J Clin Invest *97*, 2859-2865.

**Rodrigues, A.L.; De Souza, E.P.; Da Silva, S.V.; Rodrigues, D.S.; Nascimento, A.B.; Barja-Fidalgo, C.; and De Freitas, M.S.** (2007). Low expression of insulin signaling molecules impairs glucose uptake in adipocytes after early overnutrition. J Endocrinol *195*, 485-494.
**Rogers, P.J.** (1985). Returning 'cafeteria-fed' rats to a chow diet: negative contrast and effects of obesity on feeding behaviour. Physiol Behav *35*, 493-499.
**Rojas, J.; Aguirre, M.; Velasco, M.; and Bermudez, V.** (2013). Obesity genetics: a monopoly game of genes. Am J Ther *20*, 399-413.
**Rolls, B.J.; Rowe, E.A.; and Turner, R.C.** (1980). Persistent obesity in rats following a period of consumption of a mixed, high energy diet. J Physiol *298*, 415-427.
**Rosenbaum, M.; Ravussin, E.; Matthews, D.E.; Gilker, C.; Ferraro, R.; Heymsfield, S.B., . . . Leibel, R.L.** (1996). A comparative study of different means of assessing long-term energy expenditure in humans. Am J Physiol *270*, R496-504.
**Rosenbaum, M.; Vandenborne, K.; Goldsmith, R.; Simoneau, J.A.; Heymsfield, S.; Joanisse, D.R., . . . Leibel, R.L.** (2003). Effects of experimental weight perturbation on skeletal muscle work efficiency in human subjects. Am J Physiol Regul Integr Comp Physiol *285*, R183-192.
**Rosenthal, N.; and Brown, S.** (2007). The mouse ascending: perspectives for human-disease models. Nat Cell Biol *9*, 993-999.
**Ross, R.; and Rissanen, J.** (1994). Mobilization of visceral and subcutaneous adipose tissue in response to energy restriction and exercise. Am J Clin Nutr *60*, 695-703.
**Rowe, W.P.** (1978). Leukemia virus genomes in the chromosomal DNA of the mouse. Harvey Lect *71*, 173-192.
**Rozman, J.; Klingenspor, M.; and Hrabe de Angelis, M.** (2014). A review of standardized metabolic phenotyping of animal models. Mamm Genome *25*, 497-507.
**Saltiel, A.R.; and Kahn, C.R.** (2001). Insulin signalling and the regulation of glucose and lipid metabolism. Nature *414*, 799-806.
**Salvado, L.; Coll, T.; Gomez-Foix, A.M.; Salmeron, E.; Barroso, E.; Palomer, X.; and Vazquez-Carrera, M.** (2013). Oleate prevents saturated-fatty-acid-induced ER stress, inflammation and insulin resistance in skeletal muscle cells through an AMPK-dependent mechanism. Diabetologia *56*, 1372-1382.
**Sam, S.; and Mazzone, T.** (2014). Adipose tissue changes in obesity and the impact on metabolic function. Transl Res *164*, 284-292.
**Samuel, V.T.; and Shulman, G.I.** (2016). The pathogenesis of insulin resistance: integrating signaling pathways and substrate flux. J Clin Invest *126*, 12-22.
**Sasidharan, S.R.; Joseph, J.A.; Anandakumar, S.; Venkatesan, V.; Ariyattu Madhavan, C.N.; and Agarwal, A.** (2013). An experimental approach for selecting appropriate rodent diets for research studies on metabolic disorders. Biomed Res Int *2013*, 752870.
**Schmitz, J.; Evers, N.; Awazawa, M.; Nicholls, H.T.; Bronneke, H.S.; Dietrich, A., . . . Bruning, J.C.** (2016). Obesogenic memory can confer long-term increases in adipose tissue but not liver inflammation and insulin resistance after weight loss. Mol Metab *5*, 328-339.
**Schulze, M.B.; Liu, S.; Rimm, E.B.; Manson, J.E.; Willett, W.C.; and Hu, F.B.** (2004). Glycemic index, glycemic load, and dietary fiber intake and incidence of type 2 diabetes in younger and middle-aged women. Am J Clin Nutr *80*, 348-356.
**Schutz, Y.** (1997). On problems of calculating energy expenditure and substrate utilization from respiratory exchange data. Z Ernahrungswiss *36*, 255-262.
**Selman, C.; Lumsden, S.; Bunger, L.; Hill, W.G.; and Speakman, J.R.** (2001). Resting metabolic rate and morphology in mice (Mus musculus) selected for high and low food intake. J Exp Biol *204*, 777-784.
**Shen, C.L.; Zhu, W.; Gao, W.; Wang, S.; Chen, L.; and Chyu, M.C.** (2013). Energy-restricted diet benefits body composition but degrades bone integrity in middle-aged obese female rats. Nutr Res *33*, 668-676.
**Shoelson, S.E.; Lee, J.; and Goldfine, A.B.** (2006). Inflammation and insulin resistance. J Clin Invest *116*, 1793-1801.

**Sluyter, F.; Marican, C.C.; and Crusio, W.E.** (1999). Further phenotypical characterisation of two substrains of C57BL/6J inbred mice differing by a spontaneous single-gene mutation. Behav Brain Res *98*, 39-43.
**Smith, B.K.; Andrews, P.K.; and West, D.B.** (2000). Macronutrient diet selection in thirteen mouse strains. Am J Physiol Regul Integr Comp Physiol *278*, R797-805.
**Smith, B.K.; Andrews, P.K.; York, D.A.; and West, D.B.** (1999). Divergence in proportional fat intake in AKR/J and SWR/J mice endures across diet paradigms. Am J Physiol *277*, R776-785.
**Song, S.; Andrikopoulos, S.; Filippis, C.; Thorburn, A.W.; Khan, D.; and Proietto, J.** (2001). Mechanism of fat-induced hepatic gluconeogenesis: effect of metformin. Am J Physiol Endocrinol Metab *281*, E275-282.
**Speakman, J.; Hambly, C.; Mitchell, S.; and Krol, E.** (2008). The contribution of animal models to the study of obesity. Lab Anim *42*, 413-432.
**Speakman, J.R.** (2004). Obesity: the integrated roles of environment and genetics. J Nutr *134*, 2090S-2105S.
**Speakman, J.R.; Fletcher, Q.; and Vaanholt, L.** (2013). The '39 steps': an algorithm for performing statistical analysis of data on energy intake and expenditure. Dis Model Mech *6*, 293-301.
Speakman, J.R.; and Johnson, M.S. (2000). Relationships between resting metabolic rate and morphology in lactating mice: what tissues are the major contributors to resting metabolism? In Life in the Cold, G. Heldmaier, and M. Klingenspor, eds. (Berlin: Springer).
**Speakman, J.R.; Levitsky, D.A.; Allison, D.B.; Bray, M.S.; de Castro, J.M.; Clegg, D.J., . . . Westerterp-Plantenga, M.S.** (2011). Set points, settling points and some alternative models: theoretical options to understand how genes and environments combine to regulate body adiposity. Dis Model Mech *4*, 733-745.
**Stanhope, K.L.; Schwarz, J.M.; Keim, N.L.; Griffen, S.C.; Bremer, A.A.; Graham, J.L., . . . Havel, P.J.** (2009). Consuming fructose-sweetened, not glucose-sweetened, beverages increases visceral adiposity and lipids and decreases insulin sensitivity in overweight/obese humans. J Clin Invest *119*, 1322-1334.
**Stemmer, K.; Kotzbeck, P.; Zani, F.; Bauer, M.; Neff, C.; Muller, T.D., . . . Divanovic, S.** (2015). Thermoneutral housing is a critical factor for immune function and diet-induced obesity in C57BL/6 nude mice. Int J Obes (Lond) *39*, 791-797.
**Steppan, C.M.; and Lazar, M.A.** (2002). Resistin and obesity-associated insulin resistance. Trends Endocrinol Metab *13*, 18-23.
**Storer, J.B.** (1966). Longevity and gross pathology at death in 22 inbred mouse strains. J Gerontol *21*, 404-409.
**Storer, J.B.** (1967). Relation of lifespan to brain weight, body weight, and metabolic rate among inbred mouse strains. Experimental Gerontology *2*, 173-182.
**Street, J.C.; Butcher, J.E.; and Harris, L.E.** (1964). Estimating urine energy from urine nitrogen. Journal of Animal Science *23*, 1039-1041.
**Stumvoll, M.; Mitrakou, A.; Pimenta, W.; Jenssen, T.; Yki-Jarvinen, H.; Van Haeften, T., . . . Gerich, J.** (2000). Use of the oral glucose tolerance test to assess insulin release and insulin sensitivity. Diabetes Care *23*, 295-301.
**Suganami, T.; Tanaka, M.; and Ogawa, Y.** (2012). Adipose tissue inflammation and ectopic lipid accumulation. Endocr J *59*, 849-857.
**Surwit, R.S.; Feinglos, M.N.; Rodin, J.; Sutherland, A.; Petro, A.E.; Opara, E.C., . . . Rebuffe-Scrive, M.** (1995). Differential effects of fat and sucrose on the development of obesity and diabetes in C57BL/6J and A/J mice. Metabolism *44*, 645-651.
**Surwit, R.S.; Kuhn, C.M.; Cochrane, C.; McCubbin, J.A.; and Feinglos, M.N.** (1988). Diet-induced type II diabetes in C57BL/6J mice. Diabetes *37*, 1163-1167.
**Sussman, D.; Ellegood, J.; and Henkelman, M.** (2013). A gestational ketogenic diet alters maternal metabolic status as well as offspring physiological growth and brain structure in the neonatal mouse. BMC Pregnancy Childbirth *13*, 198.
**Tarantino, G.; Savastano, S.; Capone, D.; and Colao, A.** (2011). Spleen: A new role for an old player? World J Gastroenterol *17*, 3776-3784.

**Thaler, J.P.; Yi, C.X.; Schur, E.A.; Guyenet, S.J.; Hwang, B.H.; Dietrich, M.O., . . . Schwartz, M.W.** (2012). Obesity is associated with hypothalamic injury in rodents and humans. J Clin Invest *122*, 153-162.
**Thigpen, J.E.; Setchell, K.D.; Saunders, H.E.; Haseman, J.K.; Grant, M.G.; and Forsythe, D.B.** (2004). Selecting the appropriate rodent diet for endocrine disruptor research and testing studies. ILAR J *45*, 401-416.
**Thomas, L.W.** (1962). The chemical composition of adipose tissue of man and mice. Q J Exp Physiol Cogn Med Sci *47*, 179-188.
**Toye, A.A.; Lippiat, J.D.; Proks, P.; Shimomura, K.; Bentley, L.; Hugill, A., . . . Cox, R.D.** (2005). A genetic and physiological study of impaired glucose homeostasis control in C57BL/6J mice. Diabetologia *48*, 675-686.
**Tremaroli, V.; and Backhed, F.** (2012). Functional interactions between the gut microbiota and host metabolism. Nature *489*, 242-249.
**Tsai, P.P.; Pachowsky, U.; Stelzer, H.D.; and Hackbarth, H.** (2002). Impact of environmental enrichment in mice. 1: effect of housing conditions on body weight, organ weights and haematology in different strains. Lab Anim *36*, 411-419.
**Tsang, S.; Sun, Z.; Luke, B.; Stewart, C.; Lum, N.; Gregory, M., . . . Munroe, D.J.** (2005). A comprehensive SNP-based genetic analysis of inbred mouse strains. Mamm Genome *16*, 476-480.
**Tschop, M.H.; Speakman, J.R.; Arch, J.R.; Auwerx, J.; Bruning, J.C.; Chan, L., . . . Ravussin, E.** (2012). A guide to analysis of mouse energy metabolism. Nat Methods *9*, 57-63.
**Tucker, K.L.** (2007). Assessment of usual dietary intake in population studies of gene-diet interaction. Nutr Metab Cardiovasc Dis *17*, 74-81.
**Tuomilehto, J.; Lindstrom, J.; Eriksson, J.G.; Valle, T.T.; Hamalainen, H.; Ilanne-Parikka, P., . . . Finnish Diabetes Prevention Study, G.** (2001). Prevention of type 2 diabetes mellitus by changes in lifestyle among subjects with impaired glucose tolerance. N Engl J Med *344*, 1343-1350.
**Turner, M.J.; Kleeberger, S.R.; and Lightfoot, J.T.** (2005). Influence of genetic background on daily running-wheel activity differs with aging. Physiol Genomics *22*, 76-85.
**Turner, N.; Kowalski, G.M.; Leslie, S.J.; Risis, S.; Yang, C.; Lee-Young, R.S., . . . Bruce, C.R.** (2013). Distinct patterns of tissue-specific lipid accumulation during the induction of insulin resistance in mice by high-fat feeding. Diabetologia *56*, 1638-1648.
**Turner, R.T.; and Iwaniec, U.T.** (2011). Low dose parathyroid hormone maintains normal bone formation in adult male rats during rapid weight loss. Bone *48*, 726-732.
**UNAIDS, W.H.O.** (2000). Obesity: Preventing and Managing the Global Epidemic: Preventing and Managing the Global Epidemic - Report of a WHO Consultation (Who Technical Report).
**Underwood, E.A.** (1944). Lavoisier and the History of Respiration. Proc R Soc Med *37*, 247-262.
**van den Berg, S.A.; Guigas, B.; Bijland, S.; Ouwens, M.; Voshol, P.J.; Frants, R.R., . . . van Dijk, K.W.** (2010). High levels of dietary stearate promote adiposity and deteriorate hepatic insulin sensitivity. Nutr Metab (Lond) *7*, 24.
**Van der Auwera, I.; Wera, S.; Van Leuven, F.; and Henderson, S.T.** (2005). A ketogenic diet reduces amyloid beta 40 and 42 in a mouse model of Alzheimer's disease. Nutr Metab (Lond) *2*, 28.
**Veech, R.L.** (2004). The therapeutic implications of ketone bodies: the effects of ketone bodies in pathological conditions: ketosis, ketogenic diet, redox states, insulin resistance, and mitochondrial metabolism. Prostaglandins Leukot Essent Fatty Acids *70*, 309-319.
**Viardot, A.; Lord, R.V.; and Samaras, K.** (2010). The effects of weight loss and gastric banding on the innate and adaptive immune system in type 2 diabetes and prediabetes. J Clin Endocrinol Metab *95*, 2845-2850.
**Vogels, N.; Diepvens, K.; and Westerterp-Plantenga, M.S.** (2005). Predictors of long-term weight maintenance. Obes Res *13*, 2162-2168.

**Vrang, N.; Meyre, D.; Froguel, P.; Jelsing, J.; Tang-Christensen, M.; Vatin, V., . . . Larsen, P.J.** (2010). The imprinted gene neuronatin is regulated by metabolic status and associated with obesity. Obesity (Silver Spring) *18*, 1289-1296.
**Wahlsten, D.; Metten, P.; and Crabbe, J.C.** (2003). A rating scale for wildness and ease of handling laboratory mice: results for 21 inbred strains tested in two laboratories. Genes Brain Behav *2*, 71-79.
**Wang, G.; and Speakman, J.R.** (2016). Analysis of Positive Selection at Single Nucleotide Polymorphisms Associated with Body Mass Index Does Not Support the "Thrifty Gene" Hypothesis. Cell Metab *24*, 531-541.
**Wang, Q.; Perrard, X.D.; Perrard, J.L.; Mansoori, A.; Raya, J.L.; Hoogeveen, R., . . . Wu, H.** (2011). Differential effect of weight loss with low-fat diet or high-fat diet restriction on inflammation in the liver and adipose tissue of mice with diet-induced obesity. Atherosclerosis *219*, 100-108.
**Warden, C.H.; and Fisler, J.S.** (2008). Comparisons of diets used in animal models of high-fat feeding. Cell Metab *7*, 277.
**Webb, P.** (1980). The measurement of energy exchange in man: an analysis. Am J Clin Nutr *33*, 1299-1310.
**Weinstein, L.S.; Xie, T.; Qasem, A.; Wang, J.; and Chen, M.** (2010). The role of GNAS and other imprinted genes in the development of obesity. Int J Obes (Lond) *34*, 6-17.
**Weisberg, S.P.; McCann, D.; Desai, M.; Rosenbaum, M.; Leibel, R.L.; and Ferrante, A.W., Jr.** (2003). Obesity is associated with macrophage accumulation in adipose tissue. J Clin Invest *112*, 1796-1808.
**Weiss, E.C.; Galuska, D.A.; Kettel Khan, L.; Gillespie, C.; and Serdula, M.K.** (2007). Weight regain in U.S. adults who experienced substantial weight loss, 1999-2002. Am J Prev Med *33*, 34-40.
**Welch, B.L.; and Welch, A.S.** (1969). Sustained effects of brief daily stress (fighting) upon brain and adrenal catecholamines and adrenal spleen, and heart weights of mice. Proc Natl Acad Sci U S A *64*, 100-107.
**Wells, J.C.; and Fewtrell, M.S.** (2006). Measuring body composition. Arch Dis Child *91*, 612-617.
**West, D.B.; Boozer, C.N.; Moody, D.L.; and Atkinson, R.L.** (1992). Dietary obesity in nine inbred mouse strains. Am J Physiol *262*, R1025-1032.
**West, D.B.; Goudey-Lefevre, J.; York, B.; and Truett, G.E.** (1994a). Dietary obesity linked to genetic loci on chromosomes 9 and 15 in a polygenic mouse model. J Clin Invest *94*, 1410-1416.
**West, D.B.; Waguespack, J.; and McCollister, S.** (1995). Dietary obesity in the mouse: interaction of strain with diet composition. Am J Physiol *268*, R658-665.
**West, D.B.; Waguespack, J.; York, B.; Goudey-Lefevre, J.; and Price, R.A.** (1994b). Genetics of dietary obesity in AKR/J x SWR/J mice: segregation of the trait and identification of a linked locus on chromosome 4. Mamm Genome *5*, 546-552.
WHO (2016). Obesity and overweight. In Fact sheet (World Health Organization).
**Wiedemann, M.S.; Wueest, S.; Item, F.; Schoenle, E.J.; and Konrad, D.** (2013). Adipose tissue inflammation contributes to short-term high-fat diet-induced hepatic insulin resistance. Am J Physiol Endocrinol Metab *305*, E388-395.
**Wilkes, J.J.; Bonen, A.; and Bell, R.C.** (1998). A modified high-fat diet induces insulin resistance in rat skeletal muscle but not adipocytes. Am J Physiol *275*, E679-686.
**Williams, L.M.; Campbell, F.M.; Drew, J.E.; Koch, C.; Hoggard, N.; Rees, W.D., . . . Tups, A.** (2014). The development of diet-induced obesity and glucose intolerance in C57BL/6 mice on a high-fat diet consists of distinct phases. PLoS One *9*, e106159.
**Wiltshire, T.; Ervin, R.B.; Duan, H.; Bogue, M.A.; Zamboni, W.C.; Cook, S., . . . Tarantino, L.M.** (2015). Initial locomotor sensitivity to cocaine varies widely among inbred mouse strains. Genes Brain Behav *14*, 271-280.
**Winzell, M.S.; and Ahren, B.** (2004). The high-fat diet-fed mouse: a model for studying mechanisms and treatment of impaired glucose tolerance and type 2 diabetes. Diabetes *53 Suppl 3*, S215-219.

**Wishnofsky, M.** (1958). Caloric equivalents of gained or lost weight. Am J Clin Nutr *6*, 542-546.
**Wittenburg, H.; Lammert, F.; Wang, D.Q.; Churchill, G.A.; Li, R.; Bouchard, G., . . . Paigen, B.** (2002). Interacting QTLs for cholesterol gallstones and gallbladder mucin in AKR and SWR strains of mice. Physiol Genomics *8*, 67-77.
**Xu, H.; Barnes, G.T.; Yang, Q.; Tan, G.; Yang, D.; Chou, C.J., . . . Chen, H.** (2003). Chronic inflammation in fat plays a crucial role in the development of obesity-related insulin resistance. J Clin Invest *112*, 1821-1830.
**Xu, X.; Liu, C.; Xu, Z.; Tzan, K.; Wang, A.; Rajagopalan, S.; and Sun, Q.** (2012). Altered adipocyte progenitor population and adipose-related gene profile in adipose tissue by long-term high-fat diet in mice. Life Sci *90*, 1001-1009.
**Yamauchi, T.; Kamon, J.; Waki, H.; Terauchi, Y.; Kubota, N.; Hara, K., . . . Tsuboyama-Kasaoka, N.** (2001). The fat-derived hormone adiponectin reverses insulin resistance associated with both lipoatrophy and obesity. Nature medicine *7*, 941-946.
**Yang, Q.; Graham, T.E.; Mody, N.; Preitner, F.; Peroni, O.D.; Zabolotny, J.M., . . . Kahn, B.B.** (2005). Serum retinol binding protein 4 contributes to insulin resistance in obesity and type 2 diabetes. Nature *436*, 356-362.
**Ye, J.** (2013). Mechanisms of insulin resistance in obesity. Front Med *7*, 14-24.
**Ye, Z.; Huang, Y.; Liu, D.; Chen, X.; Wang, D.; Huang, D., . . . Xiao, X.** (2012). Obesity induced by neonatal overfeeding worsens airway hyperresponsiveness and inflammation. PLoS One *7*, e47013.
**York, B.; Lei, K.; and West, D.B.** (1997). Inherited non-autosomal effects on body fat in F2 mice derived from an AKR/J x SWR/J cross. Mamm Genome *8*, 726-730.
**Yoshida, C.; Shikata, N.; Seki, S.; Koyama, N.; and Noguchi, Y.** (2012). Early nocturnal meal skipping alters the peripheral clock and increases lipogenesis in mice. Nutr Metab (Lond) *9*, 78.
**Young, E.H.; Wareham, N.J.; Farooqi, S.; Hinney, A.; Hebebrand, J.; Scherag, A., . . . Sandhu, M.S.** (2007). The V103I polymorphism of the MC4R gene and obesity: population based studies and meta-analysis of 29 563 individuals. Int J Obes (Lond) *31*, 1437-1441.
**Yun, J.P.; Behan, J.W.; Heisterkamp, N.; Butturini, A.; Klemm, L.; Ji, L., . . . Mittelman, S.D.** (2010). Diet-induced obesity accelerates acute lymphoblastic leukemia progression in two murine models. Cancer Prev Res (Phila) *3*, 1259-1264.
**Zhang, Y.; Matheny, M.; Zolotukhin, S.; Tumer, N.; and Scarpace, P.J.** (2002). Regulation of adiponectin and leptin gene expression in white and brown adipose tissues: influence of beta3-adrenergic agonists, retinoic acid, leptin and fasting. Biochim Biophys Acta *1584*, 115-122.
**Zhang, Y.; Proenca, R.; Maffei, M.; Barone, M.; Leopold, L.; and Friedman, J.M.** (1994). Positional cloning of the mouse obese gene and its human homologue. Nature *372*, 425-432.
**Zurlo, F.; Lillioja, S.; Esposito-Del Puente, A.; Nyomba, B.L.; Raz, I.; Saad, M.F., . . . Ravussin, E.** (1990). Low ratio of fat to carbohydrate oxidation as predictor of weight gain: study of 24-h RQ. Am J Physiol *259*, E650-657.

# 6. APPENDIX

## 6.1. Supplementary data

2.2. Diets

**Table 14: Manufacture's information of diet composition.** Chow diet, CD, HF, HF 60, lCD, lHF 48 and lHF 75 where obtained from ssniff Spezialdiäten GmbH, Soest, Germany. LHF 78$^{cf}$ was obtained from SAFE scientific animal food & engineering, Augy France. Nutrients are shown in percent per weight.

| Ingredients [%] | Chow | CD | HF | HF 60 | lCD | lHF 48 | lHF 75 | lHF 78$^{cf}$ |
|---|---|---|---|---|---|---|---|---|
| | V1124-3 | S5745-E702 | S5745-E712 | S5745-E714 | S5745-E707 | S5745-E717 | S5745-E727 | 236HF |
| **Casein** | | 24.00 | 24.00 | 24.00 | 24.00 | 24.00 | 24.00 | 37.00 |
| **Crude protein** | 22.00 | | | | | | | |
| **Soy oil** | | 5.00 | 5.00 | 5.00 | | | | |
| **Palm oil** | | | 20.00 | 30.00 | | | | |
| **Lard** | | | | | 1.50 | 17.70 | 35.00 | 35.00 |
| **Corn oil** | | | | | 3.50 | 7.30 | 14.50 | 14.50 |
| **Crude fat** | 4.5 | | | | | | | |
| **Corn starch** | | 47.80 | 27.80 | 17.80 | 47.80 | 27.80 | 3.30 | |
| **Starch** | 34.0 | | | | | | | |
| **Maltodextrin** | | 5.60 | 5.60 | 5.60 | 5.60 | 5.60 | 5.60 | |
| **Sucrose** | 5.0 | 5.00 | 5.00 | 5.00 | 5.00 | 5.00 | 5.00 | |
| **Cellulose** | | 5.00 | 5.00 | 5.00 | 5.00 | 5.00 | 5.00 | 10.00 |
| **Crude fibre** | 3.9 | | | | | | | |
| **Crude ash** | 6.8 | | | | | | | |
| **L-Cystine** | | 5.00 | 5.00 | 5.00 | 0.20 | 0.20 | 0.20 | |
| **Choline Cl** | | 0.20 | 0.20 | 0.20 | 0.20 | 0.20 | 0.20 | |
| **Vitamins** | 1.20 | 1.20 | 1.20 | 1.20 | 1.20 | 1.20 | 1.20 | 2.50 |
| **Mineral & trace elements** | 6.00 | 6.00 | 6.00 | 6.00 | 6.00 | 6.00 | 6.00 | 1.00 |
| Calcium | 1.00 | 0.92 | 0.92 | 0.92 | 0.92 | 0.92 | 0.92 | |
| Phosphorus | 0.70 | 0.65 | 0.65 | 0.65 | 0.65 | 0.65 | 0.65 | |
| Sodium | 0.24 | 0.19 | 0.19 | 0.19 | 0.19 | 0.19 | 0.19 | |
| Magnesium | 0.21 | 0.21 | 0.21 | 0.21 | 0.21 | 0.21 | 0.21 | |
| **Fatty acids** | | | | | | | | |
| C12:0 | | 0.01 | 0.01 | 0.01 | 0.01 | 0.04 | 0.08 | |
| C14:0 | 0.01 | 0.02 | 0.21 | 0.31 | 0.04 | 0.25 | 0.49 | |
| C16:0 | 0.56 | 0.58 | 9.18 | 13.48 | 0.78 | 5.08 | 10.01 | |
| C18:0 | 0.14 | 0.18 | 1.11 | 1.56 | 0.28 | 2.54 | 5.00 | |
| C20:0 | 0.02 | 0.02 | 0.10 | 0.14 | 0.02 | 0.08 | 0.15 | |
| C16:1 | 0.03 | 0.01 | 0.05 | 0.07 | 0.05 | 0.54 | 1.06 | |
| C18:1 | 0.99 | 1.29 | 9.19 | 13.14 | 1.56 | 9.31 | 18.39 | |
| C18:2 | 2.41 | 2.65 | 4.67 | 5.68 | 2.08 | 5.72 | 11.34 | |
| C18:3 | 0.29 | 0.29 | 0.35 | 0.38 | 0.05 | 0.25 | 0.49 | |
| C20:1 | 0.01 | | | | | | | |
| C20:4 | | | | | 0.03 | 0.30 | 0.59 | |

## 3.1. High-fat diet feeding with different diets and mouse strains

**Table 15: Statistics of glucose tolerance in BL/6J mice during plant-based high-fat diet feeding.** Differences between diet groups were determined using Two-Way ANOVA with Tukey's multiple comparison test. CD, control diet (n=18); HF 48, high-fat diet with 48 kJ% of fat (n=8); HF 60, high-fat diet with 60 kJ% of fat (n=12); ns, not significant; * $p < 0.05$; ** $p < 0.01$; *** $p < 0.001$.

| Feeding duration | measure point | CD vs. HF 48 | CD vs. HF 60 | HF 48 vs. HF 60 |
|---|---|---|---|---|
| 1 week | 0 min | ns | ns | ns |
| | 15 min | ns | ns | ns |
| | 30 min | *** | *** | ns |
| | 60 min | * | ns | ns |
| | 120 min | * | ns | ** |
| 4 weeks | 0 min | *** | ns | *** |
| | 15 min | *** | ns | ** |
| | 30 min | *** | ** | * |
| | 60 min | *** | ns | *** |
| | 120 min | ** | ns | *** |
| 12 week | 0 min | * | ns | ns |
| | 15 min | ns | * | ns |
| | 30 min | *** | *** | ns |
| | 60 min | ns | *** | ns |
| | 120 min | ** | ns | ns |

**Table 16: Statistics of metabolic parameters in BL/6J mice during lard-based high-fat diet feeding.** Differences between diet groups were determined using Two-Way ANOVA with Tukey's multiple comparison test. lCD, lard-based control diet (n=12); lHF 48, lard-based high-fat diet with 48 kJ% of fat (n=12); HF 75, lard-based high-fat diet with 75 kJ% of fat (n=12); lHF 78$^{cf}$, lard-based carbohydrate free high-fat diet with 78 kJ% of fat (n=12); cf, carbohydrate free; wk, week(s); ns, not significant; * $p < 0.05$; ** $p < 0.01$; *** $p < 0.001$.

| parameter | time | lCD vs. lHF 48 | lCD vs. lHF 75 | lCD vs. lHF 78$^{cf}$ | lHF 48 vs. lHF 75 | lHF 48 vs. lHF 78$^{cf}$ | lHF 75 vs. lHF 78$^{cf}$ |
|---|---|---|---|---|---|---|---|
| Body mass gain | 0.5 wk | * | *** | ns | ns | *** | *** |
| referring to wk 0 | 1 wk | *** | *** | ns | ns | *** | *** |
| | 2 wk | *** | *** | ns | ns | *** | *** |
| | 3 wk | *** | *** | ** | ns | *** | *** |
| | 4 wk | *** | *** | *** | ns | *** | *** |
| Lean mass gain | 1 wk | ** | ns | ns | ns | *** | ns |
| referring to wk 0 | 2 wk | * | ns | ns | ns | * | ns |
| | 3 wk | ** | ns | ns | ns | * | ns |
| | 4 wk | ** | ns | ns | ns | ns | ns |
| Fat mass gain | 1 wk | ** | ** | ns | ns | ** | ** |
| referring to wk 0 | 2 wk | *** | *** | ns | ns | ** | *** |
| | 3 wk | *** | *** | ns | ns | *** | *** |
| | 4 wk | *** | *** | * | ** | *** | *** |
| Energy intake | 0.5 wk | *** | *** | ns | ns | *** | *** |
| daily | 1 wk | *** | *** | ** | ns | ns | ns |
| | 2 wk | ns | ** | ** | ns | ns | ns |
| | 3 wk | ns | ** | *** | ns | * | ns |
| | 4 wk | ns | ** | ** | ns | ns | ns |
| Energy intake | 0.5 wk | ns | ns | ns | ns | ns | ns |
| cumulative | 1 wk | ** | * | ns | ns | ns | ns |
| | 2 wk | *** | *** | ** | ns | ns | ns |

| | | | | | | | |
|---|---|---|---|---|---|---|---|
| | 3 wk | *** | *** | *** | ns | ns | ns |
| | 4 wk | *** | *** | *** | ns | ns | Ns |
| **parameter** | **time** | **lCD vs. lHF 48** | **lCD vs. lHF 75** | **lCD vs. lHF 78$^{cf}$** | **lHF 48 vs. lHF 75** | **lHF 48 vs. lHF 78$^{cf}$** | **lHF 75 vs. lHF 78$^{cf}$** |

**Table 17: Statistics of blood glucose levels during oral glucose tolerance test after 4 weeks lard-based high-fat diet feeding in BL/6J mice.** Blood glucose levels were assesses at indicated time points after glucose gavage. Differences between diet groups were determined using Two-Way ANOVA with Tukey's multiple comparison test. lCD, lard-based control diet (n=9); lHF 48, lard-based high-fat diet with 48 kJ% of fat (n=12); HF 75, lard-based high-fat diet with 75 kJ% of fat (n=10); lHF 78$^{cf}$, lard-based carbohydrate free high-fat diet with 78 kJ% of fat (n=9); cf, carbohydrate free; ns, not significant; * p < 0.05; ** p < 0.01; *** p < 0.001.

| **Time during oGTT** | **lCD vs. lHF 48** | **lCD vs. lHF 75** | **lCD vs. lHF 78$^{cf}$** | **lHF 48 vs. lHF 75** | **lHF 48 vs. lHF 78$^{cf}$** | **lHF 75 vs. lHF 78$^{cf}$** |
|---|---|---|---|---|---|---|
| 0 min | ns | ns | ns | ns | ns | ns |
| 15 min | ns | ns | ns | ns | ns | ns |
| 30 min | *** | *** | * | ns | ns | ns |
| 60 min | ns | *** | ** | ** | ns | ns |
| 120 min | ns | ns | ns | ns | ns | ns |

**Table 18: Statistics of blood glucose levels during oral glucose tolerance test after 4 weeks palm- or lard-based high-fat diet feeding in BL/6J mice.** Blood glucose levels were assesses at indicated time points after glucose gavage. Differences between diet groups were determined using Two-Way ANOVA with Tukey's multiple comparison test. Total (tAUC) and incremental (iAUC) area under glucose curves were calculated and differences between diets tested by One-Way ANOVA with Tukey's multiple comparision. tAUC, total area under the curve; iAUC, incremental area under the curve; pCD, palm-based control diet (n=18); pHF, palm-based high-fat diet with 48 kJ% fat (n=8); lCD, lard-based control diet (n=9); lHF 48, lard-based high-fat diet with 48 kJ% of fat (n=12); ns, not significant; * p < 0.05; ** p < 0.01; *** p < 0.001

| **Time during oGTT** | **lCD vs. lHF** | **lCD vs. pCD** | **lCD vs. pHF** | **lHF vs. pCD** | **lHF vs. pHF** | **pCD vs. pHF** |
|---|---|---|---|---|---|---|
| 0 min | ns | ns | *** | ns | ** | *** |
| 15 min | ns | ns | * | ** | ns | *** |
| 30 min | *** | ns | *** | *** | ns | *** |
| 60 min | ns | ns | *** | ns | *** | *** |
| 120 min | ns | ns | *** | ns | * | ** |
| tAUC | ** | ns | *** | ns | *** | *** |
| iAUC | ns | ns | ns | ns | ns | ns |

## 3.2. Baseline characterization of AKR/J and SWR/J mice

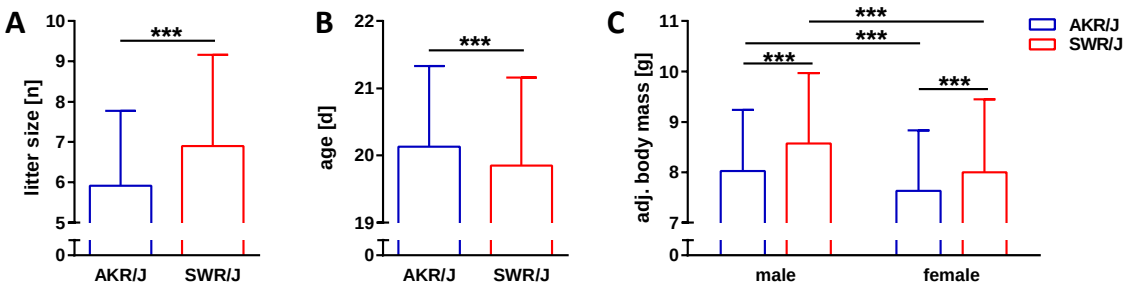


**Figure 60: Litter size, age and adjusted body mass of AKR/J and SWR/J mice at weaning. (A)** Litter size (AKR/J n= 226, SWR/J n=166) and **(B)** exact age (AKR/J n=1036, SWR/J n=946) at weaning; differences were calculated by student's t-test. **(C)** A linear relation between body weight and litter size as well as between body weight and age was

assumed. Litter size and age were used as significant correlated covariates to adjust body mass. Differences were tested using Two-way ANOVA with Tukey's multiple comparison test; male AKR/J n=538; female AKR/J n=498; male SWR/J n=500, female SWR/J n=446; ***p < 0.001.

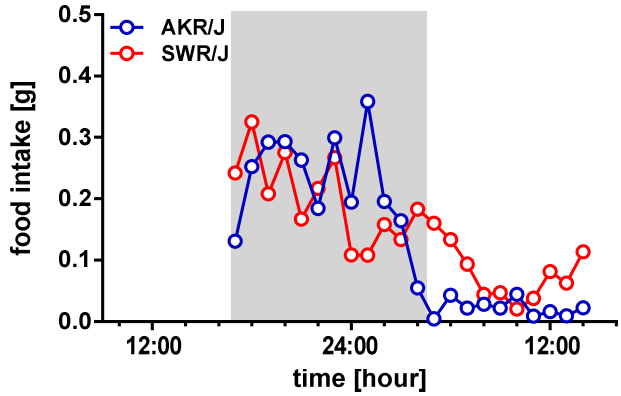


**Figure 61: Food intake in AKR/J and SWR/J mice during control diet feeding.** Food intake was detected during FDA measurements and expressed per hour; AKR/J n=16, SWR/J n=15.

## 3.3. Proximate causes for diet-induced obesity in AKR/J and SWR/J mice

**Table 19: Differences of energy expenditure during photophase between days of high-fat diet feeding.** Energy expenditure was measured by indirect calorimetry. The mean of the 12 hours of lights on represents energy expenditure of photophase. Differences between days of high-fat diet (HFD) feeding were determined using repeated measurements Two-Way ANOVA with Tukey's multiple comparison test; n=8; ns, not significant; * p < 0.05; *** p < 0.001.

| | Differences of energy expenditure during photophase between days of HFD feeding | | | | | |
|---|---|---|---|---|---|---|
| | 0 vs. 1 | 0 vs. 2 | 0 vs. 3 | 1 vs. 2 | 1 vs. 3 | 2 vs. 3 |
| AKR/J | *** | *** | *** | ns | ns | ns |
| SWR/J | ns | * | *** | ns | * | ns |

**Table 20: Differences of energy expenditure during scotophase between days of high-fat diet feeding.** Energy expenditure was measured by indirect calorimetry. The mean of the 12 hours of lights off represents energy expenditure of scotophase. Differences between days of high-fat diet (HFD) feeding were determined using repeated measurements Two-Way ANOVA with Tukey's multiple comparison test; n=8; ns, not significant; * p < 0.05; ** p < 0.01; *** p < 0.001.

| | Differences of energy expenditure during scotophase between days of HFD feeding | | | | | |
|---|---|---|---|---|---|---|
| | 0 vs. 1 | 0 vs. 2 | 0 vs. 3 | 1 vs. 2 | 1 vs. 3 | 2 vs. 3 |
| AKR/J | ns | *** | *** | * | ** | ns |
| SWR/J | * | *** | *** | ns | ** | ns |

**Table 21: Differences of resting metabolic rate between days of high-fat diet feeding.** Energy expenditure was measured by indirect calorimetry. The mean of 27 min of lowest oxygen consumption was defined and calculated as resting metabolic rate. Differences between days of high-fat diet (HFD) feeding were determined using repeated measurements Two-Way ANOVA with Tukey's multiple comparison test; n=8; ns, not significant; *** p < 0.001.

| | Differences of resting metabolic rate between days of HFD feeding | | | | | |
|---|---|---|---|---|---|---|
| | 0 vs. 1 | 0 vs. 2 | 0 vs. 3 | 1 vs. 2 | 1 vs. 3 | 2 vs. 3 |
| AKR/J | *** | *** | *** | ns | ns | ns |
| SWR/J | *** | *** | *** | ns | ns | ns |

**Table 22: Differences of daily energy expenditure between days of high-fat diet feeding.** Energy expenditure was measured by indirect calorimetry. The mean of 24 h was defined and calculated as daily energy expenditure. Differences between days of high-fat diet (HFD) feeding were determined using repeated measurements Two-Way ANOVA with Tukey's multiple comparison test; n=8; ns, not significant; * p < 0.05; ** p < 0.01; *** p < 0.001.

| | Differences of daily energy expenditure between days of HFD feeding | | | | | |
|---|---|---|---|---|---|---|
| | 0 vs. 1 | 0 vs. 2 | 0 vs. 3 | 1 vs. 2 | 1 vs. 3 | 2 vs. 3 |
| AKR/J | *** | *** | *** | ns | * | ns |
| SWR/J | * | *** | *** | ns | ** | ns |

**Table 23: Differences of maximal metabolic rate between days of high-fat diet feeding.** Energy expenditure was measured by indirect calorimetry. The mean of 27 min of highest oxygen consumption was defined and calculated as maximal metabolic rate. Differences between days of high-fat diet (HFD) feeding were determined using repeated measurements Two-Way ANOVA with Tukey's multiple comparison test; n=8; ns, not significant; ** p < 0.01.

| | Differences of maximal metabolic rate between days of HFD feeding | | | | | |
|---|---|---|---|---|---|---|
| | 0 vs. 1 | 0 vs. 2 | 0 vs. 3 | 1 vs. 2 | 1 vs. 3 | 2 vs. 3 |
| AKR/J | ns | ns | ns | ns | ns | ns |
| SWR/J | ns | ns | ** | ns | ** | ns |

## 3.4. Metabolic effects of 12 week high-fat diet feeding and their reversibility

**Table 24: Differences of resting metabolic rate between strains and diet groups.** Energy expenditure was measured by indirect calorimetry. The mean of 27 min of lowest oxygen consumption was defined and calculated as resting metabolic rate. At the age of 12 weeks AKR/J and SWR/J mice were fed either control diet (CD) or high-fat diet (HFD). After 12 weeks (wks) HFD fed mice were re-fed with control diet ad libitum (HFD-CD). Differences were calculated using Two-Way ANOVA with Tukey's multiple comparison test; n=7-9; ns, not significant; * p < 0.05; ** p < 0.01; *** p < 0.001.

| | | Differences of resting metabolic rate between groups | | | | | | | |
|---|---|---|---|---|---|---|---|---|---|
| | | 12 wks | 13 wks | 16 wks | 20 wks | 24 wks | 25 wks | 28 wks | 32 wks |
| AKR/J | CD vs. HFD | | *** | *** | *** | *** | | | |
| | CD vs HFD-CD | | | | | | ns | * | ns |
| SWR/J | CD vs. HFD | | ns | ns | ns | ns | | | |
| | CD vs. HFD-CD | | | | | | ns | ns | ns |
| CD | AKR/J vs. SWR/J | * | * | ns | ns | ns | ns | ns | ns |
| HFD | AKR/J vs. SWR/J | | ns | *** | ** | ** | | | |
| HFD-CD | AKR/J vs. SWR/J | | | | | | ns | ns | ns |

**Table 25: Differences of daily energy expenditure between strains and diet groups.** Energy expenditure was measured by indirect calorimetry. The mean of 24 h was defined and calculated as daily energy expenditure. At the age of 12 weeks AKR/J and SWR/J mice were fed either control diet (CD) or high-fat diet (HFD). After 12 weeks (wks) HFD fed mice were re-fed with control diet ad libitum (HFD-CD). Differences were calculated using Two-Way ANOVA with Tukey's multiple comparison test; n=7-9; ns, not significant; * p < 0.05; ** p < 0.01; *** p < 0.001.

| | | Differences of daily energy expenditure between groups | | | | | | | |
|---|---|---|---|---|---|---|---|---|---|
| | | 12 wks | 13 wks | 16 wks | 20 wks | 24 wks | 25 wks | 28 wks | 32 wks |
| AKR/J | CD vs. HFD | | ** | *** | *** | *** | | | |
| | CD vs HFD-CD | | | | | | ns | ** | ns |
| SWR/J | CD vs. HFD | | ns | ns | ns | ns | | | |
| | CD vs. HFD-CD | | | | | | ns | ns | ns |
| CD | AKR/J vs. SWR/J | ns | ns | ns | ns | ns | ns | ns | ns |
| HFD | AKR/J vs. SWR/J | | ns | ns | * | ** | | | |
| HFD-CD | AKR/J vs. SWR/J | | | | | | ns | ns | ns |

**Table 26: Differences of maximal metabolic rate between strains and diet groups.** Energy expenditure was measured by indirect calorimetry. The mean of 27 min of highest oxygen consumption was defined and calculated as maximal metabolic rate. At the age of 12 weeks AKR/J and SWR/J mice were fed either control diet (CD) or high-fat diet (HFD). After 12 weeks (wks) HFD fed mice were re-fed with control diet ad libitum (HFD-CD). Differences were calculated using Two-Way ANOVA with Tukey's multiple comparison test; n=7-9; ns, not significant; * $p < 0.05$; ** $p < 0.01$; *** $p < 0.001$.

| | | Differences of maximal metabolic rate between groups | | | | | | | |
|---|---|---|---|---|---|---|---|---|---|
| | | 12 wks | 13 wks | 16 wks | 20 wks | 24 wks | 25 wks | 28 wks | 32 wks |
| AKR/J | CD vs. HFD | | ns | ** | *** | *** | | | |
| | CD vs HFD-CD | | | | | | ns | ns | ns |
| SWR/J | CD vs. HFD | | * | * | ns | ns | | | |
| | CD vs. HFD-CD | | | | | | ns | ns | ns |
| CD | AKR/J vs. SWR/J | ns | ns | ns | ns | ns | ns | ns | ns |
| HFD | AKR/J vs. SWR/J | | ns | ns | * | ns | | | |
| HFD-CD | AKR/J vs. SWR/J | | | | | | ns | ns | ns |

**Tabelle 27: Differences of respiratory exchange ratio between strains and diet groups.** Carbon dioxide production and oxygen consumption were measured by indirect calorimetry. Building the ration of the two factors resulted in respiratory exchange ratio. At the age of 12 weeks AKR/J and SWR/J mice were fed either control diet (CD) or high-fat diet (HFD). After 12 weeks (wks) HFD fed mice were re-fed with control diet ad libitum (HFD-CD). Differences were calculated using Two-Way ANOVA with Tukey's multiple comparison test; n=7-9; ns, not significant; * $p < 0.05$; ** $p < 0.01$; *** $p < 0.001$.

| | | Differences of respiratory exchange ratio between groups | | | | | | | |
|---|---|---|---|---|---|---|---|---|---|
| | | 12 wks | 13 wks | 16 wks | 20 wks | 24 wks | 25 wks | 28 wks | 32 wks |
| AKR/J | CD vs. HFD | | *** | *** | *** | *** | | | |
| | CD vs HFD-CD | | | | | | *** | ns | ns |
| SWR/J | CD vs. HFD | | *** | *** | *** | *** | | | |
| | CD vs. HFD-CD | | | | | | ns | ns | ns |
| CD | AKR/J vs. SWR/J | ns | ns | ns | ns | ns | ns | ns | ns |
| HFD | AKR/J vs. SWR/J | | ns | ns | ns | ns | | | |
| HFD-CD | AKR/J vs. SWR/J | | | | | | * | ns | ns |

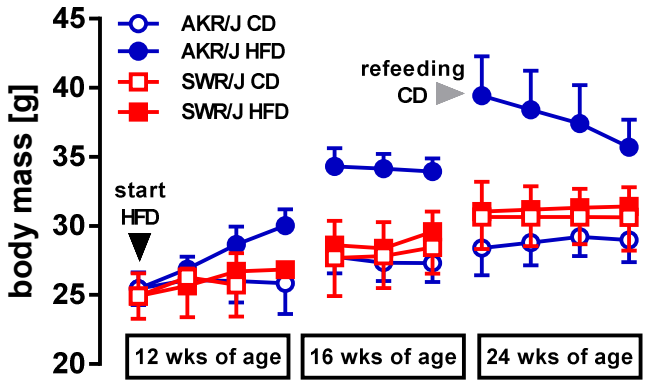


**Figure 62: Body mass of AKR/J and SWR/J mice during FDA measurements.** Body mass was measured daily during feeding drinking activity monitoring. Measurements were conducted at the age of 12 weeks when AKR/J and SWR/J mice received either control diet (CD) or high-fat diet (HFD) for 4 days, at the age of 16 weeks for 3 days and at the age of 24 weeks for 4 days when HFD fed mice were re-fed with control diet ad libitum.

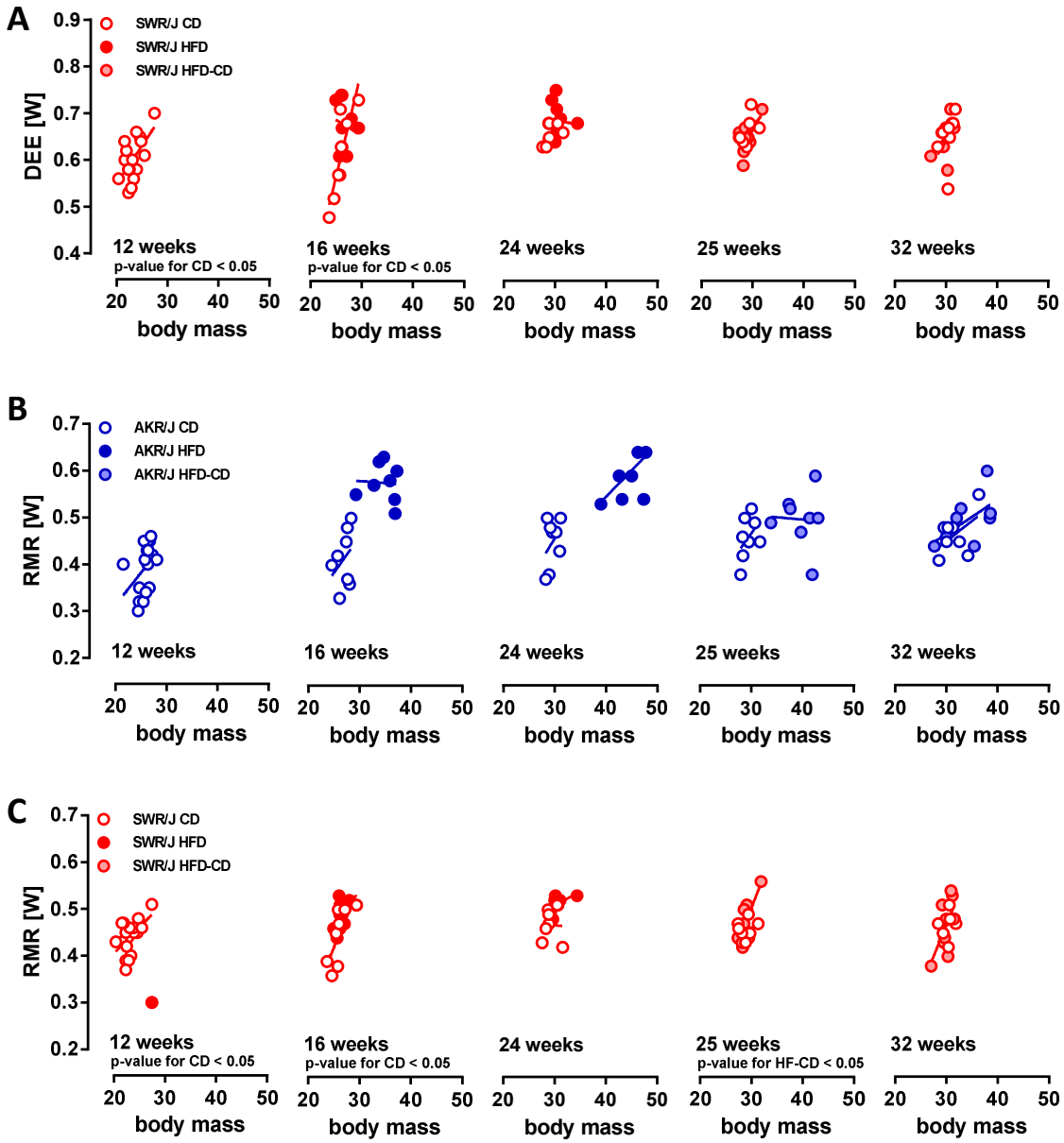


**Figure 63: Correlation of body mass and energy expenditure parameters in AKR/J and SWR/J mice.** For the measurements with 12, 16, 24, 25 and 32 weeks of age, (A) DEE of SWR/J mice (B) RMR of AKR/J mice and (C) RMR of SWR/J mice was plotted against corresponding body mass. P-Value was calculated by linear regression and significance indicated within plots; CD, control diet; HFD, high-fat diet.

**Table 28: Differences of body mass between strains and diet groups during FDA measurement.** Body mass was measured daily during feeding drinking activity (FDA) monitoring. Measurements were conducted at the age of 12 weeks (wks) when AKR/J and SWR/J mice received either control diet (CD) or high-fat diet (HFD) for 4 days, at the age of 16 weeks for 3 days and at the age of 24 weeks for 4 days when HFD fed mice were re-fed with control diet ad libitum (HFD-CD). Differences were calculated using Two-Way ANOVA with Tukey's multiple comparison test; n=4-9; ns, not significant; * $p < 0.05$; ** $p < 0.01$; *** $p < 0.001$.

| | | 12 wks of age | | | | 16 wks of age | | | 24 wks of age | | | |
|---|---|---|---|---|---|---|---|---|---|---|---|---|
| Days of FDA monitoring | | 1 | 2 | 3 | 4 | 1 | 2 | 3 | 1 | 2 | 3 | 4 |
| AKR/J | CD vs. HFD | | ns | * | ** | *** | *** | *** | *** | | | |
| | CD vs HFD-CD | | | | | | | | | *** | *** | *** |
| SWR/J | CD vs. HFD | | ns | ns | | ns | ns | ns | ns | | | |
| | CD vs. HFD-CD | | | | | | | | | ns | ns | ns |

| | | | | | | | | | | | | |
|---|---|---|---|---|---|---|---|---|---|---|---|---|
| CD | AKR/J vs. SWR/J | ns | ns | ns | | ns | ns | ns | ns | ns | ns | ns |
| HFD | AKR/J vs. SWR/J | | ns | ns | ns | *** | *** | *** | *** | | | |
| HFD-CD | AKR/J vs. SWR/J | | | | | | | | | *** | *** | *** |

**Table 29: Differences of body core temperature (mean of 24 h) between strains and diet groups during FDA measurement.** Body core temperature ($T_b$) was recorded every 5 minutes by implanted transmitter during feeding drinking activity (FDA) monitoring. Mean $T_b$ was calculated over 24 h per animal. Measurements were conducted at the age of 12 weeks (wks) when AKR/J and SWR/J mice received either control diet (CD) or high-fat diet (HFD) for 4 days, at the age of 16 weeks for 3 days and at the age of 24 weeks for 4 days when HFD fed mice were re-fed with control diet ad libitum (HFD-CD). Differences were calculated using Two-Way ANOVA with Tukey's multiple comparison test; n=4-9; ns, not significant; * $p < 0.05$; ** $p < 0.01$; *** $p < 0.001$.

| | | **12 wks of age** | | | | **16 wks of age** | | | **24 wks of age** | | | |
|---|---|---|---|---|---|---|---|---|---|---|---|---|
| Days of FDA monitoring | | 1 | 2 | 3 | 4 | 1 | 2 | 3 | 1 | 2 | 3 | 4 |
| AKR/J | CD vs. HFD | | *** | *** | *** | ns | ns | ns | ns | | | |
| | CD vs HFD-CD | | | | | | | | | ns | ns | ** |
| SWR/J | CD vs. HFD | | *** | *** | *** | ** | *** | *** | ** | | | |
| | CD vs. HFD-CD | | | | | | | | | ns | ns | ns |
| CD | AKR/J vs. SWR/J | ns | ns | ns | ns | ns | ns | ns | ns | ns | ns | ns |
| HFD | AKR/J vs. SWR/J | | ns | ns | ns | ns | ns | ns | ns | | | |
| HFD-CD | AKR/J vs. SWR/J | | | | | | | | | ns | ns | ** |

**Table 30: Differences of body core temperature (photophase) between strains and diet groups during FDA measurement.** Body core temperature ($T_b$) was recorded every 5 minutes by implanted transmitter during feeding drinking activity (FDA) monitoring. Mean $T_b$ of photophase was calculated over 12 h per animal. Measurements were conducted at the age of 12 weeks (wks) when AKR/J and SWR/J mice received either control diet (CD) or high-fat diet (HFD) for 4 days, at the age of 16 weeks for 3 days and at the age of 24 weeks for 4 days when HFD fed mice were re-fed with control diet ad libitum (HFD-CD). Differences were calculated using Two-Way ANOVA with Tukey's multiple comparison test; n=4-9; ns, not significant; * $p < 0.05$; ** $p < 0.01$; *** $p < 0.001$.

| | | **12 wks of age** | | | | **16 wks of age** | | | **24 wks of age** | | | |
|---|---|---|---|---|---|---|---|---|---|---|---|---|
| Days of FDA monitoring | | 1 | 2 | 3 | 4 | 1 | 2 | 3 | 1 | 2 | 3 | 4 |
| AKR/J | CD vs. HFD | | *** | *** | *** | ns | ns | ns | ** | | | |
| | CD vs HFD-CD | | | | | | | | | ns | ns | ns |
| SWR/J | CD vs. HFD | | ** | ns | *** | ns | ns | ns | ns | | | |
| | CD vs. HFD-CD | | | | | | | | | ns | ns | ns |
| CD | AKR/J vs. SWR/J | *** | *** | *** | *** | *** | ** | *** | *** | *** | *** | *** |
| HFD | AKR/J vs. SWR/J | | ns | ns | ns | *** | *** | *** | ** | | | |
| HFD-CD | AKR/J vs. SWR/J | | | | | | | | | *** | *** | *** |

**Table 31: Differences of body core temperature (scotophase) between strains and diet groups during FDA measurement.** Body core temperature ($T_b$) was recorded every 5 minutes by implanted transmitter during feeding drinking activity (FDA) monitoring. Mean $T_b$ of scotophase was calculated over 12 h per animal. Measurements were conducted at the age of 12 weeks (wks) when AKR/J and SWR/J mice received either control diet (CD) or high-fat diet (HFD) for 4 days, at the age of 16 weeks for 3 days and at the age of 24 weeks for 4 days when HFD fed mice were re-fed with control diet ad libitum (HFD-CD). Differences were calculated using Two-Way ANOVA with Tukey's multiple comparison test; n=4-9; ns, not significant; * $p < 0.05$; ** $p < 0.01$; *** $p < 0.001$.

| | | **12 wks of age** | | | | **16 wks of age** | | | **24 wks of age** | | | |
|---|---|---|---|---|---|---|---|---|---|---|---|---|
| Days of FDA monitoring | | 1 | 2 | 3 | 4 | 1 | 2 | 3 | 1 | 2 | 3 | 4 |
| AKR/J | CD vs. HFD | | ns | ns | ns | ns | ns | ns | ns | | | |
| | CD vs HFD-CD | | | | | | | | | *** | ** | *** |
| SWR/J | CD vs. HFD | | *** | *** | *** | ** | *** | *** | *** | | | |

| | | | | | | | | | | | | |
|---|---|---|---|---|---|---|---|---|---|---|---|---|
| | CD vs. HFD-CD | | | | | | | | | * | * | * |
| CD | AKR/J vs. SWR/J | *** | *** | *** | *** | *** | *** | *** | *** | *** | *** | *** |
| HFD | AKR/J vs. SWR/J | | ns | ns | ns | ns | ns | ns | ns | | | |
| HFD-CD | AKR/J vs. SWR/J | | | | | | | | | ns | ns | ns |

**Table 32: Differences of climbing activity between strains and diet groups during FDA measurement.** Climbing activity was defined as minutes of missing body core temperature signal of implanted transmitters. Measurements were conducted at the age of 12 weeks (wks) when AKR/J and SWR/J mice received either control diet (CD) or high-fat diet (HFD) for 4 days, at the age of 16 weeks for 3 days and at the age of 24 weeks for 4 days when HFD fed mice were re-fed with control diet ad libitum (HFD-CD). Differences were calculated using Two-Way ANOVA with Tukey's multiple comparison test; n=4-9; ns, not significant; * $p < 0.05$; ** $p < 0.01$; *** $p < 0.001$.

| | | **12 wks of age** | | | | **16 wks of age** | | | **24 wks of age** | | | |
|---|---|---|---|---|---|---|---|---|---|---|---|---|
| Days of FDA monitoring | | 1 | 2 | 3 | 4 | 1 | 2 | 3 | 1 | 2 | 3 | 4 |
| AKR/J | CD vs. HFD | | ns | ns | ns | ns | ns | ns | ns | | | |
| | CD vs HFD-CD | | | | | | | | | ns | ns | ns |
| SWR/J | CD vs. HFD | | ns | ns | * | ns | ns | ns | ns | | | |
| | CD vs. HFD-CD | | | | | | | | | ns | ns | ns |
| CD | AKR/J vs. SWR/J | *** | *** | *** | * | *** | *** | *** | *** | *** | *** | *** |
| HFD | AKR/J vs. SWR/J | | *** | *** | *** | *** | ** | *** | *** | | | |
| HFD-CD | AKR/J vs. SWR/J | | | | | | | | | ** | *** | ** |

**Table 33: Differences of energy intake (24h) between strains and diet groups during FDA measurement.** Food intake was detected by food baskets hanging at precise balances in the feeding drinking activity (FDA) device. Energy intake was calculated by multiplying food intake by energy content of the diet. Measurements were conducted at the age of 12 weeks (wks) when AKR/J and SWR/J mice received either control diet (CD) or high-fat diet (HFD) for 4 days, at the age of 16 weeks for 3 days and at the age of 24 weeks for 4 days when HFD fed mice were re-fed with control diet ad libitum (HFD-CD). Differences were calculated using Two-Way ANOVA with Tukey's multiple comparison test; n=4-9; ns, not significant; * $p < 0.05$; ** $p < 0.01$; *** $p < 0.001$.

| | | **12 wks of age** | | | | **16 wks of age** | | | **24 wks of age** | | | |
|---|---|---|---|---|---|---|---|---|---|---|---|---|
| Days of FDA monitoring | | 1 | 2 | 3 | 4 | 1 | 2 | 3 | 1 | 2 | 3 | 4 |
| AKR/J | CD vs. HFD | | *** | *** | *** | *** | * | * | ns | | | |
| | CD vs HFD-CD | | | | | | | | | *** | *** | *** |
| SWR/J | CD vs. HFD | | *** | *** | ns | * | ns | ns | ns | | | |
| | CD vs. HFD-CD | | | | | | | | | ** | ns | ns |
| CD | AKR/J vs. SWR/J | * | ns | ns | * | ns | ns | ns | *** | * | ns | ns |
| HFD | AKR/J vs. SWR/J | | *** | * | ns | ns | ns | ns | ns | | | |
| HFD-CD | AKR/J vs. SWR/J | | | | | | | | | *** | *** | *** |

**Table 34: Differences of energy intake (photophase) between strains and diet groups during FDA measurement.** Food intake was detected by food baskets hanging at precise balances in the feeding drinking activity (FDA) device. Energy intake of photophase was calculated by multiplying food intake of 12 h photophase by energy content of the diet. Measurements were conducted at the age of 12 weeks (wks) when AKR/J and SWR/J mice received either control diet (CD) or high-fat diet (HFD) for 4 days, at the age of 16 weeks for 3 days and at the age of 24 weeks for 4 days when HFD fed mice were re-fed with control diet ad libitum (HFD-CD). Differences were calculated using Two-Way ANOVA with Tukey's multiple comparison test; n=4-9; ns, not significant; * $p < 0.05$; ** $p < 0.01$; *** $p < 0.001$.

| | | **12 wks of age** | | | | **16 wks of age** | | | **24 wks of age** | | | |
|---|---|---|---|---|---|---|---|---|---|---|---|---|
| Days of FDA monitoring | | 1 | 2 | 3 | 4 | 1 | 2 | 3 | 1 | 2 | 3 | 4 |
| AKR/J | CD vs. HFD | | *** | *** | *** | ns | * | * | ns | | | |
| | CD vs HFD-CD | | | | | | | | | ns | ns | ns |

| | | | | | | | | | | | | |
|---|---|---|---|---|---|---|---|---|---|---|---|---|
| SWR/J | CD vs. HFD | | ns | ns | ns | ns | ns | ns | ns | | | |
| | CD vs. HFD-CD | | | | | | | | | *** | ns | ns |
| CD | AKR/J vs. SWR/J | *** | *** | ** | *** | *** | *** | *** | *** | *** | *** | *** |
| HFD | AKR/J vs. SWR/J | | ns | ns | ns | ** | * | ns | *** | | | |
| HFD-CD | AKR/J vs. SWR/J | | | | | | | | | ** | *** | *** |

**Table 35: Differences of energy intake (scotophase) between strains and diet groups during FDA measurement.** Food intake was detected by food baskets hanging at precise balances in the feeding drinking activity (FDA) device. Energy intake of scotophase was calculated by multiplying food intake of 12 h scotophase by energy content of the diet. Measurements were conducted at the age of 12 weeks (wks) when AKR/J and SWR/J mice received either control diet (CD) or high-fat diet (HFD) for 4 days, at the age of 16 weeks for 3 days and at the age of 24 weeks for 4 days when HFD fed mice were re-fed with control diet ad libitum (HFD-CD). Differences were calculated using Two-Way ANOVA with Tukey's multiple comparison test; n=4-9; ns, not significant; * $p < 0.05$; ** $p < 0.01$; *** $p < 0.001$.

| | | **12 wks of age** | | | | **16 wks of age** | | | **24 wks of age** | | | |
|---|---|---|---|---|---|---|---|---|---|---|---|---|
| Days of FDA monitoring | | 1 | 2 | 3 | 4 | 1 | 2 | 3 | 1 | 2 | 3 | 4 |
| AKR/J | CD vs. HFD | | *** | *** | ** | * | ns | ns | ns | | | |
| | CD vs HFD-CD | | | | | | | | | *** | *** | *** |
| SWR/J | CD vs. HFD | | *** | *** | ns | * | ns | ns | ns | | | |
| | CD vs. HFD-CD | | | | | | | | | ns | ns | ns |
| CD | AKR/J vs. SWR/J | ns | ns | ns | ns | * | * | *** | ns | ns | * | *** |
| HFD | AKR/J vs. SWR/J | | *** | *** | ns | ns | * | ns | ns | | | |
| HFD-CD | AKR/J vs. SWR/J | | | | | | | | | ns | ** | ** |

**Table 36: Differences of total activity (xyz direction) between strains and diet groups during FDA measurement.** Activity was detected by interruption of a three dimensional light beam frame in the feeding drinking activity (FDA) device. Measurements were conducted at the age of 12 weeks (wks) when AKR/J and SWR/J mice received either control diet (CD) or high-fat diet (HFD) for 4 days, at the age of 16 weeks for 3 days and at the age of 24 weeks for 4 days when HFD fed mice were re-fed with control diet ad libitum (HFD-CD). Differences were calculated using Two-Way ANOVA with Tukey's multiple comparison test; n=4-9; ns, not significant; * $p < 0.05$; ** $p < 0.01$; *** $p < 0.001$.

| | | **12 wks of age** | | | | **16 wks of age** | | | **24 wks of age** | | | |
|---|---|---|---|---|---|---|---|---|---|---|---|---|
| Days of FDA monitoring | | 1 | 2 | 3 | 4 | 1 | 2 | 3 | 1 | 2 | 3 | 4 |
| AKR/J | CD vs. HFD | | ns | ns | ns | ns | ns | ns | ns | | | |
| | CD vs HFD-CD | | | | | | | | | ns | ns | ns |
| SWR/J | CD vs. HFD | | ns | ns | ns | ns | ns | ns | ns | | | |
| | CD vs. HFD-CD | | | | | | | | | ns | ns | ns |
| CD | AKR/J vs. SWR/J | ns | ns | ns | ns | ns | ns | ns | ns | ns | ns | ns |
| HFD | AKR/J vs. SWR/J | | ns | ns | ns | ns | ns | ns | ns | | | |
| HFD-CD | AKR/J vs. SWR/J | | | | | | | | | ns | ns | ns |

**Table 37: Differences of rearing activity (z direction) between strains and diet groups during FDA measurement.** Rearing activity was detected by interruption of a light beam frame in the feeding drinking activity (FDA) device. Measurements were conducted at the age of 12 weeks (wks) when AKR/J and SWR/J mice received either control diet (CD) or high-fat diet (HFD) for 4 days, at the age of 16 weeks for 3 days and at the age of 24 weeks for 4 days when HFD fed mice were re-fed with control diet ad libitum (HFD-CD). Differences were calculated using Two-Way ANOVA with Tukey's multiple comparison test; n=4-9; ns, not significant; * $p < 0.05$; ** $p < 0.01$; *** $p < 0.001$.

| | | **12 wks of age** | | | | **16 wks of age** | | | **24 wks of age** | | | |
|---|---|---|---|---|---|---|---|---|---|---|---|---|
| Days of FDA monitoring | | 1 | 2 | 3 | 4 | 1 | 2 | 3 | 1 | 2 | 3 | 4 |
| AKR/J | CD vs. HFD | | ns | ns | ns | ns | ns | ns | ns | | | |

| | | | | | | | | | | | | |
|---|---|---|---|---|---|---|---|---|---|---|---|---|
| | CD vs HFD-CD | | | | | | | | | ns | ns | ns |
| SWR/J | CD vs. HFD | | ns | ns | | ns | * | ns | ns | | | |
| | CD vs. HFD-CD | | | | | | | | | ns | ns | ns |
| CD | AKR/J vs. SWR/J | ** | ** | *** | | *** | *** | *** | * | * | ** | ** |
| HFD | AKR/J vs. SWR/J | | ns | ns | ns | ns | ns | ns | * | | | |
| HFD-CD | AKR/J vs. SWR/J | | | | | | | | | ns | ns | ns |

**Table 38: Differences of basal glucose levels between strains and diet groups during high-fat diet feeding and refeeding control diet.** Differences were calculated using Two-Way ANOVA with Sidak multiple comparison test; ns, not significant; * p < 0.05; ** p < 0.01; *** p < 0.001; CD, control diet; HFD, high-fat diet.

| | High-fat diet feeding | | | | | Refeeding CD | |
|---|---|---|---|---|---|---|---|
| | 1.5 d | 1 wk | 4 wks | 8 wks | 12 wks | 1 wk | 4 wks |
| AKR/J: n CD/n HFD | 14/16 | 21/24 | 35/38 | 8/9 | 21/23 | 21/23 | 8/8 |
| SWR/J: n CD/ n HFD | 14/17 | 14/17 | 27/32 | 9/9 | 12/17 | 12/17 | 7/9 |
| CD: AKR/J vs. SWR/J | ns | *** | *** | ns | *** | *** | * |
| HFD: AKR/J vs. SWR/J | *** | *** | *** | *** | *** | *** | ns |

**Table 39: Differences of glucose tolerance parameters between strains and diet groups after 1.5 days high-fat diet feeding.** Differences were calculated using Two-Way ANOVA with Tukey's multiple comparison test; n=9-8; ns, not significant; * p < 0.05; ** p < 0.01; *** p < 0.001; CD, control diet; HFD, high-fat diet.

| 1.5 days HFD | Glucose measure points [min] | | | | | Area under the curve | |
|---|---|---|---|---|---|---|---|
| | 0 | 15 | 30 | 60 | 120 | tAUC | iAUC |
| AKR/J: CD vs. HFD | ns | *** | ** | ns | ns | ns | ns |
| SWR/J: CD vs. HFD | ns | *** | * | ns | ns | ns | ns |
| CD: AKR/J vs. SWR/J | ns | * | * | * | ns | ns | ns |
| HFD: AKR/J vs. SWR/J | ns | ** | ** | ns | ns | ns | ns |

**Table 40: Differences of glucose tolerance parameters between strains and diet groups after 1 week high-fat diet feeding.** Differences were calculated using Two-Way ANOVA with Tukey's multiple comparison test; n=9-8; ns, not significant; * p < 0.05; ** p < 0.01; *** p < 0.001; CD, control diet; HFD, high-fat diet.

| 1 week HFD | Glucose measure points [min] | | | | | Area under the curve | |
|---|---|---|---|---|---|---|---|
| | 0 | 15 | 30 | 60 | 120 | tAUC | iAUC |
| AKR/J: CD vs. HFD | ns | * | *** | ** | ns | ** | ns |
| SWR/J: CD vs. HFD | ns | ** | *** | ns | ns | ns | ns |
| CD: AKR/J vs. SWR/J | ns | *** | *** | ** | ns | ** | ns |
| HFD: AKR/J vs. SWR/J | ** | *** | *** | *** | ** | *** | ns |

**Table 41: Differences of glucose tolerance parameters between strains and diet groups after 4 weeks high-fat diet feeding.** Differences were calculated using Two-Way ANOVA with Tukey's multiple comparison test; n=9-8; ns, not significant; * p < 0.05; ** p < 0.01; *** p < 0.001; CD, control diet; HFD, high-fat diet.

| 4 weeks HFD | Glucose measure points [min] | | | | | Area under the curve | |
|---|---|---|---|---|---|---|---|
| | 0 | 15 | 30 | 60 | 120 | tAUC | iAUC |
| AKR/J: CD vs. HFD | ns | ns | ** | ns | ns | ns | ns |
| SWR/J: CD vs. HFD | ns | ns | ns | ns | ns | ns | ns |
| CD: AKR/J vs. SWR/J | ns | ns | ns | ** | ns | * | ns |
| HFD: AKR/J vs. SWR/J | ns | ns | * | *** | ns | *** | ns |

**Table 42: Differences of glucose tolerance parameters between strains and diet groups after 8 weeks high-fat diet feeding.** Differences were calculated using Two-Way ANOVA with Tukey's multiple comparison test; n=9-8; ns, not significant; * p < 0.05; ** p < 0.01; *** p < 0.001: CD, control diet; HFD, high-fat diet.

| 8 weeks HFD | Glucose measure points [min] | | | | | Area under the curve | |
|---|---|---|---|---|---|---|---|
| | 0 | 15 | 30 | 60 | 120 | tAUC | iAUC |
| AKR/J: CD vs. HFD | ns | ns | ** | ** | ns | *** | ns |
| SWR/J: CD vs. HFD | ns | ns | ns | ns | ns | ns | ns |
| CD: AKR/J vs. SWR/J | ns | ns | * | ns | ns | ** | ns |
| HFD: AKR/J vs. SWR/J | * | ** | *** | *** | * | *** | ** |

**Table 43: Differences of glucose tolerance parameters between strains and diet groups after 12 weeks high-fat diet feeding.** Differences were calculated using Two-Way ANOVA with Tukey's multiple comparison test; n=9-8; ns, not significant; * p < 0.05; ** p < 0.01; *** p < 0.001; CD, control diet; HFD, high-fat diet.

| 12 weeks HFD | Glucose measure points [min] | | | | | Area under the curve | |
|---|---|---|---|---|---|---|---|
| | 0 | 15 | 30 | 60 | 120 | tAUC | iAUC |
| AKR/J: CD vs. HFD | ns | * | *** | ** | ns | *** | ** |
| SWR/J: CD vs. HFD | ns | ns | ns | ns | ns | ns | ns |
| CD: AKR/J vs. SWR/J | ns | ** | ns | ns | ns | ** | ns |
| HFD: AKR/J vs. SWR/J | * | *** | *** | *** | *** | *** | *** |

**Table 44: Differences of glucose tolerance parameters between strains and diet groups after 1 weeks refeeding control diet.** Differences were calculated using Two-Way ANOVA with Tukey's multiple comparison test; n=9-8; ns, not significant; * p < 0.05; ** p < 0.01; *** p < 0.001; CD, control diet; HFD, high-fat diet.

| 1 week refeeding CD | Glucose measure points [min] | | | | | Area under the curve | |
|---|---|---|---|---|---|---|---|
| | 0 | 15 | 30 | 60 | 120 | tAUC | iAUC |
| AKR/J: CD vs. HFD | ns | ns | ns | ns | ns | ns | ns |
| SWR/J: CD vs. HFD | ns | ns | ns | ns | ns | ns | ns |
| CD: AKR/J vs. SWR/J | ns | ** | * | ** | ns | ** | ns |
| HFD: AKR/J vs. SWR/J | ns | ns | * | * | ns | * | ns |

**Table 45: Differences of glucose tolerance parameters between strains and diet groups after 4 weeks refeeding control diet.** Differences were calculated using Two-Way ANOVA with Tukey's multiple comparison test; n=9-8; ns, not significant; * p < 0.05; ** p < 0.01; *** p < 0.001; CD, control diet; HFD, high-fat diet.

| 4 weeks refeeding CD | Glucose measure points [min] | | | | | Area under the curve | |
|---|---|---|---|---|---|---|---|
| | 0 | 15 | 30 | 60 | 120 | tAUC | iAUC |
| AKR/J: CD vs. HFD | ns | * | ns | ns | ns | ns | ns |
| SWR/J: CD vs. HFD | ns | ns | ns | ns | ns | ns | ns |
| CD: AKR/J vs. SWR/J | ns | *** | *** | * | ns | *** | ns |
| HFD: AKR/J vs. SWR/J | ns | ns | * | ** | ns | ** | ns |

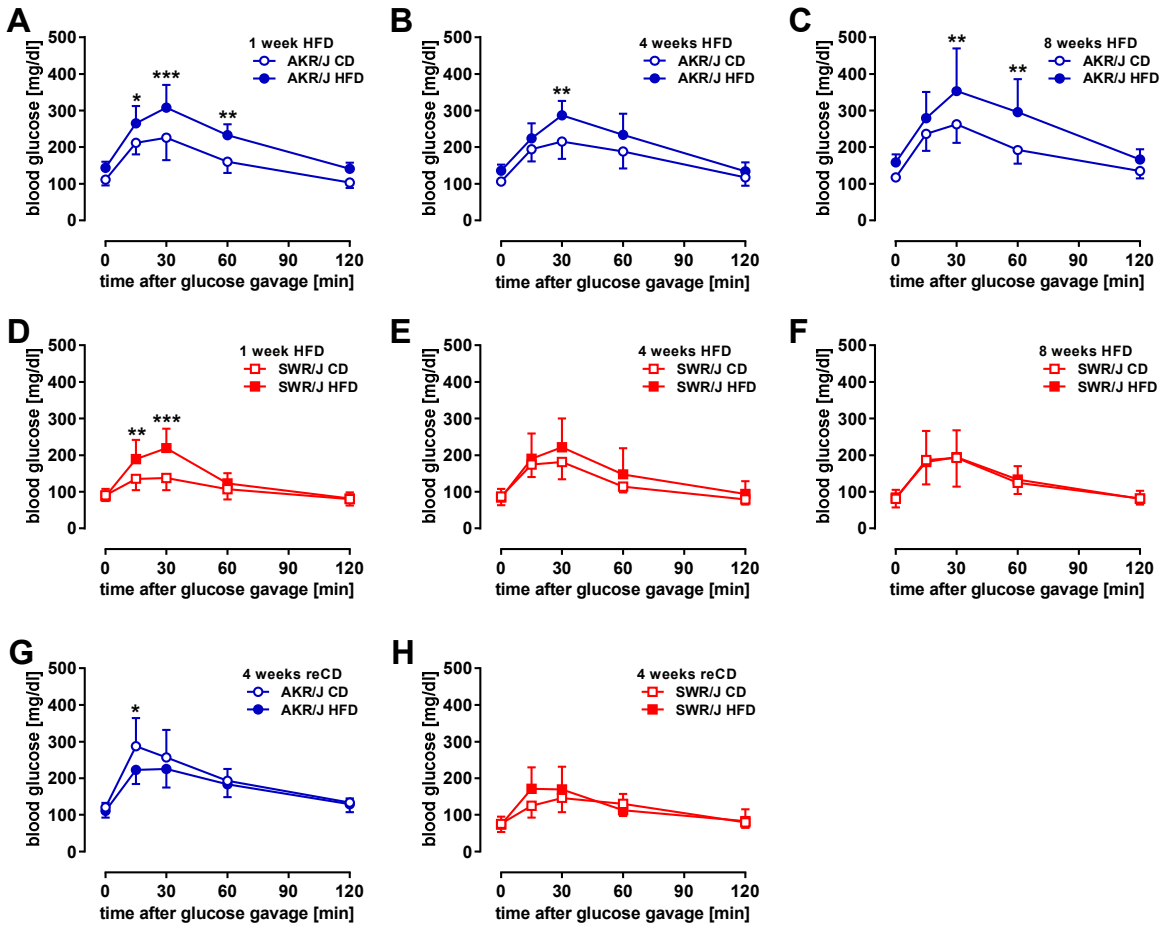


**Figure 64: Glucose tolerance of AKR/J and SWR/J mice during high-fat diet feeding and refeeding control diet.** Blood glucose curves in response to glucose gavage after **(A, D)** 1 week, **(B, E)** 4 weeks and **(C, F)** 8 weeks of high-fat diet (HFD) feeding and **(G, H)** after 4 weeks refeeding control diet (CD) in AKR/J and SWR/J mice (2.8 g glucose/kg lean mass). Differences were calculated using Two-Way ANOVA with Tukey's multiple comparison test; n=7-9; *p < 0.05; ** p < 0.01; *** p < 0.001

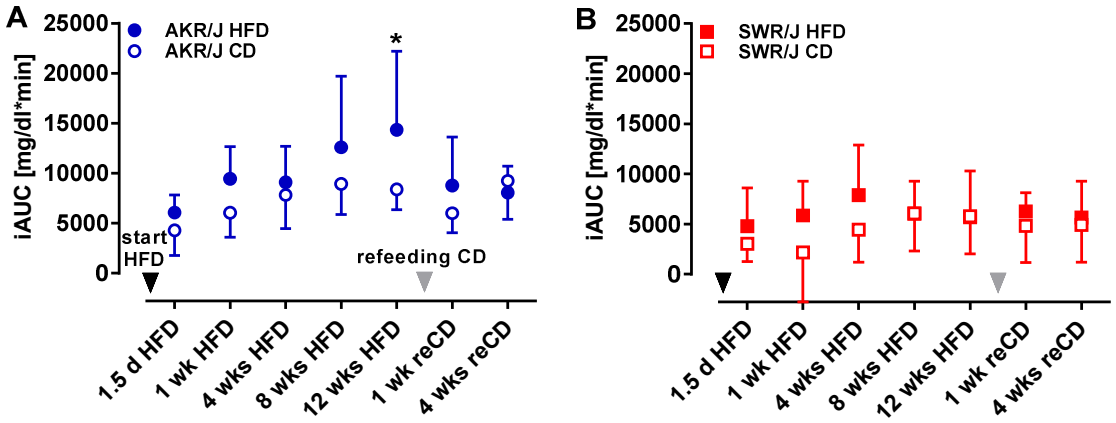


**Figure 65: Incremental area under the curve of glucose tolerance test in AKR/J and SWR/J mice.** Incremental area under the curve was calculated of oral glucose tolerance tests during high-fat diet (HFD) feeding and refeeding control diet (CD) of **(A)** AKR/J and **(B)** SWR/J mice. Differences were calculated using Two-Way ANOVA with Tukey's multiple comparison test; n=7-9; * p < 0.05.

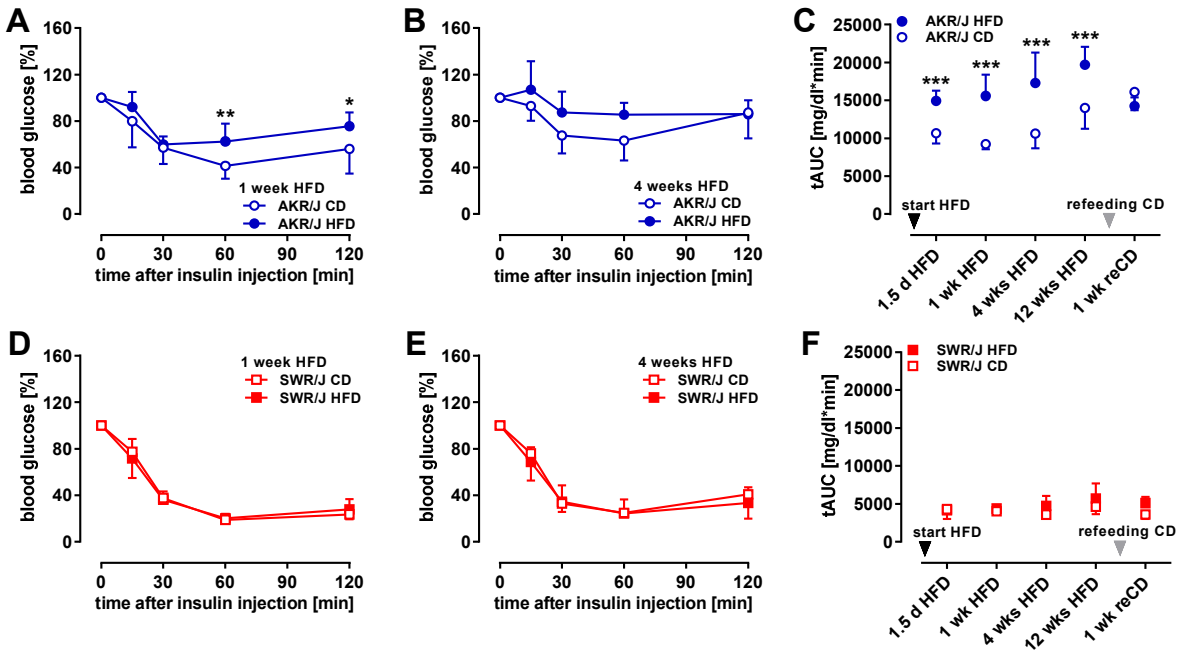


**Figure 66: Insulin tolerance of AKR/J and SWR/J mice during high-fat diet feeding and refeeding control diet.** Blood glucose curves in response to insulin injection (0.75 U/kg lean mass) after **(A, D)** 1 week and **(B, E)** after 4 weeks high-fat diet (HFD) feeding in AKR/J and SWR/J mice. Basal blood glucose levels were measured before insulin injection. Blood glucose levels 15, 30, 60 and 120 minutes after injection were calculated as %change to basal blood glucose levels. Total area under the curve was calculated based on factual blood glucose levels in **(C)** AKR/J and **(F)** SWR/J mice. Differences were calculated using Two-Way ANOVA with Tukey's multiple comparison test; n=5-8; *p < 0.05; ** p < 0.01; *** p < 0.001; CD, control diet.

**Table 46: Differences of insulin tolerance parameters between strains and diet groups after 1.5 days high-fat diet feeding.** Basal blood glucose levels were measured before insulin injection. Blood glucose levels 15, 30, 60 and 120 minutes after injection were calculated as %change to basal blood glucose levels. Differences were calculated using Two-Way ANOVA with Tukey's multiple comparison test; n=5-8; ns, not significant; * p < 0.05; ** p < 0.01; *** p < 0.001; CD, control diet; HFD, high-fat diet.

| **1.5.days HFD** | **Glucose measure points [min]** | | | | | **Area under the curve** |
|---|---|---|---|---|---|---|
| | 0 | 15 | 30 | 60 | 120 | %tAUC |
| AKR/J: CD vs. HFD | ns | ns | ns | ns | ns | ns |
| SWR/J: CD vs. HFD | ns | ns | ns | ns | ns | ns |
| CD: AKR/J vs. SWR/J | ns | ns | *** | *** | *** | *** |
| HFD: AKR/J vs. SWR/J | ns | ** | *** | *** | *** | *** |

**Table 47: Differences of insulin tolerance parameters between strains and diet groups after 1 week high-fat diet feeding.** Basal blood glucose levels were measured before insulin injection. Blood glucose levels 15, 30, 60 and 120 minutes after injection were calculated as %change to basal blood glucose levels. Differences were calculated using Two-Way ANOVA with Tukey's multiple comparison test; n=5-8; ns, not significant; * p < 0.05; ** p < 0.01; *** p < 0.001; CD, control diet; HFD, high-fat diet.

| **1 week HFD** | **Glucose measure points [min]** | | | | | **Area under the curve** |
|---|---|---|---|---|---|---|
| | 0 | 15 | 30 | 60 | 120 | %tAUC |
| AKR/J: CD vs. HFD | ns | ns | ns | ** | * | ns |
| SWR/J: CD vs. HFD | ns | ns | ns | ns | ns | ns |
| CD: AKR/J vs. SWR/J | ns | ns | * | * | *** | * |
| HFD: AKR/J vs. SWR/J | ns | ** | *** | *** | *** | *** |

**Table 48: Differences of insulin tolerance parameters between strains and diet groups after 4 weeks high-fat diet feeding.** Basal blood glucose levels were measured before insulin injection. Blood glucose levels 15, 30, 60 and 120 minutes after injection were calculated as %change to basal blood glucose levels. Differences were calculated using Two-Way ANOVA with Tukey's multiple comparison test; n=5-8; ns, not significant; * $p < 0.05$; ** $p < 0.01$; *** $p < 0.001$; CD, control diet; HFD, high-fat diet.

| 4 weeks HFD | Glucose measure points [min] | | | | | Area under the curve |
|---|---|---|---|---|---|---|
| | 0 | 15 | 30 | 60 | 120 | %tAUC |
| AKR/J: CD vs. HFD | ns | ns | ns | ns | ns | ns |
| SWR/J: CD vs. HFD | ns | ns | ns | ns | ns | ns |
| CD: AKR/J vs. SWR/J | ns | * | ** | *** | *** | *** |
| HFD: AKR/J vs. SWR/J | ns | *** | *** | *** | *** | *** |

**Table 49: Differences of insulin tolerance parameters between strains and diet groups after 12 weeks high-fat diet feeding.** Basal blood glucose levels were measured before insulin injection. Blood glucose levels 15, 30, 60 and 120 minutes after injection were calculated as %change to basal blood glucose levels. Differences were calculated using Two-Way ANOVA with Tukey's multiple comparison test; n=5-8; ns, not significant; * $p < 0.05$; ** $p < 0.01$; *** $p < 0.001$; CD, control diet; HFD, high-fat diet.

| 12 weeks HFD | Glucose measure points [min] | | | | | Area under the curve |
|---|---|---|---|---|---|---|
| | 0 | 15 | 30 | 60 | 120 | %tAUC |
| AKR/J: CD vs. HFD | ns | *** | *** | * | ns | *** |
| SWR/J: CD vs. HFD | ns | ns | ns | ns | ns | ns |
| CD: AKR/J vs. SWR/J | ns | ns | ns | *** | ** | *** |
| HFD: AKR/J vs. SWR/J | ns | *** | *** | *** | *** | *** |

**Table 50: Differences of insulin tolerance parameters between strains and diet groups after 1 week refeeding control diet.** Basal blood glucose levels were measured before insulin injection. Blood glucose levels 15, 30, 60 and 120 minutes after injection were calculated as %change to basal blood glucose levels. Differences were calculated using Two-Way ANOVA with Tukey's multiple comparison test; n=5-8; ns, not significant; * $p < 0.05$; ** $p < 0.01$; *** $p < 0.001$; CD, control diet; HFD, high-fat diet.

| 1 week refeeding CD | Glucose measure points [min] | | | | | Area under the curve |
|---|---|---|---|---|---|---|
| | 0 | 15 | 30 | 60 | 120 | %tAUC |
| AKR/J: CD vs. HFD | ns | ns | ns | ns | ns | ns |
| SWR/J: CD vs. HFD | ns | ns | ns | ns | ns | ns |
| CD: AKR/J vs. SWR/J | ns | ns | *** | *** | ** | *** |
| HFD: AKR/J vs. SWR/J | ns | * | *** | *** | *** | *** |

## 3.5. Effects of anabolic and catabolic status in AKR/J mice

**Table 51: 12 genes with most differences in expression between anabolic and catabolic eWAT according to middle criteria and low CV.** Gene expression is displayed as total reads of the transcript. Criteria for differences were ln change ≥ 1.2 or ≤ -1.2, coefficient of variation (CV) < 33 and p-value 0.01; anabolic: n=3, catabolic: n=6. Identified genes: solute carrier family 6 member 7 (Slc6a7), transient receptor potential cation channel, subfamily C, member 4 (Trpc4), POU domain, class 2, transcription factor 2 (Pou2f2), RAS protein-specific guanine nucleotide-releasing factor 1 (Rasgrf1), paired related homeobox 2 (Prrx2), hippocalcin (Hpca), SH3 and cysteine rich domain 2 (Stac2), bassoon (Bsn), SPEG complex locus (Speg), FYN binding protein (Fyb), resistin like alpha (Retnla), patatin-like phospholipase domain containing 3 (Pnpla3).

| Gene | Anabolic total reads | | | Catabolic total reads | | | ln fold change | p-value |
|---|---|---|---|---|---|---|---|---|
| | mean | SD | CV | mean | SD | CV | | |
| Slc6a7 | 44 | 13 | 30 | 543 | 168 | 31 | -2.513 | 0.002 |

| | | | | | | | | |
|---|---|---|---|---|---|---|---|---|
| Trpc4 | 29 | 8 | 29 | 124 | 36 | 29 | -1.453 | 0.003 |
| Pou2f2 | 69 | 16 | 23 | 267 | 83 | 31 | -1.353 | 0.005 |
| Rasgrf1 | 36 | 11 | 29 | 138 | 37 | 27 | -1.344 | 0.003 |
| Prrx2 | 41 | 10 | 26 | 154 | 34 | 22 | -1.323 | 0.001 |
| Hpca | 17 | 4 | 21 | 63 | 18 | 28 | -1.310 | 0.004 |
| Stac2 | 113 | 34 | 30 | 414 | 87 | 21 | -1.298 | 0.001 |
| Bsn | 45 | 13 | 29 | 159 | 47 | 29 | -1.262 | 0.005 |
| Speg | 82 | 26 | 32 | 285 | 67 | 23 | -1.246 | 0.002 |
| Fyb | 288 | 86 | 30 | 998 | 263 | 26 | -1.243 | 0.003 |
| Retnla | 8,419 | 1,894 | 22 | 2,153 | 613 | 28 | 1.364 | 0.000 |
| Pnpla3 | 6,571 | 1,909 | 29 | 1,344 | 423 | 31 | 1.587 | 0.000 |

## 3.6. Heredity of diet-induced obesity resistance – crossbreeding of AKR/J and SWR/J mice

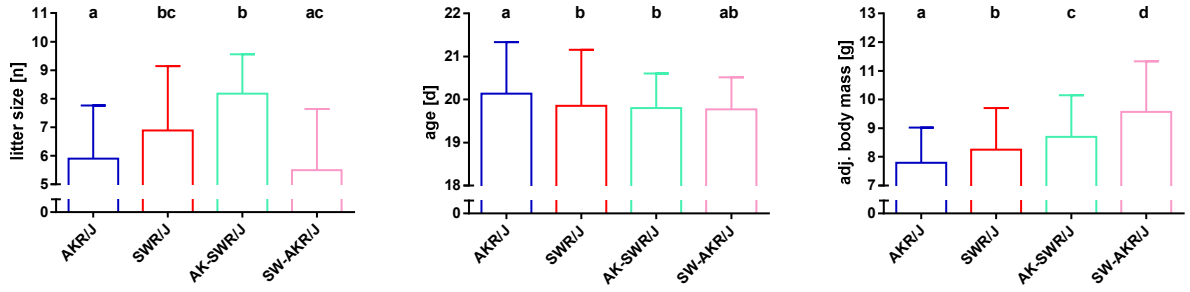


**Figure 67: Weaning characteristics of AKR/J, SWR/J, AK-SWR/J and SW-AKR/J mice. (A)** Litter size (AKR/J n= 226, SWR/J n=166, AK-SWR/J n=16, SW-AKR/J n=14) and **(B)** exact age at weaning were documented for each strain. **(C)** Adjusted body mass: linear relation between body weight and litter size as well as between body weight and age was assumed. Litter size and age were used as significant correlated covariates to adjust body mass; AKR/J: n=1036, SWR/J: n=946, AK-SWR/J: n=131, SW-AKR/J: n=70; different letters present significant differences between strains calculated using One-Way ANOVA with Tukey's multiple comparison test.

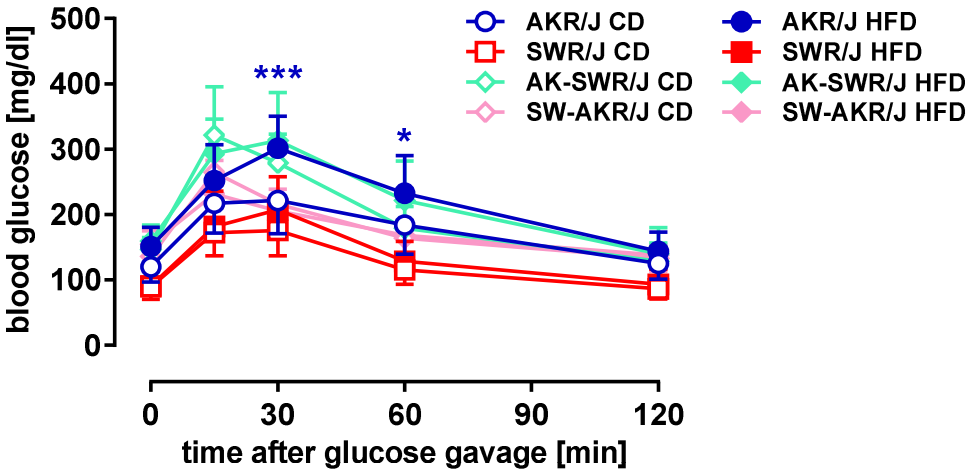


**Figure 68: Glucose tolerance test of AKR/J, AK-SWR/J, SW-AKR/J and SWR/J mice.** Blood glucose curves in response to glucose gavage (2.8 g glucose/kg lean mass) after 4 weeks of high-fat diet (HFD) feeding. Intra-strain differences between diet groups were calculated using Two-Way ANOVA with Tukey's multiple comparison test; *p < 0.05; *** p < 0.001; AKR/J (n=27, 14 CD, 13 HFD), SWR/J (n=28, 14 CD, 14 HFD), AK-SWR/J (n=27, 15 CD, 12 HFD), SW-AKR/J (n=14, 6 CD, 8 HFD).

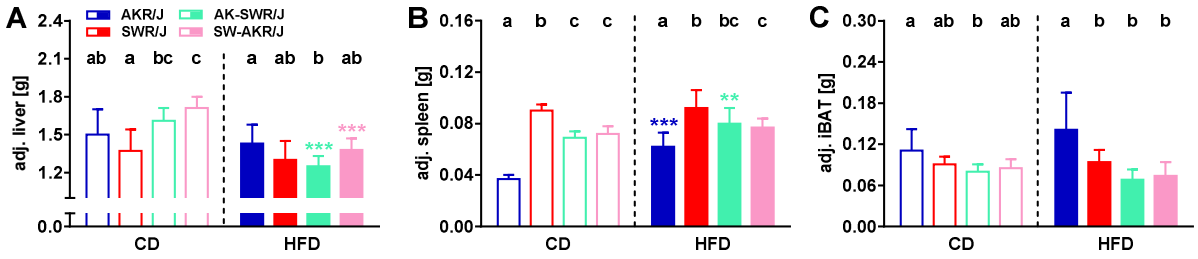


**Figure 69: Adjusted organ weight of AKR/J, AK-SWR/J, SW-AKR/J and SWR/J mice. (A)** Liver, **(B)** spleen and **(C)** intrascapular brown adipose tissue (iBAT) were weighed after dissection and masses of organs were adjusted to body mass. Differences between groups were calculated using Two-Way-ANOVA; asterisks symbolize intra-strain differences between diet groups, ** $p < 0.01$; *** $p < 0.001$; different letters present significant intra-diet group differences between strains; liver and iBAT: AKR/J (n=25, 12 CD, 13 HFD), SWR/J (n=27, 13 CD, 14 HFD), AK-SWR/J (n=38, 19 CD, 19 HFD), SW-AKR/J (n=17, 9 CD, 8 HFD); spleen: AKR/J (n=12, 6 CD, 6 HFD), SWR/J (n=12, 6 CD, 6 HFD), AK-SWR/J (n=38, 19 CD, 19 HFD), SW-AKR/J (n=17,9 CD, 8 HFD); CD, control diet; HFD, high-fat diet.

## 6.2. List of abbreviations

| | |
|---|---|
| adj. | adjusted |
| ANCOVA | analysis of covariance |
| ANOVA | analysis of variance |
| ATP | adenosine triphosphate |
| AUC | area under the curve |
| BC | body composition |
| BM | body mass |
| BMI | body mass index |
| BMR | basal metabolic rate |
| CD | control diet (soy oil based) |
| cDNA | complementary deoxyribonucleic acid |
| CHOL | cholesterol |
| $CO_2$ | carbon dioxide |
| CV | coefficient of variation |
| DEE | daily energy expenditure |
| DIO | diet-induced obesity |
| DNA | deoxyribonucleic acid |
| $E_{ass}$, E(ass) | assimilated energy |
| EDTA | ethylenediaminetetraacetic acid |
| EE | energy expenditure |
| EF(ass) | assimilation efficiency |
| $E_{in}$, E(in) | energy inflow/intake |
| ELISA | enzyme linked immunosorbent assay |
| $E_{met}$, E(met) | metabolizable energy |
| $E_{out}$, E(out) | energy outflow, |
| $E_{res}$ | resorbed energy |
| eWAT | epididymal white adipose tissue |
| FDA | Feeding drinking activity |
| FI | Food intake |

| | |
|---|---|
| Glut2 | glucose transporter 2 |
| Glut4 | glucose transporter 4 |
| HDL | high density lipoprotein |
| HF 48 | palm-oil based diet with 48 energy percent of fat |
| HF 60 | palm-oil based diet with 60 energy percent of fat |
| HFD | high-fat diet |
| HOMA-IR | homeostatic model assessment of β-cell function and insulin resistance |
| iAUC | incremental area under the curve |
| iBAT | intrascapular brown adipose tissue |
| int. | intermediate |
| ipITT | intraperitoneal insulin tolerance test |
| kJ % | energy percent |
| lCD | control diet with lard |
| lHF 48 | lard-based diet with 78 energy percent of fat |
| lHF 75 | lard-based diet with 75 energy percent of fat |
| lHF $78^{cf}$ | lard-based diet with 78 energy percent of fat, carbohydrate free |
| MMR | maximal metabolic rate |
| mRNA | messenger RNA |
| na | not applicable |
| NADH | nicotinamide adenine dinucleotide |
| NMR | nuclear magnetic resonance |
| ns | not significant |
| $O_2$ | oxygen |
| oGTT | oral glucose tolerance test |
| oPTT | oral pyruvate tolerance test |
| PBS | phosphate-buffered saline |
| qPCR | qualitative real-time polymerase chain reaction |
| QUICKI | quantitative insulin sensitivity check index |
| $R^2$ | coefficient of determination |
| RER | respiratory exchange ratio |
| RNA | ribonucleic acid |
| RT | room temperature |
| rWAT | retroperitoneal perirenal white adipose tissue |
| SPF | specified pathogen free |
| sWAT | subcutaneous white adipose tissue |
| tAUC | total area under the curve |
| $T_b$ | body core temperature |
| TRIG | triglycerides |
| vs. | versus |
| WHO | World Health Organization |
| wk, wks | week, weeks |

## 6.3. List of figures

## 6.4. List of tables

# ACKNOWLEDGEMENTS

An dieser Stelle möchte ich mich von ganzem Herzen bei allen bedanken, die mich wissenschaftlich und persönlich bei der Durchführung begleitet und zum Gelingen dieser Arbeit beigetragen haben.

An erster Stelle geht ein großes Dankeschön an Martin, der es mir ermöglicht hat diese Arbeit im Rahmen des BMBF-Projekts „Einfluss fettreicher Diäten auf die Darmpermeabilität und den Entzündungsstatus bei der Entstehung von Stoffwechselkrankheiten“ zu erforschen. Vielen Dank für dein Vertrauen, die vielen Ideen, Denkanstöße und Vorschläge, kurzum für eine rundum gute Betreuung.
Ich danke Prof. Hannelore Daniel und Prof. Dirk Haller herzlich für die Bereitschaft Zweitprüferin und Prüfungsvorsitzender zu sein sowie für die erfolgreiche Zusammenarbeit im BMBF-Projekt. Ein ganz lieber Dank gilt hier auch Veronika, Valentina und Lisa für das gute Teamwork. Ich bedanke mich bei den Tierpflegerinnen für ihre zuverlässige Arbeit.

Ein ganz großer Dank gilt der gesamten Arbeitsgruppe für ein wunderbares, hilfsbereites Arbeitsklima, in dem auch gemeinsame Events und Spaß nicht zu kurz kamen. Insbesondere danke ich Sama, Kristina, Raphaela und Sabine für beste Mittagspausen-Kaffee-Unterhaltung, dem Genius Nadine für die Lösung aller Technik- und Tierhaus-Fragen und ihre nützlichen Einfälle, Tobi für sein Ideen-Reichtum und schließlich danke an Flo, für seine fachliche Expertise, dass er nicht müde wurde auch noch die 250te Abbildung hilfreich zu kommentierten und Korrekturvorschläge für diese Arbeit zu machen.

Allen Mitdoktoranden, „Ernies“ und Freunden danke ich für aufbauende, motivierende Gespräche, beste Ablenkung zur Wissenschaft und dass ihr immer für mich da seid. Ein ganz großer Dank geht hier an Luisa, die mich aufgefangen hat. Lieber Andreas, du Meister des Hinterfragens, ich danke dir von ganzem Herzen, dass du mich ermutigt hast diese Doktorarbeit anzugehen, mich unterstützt hast und seit vielen Jahren immer an meiner Seite bist.

Zu guter Letzt möchte ich mich bei meiner Familie und besonders bei meinen Eltern bedanken. Danke für eure uneingeschränkte Unterstützung und das gute Zureden, dass ich es schon schaffen werde.

# EIDESSTATTLICHE ERKLÄRUNG

Ich erkläre an Eides statt, dass ich die bei der Fakultät Wissenschaftszentrum Weihenstephan für Ernährung, Landnutzung und Umwelt der TUM zu Promotionsprüfung vorgelegte Arbeit mit dem Titel:

**Diet-induced obesity in inbred mouse strains – identification of proximate causes, reversibility of metabolic alterations and heredity of resistance**

am Lehrstuhl für Molekulare Ernährungsmedizin unter der Anleitung und Betreuung durch Univ.-Prof. Dr. Martin Klingenspor ohne sonstige Hilfe erstellt und bei der Abfassung nur die gemäß § 6 Abs. 6 und 7 Satz 2 angegebenen Hilfsmittel benutzt habe.

Ich habe keine Organisation eingeschaltet, die gegen Entgelt Betreuerinnen und Betreuer für die Anfertigung der Dissertation sucht, oder die mir obliegende Pflichten hinsichtlich der Prüfungsleistungen für mich ganz oder teilweise erledigt.

Ich habe die Dissertation in dieser oder ähnlicher Form in keinem anderen Prüfungsverfahren als Prüfungsleitung vorgelegt.

Die vollständige Dissertation wurde noch nicht veröffentlicht.

Ich habe den angestrebten Doktorgrad noch nicht erworben und bin nicht in einem früheren Promotionsverfahren für den angestrebten Doktorgrad endgültig gescheitert.

Die öffentlich zugängliche Promotionsordnung der TUM ist mir bekannt, insbesondere habe ich die Bedeutung von § 28 (Nichtigkeit der Promotion) und § 29 (Entzug des Doktorgrades) zur Kenntnis genommen. Ich bin mir der Konsequenzen einer falschen Eidesstattlichen Erklärung bewusst.

Mit der Aufnahme meiner personenbezogenen Daten in die Alumni-Datei bei der TUM bin ich einverstanden

München, den _____ _____

Caroline Kless